



This is to certify that the

dissertation entitled

"Probing the Symmetry-Breaking Mechanism through the Electroweak Interactions of the Top Quark"

presented by

Ehab Malkawi

has been accepted towards fulfillment of the requirements for

Ph.D. degree in Physics

Date May 21, 1996

MSU is an Affirmative Action/Equal Opportunity Institution

0-12771

LIBRARY Michigan State University

PLACE IN RETURN BOX to remove this checkout from your record. TO AVOID FINES return on or before date due.

	DATE DUE	DATE DUE
MAR 0 9 2000 0 9 2 7 0 2		

MSU is An Affirmative Action/Equal Opportunity Institution choledelesus.pm3-p.

PROBING THE SYMMETRY-BREAKING MECHANISM THROUGH THE ELECTROWEAK INTERACTIONS OF THE TOP QUARK

 $\mathbf{B}\mathbf{y}$

Ehab Omar Malkawi

A DISSERTATION

Submitted to
Michigan State University
in partial fulfillment of the requirements
for the degree of

DOCTOR OF PHILOSOPHY

Department of Physics and Astronomy

1996

ABSTRACT

PROBING THE SYMMETRY-BREAKING MECHANISM THROUGH THE ELECTROWEAK INTERACTIONS OF THE TOP QUARK

By

Ehab Malkawi

Since the top quark mass is of the order of the symmetry-breaking scale, the top quark is likely to provide useful hints about the symmetry-breaking mechanism responsible for generating the gauge boson masses and at least connected with the fermion mass generation mechanism. I propose to probe the electroweak symmetrybreaking sector by measuring the effective couplings of the top quark to the gauge bosons. Different scenarios of electroweak symmetry-breaking will imply different correlations among these couplings. Using precision LEP and SLC data, I constrain the nonuniversal couplings of the top quark to the gauge bosons using the electroweak chiral Lagrangian framework. Constraining these couplings will provide an estimate for possible deviation in the gauge universality advocated in the SM. At the order of $m_t^2 \ln \Lambda^2$, in which $\Lambda \sim 4\pi v$ is the cutoff scale of the effective theory, new physics in the left-handed neutral current is already constrained by LEP data. In models with an approximate custodial symmetry, a positive new physics contribution in the left-handed charged current is preferred. The right-handed neutral current can be constrained by studying the direct detection of the top quark at the Tevatron and the LHC. At the LC, the neutral current can be better measured.

It is also interesting to note that due to the nonstandard couplings of the top quark to the gauge bosons, the upper bound on the top quark mass, from radiative corrections, can be raised from the SM bound $m_t < 200 \text{ GeV}$ to as large as 300 GeV. That is to say, if there is new physics associated with the top quark, it is possible to say that (from radiative corrections) the top quark is heavier than what the SM predicts.

Also, I present a theoretical frame work to extract the pure m_t corrections to the low energy data in the chiral Lagrangian framework. The result is useful and interesting for two reasons: First, it simplifies the whole process of calculating radiative corrections. Second, this approach is shown to clearly identify observables which are sensitive to the symmetry-breaking sector of the electroweak theory.

Finally, I present a self-contained model which demonstrates how the nonstandard top quark couplings to the gauge bosons can be generated. The model has a very rich structure and significant implications at low and high energy scales. Using the low energy data I discuss the possible constraints on the model. On the other hand, high energy colliders will provide further tests and demonstrate possible new physics especially interesting FCNC processes.

To my parents, my lovely wife, and our expected baby.

ACKNOWLEDGEMENTS

I would like to express my deepest gratitude to the people who have contributed to me and to this work:

To my thesis advisor C.-P. Yuan for teaching me high energy physics (up to date), for his calmness, and his support;

To the members of my Thesis Committee: C. Brock, W. Repko, S. D. Mahanti and A. Brown, for their support;

To my colleagues in the High Energy Theory group: Doug Carlson, Fransisco Larios, Tim Tait, Mike Wiest, Csaba Balasz, Liang-Hung Lai and Xiaoning Wang. Also to Kate Frame and Simona Murgia from the High Energy Experimental group;

To my lovely wife, Amal, for her patience, her support, and for the long nights she was waiting and standing by;

To my parents who wished to be present during my defense but could not, thanks for everything.

TABLE OF CONTENTS

LI	JIST OF TABLES		X
LIST OF FIGURES		хi	
1	The	Standard Model and Precision Tests	1
	1.1	The Electroweak Standard Model	2
	1.2	Radiative Corrections	5
		1.2.1 QED Corrections	10
	1.3	Renormalization	13
	1.4	The ϵ Parameters	28
	1.5	The SM Heavy m_t and m_H Contributions to the Low-Energy Data .	35
		1.5.1 Heavy Top Quark Contributions	35
		1.5.2 Heavy Higgs Boson Contributions	38
	1.6	Status of the SM	39
2	The	Chiral Lagrangian	48
	2.1	Physics Beyond the SM	48
	2.2	Model Independent Analysis	50

	2.3	Introduction to the Chiral Lagrangian	53
	2.4	Heavy Top Quark Contribution to the ϵ Parameters in the Chiral La-	
		grangian	61
3	Glo	bal Analysis of the Top Quark Couplings to the Electroweak	•
	Gau	ige Bosons	65
	3.1	Motivations and Perspectives	65
	3.2	The Top Quark Couplings to Gauge Bosons in the Chiral Lagrangian	
		Framework	72
	3.3	Low Energy Constraints	77
		3.3.1 General Case	78
		3.3.2 Special Case	92
		3.3.3 At the SLC	107
	3.4	Heavy Higgs Boson Limit in the SM	114
	3.5	Direct Measurement of the Top Quark Couplings	116
		3.5.1 At the Tevatron and the LHC	117
		3.5.2 At the LC	121
	3.6	Discussion and Conclusions	122
4	Hes	avy Top Quark Effects and the Scalar Sector	125
•			
	4.1	Introduction	125
	4.2	Large m_t effects in the SM	127
	4.3	Large m_t Effects In the Chiral Lagrangian	131
		4.3.1 Effective Lagrangian	136

		4.3.2 Renormalization	140
		4.3.3 Low Energy Observables	142
	4.4	One Loop Corrections in the SM	144
	4.5	One Loop Corrections with Nonstandard Top Quark Couplings	145
	4.6	Conclusions	148
5	A N	Model of Strong Flavor Dynamics for the Top Quark	150
	5.1	Introduction	150
	5.2	The Model	151
		5.2.1 The Bosonic Sector	152
		5.2.2 The Fermion Sector	156
	5.3	Low Energy Constraints	162
	5.4	High Energy Experiments	172
6	Dise	cussions and Conclusions	180
A	Ren	normalization Schemes	184
В	The	s S , T , U parameters	194
C	Hea	avy Mass Expansion	199
D	Nor	n-Linear Realization	203
	D.1	Linear Realization	203
	D 2	Non-linear Realization	204

LIST OF TABLES

1.1	The input parameters used to calculate the SM predictions in Table 1.2	. 46
1.2	Experimental and predicted values of electroweak observables for the SM. The SM predictions are calculated using the input values in Table 1.1. Columns a and b are for $\alpha_s = 0.125$ and 0.115, respectively	47
3.1	The confined range of the couplings, κ_L and κ_R for various top quark masses and for $m_H = 65 \text{ GeV}. \ldots$	100
5.1	Experimental and predicted values of electroweak observables for the SM and the proposed model (with different choices of parameters) for $\alpha_s = 0.125$ with $m_t = 175$ GeV and $m_H = 300$ GeV	178
5.2	Experimental and predicted values of electroweak observables for the SM and the proposed model (with different choices of parameters) for $\alpha_s = 0.115$ with $m_t = 175$ GeV and $m_H = 300$ GeV	179

LIST OF FIGURES

1.1	a: The Feynman diagrams contributing to the running α up to one-loop level. b: The Feynman diagrams contributing to the running α summed to all orders	14
1.2	The whole set of one-loop corrections needed to renormalize the SM parameters α , G_F , and M_Z	16
1.3	The one-loop corrections to the coupling $\gamma - e^ e^+$	19
1.4	a: The vacuum polarization function of the Z boson, up to one loop. b: The one-loop corrections to the μ decay. All corrections, except the W self-energy, are collectively denoted by $\delta G_{V,B}$	20
1.5	The top quark contribution to the epsilon parameters, at the one-loop level	37
1.6	The Higgs boson contribution to the epsilon parameters, at the one-loop level	40
2.1	The relevant Feynman diagrams in calculating the top quark contribution to the epsilon parameters using the chiral Lagrangian approach.	64
3.1	The relevant Feynman diagrams, for the nonstandard top quark couplings case and in the 't Hooft-Feynman gauge, which contribute to the order $\mathcal{O}(m_t^2 \ln \Lambda^2)$	82
3.2	A two-dimensional projection in the plane of κ_L^{NC} and κ_R^{NC} , for $m_t = 160$ GeV (solid contour) and 180 GeV (dashed contour). The Higgs boson mass is fixed, $m_H = 65$ GeV	87
3.3	A two-dimensional projection in the plane of κ_L^{NC} and κ_L^{CC} , for $m_t = 160 \text{ GeV}$ (solid contour) and 180 GeV (dashed contour). The Higgs boson mass is fixed, $m_H = 65 \text{ GeV}$	88
3.4	A two-dimensional projection in the plane of κ_R^{NC} and κ_L^{CC} , for $m_t = 160 \text{ GeV}$ (solid contour) and 180 GeV (dashed contour). The Higgs boson mass is fixed, $m_H = 65 \text{ GeV}$	89
3.5	A two-dimensional projection in the plane of κ_L^{NC} and κ_R^{NC} , for $m_t = 160$ GeV (solid contour) and 180 GeV (dashed contour), and for the heavy Higgs boson mass $m_H = 1000$ GeV	91

3.6	The allowed region of κ_L and κ_R , for $m_t = 170 \text{GeV}$, $m_H = 65 \text{GeV}$. (Note that $\kappa_L = \kappa_L^{NC} = 2\kappa_L^{CC}$ and $\kappa_R = \kappa_R^{CC}$.)	99
3.7	The allowed range of $(\kappa_L - 2\kappa_R)$ as a function of the mass of the top quark and for $m_H = 65$ GeV. (Note that $\kappa_L = \kappa_L^{NC} = 2\kappa_L^{CC}$ and $\kappa_R = \kappa_R^{CC}$.)	100
3.8	The allowed range of the coupling $\kappa_L^{CC} = \kappa_L^{NC}/2 = \kappa_L/2$ as a function of the mass of the top quark and for $m_H = 65$ GeV	101
3.9	The allowed range of the coupling $\kappa_L^{CC} = \kappa_L^{NC}/2 = \kappa_L/2$ as a function of the mass of the top quark and for $m_H = 300$ GeV	102
3.10	The allowed range of the coupling $\kappa_L^{CC} = \kappa_L^{NC}/2 = \kappa_L/2$ as a function of the mass of the top quark and for $m_H = 1000 \text{ GeV}$	103
3.11	The allowed region of κ_L^{NC} and κ_R^{NC} , for models without a SM Higgs boson and for $m_t = 170 \text{ GeV}. \dots$	104
3.12	A comparison between our model and the model in Ref. [95]. The allowed regions in both models are shown on the plane of κ_L^{NC} and κ_R^{NC} , for $m_t = 170$ GeV and $m_H = 300$ GeV	106
3.13	The allowed region of κ_L and κ_R , using the SLC measurement A_{LR} , for $m_t = 170$ GeV and $m_H = 300$ GeV	110
3.14	The allowed region of κ_L and κ_R , using LEP data and the SLC measurement of A_{LR} , for $m_t = 170$ GeV and $m_H = 300$ GeV	112
3.15	The overlapping of the two measurements A_e and A_{LR} as a function of the top quark mass. Negative values of h indicates overlapping, while positive values indicates no overlapping	113
3.16	The Feynman diagrams needed to calculate the effective couplings of the top quark to the W and Z gauge bosons	115
3.17	The allowed $ \kappa_R^{CC} $ and κ_L^{CC} are bounded within the two dashed (solid) lines for a 20% (50%) error on the measurement of the single-top production rate, for a 175 GeV top quark	120
4.1	The Feynman diagrams which contribute to ρ and τ to the order $\mathcal{O}(m_t^2 \ln \Lambda^2)$	146
5.1	The Feynman diagrams for the process $\tau \to \mu\mu\mu$	166
5.2	The lower bound on the heavy Z' mass as a function of $\sin^2 \phi$ for 3σ , $\sin^2 \beta = 0$ (solid) and $\sin^2 \beta = 1$ (dashed) and $\alpha_s = 0.125$	169
5.3	The lower bound on the heavy Z' mass as a function of $\sin^2 \phi$ for 3σ , $\sin^2 \beta = 0$ (solid) and $\sin^2 \beta = 1$ (dashed) and $\alpha_s = 0.115$	170
5.4	The event number of $\mu^{\pm}\tau^{\mp}$ produced at the LC, with a c.m. energy of 500 GeV, and for two choices of parameters	176

Chapter 1

The Standard Model and Precision Tests

The Standard Model is a $SU(3)_C \times SU(2)_L \times U(1)_Y$ gauge invariant quantum field theory of the strong and electroweak interactions. The Standard Model has been very successful in describing the fermions' (quarks and leptons) interactions via the force mediators (gauge bosons). The gauge symmetry $SU(3)_C$ is associated with the strong interaction (QCD) of the quarks via the corresponding gauge bosons known as the gluons. The remaining symmetry $SU(2)_L \times U(1)_Y$ known as the electroweak symmetry is composed of the weak $SU(2)_L$ and the hypercharge $U(1)_Y$ symmetries. The electroweak symmetry governs the unified weak and electromagnetic interactions, collectively, know as the electroweak interactions. To allow for the generation of the weak gauge boson masses the gauge symmetry $SU(2)_L \times U(1)_Y$ must be broken into the electromagnetic symmetry group $U(1)_{em}$. This breakdown is triggered through the spontaneous symmetry breaking. The intimate connection between the electroweak interactions and the symmetry breaking mechanism constitutes the major issue I will explore throughout this body of work. Therefore, throughout this study I will be mainly concentrating on the electroweak interactions. In the next section I will outline the basic features of the electroweak Standard Model. For a more detailed discussion the reader can refer to existing literature [1, 2, 3, 4, 5].

1.1 The Electroweak Standard Model

The electroweak Standard Model (SM) is based on the gauge group $SU(2)_L \times U(1)_Y$ with the following basic structures:

• The fermions are assembled in three families or generations with left-handed doublets and right-handed singlets under the $SU(2)_L$ group:

$$\begin{pmatrix} \nu_{e} \\ e \end{pmatrix}_{L}, \quad \begin{pmatrix} u \\ d \end{pmatrix}_{L}, \quad e_{R}, \quad d_{R}, \quad u_{R},
\begin{pmatrix} \nu_{\mu} \\ \mu \end{pmatrix}_{L}, \quad \begin{pmatrix} c \\ s \end{pmatrix}_{L}, \quad \mu_{R}, \quad s_{R}, \quad c_{R},
\begin{pmatrix} \nu_{\tau} \\ \tau \end{pmatrix}_{L}, \quad \begin{pmatrix} t \\ b \end{pmatrix}_{L}, \quad \tau_{R}, \quad b_{R}, \quad t_{R}.$$
(1.1)

The hypercharge quantum number Y_f of a fermion f is fixed by the Gell-Mann-Nishijima relation

$$Q_f = T_{3f} + \frac{Y_f}{2} \,, \tag{1.2}$$

where Q_f is the electric charge in units of e and T_{3f} is the weak isospin quantum number. For example, the left-handed electron e_L has $Q_e = -1$ and $T_{3e} = -1/2$. A left-handed fermion doublet will be denoted by Ψ_L whereas a right-handed fermion singlet denoted by Ψ_R . The fermionic Lagrangian is given by

$$\mathcal{L}_{FK} = \sum_{f} \overline{\Psi_L^f} i \gamma^{\mu} D_{\mu} \Psi_L^f + \sum_{f} \overline{\Psi_R^f} i \gamma^{\mu} D_{\mu} \Psi_R^f , \qquad (1.3)$$

where f = 1, 2, 3 is a family index. Also,

$$D_{\mu}\Psi_{L} = \left(\partial_{\mu} - ig\frac{\tau^{a}}{2}W_{\mu}^{a} - ig'\frac{Y}{2}B_{\mu}\right)\Psi_{L}, \qquad (1.4)$$

$$D_{\mu}\Psi_{R} = (\partial_{\mu} - ig'QB_{\mu})\Psi_{R}, \qquad (1.5)$$

where a=1,2,3 is an isospin index. The gauge boson field W^a_μ with the gauge coupling g and the gauge boson field B_μ with the gauge coupling g' are associated with the gauge groups $SU(2)_L$ and $U(1)_Y$, respectively. The Pauli matrices τ^a 's are normalized according to the relation:

$$\operatorname{Trace}(\tau^a \tau^b) = 2\delta^{ab}. \tag{1.6}$$

• There are 4 gauge bosons transmitting the electroweak force:

$$A \text{ (photon)}, \quad W^+, \quad W^-, \quad Z.$$
 (1.7)

The self-interactions of the gauge bosons are given by

$$\mathcal{L}_{GK} = -\frac{1}{4} B_{\mu\nu} B^{\mu\nu} - \frac{1}{4} W^{a}_{\mu\nu} W^{a\mu\nu} , \qquad (1.8)$$

where

$$B_{\mu\nu} = \partial_{\mu}B_{\nu} - \partial_{\nu}B_{\mu} \,, \tag{1.9}$$

$$W^a_{\mu\nu} = \partial_\mu W^a_\nu - \partial_\nu W^a_\mu + g\epsilon^{abc} W^b_\mu W^c_\nu \,, \tag{1.10}$$

and with the field definitions

$$W^{\pm} = \frac{W^1 \mp iW^2}{\sqrt{2}} \,, \tag{1.11}$$

$$Z = \cos\theta W^3 - \sin\theta B, \quad A = \sin\theta W^3 + \cos\theta B, \tag{1.12}$$

where θ is the weak mixing angle and $\cos^2 \theta = 1 - \sin^2 \theta$.

• A complex scalar doublet field with hypercharge Y = -1 implements the spontaneous symmetry-breaking

$$\Phi = \begin{pmatrix} (v + H + i\phi^0)/\sqrt{2} \\ i\phi^- \end{pmatrix}, \tag{1.13}$$

where the fields ϕ^0 and ϕ^{\pm} are called the would-be Goldstone bosons and the neutral field H is called the Higgs boson. The scalar doublet field Φ has a non-vanishing vacuum expectation value (v.e.v) $<\Phi>$, where

$$\langle \Phi \rangle = \begin{pmatrix} v/\sqrt{2} \\ 0 \end{pmatrix}. \tag{1.14}$$

The components ϕ^{\pm} , ϕ^0 are unphysical and can be gauged away in a specific gauge known as the unitary gauge. The scalar Lagrangian is given by

$$\mathcal{L}_{\Phi K} = (D_{\mu}\Phi)^{\dagger}(D^{\mu}\Phi) - \frac{\lambda}{2}\left((\Phi^{\dagger}\Phi)^2 - \frac{v^2}{2}\right)^2, \tag{1.15}$$

where

$$D_{\mu}\Phi = \left(\partial_{\mu} - ig\frac{\tau^a}{2}W_{\mu}^a + ig'\frac{1}{2}B_{\mu}\right)\Phi. \tag{1.16}$$

Because of the v.e.v, spontaneous symmetry-breaking is triggered and the W^{\pm} and Z bosons are rendered massive:

$$M_W = \frac{gv}{2}, \quad M_Z = \frac{\sqrt{g^2 + g'^2} v}{2}.$$
 (1.17)

The fermion masses are generated through the fermion interactions to the scalar doublet Φ (Yukawa interactions), e.g., for the third generation

$$\mathcal{L}_{\text{Yukawa}} = \frac{\sqrt{2}m_{t}}{v} (\overline{t}_{L} \, \overline{b}_{L}) \, \Phi \, t_{R} + \frac{\sqrt{2}m_{b}}{v} (\overline{t}_{L} \, \overline{b}_{L}) \left(-i\tau_{2}\Phi^{*}\right) b_{R} + \frac{\sqrt{2}m_{\tau}}{v} \left(\overline{\nu}_{L} \, \overline{\tau}_{L}\right) \left(-i\tau_{2}\Phi^{*}\right) \tau_{R} + \text{hermitian conjugate}. \tag{1.18}$$

Due to the generation of quark masses for both the up and down type quarks, mixing between different quark families is possible. The mixing is described by a unitary matrix V_{CKM} which consists of three mixing angles and one phase. No mixing in the lepton sector can be generated within the SM because neutrinos are massless.

The full electroweak gauge invariant SM Lagrangian can be written as

$$\mathcal{L}_{SM} = \mathcal{L}_{FK} + \mathcal{L}_{GK} + \mathcal{L}_{\Phi K} + \mathcal{L}_{Yukawa}. \tag{1.19}$$

By examining Eq. (1.19) one concludes that the SM has a certain number of free parameters: g, g', v, λ , in addition to the fermion masses m_f and the quark mixing matrix ¹. Those free parameters have to be determined from experimental data.

The parameter λ can be traded for the Higgs boson mass $m_H = v\sqrt{\lambda}$. The Higgs boson mass is experimentally constrained to be above 65 GeV [6]. Also, theoretical arguments suggest an upper bound on m_H of about 1 TeV [7, 8]. All fermion masses [9] except the top quark mass [10, 11] are below the M_Z scale [12]. Throughout this work, I will refer to fermions with masses below the M_Z scale by light fermions. Also, by low energy experiments I mean experiments operating at the M_Z scale or below.

1.2 Radiative Corrections

At tree level the low energy electroweak observables can be entirely written in terms of the three free parameters g, g', and v in addition to the light fermion masses and the quark mixing matrix V_{CKM} . The top quark mass m_t and the Higgs boson mass m_H only enter through radiative corrections. Thus, given the light fermion masses and the quark mixing matrix, three additional measurable quantities are needed to fix the free parameters g, g', and v. The three observables chosen must be precisely

¹Also, from the QCD sector, there is the strong gauge coupling g_s .

measured and theoretically calculable in a clean way. After this procedure of defining the physical input, other observables can be predicted and compared with the corresponding experimental data. Different choices of the basic measured observables correspond to different renormalization schemes. In general, loop calculations are divergent and therefore, one needs to regularize the theory. Different regularization schemes are used in the literature, e.g., using a momentum-cutoff, dimensional regularization, etc. The tree-level (bare) parameters in the Lagrangian have no direct physical meaning and can be replaced by the renormalized parameters, e.g., the bare gauge coupling g_0 can be written in terms of the renormalized coupling g_0

$$g = g_0 + \delta g \,, \tag{1.20}$$

where δg is called the coupling counterterm. The renormalized parameters are finite by definition and can be fixed by a set of measurable quantities. By this redefinition of the parameters the one-loop amplitudes are rendered finite. However, only the divergent part of the counterterm is fixed by the requirement of divergence cancelation. The finite part is somewhat arbitrary and thus calculated quantities depend on the renormalization scheme. To any perturbative order, the difference in a calculated quantity using two different renormalization schemes is of a higher order, e.g., for a one-loop calculation the difference is of the order of a two-loop correction. All renormalization schemes are equivalent if calculations are performed to all orders. Since only a perturbative fixed order calculation is usually possible, one should be consistent in defining the renormalization scheme and using the calculated numbers in that particular scheme. Different renormalization schemes are implemented in the literature. In appendix A, I discuss in some detail different renormalization schemes. Here, I briefly mention some of the most commonly used schemes:

• The Z-pole scheme, where the input observables are chosen to be:

- The electromagnetic coupling $\alpha = e^2/4\pi$ measured from electron-proton (e-p) scattering in the limit of zero momentum transfer $q^2 \to 0$ (Thomson limit) [9]

$$\alpha^{-1} = 137.0359895(61). \tag{1.21}$$

- The Fermi coupling constant G_F measured from the muon lifetime au_{μ} and the theoretical formula

$$\frac{1}{\tau_{\mu}} = \frac{G_F^2 m_{\mu}^5}{192\pi^3} \left(1 - 8 \frac{m_{\epsilon}^2}{m_{\mu}^2} \right) \left(1 + \frac{\alpha}{\pi} \left(\frac{25}{4} - \pi^2 \right) \right) \left(1 + \frac{2\alpha}{3\pi} \ln \frac{m_{\mu}}{m_{\epsilon}} \right) , \quad (1.22)$$

where QED corrections to the four-fermion interaction includes the one-loop correction and the leading correction in α^2 . The value of G_F is [9].

$$G_F = 1.166389(22) \times 10^{-5} \,\text{GeV}^{-2}$$
 (1.23)

- The Z mass [12]

$$M_Z = 91.1885 \pm 0.0022 \,\text{GeV} \,.$$
 (1.24)

In this scheme the weak mixing angle $\sin^2\theta$ is defined to all orders by the relation

$$\sin^2 \theta = 1 - \cos^2 \theta \equiv \frac{1}{2} \left(1 - \left[1 - \frac{4\pi\alpha}{\sqrt{2}G_F M_Z^2} \right]^{1/2} \right) . \tag{1.25}$$

By definition $\sin^2 \theta$ has no dependence on the top quark mass m_t and the Higgs boson mass m_H .

• The on-shell scheme where α , M_Z , and M_W are the input observables. In this scheme the weak mixing angle $\sin^2 \theta$ is defined to all orders as

$$\sin^2 \theta = 1 - \frac{M_W^2}{M_Z^2} \,. \tag{1.26}$$

Unfortunately, the W mass is not determined as precisely as M_Z [12, 13]

$$M_W = 80.26 \pm 0.16 \text{ GeV}$$
 (1.27)

Therefore, $\sin^2 \theta$ is usually extracted from other data. In this case $\sin^2 \theta$ has a strong dependence on the top quark mass m_t .

• The $\overline{\text{MS}}$ scheme where only the divergent pieces in the loop calculations are absorbed by the counterterms. In this scheme, $\sin^2 \theta$ is defined as

$$\bar{s}_{\theta}^2 = 1 - \frac{\bar{M}_W^2}{\bar{M}_Z^2} \,, \tag{1.28}$$

where $\overline{M_W}$ and $\overline{M_Z}$ are the W and Z masses defined in the \overline{MS} scheme. In this scheme the weak mixing angle $\overline{s_\theta}$ has some sensitivity on the top quark mass.

For more information on renormalization schemes, the reader can refer to appendix A.

The main goal of this work is to browse through the top quark effects to low energy data. Therefore, it is advantageous to isolate the top quark effects to low energy data completely from the input parameters. For this reason, I will work with the Z-pole scheme since $\sin^2 \theta$, by definition, does not depend on the top quark mass. The basic observables α , G_F , and M_Z can be written in terms of the parameters g, g', and v as follow

$$\alpha = \frac{g^2 g'^2}{4\pi (g^2 + g'^2)}, \quad G_F = \frac{1}{\sqrt{2}v^2}, \quad M_Z = \frac{\sqrt{g^2 + g'^2} v}{2}.$$
 (1.29)

These equations can be solved in favour of g, g', and v as a function of α , G_F , and M_Z as follow

$$v = \left(\frac{1}{\sqrt{2}G_F}\right)^{1/2}, \quad g = \frac{\sqrt{4\pi\alpha}}{\sin\theta}, \quad g' = \frac{\sqrt{4\pi\alpha}}{\cos\theta}, \tag{1.30}$$

where

$$\sin^2 \theta = 1 - \cos^2 \theta \equiv \frac{1}{2} \left(1 - \left[1 - \frac{4\pi\alpha}{\sqrt{2}G_F M_Z^2} \right]^{1/2} \right) . \tag{1.31}$$

All other derived parameters in the Lagrangian can be written in terms of the input parameters. For the W mass we have

$$M_W^2 = \cos^2 \theta \, M_Z^2 \,. \tag{1.32}$$

The photon coupling to the fermions $f - \overline{f}$ is given by

$$Q_f \sqrt{4\pi\alpha}\gamma_{\mu} \,. \tag{1.33}$$

The W^{\pm} coupling to the fermions f - f' is given by

$$\frac{\sqrt{4\pi\alpha}}{2\sqrt{2}\sin\theta}\gamma_{\mu}(1-\gamma_5). \tag{1.34}$$

The Z coupling to the fermions $f - \overline{f}$ is given by

$$\left(\sqrt{2}G_F M_Z^2\right)^{1/2} \gamma_{\mu} (g_{Vf} - g_{Af} \gamma_5) , \qquad (1.35)$$

where

$$g_{Vf} = T_{3f} - 2Q_f \sin^2 \theta \,, \quad g_{Af} = T_{3f} \,.$$
 (1.36)

For the electron $Q_e = -1$, $T_{3e} = -1/2$.

If we do not care at all about radiative corrections, it is already possible to predict the low energy observables. However, the existed low energy data are precise enough to force us into considering the radiative corrections. In the rest of this chapter I will confine the discussion to the physics at the Z-mass scale, i.e., the physics at LEP and SLC (e^+e^- colliders at the Z pole). At one-loop level, the amplitude for the process $e^-e^+ \to f\overline{f}$ near the Z resonance can be factorized and written as

$$A(e^-e^+ \to f\overline{f}) = A_\gamma + A_Z, \tag{1.37}$$

where A_{γ} and A_{Z} are the photon- and Z-exchange amplitudes, respectively. In Eq. (1.37) I have ignored contributions from box diagrams which have a negligible effect at the Z pole [14]. Near the Z peak the total cross section as a function of the center of mass (c.m.) energy (\sqrt{s}) can be written as

$$\sigma_{f\overline{f}}(s) = \sigma_{Z,f\overline{f}}(s) + \sigma_{\gamma,f\overline{f}}(s) + \sigma_{\gamma Z,f\overline{f}}(s). \tag{1.38}$$

Here, $\sigma_{Z,f\bar{f}}(s)$ is the Z contribution to the cross section defined as

$$\sigma_{Z,f\bar{f}}(s) = \sigma_{f\bar{f}}^0 \frac{s\Gamma_Z^2}{(s - M_Z^2)^2 + s^2\Gamma_Z^2/M_Z^2},$$
(1.39)

where $\sigma_{f\bar{f}}^0$ is the peak cross section which is connected to the Z partial decay widths for $Z \to e^-e^+$ and $Z \to f\bar{f}$,

$$\sigma_{f\bar{f}}^0 = \frac{12\pi\Gamma_e\Gamma_f}{M_Z^2\Gamma_Z^2} \,. \tag{1.40}$$

Eq. (1.39) is taken as the definition of the Z mass and the total decay width Γ_Z [15, 16]. Notice that Eq. (1.39) is different from the Breit-Wigner shape by the s-dependence of the width [14]. The terms $\sigma_{\gamma,f\bar{f}}(s)$ and $\sigma_{\gamma Z,f\bar{f}}(s)$ in Eq. (1.38) stand for the pure photon and the Z-photon interference contributions to the cross section.

Near the Z peak, the largest contribution to the cross section $\sigma_{f\bar{f}}(s)$ comes from the Z contribution. For the LEP physics it is customary to extract the pure QED effects and to isolate them from the Z contribution. Below I discuss the QED corrections.

1.2.1 QED Corrections

The pure photon and the Z-photon interference contributions to the cross section $\sigma_{\gamma,f\bar{f}}(s)$ and $\sigma_{\gamma Z,f\bar{f}}(s)$, are theoretically calculated and subtracted from $\sigma_{f\bar{f}}(s)$. The QED corrections can be summarized in the following items

The initial-state photon radiation is the largest source of correction to the Breit-Wigner Z-line shape. This correction causes a reduction of about 25% in the peak cross section [15]. It can be counted for through a "structure function" G(x, s) that can be deconvoluted from the measured cross section σ_f^{meas}(s)

$$\sigma_{f\overline{f}}^{\text{meas}}(s) = \int dx G(x, s) \sigma_{f\overline{f}}((1 - x)s), \qquad (1.41)$$

where x is the fraction of the initial momentum of the electron or the positron carried by the photon. The function G(x,s) is theoretically predicted to a good accuracy through renormalization group methods [17].

• The largest QED effect to the physical observables at the Z-pole comes from the change (running) in α due to the change in the energy scale from $q^2 = 0$, where α is measured, to $q^2 = M_Z^2$ where physical observables are evaluated. This effect is related to the photon vacuum polarization function which can be written as

$$\Pi_{\mu\nu}^{\gamma\gamma}(q^2) = -ig_{\mu\nu}q^2 F^{\gamma\gamma}(q^2) + q_{\mu}q_{\nu} \text{ terms}.$$
 (1.42)

Note that $\Pi_{\mu\nu}^{\gamma\gamma}(0) = 0$ due to QED gauge invariance. In defining the running coupling α at the Z-pole I only consider the light fermions contribution to the photon vacuum polarization function. Hence, from the photon exchange at one loop (see Figure 1.1a) we have

$$\frac{\alpha_0}{q^2} \to \frac{\alpha_0}{q^2} - \frac{\alpha_0}{q^2} F^{\gamma\gamma}(q^2) = \frac{\alpha_0}{q^2} [1 - F^{\gamma\gamma}(q^2)], \qquad (1.43)$$

where α_0 is the bare coupling as discussed in the next section. A redefinition (renormalization) of α_0 is performed to render it finite,

$$\alpha_0 \to \alpha \left[1 + F^{\gamma\gamma}(0) \right] \,. \tag{1.44}$$

Therefore, we get

$$\alpha(q^2) = \alpha \left(1 - F^{\gamma \gamma}(q^2) + F^{\gamma \gamma}(0) \right) \equiv \alpha \left(1 + \Delta \alpha(q^2) \right), \tag{1.45}$$

where $\Delta \alpha(q^2)$ is a finite correction to the electromagnetic coupling α . The improved summed expression for α is (see Figure 1.1b)

$$\alpha(q^2) = \frac{\alpha}{1 - \Delta\alpha(q^2)} \,. \tag{1.46}$$

In $\Delta\alpha(q^2)$ I do not include the gauge bosons or the top quark contributions which are conventionally included in the remainder of the corrections. I write the light leptons and quarks contributions to $\Delta\alpha(q^2)$ as $\Delta\alpha_\ell(q^2)$ and $\Delta\alpha_q(q^2)$, respectively. At the Z-mass scale, the leptonic contribution to α is determined accurately, $\Delta\alpha_\ell(M_Z^2) = -0.03142$ [18], whereas for the quark contribution $\Delta\alpha_q$, a perturbative calculation is not possible. The determination of $\Delta\alpha_q$ is done using a dispersion integral over the measured cross section of $e^+e^- \to$ hadrons [18]. This gives $\Delta\alpha_q(M_Z^2) = -0.0286(9)$ and therefore one obtains [18]

$$\alpha^{-1}(M_Z^2) = 128.89 \pm 0.09, \tag{1.47}$$

where the largest uncertainty is coming from the hadron contribution. The effect of the running α is significant in the radiative correction analysis near the Z pole. With the coupling $\alpha(q^2=0)$ being replaced by the running coupling $\alpha(q^2=M_Z^2)$ in the tree-level Z contribution to the cross section, one obtains what is called the improved Born approximation for physics at the Z-pole.

• Final state-photon radiations are accounted for by including a factor (1 + $3\alpha Q_f^2/4\pi$) multiplying the Z partial widths. Similarly, for the QCD corrections we include the factor $R_{\rm QCD}$ in the hadronic partial widths, where [19]

$$R_{\rm QCD} = 1 + \left(\frac{\alpha_s(M_Z^2)}{\pi}\right) - 1.4 \left(\frac{\alpha_s(M_Z^2)}{\pi}\right)^2 - 12.8 \left(\frac{\alpha_s(M_Z^2)}{\pi}\right)^3, \tag{1.48}$$

and α_s is the QCD coupling, $\alpha_s = g_s^2/4\pi$.

The remaining QED corrections due to proper vertex correction and fermion self-energies are negligibly small at the Z-pole and vanish for a real photon (s → 0) [14]. The typical size of these corrections to the form factors is about 10⁻³ relative to the tree-level [14].

By taking care of the photonic corrections theoretically and experimentally, one can concentrate on the Z contribution to the Z-pole physics. Even with the inclusion of the running coupling $\alpha(M_Z^2)$ in the Z-pole observables it has been shown that the weak radiative corrections are becoming more apparent and significant in low energy data [20]. In this case one needs to go through the whole renormalization procedure.

1.3 Renormalization

In considering the renormalization procedure at one loop one needs to consider the whole set of one-loop level contributions, which can be summarized in the following corrections:

• The vacuum polarization functions of the gauge bosons (see Figure 1.2a) written in the following form

$$\Pi_{\mu\nu}^{ij}(q^2) = -ig_{\mu\nu} \left(A^{ij}(0) + q^2 F^{ij}(q^2) \right) + q_{\mu}q_{\nu} \text{ terms}, \qquad (1.49)$$

where $i, j = W, Z, \gamma(\text{photon})$. Alternatively instead of using Z and γ one can use i, j = 3, 0 for W^3 and B, respectively. The relation between the two cases is as follow

$$A^{33} = \cos^2\theta A^{ZZ} + 2\sin\theta\cos\theta A^{\gamma Z} + \sin^2\theta A^{\gamma \gamma}, \qquad (1.50)$$

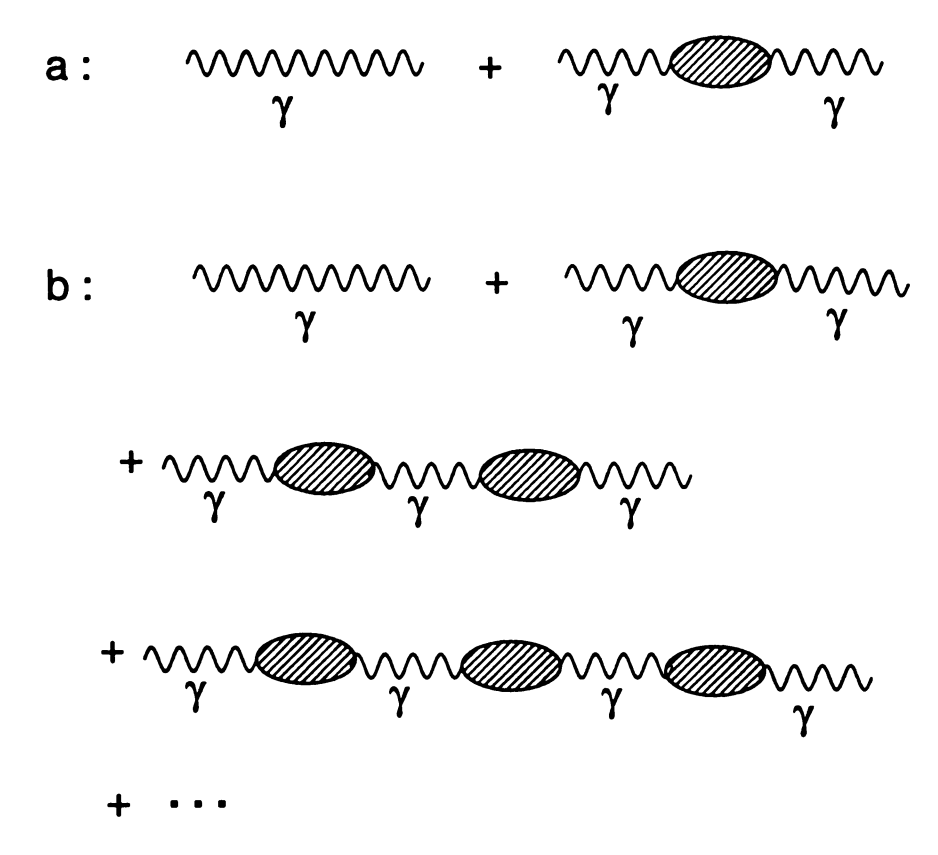


Figure 1.1: a: The Feynman diagrams contributing to the running α up to one-loop level. b: The Feynman diagrams contributing to the running α summed to all orders.

$$A^{30} = -\cos\theta\sin\theta A^{ZZ} + (\cos^2\theta - \sin^2\theta)A^{\gamma Z} + \cos\theta\sin\theta A^{\gamma Y}, \qquad (1.51)$$

$$A^{00} = \sin^2 \theta A^{ZZ} - 2\sin \theta \cos \theta A^{\gamma Z} + \cos^2 \theta A^{\gamma \gamma}, \qquad (1.52)$$

and similarly for F^{ij} . In Eq. (1.49), there is a small imaginary part which I will ignore since it does not contribute at the one-loop level.

• The contribution to the vector and the axial form factors at $q^2 = M_Z^2$ in the $Z \to f\overline{f}$ vertex from proper vertex diagrams and fermion self energies only (see Figure 1.2b)

$$(\sqrt{2}G_F M_Z^2)^{1/2} \gamma_{\mu} (\delta g_{Vf} - \delta g_{Af} \gamma_5) \,. \tag{1.53}$$

• All the one-loop corrections except the W vacuum polarization to the μ -decay amplitude at zero external momentum (see Figure 1.2c). All these corrections will be denoted by $\delta G_{V,B}$ [16]

$$\frac{\delta G_{V,B}}{\sqrt{2}} \left(\overline{e} \gamma_{\mu} (1 - \gamma_5) \nu_e \right) \left(\overline{\mu} \gamma^{\mu} (1 - \gamma_5) \nu_{\mu} \right) . \tag{1.54}$$

The input bare parameters can be written in terms of the renormalized ones and the above one-loop corrections [16].

(1) For the electromagnetic coupling I write the bare parameter α_0 in terms of the renormalized coupling α and the counterterm $\delta \alpha$ as

$$\alpha = \alpha_0 + \delta\alpha \,. \tag{1.55}$$

The one-loop corrections to the effective coupling γ - e^- - e^+ at zero momentum transfer $q^2 = 0$ are summarized in Figure 1.3. The bare coupling γ - e^- - e^+ can be written, using Eq. (1.55), as

$$e\gamma_{\mu}\left(1-\frac{1}{2}\frac{\delta\alpha}{\alpha}\right)$$
, (1.56)

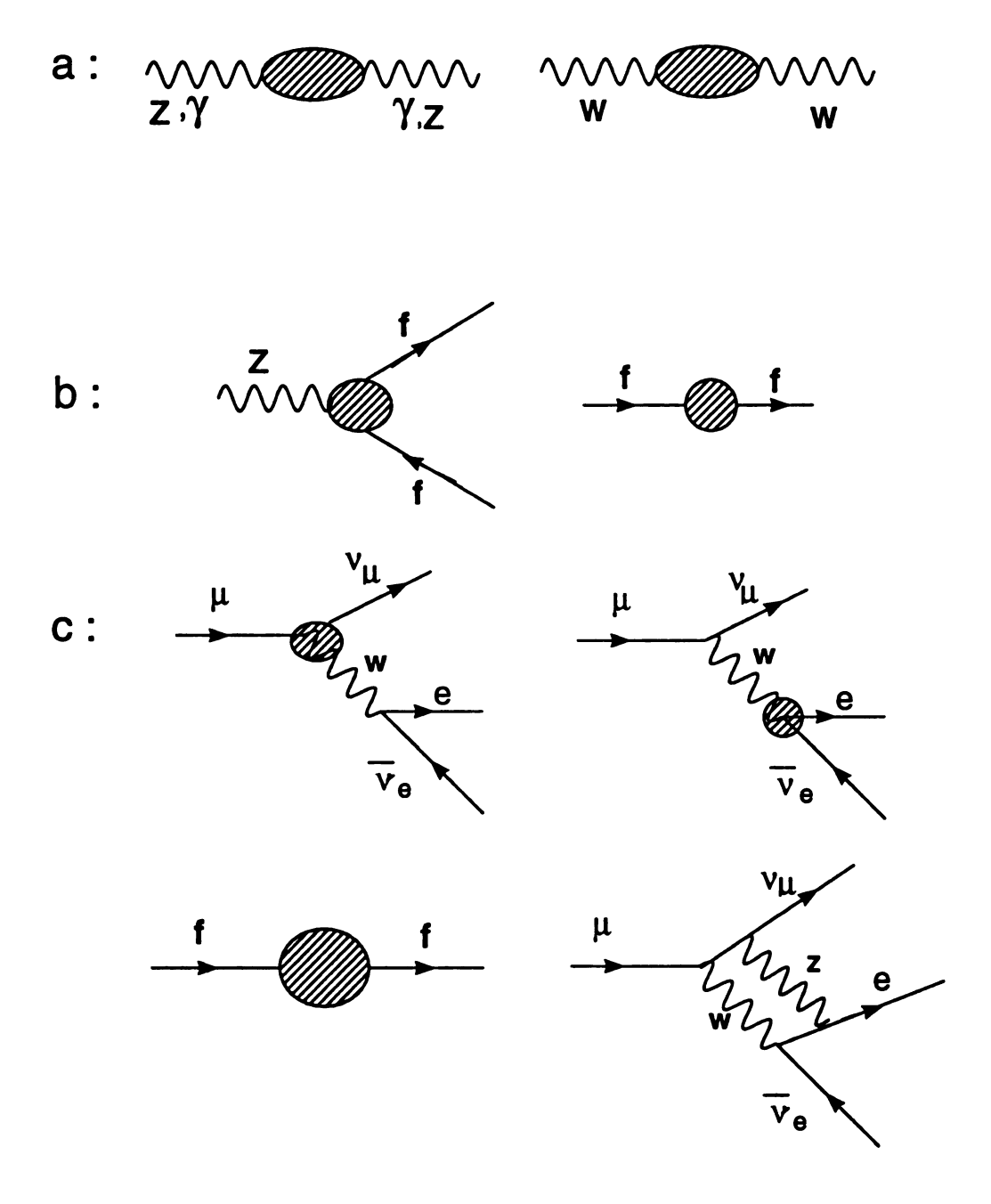


Figure 1.2: The whole set of one-loop corrections needed to renormalize the SM parameters α , G_F , and M_Z .

where $\delta \alpha / \alpha = 2 \delta e / e$. The one-loop proper vertex and self-energies calculation can be written as

$$e\gamma_{\mu}\left(\delta g_{Ve} - \gamma_5 \delta g_{Ae}\right) \,. \tag{1.57}$$

The photon wave function can be written as $(1+1/2\delta Z_{\gamma})$ where $\delta Z_{\gamma} = -F^{\gamma\gamma}(0)$. Adding all the one-loop corrections, one finds

$$e\gamma_{\mu} \left(1 - \frac{1}{2} \frac{\delta \alpha}{\alpha} - \frac{v_e}{2 \sin \theta \cos \theta} \frac{A^{\gamma Z}(0)}{M_Z^2} + \delta g_{Ve} + \frac{1}{2} \delta Z_{\gamma} \right)$$

$$+ e\gamma_{\mu} \gamma_5 \left(\delta g_{Ae} - \frac{a_e}{2 \sin \theta \cos \theta} \frac{A^{\gamma Z}(0)}{M_Z^2} \right) , \qquad (1.58)$$

where $v_e = -1/2 + 2\sin^2\theta$ and $a_e = -1/2$ are the vector and axial-vector couplings of the Z boson to e^-e^+ .

In pure QED no γ -Z mixing exists and using the QED Ward identity one finds $\delta g_{Ve} = \delta g_{Ae} = 0$ [21]. Therefore, the renormalized coupling reduces to

$$e\left(1 - \frac{1}{2}\frac{\delta\alpha}{\alpha} + \frac{1}{2}\delta Z_{\gamma}\right). \tag{1.59}$$

By requiring that, in the limit $q^2 = 0$, the renormalized coupling reduces to (e) we conclude that

$$\frac{\delta\alpha}{\alpha} = \delta Z_{\gamma} = -F^{\gamma\gamma}(0) \,. \tag{1.60}$$

In the SM case we have to include the γ -Z mixing which is mainly due to the W-boson loop. In the SM case one finds that the electromagnetic Ward-Takahashi identity guarantees [21]

$$\delta g_{Ae} + \frac{1}{4\sin\theta\cos\theta} \frac{A^{\gamma Z}(0)}{M_Z^2} = 0. \tag{1.61}$$

Also, one finds

$$\delta g_{Ve} + \frac{1 - 4\sin^2\theta}{4\sin\theta\cos\theta} \frac{A^{\gamma Z}}{M_Z^2}(0) = -\frac{\sin^2\theta}{\sin\theta\cos\theta} \frac{A^{\gamma Z}}{M_Z^2}(0). \tag{1.62}$$

Therefore the coupling reduces to

$$e\left(1 - \frac{1}{2}\frac{\delta\alpha}{\alpha} + \frac{1}{2}\delta Z_{\gamma} - \frac{\sin^2\theta}{\sin\theta\cos\theta} \frac{A^{\gamma Z}(0)}{M_Z^2}\right). \tag{1.63}$$

From which one finds

$$\frac{\delta\alpha}{\alpha} = -F^{\gamma\gamma}(0) - \frac{2\sin\theta}{\cos\theta} \frac{A^{\gamma Z}(0)}{M_Z^2} \,. \tag{1.64}$$

(2) For the Z-mass renormalization I consider the one-loop corrections to the Z boson propagator (see Figure 1.4a). One finds

$$\frac{1}{q^2 - M_{Z0}^2} \to \frac{1}{q^2 - M_{Z0}^2} \left(1 - \frac{A^{ZZ}(0) + q^2 F^{ZZ}(q^2)}{q^2 - M_{Z0}^2} \right) . \tag{1.65}$$

The full or dressed propagator is

$$\frac{1}{q^2 - M_{Z0}^2} \to \frac{1}{q^2 - M_{Z0}^2} \left(\frac{1}{1 + \frac{A^{ZZ}(0) + q^2 F^{ZZ}(q^2)}{q^2 - M_{Z0}^2}} \right) = \frac{1}{q^2 - M_{Z0}^2 + A^{ZZ}(0) + q^2 F^{ZZ}(q^2)} .$$
(1.66)

The physical mass M_Z is identified with the position of the pole

$$q^2 - M_{Z0}^2 + A^{ZZ}(0) + q^2 F^{ZZ}(q^2) = 0$$
 at $q^2 = M_Z^2$. (1.67)

Hence defining the mass counterterm as

$$M_Z^2 = M_{Z0}^2 + \delta M_Z^2 \,, \tag{1.68}$$

one finds

$$\frac{\delta M_Z^2}{M_Z^2} = -\frac{A^{ZZ}(0)}{M_Z^2} - F^{ZZ}(M_Z^2). \tag{1.69}$$

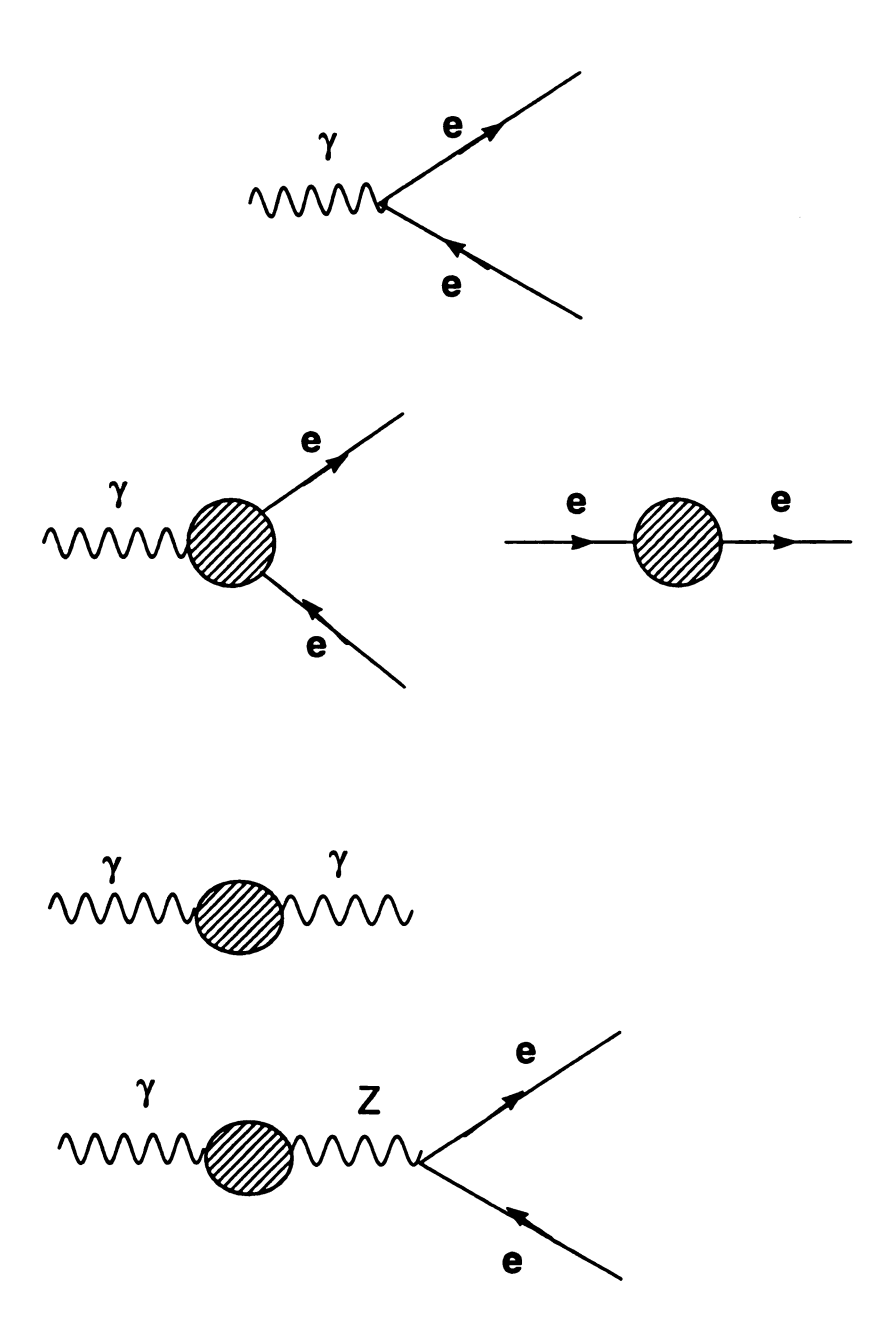
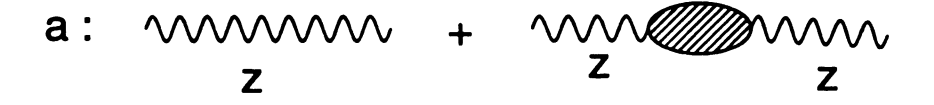


Figure 1.3: The one-loop corrections to the coupling $\gamma - e^- - e^+$.



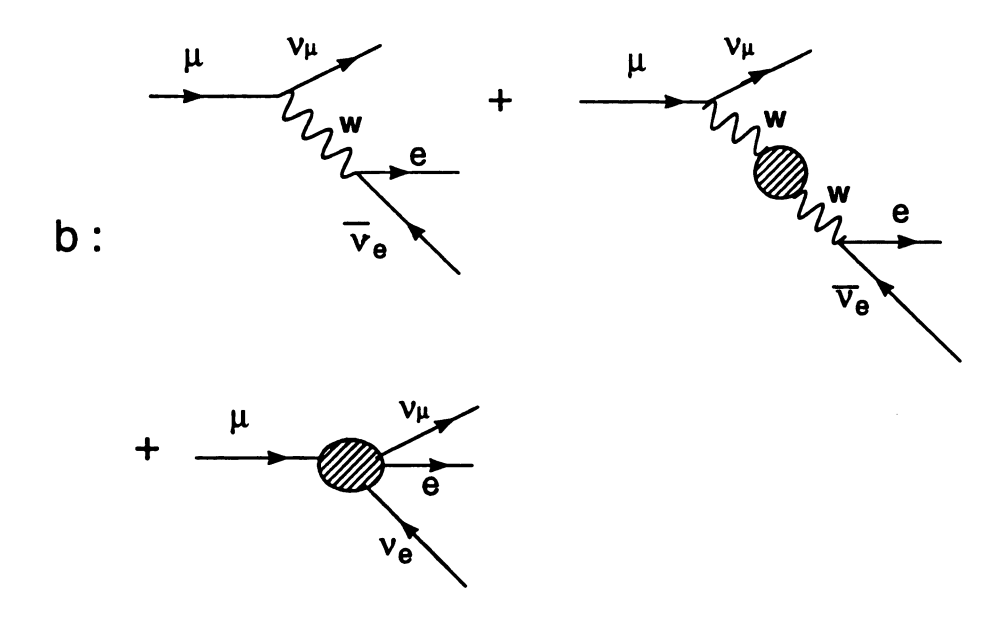


Figure 1.4: a: The vacuum polarization function of the Z boson, up to one loop. b: The one-loop corrections to the μ decay. All corrections, except the W self-energy, are collectively denoted by $\delta G_{V,B}$.

(3) For the Fermi coupling G_F , I compute the one-loop correction to the μ decay (see Figure 1.4b). I denote all the proper vertex, box and self energies corrections by $\delta G_{V,B}$. Writing the counterterm as

$$G_F = G_{F0} + \delta G_F \,, \tag{1.70}$$

and adding the one-loop calculations with the counterterm to the μ -decay amplitude, one finds

$$G_F \left(1 - \frac{\delta G_F}{G_F} - \frac{A^{WW}(0) + q^2 F^{WW}(q^2)}{q^2 - M_{W0}^2} + \frac{\delta G_{V,B}}{G_F} \right). \tag{1.71}$$

At $q^2 = 0$ we have

$$G_F \left(1 - \frac{\delta G_F}{G_F} + \frac{A^{WW}(0)}{M_W^2} + \frac{\delta G_{V,B}}{G_F} \right)$$
 (1.72)

By requiring that Eq. (1.72) reduces to G_F one finds

$$\frac{\delta G_F}{G_F} = \frac{A^{WW}(0)}{M_W^2} + \frac{\delta G_{V,B}}{G_F} \,. \tag{1.73}$$

All other derived quantities can be written in terms of the renormalized α , G_F , M_Z , and their counterterms. The renormalized weak mixing angle can be derived as follows

$$\sin^2\theta = \sin^2\theta_0 + \delta\sin^2\theta, \quad \cos^2\theta = \cos^2\theta_0 + \delta\cos^2\theta, \tag{1.74}$$

where

$$\sin^2\theta_0 \cos^2\theta_0 = \frac{\pi\alpha_0}{\sqrt{2}G_{F0}M_{Z0}^2}.$$
 (1.75)

Therefore, one finds

$$\delta \cos^2 \theta = -\delta \sin^2 \theta = \frac{\sin^2 \theta \cos^2 \theta}{\cos^2 \theta - \sin^2 \theta} \left(-\frac{\delta \alpha}{\alpha} + \frac{\delta G_F}{G_F} + \frac{\delta M_Z^2}{M_Z^2} \right), \tag{1.76}$$

where $\sin^2 \theta$ is defined to all orders as

$$\sin^2 \theta = 1 - \cos^2 \theta \equiv \frac{1}{2} \left(1 - \left[1 - \frac{4\pi\alpha}{\sqrt{2}G_F M_Z^2} \right]^{1/2} \right) . \tag{1.77}$$

Equivalently,

$$\sin^2\theta \cos^2\theta = \frac{\pi\alpha}{\sqrt{2}G_F M_Z^2} \quad \text{and} \quad \cos^2\theta = 1 - \sin^2\theta \ . \tag{1.78}$$

The renormalized W mass can be derived from the tree-level relation

$$M_{W0}^2 = \cos^2\theta_0 M_{Z0}^2 \,. \tag{1.79}$$

One finds

$$M_W^2 = M_{W0}^2 + \delta M_W^2 = \cos^2 \theta \,_0 M_{Z0}^2 + \delta M_W^2 = \cos^2 \theta \, M_Z^2 + \delta M_W^2 - \frac{M_Z^2 \cos^2 \theta}{\sin^2 \theta - \cos^2 \theta} \left(\sin^2 \theta \, \frac{\delta \alpha}{\alpha} - \sin^2 \theta \, \frac{\delta G_F}{G_F} - \cos^2 \theta \, \frac{\delta M_Z^2}{M_Z^2} \right) \,. \tag{1.80}$$

By demanding that M_W coincides with the physical (on-shell) mass, the counterterm δM_W^2 is fixed

$$\frac{\delta M_W^2}{M_W^2} = -\frac{A^{WW}(0)}{M_W^2} - F^{WW}(M_W^2). \tag{1.81}$$

In summary, the tree-level (bare) S matrix

$$S_0 = S_0(\alpha_0, G_{F0}, M_{Z0}^2), (1.82)$$

is replaced at one-loop level by a finite physical S matrix

$$S_0 \to S(\alpha, G_F, M_Z^2) + \delta S(\alpha, G_F, M_Z^2, m_t, m_H), \qquad (1.83)$$

where δS encompasses the one-loop corrections and the induced shift in the renormalized quantities. Notice that m_t and m_H only appear in the radiative corrections.

The tree-level amplitude $Z \to f\overline{f}$ can be written as

$$A(e^{-}e^{+} \to Z \to f\overline{f}) = \frac{\sqrt{2}G_{F0}M_{Z0}^{2}}{q^{2} - M_{Z0}^{2}} \overline{v_{e}} \gamma_{\mu} \left(-\frac{1}{2} + 2\sin^{2}\theta_{0} + \gamma_{5}\frac{1}{2}\right) u_{e} \times \overline{v_{f}} \gamma_{\mu} \left(T_{3f} - 2Q_{f}\sin^{2}\theta_{0} - \gamma_{5}T_{3f}\right) u_{f}.$$
(1.84)

Next, I include all the one-loop corrections and the counterterms to the amplitude A. Notice that the photon-Z mixing will also contribute to the amplitude. One finds

$$A(e^{-}e^{+} \rightarrow Z \rightarrow f\overline{f}) = \frac{\sqrt{2}G_{F}M_{Z}^{2}}{q^{2} - M_{Z}^{2}} \left(1 - \frac{\delta G_{F}}{G_{F}} - \frac{\delta M_{Z}^{2}}{M_{Z}^{2}} - F^{ZZ}(M_{Z}^{2}) - \frac{dF^{ZZ}}{dq^{2}}(M_{Z}^{2})\right)$$

$$\overline{v_{e}}\gamma_{\mu} \left(g_{Ve} + \Delta g_{Ve} - \gamma_{5} \left[g_{Ae} + \Delta g_{Ae}\right]\right) u_{e} \times$$

$$\overline{v_{f}}\gamma_{\mu} \left(g_{Vf} + \Delta g_{Vf} - \gamma_{5} \left[g_{Af} + \Delta g_{Af}\right]\right) u_{f}, \qquad (1.85)$$

where to simplify the notation, I defined

$$g_{Vf} = T_{3f} - 2Q_f \sin^2 \theta \,, \quad g_{Af} = T_{3f} \,, \tag{1.86}$$

$$\Delta g_{Vf} = 2Q_f \delta \sin^2 \theta + \delta g_{Vf} - 2Q_f \sin \theta \cos \theta \left(\frac{A^{\gamma Z}(0)}{M_Z^2} + F^{\gamma Z}(M_Z^2) \right) , \qquad (1.87)$$

$$\Delta g_{Af} = \delta g_{Af} \,. \tag{1.88}$$

This result is slightly different from the result given in Ref. [16] by the inclusion of the term $A^{\gamma Z}(0)$ in Eq. (1.87). At one-loop level, fermions do not contribute to $A^{\gamma Z}(0)$, i.e., $A_f^{\gamma Z}(0) = 0$. However, there is a small contribution from the W-boson loop [14].

Determining the amplitude enables us to calculate all physical observables at LEP, namely the partial decay widths, the forward-backward asymmetries, and the polarization measurements A_e and A_τ . The partial-decay widths can be written as follow

$$\Gamma(Z \to f\overline{f}) = \frac{G_F M_Z^3}{6\pi\sqrt{2}} N_C \left(1 - \frac{\delta G_F}{G_F} - \frac{\delta M_Z^2}{M_Z^2} - F^{ZZ}(M_Z^2) - \frac{dF^{ZZ}}{dq^2} (M_Z^2) \right) \times \left([g_{Vf} + \Delta g_{Vf}]^2 + [g_{Af} + \Delta g_{Af}]^2 \right) , \qquad (1.89)$$

where N_C is a color factor, $N_C = 3$ for a quark final state and 1 otherwise. The leptonic forward-backward asymmetry can be written as

$$A_{FB}^{\ell} = \frac{3[g_{A\ell} + \Delta g_{A\ell}]^2 [g_{V\ell} + \Delta g_{V\ell}]^2}{\left([g_{A\ell} + \Delta g_{A\ell}]^2 + [g_{V\ell} + \Delta g_{V\ell}]^2\right)^2} ,$$
 (1.90)

where I have assumed lepton universality in A_{FB}^{ℓ} . In the SM, lepton universality is a valid statement. However, In chapter 5 I will discuss a model, different from the SM, which may break lepton universality. In the following discussion I will continue with the assumption of lepton universality. The e and τ polarization observables A_e and A_{τ} can be written as

$$A_f = \frac{2[g_{Af} + \Delta g_{Af}][g_{Vf} + \Delta g_{Vf}]}{([g_{Af} + \Delta g_{Af}]^2 + [g_{Vf} + \Delta g_{Vf}]^2)},$$
(1.91)

where f stands for e or τ .

If we ignore for the moment the non-oblique corrections to the form-factors Δg_{Vf} and Δg_{Af} ($\delta g_{Vf} = \delta g_{Af} = 0$) then it is clear that only oblique corrections (corrections independent of the fermion flavor) are present. Also, one finds that all LEP observables can be written in terms of three combinations of oblique corrections. The first correction is the one multiplying the partial decay width in Eq. (1.89), namely

$$\left(-\frac{\delta G_F}{G_F} - \frac{\delta M_Z^2}{M_Z^2} - F^{ZZ}(M_Z^2) - \frac{F^{ZZ}}{dq^2}(M_Z^2)\right).$$
(1.92)

The second one is seen clearly from the ratio

$$\frac{\Delta g_{Vf}}{g_{Af}} = 4|Q_f| \left(\delta \sin^2 \theta - \sin \theta \cos \theta \left[\frac{A^{\gamma Z}(0)}{M_Z^2} + F^{\gamma Z}(M_Z^2) \right] \right). \tag{1.93}$$

The third one is given in terms of the W mass, which can be seen clearly from Eq. (1.80). From Eq. (1.80) one can extract the third oblique correction,

$$\frac{M_W^2}{\cos^2\theta M_Z^2} = 1 + \frac{\delta M_W^2}{M_W^2} - \frac{\sin^2\theta}{\sin^2\theta - \cos^2\theta} \left(\frac{\delta\alpha}{\alpha} - \frac{\delta G_F}{G_F} - \frac{\cos^2\theta}{\sin^2\theta} \frac{\delta M_Z^2}{M_Z^2} \right). \tag{1.94}$$

To summarize, ignoring all non-oblique corrections, there are only three combinations of oblique corrections which affect the Z-pole observables.

To include the non-oblique corrections one has to make some general assumptions to make the analysis simple and useful as a model independent tool. Before I do this I consider the measurements of $\Gamma(Z \to \mu^- \mu^+)$, A_{FB}^{μ} , and M_W with the non-oblique corrections included. I combine the term $\Delta g_{A\mu}$ with the oblique correction to the decay width $\Gamma(Z \to \mu^- \mu^+)$ and define the first parameter $\Delta \rho$ where

$$\Delta \rho \equiv -\frac{\delta G_F}{G_F} - \frac{\delta M_Z^2}{M_Z^2} - F^{ZZ}(M_Z^2) - \frac{F^{ZZ}}{dq^2}(M_Z^2) - 4\Delta g_{A\mu}. \tag{1.95}$$

Using the form-factors ratio extracted from A_{FB}^{μ} one finds

$$\frac{g_{V\mu} + \Delta g_{V\mu}}{g_{A\mu} + \Delta g_{A\mu}} = 1 - 4\sin^2\theta - 2\Delta g_{V\mu} + 2(1 - 4\sin^2\theta)\Delta g_{A\mu}. \tag{1.96}$$

I define the second parameter $\Delta k'$ where

$$\frac{g_{V\mu} + \Delta g_{V\mu}}{g_{A\mu} + \Delta g_{A\mu}} \equiv 1 - 4\sin^2\theta \left(1 + \Delta k'\right). \tag{1.97}$$

From which one concludes

$$\Delta k' = \frac{1}{2\sin^2\theta} \left(\Delta g_{V\mu} - (1 - 4\sin^2\theta) \Delta g_{A\mu} \right). \tag{1.98}$$

Using the parameters $\Delta \rho$ and $\Delta k'$ one can write the observables $\Gamma(Z \to \mu^- \mu^+)$ and A_{FB}^{μ} as

$$\Gamma(Z \to \mu^- \mu^+) = \frac{G_F M_Z^3}{24\pi\sqrt{2}} (1 + \Delta\rho) \left(\left[1 - 4\sin^2\theta \left(1 + \Delta k' \right) \right]^2 + 1 \right) , \tag{1.99}$$

$$A_{FB}^{\mu} = \frac{3\left[1 - 4\sin^2\theta \left(1 + \Delta k'\right)\right]^2}{\left(1 + \left[1 - 4\sin^2\theta \left(1 + \Delta k'\right)\right]^2\right)^2} \ . \tag{1.100}$$

It is worth mentioning that one needs to assume only e- μ universality to extract $\Delta k'$ from the forward-backward asymmetries A_{FB}^{μ} . So far there is no need to include the τ letpon in the universality assumption. Finally, using Eq. (1.80) and the expression for $\left(1 - \frac{M_W^2}{M_Z^2}\right) \frac{M_W^2}{M_Z^2}$, I introduce the third parameter Δr_W where

$$\left(1 - \frac{M_W^2}{M_Z^2}\right) \frac{M_W^2}{M_Z^2} \equiv \frac{\pi \alpha(M_Z^2)}{\sqrt{2} G_F M_Z^2 (1 - \Delta r_W)} \,.$$
(1.101)

Using Eq. (1.80) one finds

$$\Delta r_W = \frac{\delta G_F}{G_F} - \frac{\delta \alpha}{\alpha} + \frac{\cos^2 \theta}{\sin^2 \theta} \frac{\delta M_Z^2}{M_Z^2} + \frac{\sin^2 \theta - \cos^2 \theta}{\sin^2 \theta} \frac{\delta M_W^2}{M_W^2}.$$
 (1.102)

One should remember that the term $\delta\alpha/\alpha$ in Eq. (1.102) does not include the light fermions contribution which has been absorbed in $\alpha(M_Z^2)$ as discussed earlier. Notice that in the improved Born approximation (including only the QED corrections) $\Delta\rho$, $\Delta k'$, and Δr_W vanish by definition.

In terms of the one-loop corrections we found earlier one can write explicitly the quantities $\Delta \rho$, Δr_W , and $\Delta k'$ as follow

$$\Delta \rho = \frac{A^{ZZ}(0)}{M_Z^2} - \frac{A^{WW}(0)}{M_W^2} - M_Z^2 \frac{dF^{ZZ}}{dq^2} (M_Z^2) - \frac{\delta G_{V,B}}{G_F} - 4\delta g_{A\ell}, \qquad (1.103)$$

$$\Delta r_{W} = -\frac{\cos^{2}\theta}{\sin^{2}\theta} \left(\frac{A^{ZZ}(0)}{M_{Z}^{2}} - \frac{A^{WW}(0)}{M_{W}^{2}} \right) - \frac{\cos^{2}\theta}{\sin^{2}\theta} F^{ZZ}(M_{Z}^{2}) + F^{\gamma\gamma}(0)$$
$$-\frac{\sin^{2}\theta - \cos^{2}\theta}{\sin^{2}\theta} F^{WW}(M_{W}^{2}) + \frac{2\sin\theta}{\cos\theta} \frac{A^{\gamma Z}(0)}{M_{Z}^{2}} + \frac{\delta G_{V,B}}{G_{F}}, \qquad (1.104)$$

$$\Delta k' = \frac{\cos^2 \theta}{\cos^2 \theta - \sin^2 \theta} \left(\frac{A^{WW}(0)}{M_W^2} - \frac{A^{ZZ}(0)}{M_Z^2} - F^{ZZ}(M_Z^2) + F^{\gamma\gamma}(0) \right) +$$

$$\frac{2 \sin \theta \cos \theta}{\cos^2 \theta - \sin^2 \theta} \frac{A^{\gamma Z}(0)}{M_Z^2} + 2 \sin \theta \cos \theta F^{\gamma Z}(M_Z^2) +$$

$$\frac{\cos^2 \theta}{\cos^2 \theta - \sin^2 \theta} \frac{\delta G_{V,B}}{G_F} + \delta g_{V\ell} - (1 - 4 \sin^2 \theta) \delta g_{A\ell}. \tag{1.105}$$

Now I expand my scope and take a further step into the analysis. The definition of the parameters $\Delta \rho$, Δr_W , and $\Delta k'$ in terms of the physical observables $\Gamma(Z \to \mu^- \mu^+)$, A_{FB}^{μ} , and M_W nominate these parameters to be used as a model independent probe. The parameters $\Delta \rho$, Δr_W , and $\Delta k'$ are equipped to describe radiative corrections due to any model which is identical in its tree-level low energy part to that of the SM. Therefore, I will proceed with this aim in mind.

To include additional observables in the model independent analysis I will make some general assumptions [16, 22, 23]. I start by assuming $e^{-\mu-\tau}$ lepton universality. As mentioned before, lepton universality is a valid statement in the SM. Consequently, all leptonic partial decay widths and forward-backward asymmetries are uniquely determined by $\Delta \rho$ and $\Delta k'$. Similarly for the polarization measurements A_e and A_{τ} . In the case of lepton universality one can use the average lepton measurements $\Gamma(Z \to \ell^- \ell^+)$ and A_{FB}^{ℓ} in defining $\Delta \rho$ and $\Delta k'$. To include the quark measurements, i.e., the hadronic widths and the forward-backward asymmetries, further assumptions are needed. I assume that all relevant deviations from the SM are only contained in the vacuum polarization functions, i.e., through oblique corrections. This may be a reasonable assumption except for the b quark which I handle separately. In the b-quark case, there is a large non-oblique correction to the decay width $\Gamma(Z \to b\bar{b})$ due to vertex diagrams involving the top quark. This correction can not be expressed in terms of the parameters we defined above. Therefore, I follow Refs. [16, 22, 23] by introducing an additional parameter ϵ_b to describe this non-oblique correction. I will discuss this parameter in the next section.

To summarize this section, all precision electroweak observables at the Z pole, under some general assumptions, can be written in terms of four quantities Δr_W , $\Delta \rho$, $\Delta k'$, and ϵ_b (to be discussed below). These quantities can be deduced easily from the experimental measurements $\Gamma(Z \to \ell^- \ell^+)$, A_{FB}^{ℓ} (assuming lepton universality),

 M_W , and $\Gamma(Z \to b\bar{b})$. This result provides a straight-forward method to check for the validity of the theory against the experimental data. The theory under investigation includes a more general set of models and not exclusively the SM. All models which are identical in their low-energy tree-level sectors to that of the SM and only differ by radiative corrections can be included in the model independent analysis. Examples include the Minimal Supersymmetric Standard Model (MSSM), Technicolor (TC) models, multi-Higgs doublets models, etc.

1.4 The ϵ Parameters

From the previous section, we found that all electroweak radiative corrections can be parameterized by a set of four parameters. This result is interesting because one does not need to worry about the whole renormalization procedure any more. To parameterize the electroweak radiative corrections, it is useful to separate different possible effects into different parameters. In other words, to disentangle new physics effects it is very useful to choose the parameters so that some are sensitive to specific types of new physics. In this work where I am interested in the top quark contributions to low energy data, the temptation is high to choose some parameters to be very sensitive to the top quark mass effect.

A well-known parameterization can be implemented to our case based on the scheme used in Refs. [16, 22, 23], where the electroweak radiative corrections can be parameterized by 4 independent parameters, three of those parameters ϵ_1 , ϵ_2 , and ϵ_3 are proportional to the popular T, U, and S parameters [24]. The fourth one; ϵ_b describes the relevant non-oblique corrections to the proper vertex $Z \to b\bar{b}$ [16, 22, 23]. A similar parameterization to ϵ_b is discussed in Ref. [25]. In appendix B, I discuss briefly the S, U, and T parameters. Also, I discuss their relation to the epsilon

parameters.

I write the electroweak precision observables as

$$O_i = O_i|_B \left(1 + \sum_{j=1}^4 a_{ij}\epsilon_j\right),$$
 (1.106)

where, $O_i|_B$ is the corresponding prediction of the theory in the improved Born approximation (i.e., with the QED and QCD corrections). The four dimensionless parameters ϵ_1 , ϵ_2 , ϵ_3 , and ϵ_b contain the genuine electroweak radiative corrections. All dependence on m_t and m_H comes through these parameters. The quantities a_{ij} are fixed numerical constants.

In principle there are many different ways to parameterize the electroweak corrections. In this work, I follow the parameterization in Refs. [16, 22, 23] given in terms of the epsilon parameters. The parameters ϵ_1 , ϵ_2 , ϵ_3 are given in terms of the previously defined parameters $\Delta \rho$, $\Delta k'$, and Δr_W

$$\epsilon_1 = \Delta \rho \,, \tag{1.107}$$

$$\epsilon_2 = \cos^2 \theta \,\Delta \rho + \frac{\sin^2 \theta}{\cos^2 \theta - \sin^2 \theta} \Delta r_W - 2\sin^2 \theta \,\Delta k' \,, \tag{1.108}$$

$$\epsilon_3 = \cos^2 \theta \,\Delta \rho + (\cos^2 \theta \, - \sin^2 \theta) \Delta k' \,. \tag{1.109}$$

For the parameter ϵ_b I write the partial-decay width $Z \to b \bar b$ as follows

$$\Gamma_b = \frac{G_F M_Z^3}{2\pi\sqrt{2}} \left(1 + \Delta\rho\right) \left(\left(g_{Vb}^N\right)^2 + \left(g_{Ab}^N\right)^2 \right) \left(1 + \frac{\alpha(M_Z^2)}{12\pi}\right) R_{QCD}, \tag{1.110}$$

where R_{QCD} is the QCD correction given in Eq. (1.48),

$$R_{QCD} = 1 + \left(\frac{\alpha_s(M_Z^2)}{\pi}\right) - 1.4 \left(\frac{\alpha_s(M_Z^2)}{\pi}\right)^2 - 12.8 \left(\frac{\alpha_s(M_Z^2)}{\pi}\right)^3, \tag{1.111}$$

and α_s is the QCD coupling, $\alpha_s = g_s^2/4\pi$. The quantities g_{Vb}^N and g_{Ab}^N are defined as follow [16, 22]

$$g_{Ab}^{N} = -\frac{1}{2}(1 + \epsilon_b), \qquad (1.112)$$

$$\frac{g_{Vb}^{N}}{g_{Ab}^{N}} = \frac{1 - 4/3(1 + \Delta k')\sin^{2}\theta + \epsilon_{b}}{1 + \epsilon_{b}}.$$
(1.113)

One should notice that Eqs. (1.112) and (1.113) are just auxiliary equations. So far they do not mean that relevant physics is only coming through the b_L - $\overline{b_L}$ -Z vertex. In fact, from Eq. (1.110), the correct assumption is that relevant physics will modify the decay width Γ_b . To put it differently, the combination of relevant physics to both the b_L - $\overline{b_L}$ -Z and b_R - $\overline{b_R}$ -Z vertices which contributes to Γ_b is simply parameterized by ϵ_b (cf. Eq. (1.124)). However, if one is interested in other observables, e.g., A_b (see below), then an additional assumption is needed. The assumption is that the only relevant new physics is coming through the b_L - $\overline{b_L}$ -Z vertex. The reason is simply that another combination of the neutral left- and right-handed b quark couplings will enter these observables. I will adopt this assumption since the observable A_b is not sensitive to the top quark mass (see Eq. (1.141)) and also it does not show a deviation from the SM (see Table 1.2).

In terms of the one-loop corrections we found for the parameters $\Delta \rho$, Δr_W , and $\Delta k'$, one can write the parameters ϵ_1 , ϵ_2 , and ϵ_3 as follow

$$\epsilon_1 = e_1 - e_5 - \frac{\delta G_{V,B}}{G_F} - 4\delta g_{A\ell}, \qquad (1.114)$$

$$\epsilon_2 = e_2 - \sin^2 \theta \, e_4 - \cos^2 \theta \, e_5 - \frac{2 \sin \theta}{\cos \theta} \, e_6 - \frac{\delta G_{V,B}}{G_F} - \delta g_{V\ell} - 3\delta g_{A\ell} \,,$$
 (1.115)

$$\epsilon_{3} = e_{3} + \cos^{2}\theta \, e_{4} - \cos^{2}\theta \, e_{5} + \frac{\cos\theta}{\sin\theta} \, e_{6} + \frac{\cos^{2}\theta \, - \sin^{2}\theta}{2\sin^{2}\theta} \delta g_{V\ell} - \frac{1 + 2\sin^{2}\theta}{2\sin^{2}\theta} \delta g_{A\ell} \, . (1.116)$$

Here I define the following quantities

$$e_1 = \frac{A^{ZZ}(0)}{M_Z^2} - \frac{A^{WW}(0)}{M_W^2} \,, \tag{1.117}$$

$$e_2 = F^{WW}(M_W^2) - F^{33}(M_Z^2),$$
 (1.118)

$$e_3 = \frac{\cos \theta}{\sin \theta} F^{30}(M_Z^2) \,, \tag{1.119}$$

$$e_4 = F^{\gamma\gamma}(0) - F^{\gamma\gamma}(M_Z^2), \qquad (1.120)$$

$$e_5 = M_Z^2 \frac{dF^{ZZ}}{dq^2} (M_Z^2) , (1.121)$$

$$e_6 = \frac{A^{\gamma Z}(0)}{M_Z^2} \,. \tag{1.122}$$

For the parameter ϵ_b , I write the one-loop corrections to the vector- and axialform factors δg_{Vb} and δg_{Ab} , which are due to proper vertex diagrams and b-quark self energy, as

$$\delta g_{Vb} = -\frac{1}{2} (e_b + \delta g_{Vd}), \quad \delta g_{Ab} = -\frac{1}{2} (e_b + \delta g_{Ad}).$$
 (1.123)

In Eq. (1.123) I split the corrections to δg_{Vb} and δg_{Ab} into two parts, the first part e_b encompass all non-oblique corrections due to the top quark mass. (Notice that the relevant m_t corrections are only in the left-handed current.) The second part includes the vector and axial-vector corrections independent of the top quark mass g_{Vd} and g_{Ad} , which are identical, in the SM, to the d-quark vertex corrections. Calculating the Γ_b decay width using Eq. (1.89) and comparing with Eq. (1.110) one finds

$$\epsilon_b = e_b + \frac{1}{2 - \frac{4}{3}\sin^2\theta} \left[\left(1 - \frac{4}{3}\sin^2\theta \right) \delta g_{Vd} + \delta g_{Ad} \right] + \frac{1}{2 - \frac{4}{3}\sin^2\theta} \left[\frac{2}{3} \left(1 - \frac{4}{3}\sin^2\theta \right) \delta g_{V\ell} - \frac{2}{3} \left(-5 + \frac{8}{3}\sin^2\theta \right) \delta g_{A\ell} \right]. \tag{1.124}$$

Note that the parameters ϵ_1 , ϵ_2 , ϵ_3 , and ϵ_b can be written in terms of the basic measurements $\Gamma_{\mu} = \Gamma(Z \to \mu^{-}\mu^{+})$, A_{FB}^{μ} , M_{W} , and Γ_{b} . To do this let us first rewrite the parameters $\Delta \rho$, Δr_{W} , and $\Delta k'$ in terms of ϵ_1 , ϵ_2 , and ϵ_3 . Using Eqs. (1.107)–(1.109) one finds

$$\Delta \rho = \epsilon_1 \,, \tag{1.125}$$

$$\Delta r_W = -\frac{\cos^2 \theta}{\sin^2 \theta} \,\epsilon_1 + \frac{\cos^2 \theta - \sin^2 \theta}{\sin^2 \theta} \,\epsilon_2 + 2 \,\epsilon_3 \,, \tag{1.126}$$

$$\Delta k' = \frac{1}{\cos^2 \theta - \sin^2 \theta} \left(\epsilon_3 - \cos^2 \theta \ \epsilon_1 \right) . \tag{1.127}$$

Using Eqs. (1.99)–(1.101) and (1.110) one finds

$$\Gamma_{\mu} = \Gamma_{\mu}|_{B} (1 + 1.20\epsilon_{1} - 0.26\epsilon_{3}) ,$$
 (1.128)

$$A_{FB}^{\mu} = A_{FB}^{\mu}|_{B} \left(1 + 34.60\epsilon_{1} - 45.00\epsilon_{3}\right), \tag{1.129}$$

$$\frac{M_W^2}{M_Z^2} = \left(\frac{M_W^2}{M_Z^2}\right)|_B \left(1 + 1.43\epsilon_1 - 1.00\epsilon_2 - 0.86\epsilon_3\right) , \qquad (1.130)$$

$$\Gamma_b = \Gamma_b|_B (1 + 1.41\epsilon_1 - 0.54\epsilon_3 + 2.93\epsilon_b) ,$$
 (1.131)

where $O|_B$ stands for the observable O in the improved Born approximation (including the QED and QCD corrections only). Other observables can be written in terms of the epsilon parameters [26] as long as they satisfy the conditions we mentioned before.

• The charged leptonic decays will be identical to Γ_{μ} as long as lepton universality is satisfied. In this case, one can use the average leptonic decay width Γ_{ℓ} . Similarly for the leptonic forward-backward asymmetries A_{FB}^{ℓ} .

• The polarization measurements A_{ϵ} and A_{τ} are identical, assuming leptonic universality, where

$$A_{\epsilon} = 2 \frac{\left(g_{V\epsilon} + \Delta g_{V\epsilon}\right) \left(g_{A\epsilon} + \Delta g_{A\epsilon}\right)}{\left(g_{V\epsilon} + \Delta g_{V\epsilon}\right)^2 + \left(g_{A\epsilon} + \Delta g_{A\epsilon}\right)^2} . \tag{1.132}$$

One finds

$$A_{\epsilon} = A_{\tau} = A_{\epsilon}|_{B} (1 + 17.3\epsilon_{1} - 22.5\epsilon_{3}) . \tag{1.133}$$

• The observable A_{LR} is measured at SLC using polarized initial e^-e^+ beam and at the Z peak. Under the general assumptions I mentioned before, the observables A_e at LEP and A_{LR} at SLC measure the same quantity, i.e.,

$$A_{LR} = 2 \frac{(g_{Ve} + \Delta g_{Ve})(g_{Ae} + \Delta g_{Ae})}{(g_{Ve} + \Delta g_{Ve})^2 + (g_{Ae} + \Delta g_{Ae})^2} = A_e.$$
 (1.134)

Thus, one simply has

$$A_{LR} = A_e = A_e|_B (1 + 17.3\epsilon_1 - 22.5\epsilon_3) . (1.135)$$

• The total decay width of the Z boson Γ_Z

$$\Gamma_Z = \Gamma_Z|_B (1 + 1.35\epsilon_1 - 0.46\epsilon_3 + 0.35\epsilon_b) . \tag{1.136}$$

• The observable $R_{\ell} = \Gamma_h/\Gamma_{\ell}$, the ratio of the partial widths $Z \to \text{hadrons}$ and $Z \to \ell^- \ell^+$,

$$R_{\ell} = R_{\ell}|_{B} \left(1 + 0.28\epsilon_{1} - 0.36\epsilon_{3} + 0.50\epsilon_{b}\right). \tag{1.137}$$

• For the hadronic peak cross-section σ_h , where

$$\sigma_h = \frac{12\pi\Gamma_e\Gamma_h}{M_Z^2\Gamma_Z^2},\tag{1.138}$$

one finds

$$\sigma_h = \sigma_h|_B \left(1 + 0.03\epsilon_1 - 0.04\epsilon_3 + 0.20\epsilon_b\right). \tag{1.139}$$

• The observable $R_b = \Gamma_b/\Gamma_h$, the ratio of the partial widths $Z \to b \, \bar{b}$ and $Z \to hadrons$,

$$R_b = R_b|_B \left(1 + 0.06\epsilon_1 - 0.07\epsilon_3 + 1.79\epsilon_b\right). \tag{1.140}$$

• For the polarization measurement of A_b (at SLC), the dependence on the non-oblique corrections is not exactly given by ϵ_b (see Eq. (1.124)). Nevertheless, with the assumption that the relevant effect enters through e_b one can ignore the other contributions, i.e., δg_{Vd} and δg_{Ad} defined in Eq. (1.123). In this case, one finds

$$A_b = A_b|_B (1 + 0.23\epsilon_1 - 0.29\epsilon_3 + 0.16\epsilon_b) . {(1.141)}$$

• The polarization measurement of A_c (at SLC)

$$A_c = A_c|_B (1 + 1.71\epsilon_1 - 2.22\epsilon_3) . (1.142)$$

• The b-quark forward-backward asymmetry A_{FB}^{b}

$$A_{FB}^{b} = A_{FB}^{b}|_{B} (1 + 17.53\epsilon_{1} - 22.80\epsilon_{3} + 0.16\epsilon_{b}) . \tag{1.143}$$

• The c-quark forward-backward asymmetry A_{FB}^{c}

$$A_{FB}^{c} = A_{FB}^{c}|_{B} (1 + 19.01\epsilon_{1} - 24.72\epsilon_{3}) . {(1.144)}$$

• Finally, the measurement of $R_c = \Gamma_c/\Gamma_h$, the ratio of the partial widths $Z \to c\bar{c}$ and $Z \to \text{hadrons}$,

$$R_c = R_c|_B (1 + 0.116\epsilon_1 - 0.151\epsilon_3 - 0.5\epsilon_b) . {(1.145)}$$

Therefore, using the above equations and the low energy experimental data, one can fit the parameters ϵ_1 , ϵ_2 , ϵ_3 , and ϵ_b . A direct comparison with the theory is possible by calculating the theoretical values of these parameters and then comparing with the extracted experimental values.

1.5 The SM Heavy m_t and m_H Contributions to the Low-Energy Data

The important property of the epsilon parameters is that, for all observables at the Z pole, the whole dependence on m_t and m_H enters only through these parameters. Therefore, to calculate the m_t and m_H contributions to the low energy data it is enough to calculate their contributions to ϵ_1 , ϵ_2 , ϵ_3 , and ϵ_b . In this section, I treat the top quark mass m_t and the Higgs boson mass m_H as heavy mass scales and calculate their contributions at one-loop level to ϵ_1 , ϵ_2 , ϵ_3 , and ϵ_b in the SM. Using the heavy mass expansion (discussed in appendix C) and keeping only the leading contributions of m_t and m_H I determine their contributions to the epsilon parameters.

1.5.1 Heavy Top Quark Contributions

In this case, only the vacuum polarization functions and the quantity e_b are sensitive to the top quark mass (see Figure 1.5). One can perform the calculations in any gauge, since the result is gauge invariant. I use dimensional regularization and define

$$\Delta = -\frac{2}{n-4} - \gamma - \ln 4\pi \,, \tag{1.146}$$

where n is the space-time dimension and $\gamma = 0.577...$ is the Euler's constant. I keep only the leading contributions of m_t .

• For the photon

$$A^{\gamma\gamma}(0) = 0, \qquad (1.147)$$

$$F^{\gamma\gamma}(M_Z^2) = \frac{g^2}{16\pi^2} \frac{16\sin^2\theta}{9} \left(\Delta - \ln m_t^2\right) \,. \tag{1.148}$$

• For the Z boson

$$A^{ZZ}(0) = -\frac{g^2}{16\pi^2} \frac{3m_t^2}{2\cos^2\theta} \left(\Delta - \ln m_t^2\right) , \qquad (1.149)$$

$$F^{ZZ}(M_Z^2) = \frac{g^2}{16\pi^2} \frac{1}{\cos^2 \theta} \left(\frac{1}{2} - \frac{4}{3} \sin^2 \theta + \frac{16}{9} \sin^4 \theta \right) \left(\Delta - \ln m_t^2 \right). \tag{1.150}$$

 \bullet For the W boson

$$A^{WW}(0) = \frac{g^2}{16\pi^2} \frac{3m_t^2}{2} \left(-\Delta - \frac{1}{2} + \ln m_t^2 \right) , \qquad (1.151)$$

$$F^{WW}(M_Z^2) = \frac{g^2}{16\pi^2} \left(\Delta - \ln m_t^2 \right) \,. \tag{1.152}$$

• For the γ -Z mixing

$$A^{\gamma Z}(0) = 0, (1.153)$$

$$F^{\gamma Z}(M_Z^2) = \frac{g^2}{16\pi^2} \frac{4\sin\theta}{3\cos\theta} \left(\frac{1}{2} - \frac{4}{3}\sin^2\theta\right) \left(\Delta - \ln m_t^2\right). \tag{1.154}$$

• For the proper vertex e_b

$$e_b = -\frac{g^2}{16\pi^2} \frac{m_t^2}{2M_W^2} \,. \tag{1.155}$$

Therefore, we find

$$\epsilon_1 = \Delta \rho = \frac{A^{ZZ}(0)}{M_Z^2} - \frac{A^{WW}(0)}{M_W^2} = \frac{g^2}{16\pi^2} \frac{3m_t^2}{4M_W^2} = \frac{3G_F m_t^2}{8\sqrt{2}\pi^2},\tag{1.156}$$

$$\epsilon_2 = F^{WW}(M_W^2) - F^{33}(M_Z^2) = -\frac{G_F M_W^2}{4\sqrt{2}\pi^2} \ln(m_t^2), \qquad (1.157)$$

$$\epsilon_3 = \frac{\cos \theta}{\sin \theta} F^{30}(M_Z^2) = -\frac{G_F M_W^2}{12\sqrt{2}\pi^2} \ln(m_t^2) , \qquad (1.158)$$

$$\epsilon_b = -\frac{G_F m_t^2}{4\sqrt{2}\pi^2}.\tag{1.159}$$

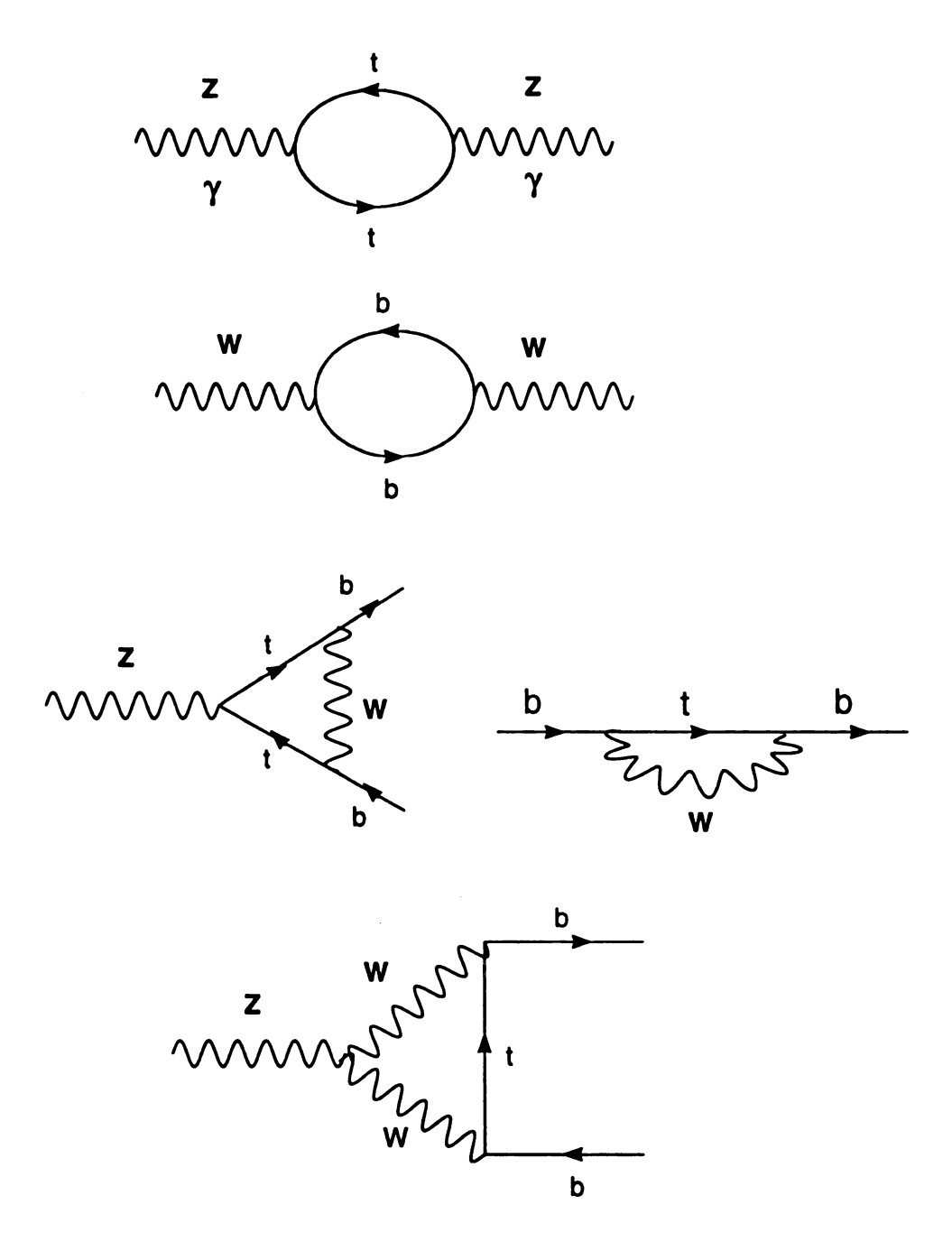


Figure 1.5: The top quark contribution to the epsilon parameters, at the one-loop level.

1.5.2 Heavy Higgs Boson Contributions

For the heavy Higgs boson case, I calculate the vacuum polarization functions to the leading order in m_H (see Figure 1.6). Due to the screening theorem [27], at one-loop level, the leading dependence on the heavy Higgs boson mass in low energy physical observables can be at most a logarithmic dependence. All vertex corrections are negligible because of the small light fermions masses.

- At tree level, the Higgs boson does not couple to the photon. Thus, the Higgs boson does not contribute to $A^{\gamma\gamma}(0)$ and $F^{\gamma\gamma}(M_Z^2)$ up to one loop. Similarly, there is no contribution to $A^{\gamma Z}(0)$ and $F^{\gamma Z}(M_Z^2)$.
- For the Z boson

$$A^{ZZ}(0) = \frac{g^2}{16\pi^2 \cos^2 \theta} \left(-\frac{m_H^2}{8} - \frac{3}{4} M_Z^2 \ln(m_H^2) \right) , \qquad (1.160)$$

$$F^{ZZ}(M_Z^2) = -\frac{g^2}{16\pi^2 \cos^2 \theta} \left(\frac{\ln(m_H^2)}{12} \right) . \tag{1.161}$$

• For the W boson

$$A^{WW}(0) = \frac{g^2}{16\pi^2} \left(-\frac{m_H^2}{8} - \frac{3}{4} M_W^2 \ln(m_H^2) \right) , \qquad (1.162)$$

$$F^{WW}(M_Z^2) = -\frac{g^2}{16\pi^2} \left(\frac{\ln(m_H^2)}{12}\right). \tag{1.163}$$

Therefore, one finds

$$\epsilon_1 = \Delta \rho = \frac{A^{ZZ}(0)}{M_Z^2} - \frac{A^{WW}(0)}{M_W^2} = -\frac{3G_F M_W^2 \sin^2 \theta}{8\sqrt{2}\pi^2 \cos^2 \theta} \ln(m_H^2), \qquad (1.164)$$

$$\epsilon_2 = F^{WW}(M_W^2) - F^{33}(M_Z^2) = 0,$$
(1.165)

$$\epsilon_3 = \frac{\cos \theta}{\sin \theta} F_{30}(M_Z^2) = \frac{G_F M_W^2}{24\sqrt{2}\pi^2} \ln(m_H^2). \tag{1.166}$$

The parameter ϵ_b is not sensitive to the Higgs boson mass because the Higgs boson couples to the b quark with a coupling strength proportional to the b-quark mass m_b (Yukawa coupling). In fact, in the limit of ignoring the bottom quark mass m_b , the Higgs boson contribution to ϵ_b vanishes.

1.6 Status of the SM

In general, precision tests performed at LEP, SLC, and the Tevatron have confirmed to a large accuracy the SM predictions. One-loop and even in some cases two-loop corrections to the SM have been implemented and checked against the low energy data [26, 28, 29]. Using the input values in Table 1.1, the SM predictions for the low energy physical observables have been calculated [30]. In Table 1.2, I tabulate the new data [12] and the corresponding SM predictions [30]. The SM predictions are calculated for two values of $\alpha_s(M_Z^2)$, 0.125 and 0.115, respectively. The top quark and Higgs boson masses used in the SM predictions are $m_t = 175$ GeV and $m_H = 300$ GeV, respectively. The only sensitive measurements for $\alpha_s(M_Z^2)$ are the total Z decay width Γ_Z , the ratio $R_\ell = \Gamma_h/\Gamma_\ell$, and the hadronic peak cross-section σ_h (see Eq. (1.138).

With all the accumulated success of the SM, there are only a few hints of possible deviations from the SM that have been reported recently. Among those measurements are: the LEP observation of a small excess in the measurement $R_b = \Gamma_b/\Gamma_h$, the ratio of the partial widths $Z \to b\bar{b}$ and $Z \to hadrons$, of about 3.5 σ [12]. Also at LEP there is the measurement of $R_c = \Gamma_c/\Gamma_h$, ratio of the partial widths $Z \to c\bar{c}$ and $Z \to hadrons$, with a deficit of about 2.5 σ [12]. At the SLC, a deviation from the SM has been seen in the measurement of A_{LR} of about 2.8 σ [31]. At the Tevatron, an

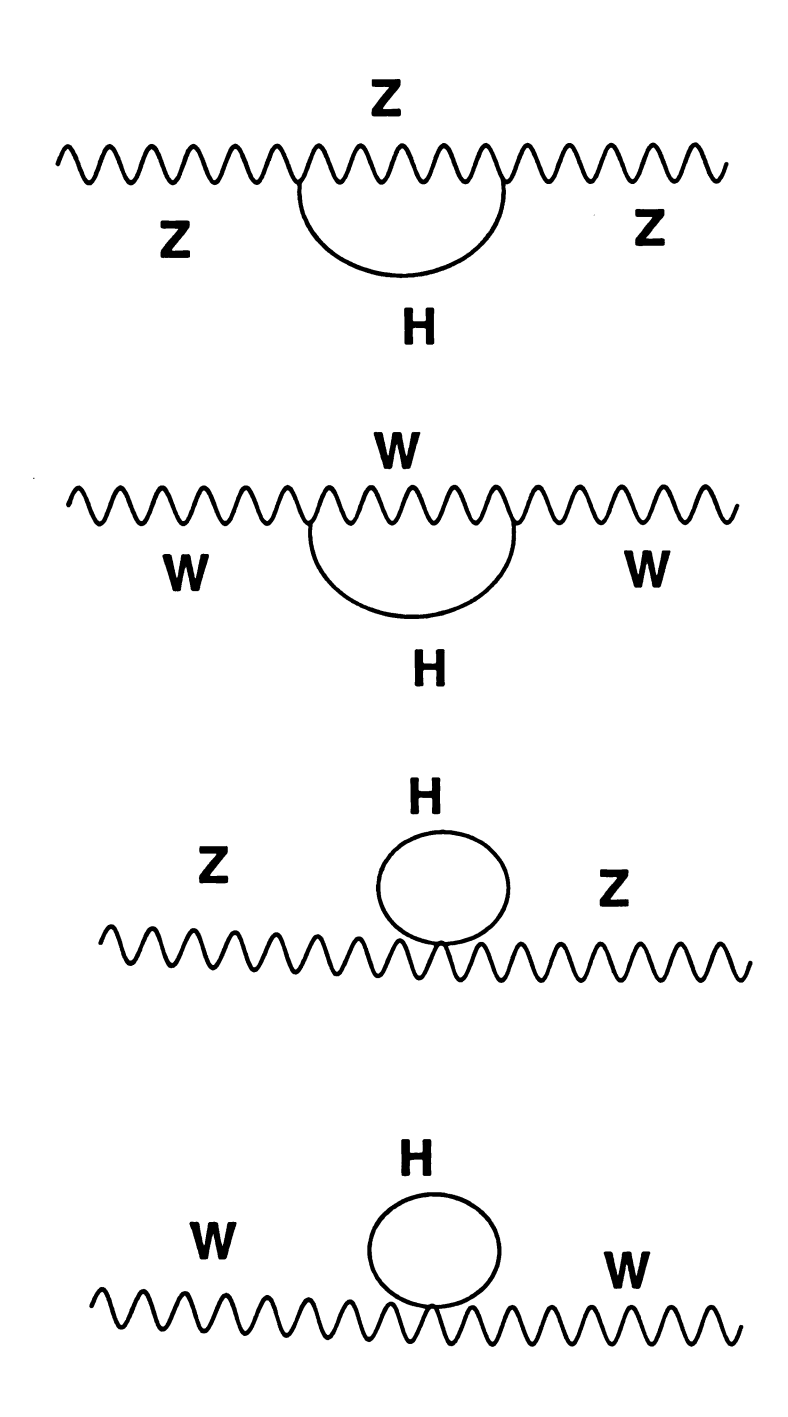


Figure 1.6: The Higgs boson contribution to the epsilon parameters, at the one-loop level.

excess of large E_t jets has been reported [32]. Finally, there is the issue of the QCD coupling $\alpha_s(M_Z^2)$ [33]. From the LEP electroweak fit at the Z pole, the extracted value for the QCD coupling is $\alpha_s(M_Z^2) = 0.125 \pm 0.004$ [12]. The LEP and SLC combined fit gives $\alpha_s(M_Z^2) = 0.123 \pm 0.004$ [12]. These fits are not consistent with the evolved value $\alpha_s(M_Z^2) \sim 0.11$ coming from the measured α_s at $|q^2| \ll M_Z^2$ in deep inelastic scattering (DIS) [9], or with the value of $\alpha_s \sim 0.115$ from lattice QCD [9]. As it is argued by Shifman [34], the tendency of lower values of $\alpha_s(M_Z^2)$; determined form low energy observables, as compared to the higher values of $\alpha_s(M_Z^2)$; measured at LEP and SLC, presents a serious discrepancy that could be a signal for new physics.

The new LEP and SLC data show some interesting features which did not manifest themselves in the old reported LEP and SLC data (before the summer of 1995) [35]. In fact, by the time I started this work the new data was not available. The old data reported an excess of about 2.0σ in R_b . No significant deviation in R_c was observed then (within 1.0σ). All other measurements like $R_{\ell} = \Gamma_h/\Gamma_{\ell}$, A_{FB}^{ℓ} , A_c , A_{τ} , Γ_h , A_b , A_c , and A_{LR} where consistent with the SM.

As I discussed in the previous sections, based on a few general assumptions, all low energy data at LEP, SLC, and the Tevatron measurement of M_W can be expressed in terms of 4-independent parameters ϵ_1 , ϵ_2 , ϵ_3 , and ϵ_b . The assumptions made are that new physics appear in the vacuum polarization functions and/or the $Z \to b\bar{b}$ vertex. The epsilon parameters contain the genuine electroweak corrections including the top quark and the Higgs boson contributions. Unfortunately, in defining the ϵ parameters no relevant new physics in the observable Γ_c is assumed. Given the above assumptions in defining the ϵ parameters, the reported anomaly in $R_c = \Gamma_c/\Gamma_h$ has a very small dependence on ϵ_b [see Eq. (1.145)] which cannot explain the large deficit in R_c . Therefore, to use the ϵ parameters one has to ignore the anomaly in R_c . In fact, as argued by Shifman [33], the size of the anomaly in R_c cannot be given by any

perturbative physics.

Using the leptonic data, i.e., Γ_{ℓ} and the asymmetries combined with the W mass, the fit of ϵ_1 and ϵ_3 shows interesting features [36]: the good agreement with the SM, the evidence for weak corrections, and the preference for a light Higgs boson. Lighter Higgs boson implies lighter top quark mass. Including the hadronic data (except R_c) does not alter the correlation between ϵ_1 and ϵ_3 . However, the fitted ϵ_b is departed from the SM by about 2σ . Therefore, the conclusion is that, by ignoring the anomaly in R_c , the SM predictions for ϵ_1 , ϵ_2 , and ϵ_3 , are in good agreement with the fitted experimental values. However, the SM prediction for ϵ_b is not consistent with the low energy data at the 2σ level.

The electroweak data can be used to predict quantities like the top quark mass, the W mass, the Higgs boson mass, and $\alpha_s(M_Z^2)$. The new data predicts the top quark mass to be [12]

$$m_t = 170 \pm 10 \pm 19 \tag{1.167}$$

where the central value and the first error refer to $m_H = 300$ GeV. The second error corresponds to the variation of the central value when varying m_H in the interval $60 \text{ GeV} \leq m_H \leq 1000 \text{ GeV}$. This is consistent with the top quark mass reported from the observation of the top quark at the Tevatron by CDF [10] and DØ [11].

Up to one loop, the Higgs boson contribution to the low energy observables can be at most a logarithmic contribution [27]. This makes the determination of m_H more difficult than m_t . Also, because the effects of m_t and m_H are correlated, the determination of m_H is more difficult without a precise measurement of m_t . Electroweak precision tests show a preference for a light Higgs boson [6, 36]. However, as argued in Ref. [37], LEP precision data, upon excluding the observables R_b and R_c , does not imply a strong bound on the Higgs bosons mass, i.e., m_H can still be as large as 1

TeV.

If one takes the new discrepancies seriously, i.e., is not mere statistics, then one needs to understand the sources of these anomalies. Before the announcement of the new data, the observed anomaly in R_b in the old data, has triggered the hope to detect new physics. In fact, it was observed [34, 38] that if there was new physics in R_b then the LEP fit of $\alpha_s(M_Z^2)$ would go down to $\alpha_s(M_Z^2) \sim 0.11$ in better agreement with the DIS and QCD values of $\alpha_s(M_Z^2)$. With the inclusion of the new data, the need for new physics is indeed more apparent. In fact, as discussed below, many attempts have been made to explain the observed anomalies. Even though my work is not completely oriented toward explaining these anomalies, part of it is. In the next chapter I will discuss my general motivations for launching into this work. Below, I will mention briefly mine and other's efforts to understand these deviations.

If we assume that the reported anomalies are not mere statistics, then we can advocate specific types of new physics which can tackle these experimental anomalies. The problem is that the anomalies reported recently as a whole represent a confusing picture. The argument given [36] is as follows: The measurement of Γ_h at the Z pole is precise with uncertainty of about ± 3 MeV. However, the access in Γ_b by 11 MeV and the deficit in Γ_c by 32 MeV amounts to a deficit in the sum $\Gamma_b + \Gamma_c$, which enters the hadronic width Γ_h , by 21 MeV. This deficit is far too large compared with the accuracy of the measurement of Γ_h . Even with the inclusion of the ambiguity of α_s , coming from the M_Z scale or the DIS physics, $\delta \alpha_s = \pm 0.007$ which corresponds to ± 4 MeV shift in Γ_h , the total shift in Γ_h does not amount to that of $\Gamma_b + \Gamma_c$. Therefore, a shift in the partial decay widths of the light quarks is needed. This shift must be tuned up to account for the accuracy of Γ_h . The problem then is how to produce the shifts seen in R_b and R_c while not affecting other precise data, especially that of the leptonic sector. This is not a trivial task and I think building a natural model to cure

all these anomalies altogether is extremely difficult (ad hoc).

One possibility to explain the anomaly in R_b is through the top quark. As I discussed in section 1.4, the decay width Γ_b has a strong dependence on the top quark mass. Therefore, assuming the top quark couplings to the gauge bosons [39, 40, 41] are different from the SM may be a plausible explanation to the anomaly in R_b . In chapter 3, I will discuss in detail a general treatment for studying the anomalous top quark couplings from the low energy data using a model independent analysis. Unfortunately, such a scenario can not accommodate the anomaly in R_c because, in the general model discussed in chapter 3, there is no mechanism to affect the charm couplings through the top quark.

In chapter 5, I discuss a special model in which the third generation of fermions undergoes a different SU(2) interaction from the first two generation of fermions. The SU(2) symmetry associated with the third generation exhibits a strong flavor dynamics which leads to a modification in the Z-boson couplings to the fermions (as compared to the SM). Nevertheless, due to the accuracy of LEP data the constraints on the free parameters of the model are so severe that this model can account for the deviation in R_b from the SM at the 3σ level. Even though R_c is shifted in the needed direction, the predicted value is still outside the 2σ range of the data. Therefore, one cannot explain the anomaly in R_c entirely based on this proposed model. By the time this part of my work was going through a final revision, a similar model was proposed in Ref. [42]. Also, I have become aware of another similar model discussed before [43].

Other efforts to explain these anomalies have been done by many theorists. The reported anomalies can not be understood within the fully MSSM [44, 45]. According to Ref. [44], the MSSM with additional high energy scale effects may be a suitable candidate to explain the observed anomalies in the data. A fit on $\alpha_s(M_Z^2) = 0.116$

with large R_b and large A_{LR} can be achieved. However, such a model predicts light superpartners below 100 GeV, a result which may rule out such a model if light superpartners are not found at LEP2 and FNAL. In Ref. [45] a SUSY model with four generations is proposed to explain R_b while ignoring the problem of R_c . In Ref. [46], a composite model of a forth heavy fermion family has been assumed. The model can explain the anomaly in R_b but not the anomaly in R_c . A common feature among these models is that they all predict some light particles with masses around the M_W scale. Such models may be ruled out if nothing is observed at LEP-II and at the Tevatron.

As it is argued in Refs. [43, 47], non-commuting extended technicolor (ETC) is a possible candidate to give rise to a large R_b which is consistent with the data. Other efforts are oriented towards the inclusion of an extra Z' gauge boson [48, 49, 50]. Some of these models seem to explain the R_b anomaly but not R_c . In Ref. [49] an extra Z' is coupled to the third family through an additional U(1) gauge symmetry. This model may explain the anomaly in R_b and in $\alpha_s(M_Z^2)$. Other authors [50] claim to explain the R_b anomaly, $\alpha_s(M_Z^2)$, and R_c on the expense of building ad hoc models.

The anomaly in the SLC measurement of A_{LR} is difficult to realize because LEP measures a similar quantity A_{ϵ} which is in a very excellent agreement with the SM. In fact, in the SM and in many other extensions the two observables are identical. It is true that the two measurements refer to different observables, nevertheless, it is hard to imagine new physics which would affect one and not the other. In Ref. [51], the authors discuss the possibility of new physics which would reconcile the measurements of A_{LR} and A_{ϵ} . They conclude that the only possible way to reconcile the two measurements is through an additional Z' boson coupled almost exclusively to quarks and with a mass almost degenerate with the Z boson mass. They also conclude that the Z' must have an almost vanishing coupling to the leptons.

Table 1.1: The input parameters used to calculate the SM predictions in Table 1.2.

Input	Value	
$\alpha_s(M_Z^2)$	a: 0.125	
	b: 0.115	
$\alpha(M_Z^2)$	128.89(9)	
M_Z	91.1885(22) GeV	
G_F	$1.166389(22) \times 10^{-5} \mathrm{GeV}^-$	
$\sin^2 \theta$	0.2312(3)	
m_t	175 GeV	
m_H	300 GeV	

Summarizing this section [30, 36],

- The precision electroweak experiments at LEP and SLC test the SM predictions at a few times 10⁻³. A need for electroweak corrections is demonstrated.
- All data agree well with the predictions of the SM except for R_b which shows an access of about 3.5σ, R_c which shows a deficit of about 2.5σ, and A_{LR} with a deviation of about 2.8σ. Combining the two data R_b and R_c alone rule out the SM at 99.99% confidence level (C.L.) for m_t > 170 GeV [30]. (i.e., a lower m_t is preferred.)
- There are many different scenarios which can explain the access in R_b . So far, it is not possible to understand the anomaly in R_c , it may even be beyond the perturbative region [33]. It is also extremely difficult to understand the anomaly in A_{LR} .

Table 1.2: Experimental and predicted values of electroweak observables for the SM. The SM predictions are calculated using the input values in Table 1.1. Columns a and b are for $\alpha_s = 0.125$ and 0.115, respectively.

Observables	Experimental data	SM	
		a	b
LEP			
g _{Ve}	-0.0368 ± 0.0017	-0.0367	-0.0367
g _{Ae}	-0.50115 ± 0.00052	-0.5012	-0.5012
$g_{V\mu}/g_{Ve}$	1.01 ± 0.14	1.00	1.00
$g_{A\mu}/g_{Ae}$	1.0000 ± 0.0018	1.0000	1.0000
$g_{V\tau}/g_{Ve}$	1.008 ± 0.071	1.000	1.000
$g_{A\tau}/g_{Ae}$	1.0007 ± 0.0020	1.0000	1.0000
$\Gamma_{oldsymbol{Z}}$	2.4963 ± 0.0032	2.4978	2.4922
R_e	20.797 ± 0.058	20.784	20.716
R_{μ}	20.796 ± 0.043	20.784	20.716
$R_{ au}$	20.813 ± 0.061	20.831	20.716
σ_h^0	41.488 ± 0.078	41.437	41.490
A _e	0.1390 ± 0.0089	0.1439	0.1439
$A_{ au}$	0.1418 ± 0.0075	0.1439	0.1439
A_{ϵ}^{FB}	0.0157 ± 0.0028	0.0157	0.0157
A_e^{FB} A_μ^{FB} A_τ^{FB}	0.0163 ± 0.0016	0.0157	0.0157
A_{τ}^{FB}	0.0206 ± 0.0023	0.0157	0.0157
$R_{\mathbf{b}}$	0.2219 ± 0.0017	0.2157	0.2157
R_c	0.1543 ± 0.0074	0.1721	0.1721
SLC			
A_{LR}	0.1551 ± 0.0040	0.1439	0.1439
R_{b}	0.2171 ± 0.0054	0.2157	0.2157
A_b	0.841 ± 0.053	0.934	0.934
$A_{\mathbf{c}}$	0.606 ± 0.090	0.666	0.666
Tevatron			
M_{W}	80.26 ± 0.16	80.32	80.32

Chapter 2

The Chiral Lagrangian

2.1 Physics Beyond the SM

As I discussed in chapter 1, the SM has proven to be very successful in accommodating all precision measurements available so far; with the exception of a few observables. Among those observables are R_b and R_c at LEP with deviations of about 3.5 σ and 2.5 σ , respectively [12]. Also at the SLC there is the A_{LR} measurement with a deviation of about 2.8σ [31]. At the Tevatron there is the observation of an excess of large E_t jets [32]. Despite the success of the SM as a whole, there are two main points regarding the SM one should bear in mind. The first point is that some parts of the SM remain untested, examples include the top quark interactions with the electroweak gauge bosons which is the main theme of this work. It is only recently that the first direct observation of the top quark has been made [10, 11]. With a top quark mass much larger than the Z mass, physics of the top quark is still premature. In chapter 3, I will discuss in detail the possibility of anomalous top quark couplings to the gauge bosons. A second example is the study of the gauge boson self-interactions [52]. The current available energy at LEP which is around the Z-mass scale, does not permit a direct test on the gauge boson self-interactions. It is only through radiative corrections that such couplings can be examined. There has been several attempts to study the $SU(2)_L \times U(1)_Y$ gauge structure using the low energy data at LEP/SLC and other low energy data [25, 53, 78]. With the upgrade collider LEP-II with an energy of about twice the Z mass, a direct test will be available in the future [54]. A third example is the Higgs sector, which is responsible for the symmetry-breaking mechanism. The Higgs boson is still a hypothetical particle. Direct search at LEP only led to a lower constraint on the Higgs boson mass to be larger than 65.2 GeV [6]. From radiative corrections, the Higgs boson mass still can be as large as 1 TeV [37].

The second point about the status of the SM is that despite the celebrated success of the SM, there is little faith that the SM is the final theory. The reasons behind this are fundamental and basic. Some of these reasons are

- No unification in the gauge couplings g, g', and g_s can be attained within the SM framework. Furthermore, gravity is a totally ignored subject in the SM.
- The SM contains many arbitrary parameters with no apparent connections, e.g., fermion masses and quark mixings.
- The SM provides no prediction for the fermion masses, the quark mixings, the Higgs boson mass, and why the number of generations is 3.
- The SM provides no satisfactory explanation for the symmetry-breaking mechanism which takes place and gives rise to the observed mass spectrum of the gauge bosons and fermions (see chapter 3). The Higgs boson is still a hypothetical particle. In fact the sole existence of the Higgs boson by itself is a debated issue [55].
- The SM does not explain the large and unnatural difference between light and heavy quark masses. The question of why the top quark is so much heavier

than the other quarks, or to put it differently why all the quarks, except the top quark, have small masses relative to the symmetry-breaking scale v = 246 GeV.

 Other issues are not contemplated within the SM, examples include neutrino masses, the observed CP violation in the Kaon system, strong CP violation, etc.

If one holds the belief that the SM is not a fundamental theory, then many questions arise. How come the SM is so successful? Is the success of the SM an accident, or is there a link between the "fundamental" theory and the SM? Where is the new physics? How to reach for it? ... These are some of the questions that one hopes to answer in the on going efforts to understand nature.

2.2 Model Independent Analysis

Based on the belief that the SM is not the whole story, the search for physics beyond the SM is a continuous effort. One can investigate the possible existence for physics beyond the SM through a systematic model by model study. An example may be a grand unified theory (GUT) valid up to some high energy scale. Evolving that theory down to the electroweak scale permits a direct comparison between the prediction of the theory and the precision low energy data [56], or at least one may be able to set some constraints on the free parameter space of the model under study. Such an approach provides a consistent analysis for low energy data because the full theory under investigation is at hand. Other examples of this approach include Supersymmetry (SUSY) models [57] and TC along with its revised versions [47, 58, 59]. (For a review see Refs. [25, 60].) However, such approach is cumbersome and time consuming because of the need to go over the whole model and pin point

all of its characteristics at low energy.

A useful alternative method in searching for new physics is the model independent analysis. There are two common approaches in searching for new physics using a model independent analysis. The first approach is by characterizing all energy effects at low energy using a few parameters. As I discussed in chapter 1, such an approach is possible, e.g., using the epsilon parameters [16, 22, 23] or the S, T, U quantities [24] (see appendix B). Then by simply calculating theses quantities in any model and comparing with the corresponding values extracted from the low energy data one can judge whether a specific model is compatible with the low energy data or not. However, one should admit that using these parameters does not allow for a general treatment of all possible models. this is true because in defining these parameters certain assumptions are implemented. For example, in these parameterizations one assumes that at the tree level the low energy part of any model should reduce to that of the SM. Difference is only allowed in radiative corrections. Other assumptions include lepton universality in defining the epsilon parameters. In the S, T, U parameters one assumes that the only relevant physics is coming through the vacuum polarization, i.e., oblique corrections, and so on.

The second approach to the model independent analysis is the effective Lagrangian approach [61, 62, 63]. In this case, under general assumptions, one can effectively describe new physics effects to low energy data with no regard to the actual mechanism at the high energy scale. The use of effective Lagrangians began with the introduction of the non-linear σ -model [64] in the early 60's as an effective theory for the strong interactions. The theoretical basis of the effective Lagrangian method was formulated by the late 60's [65, 66].

In general, realistic models of new physics at high energy scales generate a host of effective operators at the low energy scale. The effective theory is valid below some high energy scale Λ above which the effective theory breaks down. Depending on the underlying physics one can resort to two different approaches in constructing the effective Lagrangian. The first approach is if the underlying physics is decoupling [67]. In this case, the effective operators are usually suppressed by some power of a high mass scale Λ . Therefore, the effective Lagrangian can be expanded in powers of $1/\Lambda$ or equivalently in terms of increasingly suppressed higher dimensional operators [68]. (For this effective Lagrangian, the $SU(2)_L \times U(1)_Y$ gauge symmetry is linearly realized by inserting more Higgs doublet fields in the effective operators.) The second approach is if the underlying physics is non-decoupling. In this case, the contributions due to physics above Λ need not be suppressed by powers of $1/\Lambda$. Therefore, in the non-decoupling case, an expansion in powers of momenta is performed and the effective Lagrangian is known as the chiral Lagrangian [68, 69]. (For the chiral Lagrangian, the $SU(2)_L \times U(1)_Y$ gauge symmetry is non-linearly realized, see appendix D.)

The effective Lagrangian can be taken to respect the gauge invariance of the SM. The disadvantage of the effective Lagrangian is that it involves a large body of free parameters, making the whole approach a tedious one for a general treatment. To simplify the whole approach usually one resorts to a limited class of effective operators which are sensitive to the case under study. Some recent efforts have been implemented to account for a broader class of effective operators than has previously been considered [70].

The chiral Lagrangian constitutes a powerful approach in describing the phenomenon of spontaneous symmetry breaking [71]. It provides a systematic way to effectively incorporate new physics without adhering to a limited scenario of the symmetry-breaking mechanism as long as the electroweak symmetry is spontaneously (as opposed to dynamically) broken. For example, one does not have to be confined to the assumed SM Higgs mechanism and therefore, the Higgs boson is not an essential

part of the basic structure of the chiral Lagrangian. In the next section I discuss in some detail the structure of the electroweak chiral Lagrangian. For more details, the reader can refer to the literature [62, 72, 73, 74, 75, 76, 77, 78].

In the effective Lagrangian approach one can understand the reason why the SM is so successful, it is because the SM is viewed only as a low energy effective theory. The success of the SM simply indicates the irrelevant effect of higher dimensional operators.

Another thing to mention is that the use of the effective Lagrangian does not necessarily stem from our ignorance of the full dynamics. In fact, as pointed out by H. Georgi in Ref. [76], the effective field theory framework is not only simpler and more transparent, but it actually provides a deeper insight into the relevant physics at the distance scale that is relevant to the current experimental data.

2.3 Introduction to the Chiral Lagrangian

The chiral Lagrangian approach has been used in understanding the low energy strong interactions because it can systematically describe the phenomenon of spontaneous symmetry-breaking [71]. In fact, the chiral Lagrangian found its greatest development in the context of strong interactions [79], e.g., $\pi\pi$ scattering. Recently, the chiral Lagrangian technique has been widely used in studying the electroweak sector [62, 72, 74, 75, 76, 77, 78], to which this work has been directed.

The chiral Lagrangian can be constructed based solely on symmetry principles with no other assumptions regarding any explicit dynamics. Thus, it is the most general effective Lagrangian that can accommodate any truly fundamental theory possessing that symmetry at low energy. Since one is interested in the low energy behavior of such a theory, an expansion in powers of the external momentum is

performed in the chiral Lagrangian [69].

In general, one starts from a Lie group G which breaks down spontaneously into a subgroup H, hence a Goldstone boson for every broken generator is to be introduced [80]. I consider the case where $G = SU(2)_L \times U(1)_Y$ and $H = U(1)_{em}$. There are three Goldstone bosons generated by this breakdown, ϕ^a , a = 1, 2, 3 which are eventually eaten by W^{\pm} and Z and become the longitudinal degrees of freedom of these gauge bosons.

The Goldstone bosons transform non-linearly under G but linearly under the subgroup H. A convenient way to handle this is to introduce the matrix field

$$\Sigma = \exp\left(i\frac{\phi^a \tau^a}{v_a}\right) \,, \tag{2.1}$$

where τ^a , a=1,2,3 are the Pauli matrices normalized as: Trace $(\tau^a\tau^b)=2\delta_{ab}$. Because of $U(1)_{\rm em}$ invariance $v_1=v_2=v$, but is not necessarily equal to v_3 . The matrix field Σ transforms under G as

$$\Sigma \to \Sigma' = \exp\left(i\frac{\alpha^a \tau^a}{2}\right) \Sigma \exp(-iy\frac{\tau^3}{2}),$$
 (2.2)

where $\alpha^{1,2,3}$ and y are the group parameters of G.

In the SM, being a special case of the chiral Lagrangian, v = 246 GeV is the vacuum expectation value of the Higgs boson field. Also $v_3 = v$ arises from the approximate custodial SU(2) symmetry in the SM. It is this symmetry that is responsible for the SM tree-level relation

$$\rho = \frac{M_W^2}{M_Z^2 c_\theta^2} = 1 \,, \tag{2.3}$$

where $c_{\theta}^2 = 1 - s_{\theta}^2$ and s_{θ}^2 is the weak mixing angle defined in the on-shell scheme (see appendix A). Low energy data already constrains ρ to be 1 within about 0.1%

accuracy [60]. Therefore, in this work, I will assume the full theory guarantees that $v_1 = v_2 = v_3 = v$.

Out of the Goldstone bosons and the gauge boson fields one can construct the bosonic gauge invariant terms in the chiral Lagrangian

$$\mathcal{L}_{B} = -\frac{1}{4} W_{\mu\nu}^{a} W^{\mu\nu a} - \frac{1}{4} B_{\mu\nu} B^{\mu\nu} + \frac{1}{4} v^{2} \operatorname{Tr} \left(D_{\mu} \Sigma^{\dagger} D^{\mu} \Sigma \right) , \qquad (2.4)$$

where the covariant derivative

$$D_{\mu}\Sigma = \partial_{\mu}\Sigma - igW_{\mu}^{a}\frac{\tau^{a}}{2}\Sigma + ig'\Sigma B_{\mu}\frac{\tau^{3}}{2}.$$
 (2.5)

Under G, the covariant derivative transforms as

$$D_{\mu}\Sigma \to (D_{\mu}\Sigma)' = \exp\left(i\frac{\alpha^a \tau^a}{2}\right) D_{\mu}\Sigma \exp(-iy\frac{\tau^3}{2}).$$
 (2.6)

In the unitary gauge $\Sigma = 1$, one can easily see how the gauge bosons acquire their masses. In the unitary gauge, the mass term in the Lagrangian reduces to

$$\mathcal{L}_{m} = \frac{1}{4} v^{2} \operatorname{Tr} \left(D_{\mu} \Sigma^{\dagger} D^{\mu} \Sigma \right) \to \frac{1}{4} v^{2} \operatorname{Tr} \left(\left[-g W_{\mu}^{a} \frac{\tau^{a}}{2} + g' B_{\mu} \frac{\tau^{3}}{2} \right]^{2} \right)$$

$$= \frac{1}{8} v^{2} \left(g^{2} W_{\mu}^{a} W^{\mu a} - 2g g' W_{\mu}^{3} B^{\mu} + g'^{2} B_{\mu} B^{\mu} \right). \tag{2.7}$$

Using the field definitions in Eqs. (1.11) and (1.12) one recovers the gauge boson masses given in Eq. (1.17)

$$\mathcal{L}_{m} = \frac{g^{2}v^{2}}{4}W_{\mu}^{+}W^{\mu-} + \frac{g^{2}v^{2}}{8\cos^{2}\theta}Z_{\mu}Z^{\mu}. \tag{2.8}$$

The W and Z masses are

$$M_W^2 = \frac{g^2 v^2}{4} , \quad M_Z^2 = \frac{g^2 v^2}{4 \cos^2 \theta} .$$
 (2.9)

The difference between the non-linear and the linear realizations is that in a general gauge, the non-linear realization produces other complicated terms in powers of the Goldstone bosons. (See appendix D for details.) In general, one finds

$$\mathcal{L}_{m} = M_{W}^{2} W_{\mu}^{+} W^{\mu -} + \frac{M_{Z}^{2}}{2} Z_{\mu} Z^{\mu} + \partial_{\mu} \phi^{+} \partial^{\mu} \phi^{-} + \frac{1}{2} \partial_{\mu} \phi^{3} \partial^{\mu} \phi^{3} + \dots,$$
 (2.10)

where the fields ϕ^{\pm} are defined as

$$\phi^{\pm} = \frac{\phi^1 \mp i\phi^2}{\sqrt{2}} \,. \tag{2.11}$$

Fermions can be included in the context of the chiral Lagrangian by assuming that they transform under $G = SU(2)_L \times U(1)_Y$ as [74]

$$f \to f' = e^{iyQ_f} f, \tag{2.12}$$

where Q_f is the electromagnetic charge of fermion f.

Out of the fermion fields f_1 , f_2 , with the condition $Q_{f_1} - Q_{f_2} = 1$, and the Goldstone bosons matrix field Σ the usual linearly realized fields Ψ (see section 1.1) can be constructed. For example, the left-handed fermions $[SU(2)_L]$ doublet] are constructed as

$$\Psi_L = \Sigma F_L = \Sigma \begin{pmatrix} f_1 \\ f_2 \end{pmatrix}_L. \tag{2.13}$$

One can easily show that Ψ_L transforms under G linearly as follows

$$\Psi_L \to \Psi_{L'} = \exp\left(i\frac{\alpha^a \tau^a}{2}\right) \Sigma \exp\left(-iy\frac{\tau^3}{2}\right) \exp\left(iy\left[\frac{\tau^3}{2} + \frac{Y}{2}\right]\right) F_L$$

$$= \exp\left(i\frac{\alpha^a \tau^a}{2}\right) \exp(iy\frac{Y}{2}) \Psi, \qquad (2.14)$$

where in Eq. (2.14) I wrote the fermion charge Q_f in terms of the Gell-Mann-Nishijima relation defined in Eq. (1.2)

$$Q = T_3 + \frac{Y}{2} \,, \quad T_3 = \frac{\tau^3}{2} \,. \tag{2.15}$$

Therefore, under the group $G=SU(2)_L \times U(1)_Y$

$$\Psi_L \to \Psi'_L = g \, \Psi_L \,, \tag{2.16}$$

where

$$g = \exp(i\frac{\alpha^a \tau^a}{2}) \exp(i\frac{yY}{2}) \in G.$$
 (2.17)

Linearly realized right-handed fermions Ψ_R [SU(2)_L singlet] simply coincide with F_R : i.e.,

$$\Psi_R = F_R = \begin{pmatrix} f_1 \\ f_2 \end{pmatrix}_R. \tag{2.18}$$

Out of the defined fields with their specified transformations it is straightforward to construct a Lagrangian which is invariant under $SU(2)_L \times U(1)_Y$. In constructing the low energy chiral Lagrangian, one can use either the fermionic basis Ψ_L and Ψ_R or the basis f_1 and f_2 . The two basis lead to an identical physical S matrix in virtue of Coleman's theorem [66, 81].

In constructing the chiral Lagrangian, I will follow Ref. [74] and define the composite fields as

$$\Sigma^{a}_{\mu} = -\frac{i}{2} \text{Tr}(\tau^{a} \Sigma^{\dagger} D_{\mu} \Sigma) . \tag{2.19}$$

Under the gauge transformation element $g \in G$ and using Eqs. (2.2) and (2.6), one finds that the composite fields transform as:

$$\Sigma_{\mu}^{a} \to \Sigma_{\mu}^{\prime a} = -\frac{i}{2} \operatorname{Tr} \left(\exp(-iy\frac{\tau^{3}}{2}) \tau^{a} \exp(iy\frac{\tau^{3}}{2}) \Sigma^{\dagger} D_{\mu} \Sigma \right) . \tag{2.20}$$

From which one concludes that under a general gauge transformation

$$\Sigma_{\mu}^{3} \to \Sigma_{\mu}^{\prime 3} = \Sigma_{\mu}^{3},$$
 (2.21)

and

$$\Sigma_{\mu}^{\pm} \to \Sigma_{\mu}^{\prime \pm} = e^{\pm iy} \Sigma_{\mu}^{\pm} \,, \tag{2.22}$$

where

$$\Sigma_{\mu}^{\pm} = \frac{1}{\sqrt{2}} (\Sigma_{\mu}^{1} \mp i \Sigma_{\mu}^{2}). \tag{2.23}$$

The field Σ^3_{μ} behaves as a neutral matter field while the two fields Σ^{\pm}_{μ} behave as charged matter fields with $Q=\pm 1$. By a matter field I mean a field which does not transform as a gauge boson field under the symmetry group H.

In a general gauge, Σ^3_μ can be expanded as

$$\Sigma_{\mu}^{3} = \frac{1}{v^{2}} \partial_{\mu} \phi^{3} - \frac{1}{2} \frac{g}{\cos \theta} Z_{\mu} - \frac{ig}{v} \left(W_{\mu}^{+} \phi^{-} - W_{\mu}^{-} \phi^{+} \right) - \frac{i}{v} \left(\phi^{+} \partial_{\mu} \phi^{-} - \phi^{-} \partial_{\mu} \phi^{+} \right) + \dots$$
(2.24)

The composite field Σ_{μ}^{+} can be expanded as

$$\Sigma_{\mu}^{+} = \frac{1}{v^{2}} \partial_{\mu} \phi^{+} - \frac{1}{2} g W_{\mu}^{+} - \frac{ig}{v} \left(\phi^{+} \left[\cos \theta Z_{\mu} + \sin \theta A_{\mu} \right] - \phi^{3} W_{\mu}^{+} \right) + \frac{i}{v} \left(\phi^{+} \partial_{\mu} \phi^{3} - \phi^{3} \partial_{\mu} \phi^{+} \right) + \dots$$
(2.25)

The component Σ_{μ}^{-} is just the Hermitian conjugate of Σ_{μ}^{+} . In the unitary gauge $\Sigma = 1$ one finds that the composite fields reduce to the physical gauge bosons, *i.e.*,

$$\Sigma_{\mu}^{3} = -\frac{1}{2} \frac{g}{\cos \theta} Z_{\mu} \,, \tag{2.26}$$

and

$$\Sigma_{\mu}^{\pm} = -\frac{1}{2}gW_{\mu}^{\pm} \,. \tag{2.27}$$

Using the non-linear realization technique for $G=SU(2)_L \times U(1)_Y$ and $H=U(1)_{em}$ one finds that the conserved generator Q (electric charge) is associated with the B_{μ}

gauge boson rather than the photon A_{μ} [77]. Therefore, in constructing the chiral Lagrangian, the covariant derivative of a fermion f will include the B_{μ} gauge boson field rather than the A_{μ} boson field (see below).

The main observation is that the bosonic fields Σ_{μ}^{3} , Σ_{μ}^{\pm} combined with the fermionic fields f_{1} , f_{2} , ..., only feel the electromagnetic transformation $U(1)_{\rm em}$ even though the whole gauge symmetry is $SU(2)_{L} \times U(1)_{Y}$. This is a very important observation because it enables us to write an invariant Lagrangian under the gauge group $SU(2)_{L} \times U(1)_{Y}$ simply by requiring the Lagrangian (constructed from Σ_{μ}^{a} , B_{μ} , and $F_{L,R}$) to be invariant under $U(1)_{\rm em}$. For example, consider the top and bottom quarks. From Eqs. (2.13) and (2.18) one has

$$F = \begin{pmatrix} t \\ b \end{pmatrix} = F_L + F_R \,, \tag{2.28}$$

with $f_1 = t$ and $f_2 = b$. The SM Lagrangian involving the t and b quarks can be deduced from

$$\mathcal{L}_{0} = \overline{F} i \gamma^{\mu} \left(\partial_{\mu} - i g' \left[\frac{Y}{2} + \frac{\tau^{3}}{2} \right] B_{\mu} \right) F - \overline{F} M F$$

$$- \overline{F}_{L} \gamma^{\mu} \tau^{a} F_{L} \Sigma_{\mu}^{a} + \mathcal{L}_{B} , \qquad (2.29)$$

where the hypercharge number is Y = 1/3 and M is a diagonal mass matrix

$$M = \begin{pmatrix} m_t & 0 \\ 0 & m_b \end{pmatrix} . (2.30)$$

 \mathcal{L}_0 is invariant under G and the electric charges of t and b quarks are given by the relation $Y/2 + T^3$, where $T^3 = \tau^3/2$ is the weak isospin quantum number $(T_t^3 = 1/2)$ and $T_b^3 = -1/2$. The terms in Eq. (2.29) are not the only possible gauge invariant dimension four operators. In fact, the chiral Lagrangian permits the inclusion of other terms while keeping the gauge invariance maintained. In chapter 3, I discuss how to parameterize the anomalous top quark couplings using the chiral Lagrangian framework.

Here is a final note regarding the physical Higgs boson. It is known that the gauge bosons acquire their masses through the spontaneous symmetry-breaking mechanism. The bosonic Lagrangian \mathcal{L}_B in Eq. (2.4) only involves the gauge bosons and the unphysical Goldstone bosons. The Higgs boson is not a part of the Lagrangian \mathcal{L}_B . This indicates that the chiral Lagrangian can account for the mass generation of the gauge bosons without the actual details of the symmetry-breaking mechanism. Furthermore, the fermion mass term is also allowed in the chiral Lagrangian,

$$-m_{f_i}\overline{f_i}f_i, \qquad (2.31)$$

because it is invariant under G, where the fermion field f_i transforms as in Eq. (2.12).

From this it is clear that the Higgs boson is not a necessary element in constructing the low energy effective Lagrangian. This indicates that the SM Higgs mechanism is just one example of the possible spontaneous symmetry-breaking scenarios which might take place in nature and still be described within the chiral Lagrangian framework. However, a Higgs boson field can be inserted in the chiral Lagrangian as an additional field $(SU(2)_L \times U(1)_Y)$ singlet with arbitrary couplings to the rest of the fields. To retrieve the SM Higgs boson at tree level, one can simply substitute the fermion mass m_f by $g_f v$ and v by v + H in \mathcal{L}_0 [see Eqs. (2.4) and (2.29)], where $g_f = m_f/v$ is the Yukawa coupling for fermion f and H is the Higgs boson field. Hence, one gets the Higgs Lagrangian

$$\mathcal{L}_{H} = \frac{1}{2} \partial_{\mu} H \partial^{\mu} H - \frac{1}{2} m_{H}^{2} H^{2} - V(H) + \frac{1}{2} v H \operatorname{Tr} \left(D_{\mu} \Sigma^{\dagger} D^{\mu} \Sigma \right) + \frac{1}{4} H^{2} \operatorname{Tr} \left(D_{\mu} \Sigma^{\dagger} D^{\mu} \Sigma \right) , \qquad (2.32)$$

where V(H) describes the Higgs boson self-interaction. In the SM, V(H) is given by

$$V(H) = -\frac{m_H^2}{8v^2} \left(4vH^3 + H^4 \right) \,. \tag{2.33}$$

Each term in Eq. (2.32) is separately gauge invariant because H is electromagnetically neutral. The coefficients of the last two terms in Eq. (2.32) can be arbitrary for a chiral Lagrangian with a scalar field other than the SM Higgs boson.

2.4 Heavy Top Quark Contribution to the ϵ Parameters in the Chiral Lagrangian

In chapter 1, I calculated the top quark leading contributions to the epsilon parameters in the SM. In this section, I repeat these calculations using the chiral Lagrangian framework. There are some differences in the Feynman diagrams between the SM and the chiral Lagrangian case. The dimension-four gauge boson couplings to the fermions are the same as in the SM. However, the Goldstone bosons couplings to the fermions are different. What is important to our case are the vertices ϕ^3 -t- \bar{t} , and ϕ^{\pm} -t- \bar{t} . In Figure 2.1, I show the relevant Feynman diagrams to the epsilon parameters in the chiral lagrangian. For the case of the ϵ_b parameter one needs to include an additional Feynman diagram (see Figure 2.1f) which appears because of the non-linear realization of the chiral Lagrangian. The calculations are performed in the 't Hooft-Feynman gauge. Calculations have been cross-checked in the Landau and unitary gauges, they all agree as they should. Using the heavy mass expansion discussed in appendix C, one finds

• For the photon

$$A^{\gamma\gamma}(0) = 0, (2.34)$$

$$F^{\gamma\gamma}(M_Z^2) = \frac{g^2}{16\pi^2} \frac{16\sin^2\theta}{9} \left(\Delta - \ln m_t^2\right). \tag{2.35}$$

• For the Z boson

$$A^{ZZ}(0) = -\frac{g^2}{16\pi^2} \frac{3m_t^2}{2\cos^2\theta} \left(\Delta - \ln m_t^2\right) , \qquad (2.36)$$

$$F^{ZZ}(M_Z^2) = \frac{g^2}{16\pi^2} \frac{1}{\cos^2 \theta} \left(\frac{1}{2} - \frac{4}{3} \sin^2 \theta + \frac{16}{9} \sin^4 \theta \right) \left(\Delta - \ln m_t^2 \right). \tag{2.37}$$

• For the W boson

$$A^{WW}(0) = \frac{g^2}{16\pi^2} \frac{3m_t^2}{2} \left(-\Delta - \frac{1}{2} + \ln m_t^2 \right) , \qquad (2.38)$$

$$F^{WW}(M_Z^2) = \frac{g^2}{16\pi^2} \left(\Delta - \ln m_t^2 \right) \,. \tag{2.39}$$

• For the γ -Z mixing

$$A^{\gamma Z}(0) = 0, (2.40)$$

$$F^{\gamma Z}(M_Z^2) = \frac{g^2}{16\pi^2} \frac{4\sin\theta}{3\cos\theta} \left(\frac{1}{2} - \frac{4}{3}\sin^2\theta\right) \left(\Delta - \ln m_t^2\right). \tag{2.41}$$

• For the proper vertex e_b one has to include all the relevant Feynman diagrams (see Figure 2.1c,d,e,f). One finds

$$e_b = -\frac{G_F m_t^2}{4\sqrt{2}\pi^2} \,. \tag{2.42}$$

Therefore, we find

$$\epsilon_1 = \Delta \rho = \frac{A^{ZZ}(0)}{M_Z^2} - \frac{A^{WW}(0)}{M_W^2} = \frac{g^2}{16\pi^2} \frac{3m_t^2}{4M_W^2} = \frac{3G_F m_t^2}{8\sqrt{2}\pi^2},$$
 (2.43)

$$\epsilon_2 = F^{WW}(M_W^2) - F^{33}(M_Z^2) = -\frac{G_F M_W^2}{4\sqrt{2}\pi^2} \ln(m_t^2), \qquad (2.44)$$

$$\epsilon_3 = \frac{\cos \theta}{\sin \theta} F^{30}(M_Z^2) = -\frac{G_F M_W^2}{12\sqrt{2}\pi^2} \ln(m_t^2) , \qquad (2.45)$$

and

$$\epsilon_b = -\frac{G_F m_t^2}{4\sqrt{2}\pi^2} \,. \tag{2.46}$$

The result we obtained here is identical to the result in section 1.5, as expected. By virtue of Coleman's theorem [66, 81] the linear and non-linear realizations lead to the same physical observables. The equivalence between the two approaches is verified at one loop for the heavy top quark contribution to the low energy data.

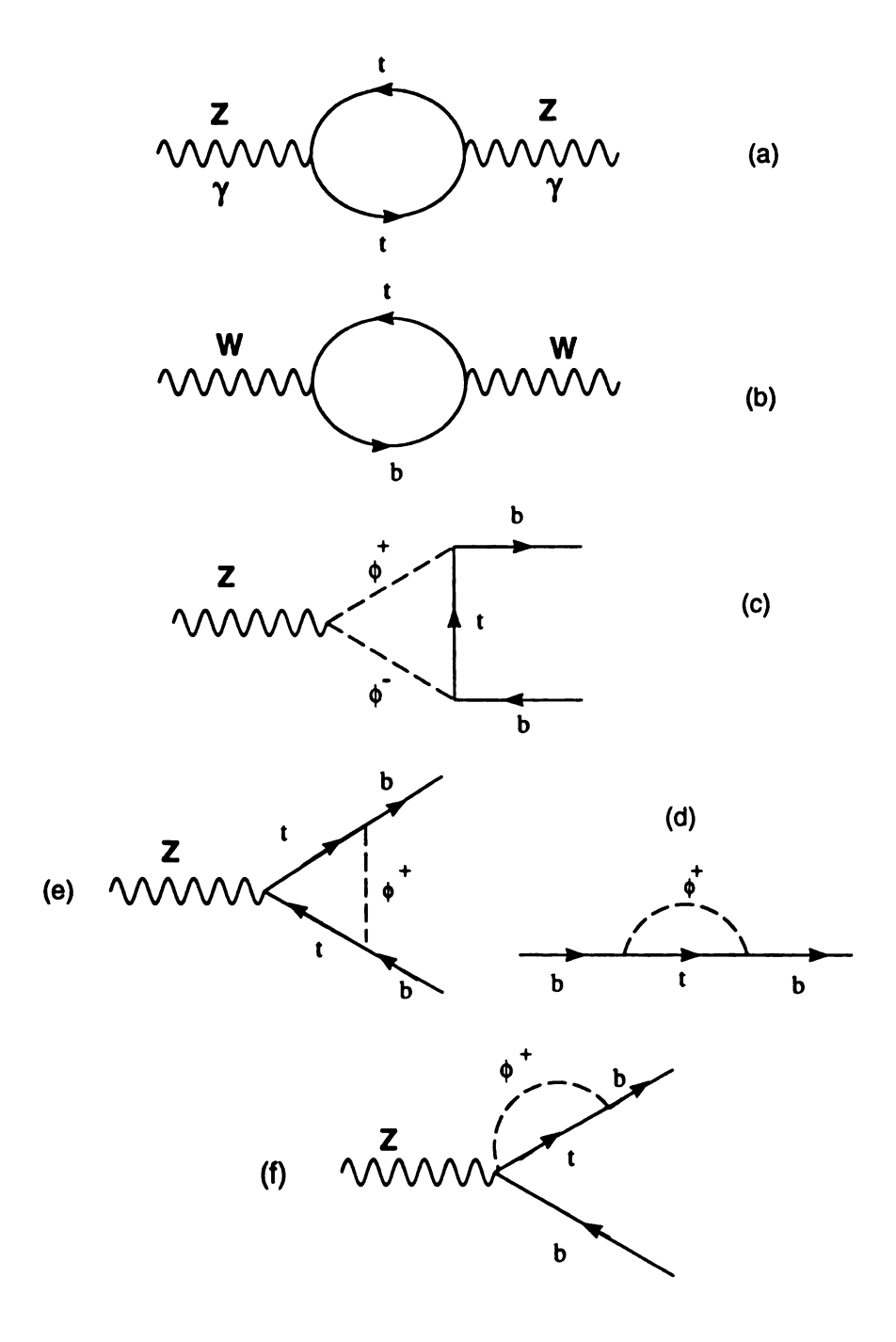


Figure 2.1: The relevant Feynman diagrams in calculating the top quark contribution to the epsilon parameters using the chiral Lagrangian approach.

Chapter 3

Global Analysis of the Top Quark Couplings to the Electroweak Gauge Bosons

3.1 Motivations and Perspectives

As I discussed in chapter 2, there is little faith that the SM is the final theory. The reasons behind this are fundamental and basic (see chapter 2). One of the most important reasons is the assumed SM symmetry-breaking scenario. The SM assumes the symmetry breaking is a result of the dynamics of a complex scalar doublet Φ . The scalar doublet acquires a v.e.v along the direction of the Higgs boson field. The simple SM scenario suffers a great difficulty if the SM is viewed as a fundamental theory. If the SM is valid up to all energies then the scalar sector is trivial (non-interacting) [82]. This triviality is problematic because of the need for a self-interacting scalar sector to generate the W and Z masses through the symmetry-breaking mechanism. To solve the triviality aspect of the SM scalar sector one has to assume that the scalar potential $V(\phi)$ is only valid below some energy cutoff scale Λ . Therefore, the SM can only be viewed as a low energy description of an effective theory which is only valid up to the energy cutoff scale Λ . Another problem in the SM scalar sector is that the loop corrections to the Higgs boson mass are quadratically divergent and

counterterms must be adjusted order by order in the perturbative expansion to cancel the quadratic divergencies. If the SM is embedded in a larger fundamental theory with heavy mass scales then the divergencies in the loop corrections to m_H depend on the square of the heavy mass scales. In order to keep m_H light, as required by unitarity conditions discussed below, there must be a deliberate cancellation of all the quadratic divergencies by the appropriate counterterms and to all orders. This cancellation is viewed by many as an unnatural aspect in the scalar sector which is known as the fine-tuning problem.

The most recent experimental bound on the Higgs boson mass comes from the direct search at LEP [6]

$$m_H > 65.2 \text{ GeV}$$
 at 95% C.L. (3.1)

As concluded in Refs. [6, 36], electroweak precision tests show a preference for a light Higgs boson although the allowed range of m_H is still wide enough due to the soft non-decoupling Higgs boson contribution to low energy data at one-loop level (logarithmic contribution [27]). On the other hand, as indicated in Ref. [37], LEP precision data, upon excluding the observables R_b and R_c , does not imply a strong bound on the Higgs bosons mass, i.e., m_H can still be as large as 1 TeV. The requirement of the consistency of the SM scalar sector implies some theoretical bounds on the Higgs mass. Unitarity of the perturbative partial wave amplitudes [8] implies an upper bound on the Higgs mass [83, 84]

$$m_H < 860 \text{ GeV}$$
 . (3.2)

The triviality aspect of the scalar sector and the requirement of new physics to appear at a high energy scale Λ (of the order of 1 TeV) implies a perturbative upper bound

on the Higgs boson mass [83]

$$m_H < 1 \text{ TeV}. \tag{3.3}$$

The higher the energy scale Λ is the lower the Higgs boson mass will be, e.g., for $\Lambda \sim \Lambda_{PL}$ and for $m_t \sim 175$ GeV one finds [85]:

$$m_H < 200 \text{ GeV}, \tag{3.4}$$

where Λ_{PL} is the Planck scale. Careful estimates of the triviality using the lattice [86] places a somewhat tighter limit

$$m_H < 640 \text{ GeV}$$
 (3.5)

Theoretical lower bounds on the Higgs mass come from the vacuum stability [87]. The lower limit is a function of the top quark mass and of the cutoff scale Λ . The dependence on the top quark mass comes because the Higgs boson coupling to the top quark is proportional to m_t (Yukawa coupling). Recent analysis of the vacuum stability [85, 88] concludes that if the cutoff scale Λ is as large as the Planck scale Λ_{PL} then for $m_t \sim 175$ GeV, the SM Higgs boson mass must be larger than about 120 GeV.

Many attempts to offer alternative scenarios for the symmetry-breaking mechanism are discussed in literature. A general trend among all alternatives is that new physics appear at or below the TeV scale. Examples include MSSM [89], technicolor models [58, 89] and possibly extended technicolor sectors to account for the fermion masses [47, 59]. Other examples include top-mode condensate models [90] and a strongly interacting Higgs sector [91].

In this chapter, I study how to use the top quark to probe the origin of the spontaneous symmetry-breaking and the generation of fermion masses. I start the

discussion with a brief description of the top quark. The top quark is the $T_3 = +1/2$ member of the weak isospin doublet containing the bottom quark with an electric charge Q = +2/3. The existence of the top quark has been confirmed recently by the CDF and DØ experiments [10, 11] at the Tevatron proton-antiproton collider with a center of mass (c.m.) energy of 1.8 TeV. Before this direct observation of the top quark, there were strong experimental and theoretical arguments suggesting that the top quark must exist [92]; e.g., the measurement of the weak isospin quantum number of the left-handed b quark $T_3 = -1/2$ suggests that the b quark should have an isospin partner, namely the top quark. By 1994, from a negative result of direct search at the Tevatron, assuming SM top quark, DØ concluded that m_t has to be larger than 131 GeV [93]. In the same year, data were presented by the CDF group at FNAL to support the existence of a heavy top quark with mass $m_t \sim 174 \pm 20$ GeV [94]. In 1995, both CDF and DØ announced the discovery of the top quark. From the recent observation of top quark events at CDF and DØ a fit of the mass distribution leads to the CDF top quark mass [10]

$$m_t = 176 \pm 9 \text{ GeV},$$
 (3.6)

and the DØ top quark mass [11]

$$m_t = 170 \pm 18 \text{ GeV},$$
 (3.7)

where the second error is the estimated systematic uncertainty. Furthermore, a recent study [12] based on the analysis of all available LEP data concludes that the SM top quark mass is

$$m_t = 178 \pm 8^{+17}_{-20} \text{ GeV} \,.$$
 (3.8)

The central value and the first error quoted refer to $m_H = 300$ GeV. The second

errors correspond to the variation of the central value when varying m_H in the interval $60 \text{ GeV} \leq m_H \leq 1000 \text{ GeV}$.

Despite the recent success in the observation of the top quark and its mass measurement, there are no compelling reasons to believe that the top quark couplings to the weak gauge bosons should be of the SM nature. The CDF and DØ measurements of the top quark mass are from a fit on the mass distribution, *i.e.*, from kinematics, no conclusions can be drawn regarding interactions or dynamics. Therefore, using the top quark radiative corrections to the low energy data is the only available approach, so far, to study the top quark interactions. Because the top quark is heavy relative to the other observed fundamental particles, one expects that any underlying theory at high energy scale $\Lambda \gg m_t$ will easily reveal itself at low energy through the effective interactions of the top quark to the gauge bosons. Also, because the top quark mass is of the order of the Fermi scale $v = (\sqrt{2}G_F)^{-1/2} = 246 \,\text{GeV}$, which characterizes the electroweak symmetry-breaking scale, the top quark may be a useful tool to probe the symmetry-breaking sector. It is this connection between the top quark weak-interactions and the symmetry-breaking mechanism that I would like to investigate throughout the discussion of this chapter.

Since the fermion mass generation can be closely related to the electroweak symmetry-breaking, one expects some residual effects of this breaking to appear in accordance with the generated mass [47, 59, 95]. This means that new effects should be more apparent in the top quark sector than any other light sector of the theory. Therefore, it is important to study the top quark system as a direct tool to probe new physics effects.

In the SM, which is a renormalizable theory, the couplings of the top quark to gauge bosons are fixed by the linear realization of the gauge symmetry $SU(2)_L \times U(1)_Y$. However, the top quark mass is a free parameter in the theory (SM) and

need to be measured experimentally. If the top quark is not a SM quark, then the couplings of the top quark to gauge bosons can be different from the SM. Also, the effective theory describing the top quark interactions at low energy can be non-renormalizable. Therefore, to conclude upon the properties of the top quark from the radiative corrections is less vital and predictive. Nevertheless, precision data at this stage are our best hope to look for any possible deviation in the top quark sector from the SM, until a direct measurement of the top quark interactions can be made.

To study the couplings of the top quark to the gauge bosons, I will first use the precision data at LEP/SLC to constrain these couplings in a model independent approach, then I will examine how to improve our knowledge about the top quark couplings at the current and future colliders. In addition, I will discuss how to use this knowledge to probe the symmetry-breaking mechanism.

It is generally believed that new physics is likely to come in via processes involving longitudinal gauge bosons (equivalent to Goldstone bosons) and/or heavy fermions such as the top quark. One commonly discussed method to probe the electroweak symmetry sector is to study the interactions among the longitudinal gauge bosons in the TeV region. Tremendous work has been done in the literature [96]. However, this is not the subject of this work. As I argued above, the top quark plays an important role in the search for new physics. Because of its heavy mass, new physics will feel its presence easily and eventually may show up in its couplings to the gauge bosons. If the top quark is a participant in a dynamical symmetry-breaking mechanism, e.g., through the $\bar{t}t$ condensate (top-mode Standard Model) [90] which is suggested by the fact that its mass is of the order of the Fermi scale v, then the top quark is one of the best candidates for the search for new physics.

An attempt to study the nonuniversal interactions of the top quark has been carried out in Ref. [95] by Peccei et al. However, in that study only the vertex

t-t-Z was considered based on the assumption that this is the only vertex which gains a significant modification due to a speculated dependence of the coupling strength on the fermion mass: $\kappa_{ij} \leq \mathcal{O}\left(\frac{\sqrt{m_i m_j}}{v}\right)$, where κ_{ij} parameterizes some new dimensional-four interactions among gauge bosons and fermions i and j. However, this is not the only possible pattern of interactions, e.g., in some extended technicolor models [59] one finds that the nonuniversal residual interactions associated with the vertices $b_L - \overline{b_L} - Z$, $t_L - \overline{t_L} - Z$, and $t_L - \overline{b_L} - W$ to be of the same order. In Section 3.4, I discuss the case of the SM with a heavy Higgs boson $(m_H > m_t)$ in which we find the size of the nonuniversal effective interactions $t_L - \overline{t_L} - Z$ and $t_L - \overline{b_L} - W$ to be of the same order but with a negligible $b_L - \overline{b_L} - Z$ effect.

Here is the outline of my approach to the analysis. First, I use the chiral Lagrangian approach [66, 69, 71, 72] to construct the most general $SU(2)_L \times U(1)_Y$ invariant effective Lagrangian including up to dimension-four operators for the top and bottom quarks. Then I deduce the SM (with and without a scalar Higgs boson) from this Lagrangian, and only consider new physics effects which modify the top quark couplings to gauge bosons and possibly the vertex b_L - $\overline{b_L}$ -Z. With this in hand, I perform a comprehensive analysis using precision data from LEP/SLC. I include the contributions from the vertex t-b-W in addition to the vertex t-t-Z, and discuss the special case of having a comparable size in b-b-Z as in t-t-Z. Second, I build an effective model with an approximate custodial symmetry ($\rho \approx 1$) connecting the t-t-Z and t-b-W couplings. This reduces the number of parameters in the effective Lagrangian and strengthens its structure and predictability. After examining what we have learned from the LEP and SLC data, I study how to improve our knowledge on these couplings at the Tevatron, the LHC (Large Hadron Collider) and the LC (Linear Collider) [97]. (I use LC to represent a generic e-e+ supercollider.)

The rest of this chapter is organized as follows. In Section 3.2, I parameterize the

anomalous top quark couplings using the chiral Lagrangian framework. In Section 3.3, I present the complete analysis of the top quark interactions with gauge bosons using LEP data for various scenarios of symmetry-breaking mechanism. Also, I discuss how the SLC measurement of A_{LR} can contribute to the study of the top quark couplings to the gauge bosons. In Section 3.4, I discuss the heavy Higgs limit $(m_H > m_t)$ in the SM model as an example of our proposed effective model at the top quark mass scale. In Section 3.5, I discuss how the Tevatron, LHC, and LC can contribute to the measurement of these couplings. Some discussion and conclusions are given in Section 3.6.

3.2 The Top Quark Couplings to Gauge Bosons in the Chiral Lagrangian Framework

I will concentrate my discussion on the b and t quarks. Precision tests at LEP and SLC have shown that the interactions among the other light fermions and the gauge bosons agree very well with the SM, with the exception of the recent observed deviations in A_{LR} at SLC and in R_b and R_c at LEP. As discussed in chapter 1, if the anomaly in R_c persists in the future then it is unlikely for us to be able to understand such a large deviation within any perturbative model. Therefore, I will ignore this measurement in my discussion. (I will come back later to say a few words about R_c .) To simplify the discussion on the proposed new top quark interactions, I will ignore all possible mixings of the top and bottom quarks with the other light fermions. In case there exists a fourth generation with heavy fermions, there can be a substantial impact on the Cabibbo-Kobayashi-Maskawa (CKM) matrix element V_{tb} . To be discussed below, this effect is effectively included in the nonstandard couplings of t-b-W of the effective Lagrangian at low energy scale.

Taking advantage of the chiral Lagrangian approach (see chapter 2), nonstandard interaction terms, invariant under $SU(2)_L \times U(1)_Y$, are allowed in addition to the standard terms in Eq. (2.29). These terms are

$$\mathcal{L}_{1} = -\kappa_{L}^{NC} \overline{t_{L}} \gamma^{\mu} t_{L} \Sigma_{\mu}^{3} - \kappa_{R}^{NC} \overline{t_{R}} \gamma^{\mu} t_{R} \Sigma_{\mu}^{3}
- \sqrt{2} \kappa_{L}^{CC} \overline{t_{L}} \gamma^{\mu} b_{L} \Sigma_{\mu}^{+} - \sqrt{2} \kappa_{L}^{CC\dagger} \overline{b_{L}} \gamma^{\mu} t_{L} \Sigma_{\mu}^{-}
- \sqrt{2} \kappa_{R}^{CC} \overline{t_{R}} \gamma^{\mu} b_{R} \Sigma_{\mu}^{+} - \sqrt{2} \kappa_{R}^{CC\dagger} \overline{b_{R}} \gamma^{\mu} t_{R} \Sigma_{\mu}^{-},$$
(3.9)

where κ_L^{NC} , κ_R^{NC} are two arbitrary real parameters, κ_L^{CC} , κ_R^{CC} are two arbitrary complex parameters, and the superscript NC and CC denote neutral and charged currents, respectively. The composite fields Σ_{μ}^a , a=1,2,3 are discussed in chapter 2. In the unitary gauge, the Lagrangian above reduces to

$$\mathcal{L}_{1} = \frac{g}{4\cos\theta_{W}} \bar{t} \left(\kappa_{L}^{NC} \gamma^{\mu} (1 - \gamma_{5}) + \kappa_{R}^{NC} \gamma^{\mu} (1 + \gamma_{5}) \right) t Z_{\mu}
+ \frac{g}{2\sqrt{2}} \bar{t} \left(\kappa_{L}^{CC} \gamma^{\mu} (1 - \gamma_{5}) + \kappa_{R}^{CC} \gamma^{\mu} (1 + \gamma_{5}) \right) b W_{\mu}^{+}
+ \frac{g}{2\sqrt{2}} \bar{b} \left(\kappa_{L}^{CC\dagger} \gamma^{\mu} (1 - \gamma_{5}) + \kappa_{R}^{CC\dagger} \gamma^{\mu} (1 + \gamma_{5}) \right) t W_{\mu}^{-}.$$
(3.10)

A few remarks are in order regarding the Lagrangian \mathcal{L}_1 in Eqs. (3.9) and (3.10).

- (1) In principle, \mathcal{L}_1 can include nonstandard neutral currents $\overline{b_L}\gamma_\mu b_L$ and $\overline{b_R}\gamma_\mu b_R$. For the left-handed neutral current $\overline{b_L}\gamma_\mu b_L$ I discuss two cases:
 - (a) The effective left-handed vertices $t_L \overline{t_L} Z$, $t_L \overline{b_L} W$, and $b_L \overline{b_L} Z$ are comparable in size as in some extended technicolor models [47, 59]. In this case, the top quark contribution to low energy observables through radiative corrections is of a higher order, *i.e.*, the top quark contribution will be suppressed by $1/16\pi^2$ relative to the *b*-quark contribution. In this case, as I will discuss in the next section, the constraints derived from low energy data on the nonstandard couplings are so stringent (of the order of a few

- percent) that it would be a challenge to directly probe the nonstandard top quark couplings at the Tevatron, the LHC, and the LC.
- (b) The effective left-handed vertex $b_L \overline{b_L} Z$ is small as compared to the t-t-Z and t-b-W vertices. I will devote most of this work to the case where the vertex $b_L \overline{b_L} Z$ is not modified by the dynamics of the symmetry breaking. This assumption leads to interesting conclusions to be seen in the next section. In this case one needs to consider the contributions of the top quark to low energy data through loop effects. A specific model with such properties is given in Section 3.4.
- (2) I will assume that $b_R \overline{b_R} Z$ is not modified by the dynamics of the electroweak symmetry-breaking. This is the case in the extended technicolor models discussed in Ref. [47, 59]. The model discussed in Section 3.4 is another example.
- (3) The right-handed charged current contribution κ_R^{CC} in Eqs. (3.9) and (3.10) is expected to be suppressed by the bottom quark mass. This can be understood in the following way. If b is massless (m_b = 0), then the left- and right-handed b fields can be associated with different global U(1) quantum numbers. (U(1) is a chiral group, not the hypercharge group.) Since the underlying theory has an exact SU(2)_L × U(1)_Y symmetry at high energy, the charged currents are purely left-handed before the symmetry is broken. After the symmetry is spontaneously broken and for a massless b the U(1) symmetry associated with b_R remains exact (chiral invariant) so it is not possible to generate right-handed charged currents. Thus κ_R^{CC} is usually suppressed by the bottom quark mass although it could be enhanced in some models with a larger group G, i.e., in models containing additional right-handed gauge bosons.

I observed that in the limit of ignoring the bottom quark mass, κ_R^{CC} does not

contribute to the low energy data through loop insertion at the order $m_t^2 \ln \Lambda^2$, therefore one cannot constrain κ_R^{CC} from the LEP data. However, at the Tevatron and the LHC κ_R^{CC} can be measured by studying the direct detection of the top quark and its decays. This will be discussed in Section 3.5

It is worth mentioning that the photon does not participate in the new nonuniversal interactions as described by the chiral Lagrangian \mathcal{L}_1 in Eq. (3.10) because the $U(1)_{\rm em}$ symmetry remains an exact symmetry of the effective theory. Any new physics can only contribute to the universal interactions of the photon to charged fields. This effect can simply be absorbed in redefining the electromagnetic fine structure constant α , hence no new t-t-A or b-b-A interaction terms will appear in the effective Lagrangian after a proper renormalization of α and the wave functions of the particle fields.

In this analysis, I will discuss an effective model with and without the Higgs boson. In the case of a light Higgs boson $(m_H < m_t)$ I will include the Higgs boson field in the chiral Lagrangian as a part of the light fields with no new physics being associated with it. In the heavy Higgs boson case $(m_H > m_t)$, one should integrate out the Higgs boson field from the tree-level Lagrangian. Thus, one is left with an effective Lagrangian which contains the heavy Higgs boson effects and the additional nonstandard couplings κ_L^{NC} , κ_R^{NC} , κ_L^{CC} , and κ_R^{CC} . The Higgs boson contribution to the low energy effective Lagrangian (for energies $E \ll m_t$) is only relevant in the gauge sector. This is true because, as discussed in section 1.5, the Higgs boson couplings to light fermions are negligible. However, the top quark couplings to the gauge bosons will be affected by the heavy Higgs boson due to the large Yukawa coupling (m_t/v) . In fact, a heavy Higgs boson may be the source for the nonstandard couplings of the top quark κ_L^{NC} , κ_R^{NC} , κ_L^{NC} , and κ_R^{NC} . Finally, I will consider the possibility of a spontaneous symmetry-breaking scenario without including a SM Higgs boson in the

full theory. In this case I consider the effects on the low energy data from the new physics parameterized by the nonstandard interaction terms in \mathcal{L}_1 in Eq. (3.10) and the contributions from the SM without a Higgs boson.

As I discussed above, one possibility of new physics effects is the modification of the vertices b-b-Z, t-t-Z, and t-b-W in the effective Lagrangian by the same order of magnitude [47, 59]. In this case, only the vertex b-b-Z can have large contributions to low energy data while, based on the dimensional counting method, the contributions from the other two vertices t-t-Z and t-b-W are suppressed by $1/16\pi^2$ due to their insertion in loops.

In this case, one can use Γ_b (the partial decay width of the Z boson to $\bar{b}b$) to constrain the b-b-Z coupling. Denote the nonstandard b-b-Z vertex as

$$\frac{g}{4\cos\theta}\kappa\gamma_{\mu}(1-\gamma_5)\,,\tag{3.11}$$

which is purely left-handed. In some extended technicolor models, discussed in Ref. [47, 59], this nonstandard effect arises from the same source as the mass generation of the top quark, therefore κ depends on the top quark mass.

As I discussed in chapter 1, the nonuniversal contribution to Γ_b is parameterized by a measurable parameter denoted as ϵ_b [16, 22, 23]. Using all LEP data, a fit on ϵ_b yields the value [38]

$$\epsilon_b (10^3) = 0.0 \pm 3.9. \tag{3.12}$$

The SM contribution to ϵ_b is calculated in Ref. [26], e.g., for a 170 GeV top quark

$$\epsilon_b^{\text{SM}} (10^3) = -6.15 \ . \tag{3.13}$$

The contribution from κ to ϵ_b is

$$\epsilon_b = -\kappa \,. \tag{3.14}$$

Within a 95% confidence level (C.L.), one finds that

$$-14.2 \le \kappa \,(10^3) \le 1.9\,. \tag{3.15}$$

As an example, the simple commuting extended technicolor model presented in Ref. [59] predicts that

$$\kappa \approx \frac{1}{2} \xi^2 \frac{m_t}{4\pi v} \,, \tag{3.16}$$

where ξ is of order 1. Also in that model the top quark couplings κ_L^{NC} , κ_R^{NC} , and κ_L^{CC} , as defined in Eqs. (3.9) and (3.10), are of the same order as κ . For a 170 GeV top quark mass, this model predicts

$$\kappa (10^3) \approx 27.5 \, \xi^2 \,.$$
 (3.17)

Hence, such a model is likely to be excluded by using the low energy data constraints [see Eq. (3.15)].

3.3 Low Energy Constraints

In this section, I will devote the discussion to models in which the nonstandard b-b-Z coupling can be ignored relative to the t-t-Z and t-b-W couplings. In this case, the nonstandard couplings contribute to low energy observables at the quantum level, i.e., through loop insertion. I will first discuss the general case where no relations between the nonstandard couplings are assumed. Later, I will impose a relation between κ_L^{NC} and κ_L^{CC} which are defined in Eqs. (3.9) and (3.10) using an effective model with an approximate custodial symmetry.

3.3.1 General Case

In general, the chiral Lagrangian has a complicated structure and many arbitrary coefficients which weaken its predictive power. Still, with a few further assumptions, based on the status of present low energy data, the chiral Lagrangian can provide a useful approach to confine the coefficients parameterizing new physics effects.

In this subsection, I provide a general treatment for the case under study with minimal imposed assumptions in the chiral Lagrangian. I only impose the assumption that the vertex b-b-Z is not modified by the dynamics. In the chiral Lagrangian \mathcal{L}_1 , as defined in Eqs. (3.9) and (3.10), there are six independent parameters (κ 's) which need to be constrained using precision data. Throughout this paper, I will only consider the insertion of κ 's once in one-loop diagrams by assuming that these nonstandard couplings are small; $\kappa_{L,R}^{NC,CC}$ < 1. At the one-loop level the imaginary parts of the couplings do not contribute to those LEP observables of interest. Thus, hereafter I drop the imaginary pieces from the effective couplings, which reduces the number of relevant parameters to four. Since the bottom quark mass is small as compared to the top quark mass, the non-standard coupling κ_R^{CC} does not contribute to low energy observables up to the order $m_t^2 \ln \Lambda^2$ in the $m_b \to 0$ limit. With these observations we conclude that only the three parameters κ_L^{NC} , κ_R^{NC} and κ_L^{CC} (to bear in mind, this is really $\mathrm{Re}(\kappa_L^{CC})$) can be constrained at LEP. The nonstandard coupling κ_R^{CC} can be studied using the CLEO measurement of $b \to s\gamma$. An effective model with only one nonstandard coupling κ_R^{CC} was studied in Ref. [98], a constraint on the right-handed charged current coupling $\kappa_R^{\rm CC}$ was set using the CLEO measurement of $b \to s\gamma$. The authors concluded that $\kappa_R^{\rm CC}$ is well constrained to within a few percent from its SM value ($\kappa_R^{\text{CC}} = 0$). This provides a complementary information to our constraint on κ_L^{NC} , κ_R^{NC} , and κ_L^{CC} .

As I discussed in chapter 1, the new physics contribution to low energy observables, under a few general assumptions, can be parameterized by 4-independent parameters ϵ_1 , ϵ_2 , ϵ_3 , and ϵ_b . In our case, the general assumptions are satisfied, namely all the contributions of κ_L^{NC} , κ_R^{NC} , κ_L^{CC} , and κ_R^{CC} to low energy observables are contained in the oblique corrections, i.e., the vacuum polarization functions of the gauge bosons, and the non-oblique corrections to the vertex b-b-Z. Therefore, it is enough to calculate the new physics contribution to the ϵ parameters in order to isolate all effects to low energy observables. As discussed in chapter 1, the ϵ parameters are derived from four basic measured observables, Γ_ℓ (the partial width of Z to a charged lepton pair), A_{FB}' (the forward-backward asymmetry at the Z peak for the charged lepton ℓ), M_W/M_Z , and Γ_b (the partial width of Z to a $b\bar{b}$ pair). The expressions of these observables in terms of ϵ 's are given in chapter 1. Since the top quark will only contribute to the vacuum polarization functions and the the vertex b-b-Z, I am only interested in the following terms

$$\epsilon_1 = e_1 - e_5 \,, \tag{3.18}$$

$$\epsilon_2 = e_2 - \cos^2 \theta \, e_5 \,, \tag{3.19}$$

$$\epsilon_3 = e_3 - \cos^2 \theta \, e_5 \,, \tag{3.20}$$

$$\epsilon_b = e_b \,, \tag{3.21}$$

where e_1 , e_2 , e_3 , e_5 , and e_b are defined in chapter 1 as follow

$$e_1 = \frac{A^{ZZ}(0)}{M_Z^2} - \frac{A^{WW}(0)}{M_W^2} \,, \tag{3.22}$$

$$e_2 = F^{WW}(M_W^2) - F^{33}(M_Z^2),$$
 (3.23)

$$e_3 = \frac{\cos \theta}{\sin \theta} F^{30}(M_Z^2) \,, \tag{3.24}$$

$$e_5 = M_Z^2 \frac{dF^{ZZ}}{dq^2} (M_Z^2) \,. \tag{3.25}$$

The quantity e_b is defined through the proper vertex corrections

$$V_{\mu}\left(Z \to b\bar{b}\right) = -\frac{g}{2c}e_{b}\gamma_{\mu}\frac{1-\gamma_{5}}{2}.$$
(3.26)

As we found in section 1.5, the parameters ϵ_1 and ϵ_b depend quadratically on m_t . Therefore, ϵ_1 and ϵ_b are sensitive to any new physics coming through the top quark. On the contrary, ϵ_2 and ϵ_3 have at most a logarithmic dependence on m_t . Hence, in our effective model, the significant constraints on the parameters κ_L^{NC} , κ_R^{NC} , and κ_L^{CC} are only coming from ϵ_1 and ϵ_b .

Non-renormalizability of the effective Lagrangian presents a major issue of how to find a scheme to handle both the divergent and the finite pieces in loop calculations [99, 100]. Such a problem arises because one does not know the underlying theory; hence, no matching can be performed to extract the correct scheme to be used in the effective Lagrangian [61]. One approach is to associate the divergent piece in loop calculations with a physical cutoff Λ , the upper scale at which the effective Lagrangian is valid [74]. In the chiral Lagrangian approach this cutoff Λ is taken to be $4\pi v \sim 3 \text{ TeV} [61]^1$. For the finite piece no completely satisfactory approach is available [99]. I assume that the underlying full theory is renormalizable. In this case, the cutoff scale Λ serves as the infrared cutoff of the operators in the effective Lagrangian. Due to the renormalizability of the full theory, from renormalization group analysis, one concludes that the same cutoff Λ should also serve as the ultraviolet cutoff of the effective Lagrangian in calculating Wilson coefficients. Hence, in the dimensional regularization scheme, $1/\epsilon$ is replaced by $\ln(\Lambda^2/\mu^2)$, where $\epsilon = (4-n)/2$ and n is the

¹The scale $4\pi v \sim 3$ TeV is only meant to indicate the typical cutoff scale. It is equally probable to have, say, $\Lambda = 1$ TeV.

space-time dimension. Furthermore, the renormalization scale μ is set to be m_t , the heaviest mass scale in the effective Lagrangian of interest.

To perform calculations using the chiral Lagrangian, one should arrange the contributions in powers of $1/4\pi v$ and then include all diagrams up to the desired power. In a general R_{ξ} gauge ($\Sigma \neq 1$), the couplings of the Goldstone bosons to the fermions should also be included in Feynman diagram calculations. These couplings can be easily found by expanding the terms in \mathcal{L}_1 as given in Eq. (3.9). The relevant Feynman diagrams are shown in Figure 3.1. Calculations are done for a general R_{ξ} gauge. (I have also checked the calculations in the 't Hooft-Feynman gauge, the Landau gauge, and the unitary gauge. All agree as expected.)

I calculate the contribution to ϵ_1 and ϵ_b due to the new interaction terms in the chiral Lagrangian (see Eqs. (3.9) and (3.10)) using the dimensional regularization scheme and taking the bottom mass to be zero. At the end of the calculation, as I discussed above, I replace the divergent piece $1/\epsilon$ by $\ln(\Lambda^2/m_t^2)$ for $\epsilon = (4-n)/2$ where n is the space-time dimension. Since I am mainly interested in new physics associated with the top quark couplings to gauge bosons, I will restrict myself to the leading contribution enhanced by the top quark mass, *i.e.*, of the oder of $m_t^2 \ln \Lambda^2$. The result of the calculation is as follows

• The vacuum polarization function of the Z boson is (see Figure 3.1a)

$$A^{ZZ}(0) = \frac{M_Z^2}{4\pi^2} \frac{3m_t^2}{v^2} \left(-\kappa_L^{NC} + \kappa_R^{NC} \right) \frac{1}{\epsilon}$$
 (3.27)

• The vacuum polarization function of the W boson is (see Figure 3.1b)

$$A^{WW}(0) = \frac{M_W^2}{4\pi^2} \frac{3m_t^2}{v^2} \left(-\kappa_L^{CC}\right) \frac{1}{\epsilon} \tag{3.28}$$

• Figure 3.1c yields the result

$$\frac{ig}{4\cos\theta} \frac{m_t^2}{4\pi^2 v^2} \left(-2\kappa_L^{CC}\right) \gamma_\mu \left(1 - \gamma_5\right) \frac{1}{\epsilon} \tag{3.29}$$

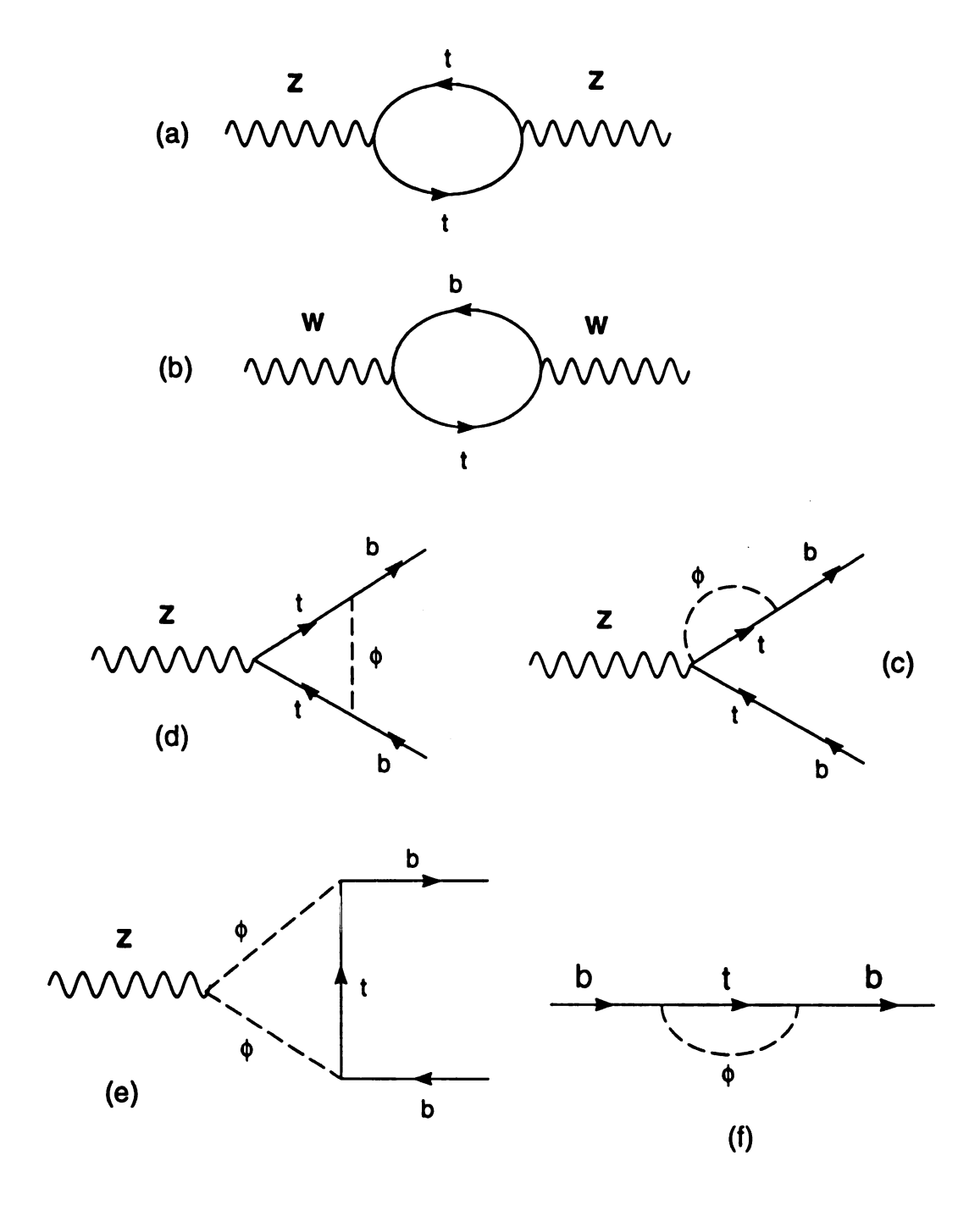


Figure 3.1: The relevant Feynman diagrams, for the nonstandard top quark couplings case and in the 't Hooft-Feynman gauge, which contribute to the order $\mathcal{O}(m_t^2 \ln \Lambda^2)$.

A similar diagram with the other b quark leg attached to the Goldstone boson yields the same result.

• Figure 3.1d yields the result

$$\frac{ig}{4\cos\theta} \frac{m_t^2}{4\pi^2 v^2} \left(-2\cos^2\theta \,\kappa_L^{CC} + \frac{1}{4}\kappa_R^{NC} - \kappa_L^{NC} \right) \gamma_\mu \left(1 - \gamma_5 \right) \frac{1}{\epsilon} \tag{3.30}$$

• Figure 3.1e yields the result

$$\frac{ig}{4\cos\theta} \frac{m_t^2}{4\pi^2 v^2} \left(-\cos^2\theta + \frac{1}{2} \right) \kappa_L^{CC} \gamma_\mu \left(1 - \gamma_5 \right) \frac{1}{\epsilon} \tag{3.31}$$

• The b-quark self energy (Figure 3.1f) yields the result

$$-\frac{3m_t^2}{16\pi^2v^2}\gamma_\mu p^\mu \left(\kappa_L^{CC}\right) (1-\gamma_5) \frac{1}{\epsilon} \tag{3.32}$$

Therefore, one finds

$$\delta\epsilon_1 = \frac{G_F}{2\sqrt{2}\pi^2} 3m_t^2 (-\kappa_L^{NC} + \kappa_R^{NC} + \kappa_L^{CC}) \ln \frac{\Lambda^2}{m_t^2} , \qquad (3.33)$$

$$\delta\epsilon_b = \frac{G_F}{2\sqrt{2}\pi^2} m_t^2 \left(-\frac{1}{4} \kappa_R^{NC} + \kappa_L^{NC} \right) \ln \frac{\Lambda^2}{m_t^2} , \qquad (3.34)$$

where $\delta\epsilon_1$ denotes the new physics contribution to ϵ_1 and similarly for $\delta\epsilon_b$. Notice that ϵ_2 and ϵ_3 do not contribute at this order. It is interesting to note that κ_L^{CC} does not contribute to ϵ_b up to this order which can be understood from Eq. (3.10). If $\kappa_L^{CC} = -1$ then there is no net t-b-W coupling in the chiral Lagrangian after including both the standard and nonstandard contributions. Hence, no dependence on the top quark mass can be generated, i.e., the nonstandard κ_L^{CC} contribution to ϵ_b must cancel the SM contribution when $\kappa_L^{CC} = -1$, independently of the couplings of the neutral current. From this observation and because the SM contribution to ϵ_b is finite, I conclude that κ_L^{CC} cannot contribute to ϵ_b at the order of interest. In Ref. [101] a

similar calculation for ϵ_b was performed and the author claimed to get a different result from the one above. However, the author included only the vertex corrections to calculate the physical quantity ϵ_b , which is not complete because the wave function corrections to the b quark must be included.

In Eqs. (3.33) and (3.34) I set the renormalization scale μ to be equal to m_t , which is the natural scale to be used in this study because the top quark is considered to be the heaviest mass scale in the effective Lagrangian. I have assumed that all other heavy fields have been integrated out to modify the effective couplings of the top quark to gauge bosons at the scale m_t in the chiral Lagrangian. Here, I ignore the effect of the running couplings from the top quark mass scale down to the Z boson mass scale which is a reasonable approximation for this study.

To constrain these nonstandard couplings one needs to have both the experimental values and the SM predictions of ϵ 's. The experimental data is given in Table 1.2. From these low energy data, a fit for ϵ_1 and ϵ_b yields the values [36]

$$\epsilon_1^{\text{exp.}} (10^3) = 3.8 \pm 1.5,$$

$$\epsilon_b^{\text{exp.}} (10^3) = 0.0 \pm 3.9.$$
(3.35)

The SM contribution to ϵ 's have been calculated in Ref. [26]. I include these contributions in the analysis in accordance with the assumed Higgs boson mass. If the low energy theory contains a SM Higgs boson, i.e., there is a light Higgs boson $(m_H < m_t)$, then the calculated values of the ϵ 's include both the SM contribution calculated in Ref. [26] and the new physics contribution derived from the effective couplings of the top quark to gauge bosons. In the heavy Higgs boson case $(m_H > m_t)$, one should integrate out the Higgs boson field from the tree-level Lagrangian. Thus, one is left with an effective Lagrangian which contains the heavy Higgs boson effects and the additional nonstandard couplings κ_L^{NC} , κ_R^{NC} , κ_L^{CC} , and κ_R^{CC} . Up to

one loop, the Higgs boson contribution to the low energy effective Lagrangian (for $M_W < E \ll m_H$) is only relevant in the gauge sector. This is true because, as discussed in section 1.5, the Higgs boson couplings to light fermions are negligible. The effective Lagrangian after integrating out the heavy Higgs boson field can be written as

$$\mathcal{L}_{eff} = -\frac{1}{2} W_{\mu\nu}^{+} W^{-\mu\nu} - \frac{1}{4} (1 - e_2) W_{\mu\nu}^{3} W^{3\mu\nu} - \frac{1}{4} B_{\mu\nu} B^{\mu\nu} - \frac{1}{2} \sin\theta \cos\theta e_3 B_{\mu\nu} W^{3\mu\nu} - \frac{1}{2} M_Z^2 Z_{\mu} Z^{\mu} - M_Z^2 \cos^2\theta (1 + e_1) W_{\mu}^{+} W^{-\mu} , \qquad (3.36)$$

where

$$e_1 = \frac{A^{ZZ}(0)}{M_Z^2} - \frac{A^{WW}(0)}{M_W^2} = -\frac{3G_F M_W^2 \sin^2 \theta}{8\sqrt{2}\pi^2 \cos^2 \theta} \ln(m_H^2), \qquad (3.37)$$

$$e_2 = F^{WW}(M_W^2) - F^{33}(M_Z^2) = 0,$$
 (3.38)

$$e_3 = \frac{\cos \theta}{\sin \theta} F_{30}(M_Z^2) = \frac{G_F M_W^2}{24\sqrt{2}\pi^2} \ln(m_H^2). \tag{3.39}$$

However, the top quark couplings to the gauge bosons will be affected by the heavy Higgs boson due to the large Yukawa coupling (m_t/v) . In fact, a heavy Higgs boson may be the source for the nonstandard couplings of the top quark κ_L^{NC} , κ_R^{NC} , κ_L^{CC} , and κ_R^{CC} . In section 3.4, I calculate the heavy Higgs boson effect to the nonstandard top quark couplings. Finally, I consider the case of a spontaneous symmetry scenario without a Higgs boson. In this case, I subtract the Higgs boson contribution from the SM values of the ϵ parameters given in Ref. [26]. In this scenario, the nonstandard top quark couplings to gauge bosons are viewed as not due to an assumed heavy Higgs boson but possibly to some residual effects of a new symmetry-breaking mechanism.

First, I consider the light Higgs boson case $(m_H < m_t)$. Choosing $m_t = 160$ and 180 GeV, respectively, and taking $m_H = 65$ GeV, I span the parameter space defined by $-1 \le \kappa_L^{NC} \le 1$, $-1 \le \kappa_R^{NC} \le 1$, and $-1 \le \kappa_L^{CC} \le 1$. Within 95% C.L.

and including both the SM and the new physics contributions, the allowed region of these three parameters is found to form a thin slice in the specified volume. The two-dimensional projections of this slice are shown in Figures 3.2, 3.3, and 3.4. These nonstandard couplings (κ 's) do exhibit some interesting features.

- (1) As a function of the top quark mass, the allowed volume for the top quark couplings to the gauge bosons shrinks as the top quark becomes more massive.
- (2) New physics prefers positive κ_L^{NC} , see Figures 3.2 and 3.3. For $\kappa_R^{NC} = 0$, κ_L^{NC} is constrained within -0.05 to 0.17 (0.0 to 0.15) for a 160 (180) GeV top quark.
- (3) New physics prefers $\kappa_L^{CC} \approx -\kappa_R^{NC}$. This is clearly shown in Figure 3.4 which is the projection of the allowed volume in the plane containing κ_R^{NC} and κ_L^{CC} .

The preference for a positive κ_L^{NC} is triggered by ϵ_b . For $m_t=170$ GeV and $m_H=65$ GeV, the experimental value of ϵ_b is

$$\epsilon_b^{\text{exp.}} = 0.0 \pm 3.9 \,, \tag{3.40}$$

which is larger than the SM value

$$\epsilon_b^{\rm SM} = -6.15. \tag{3.41}$$

Therefore, the new physics contribution to ϵ_b favors positive values in order to be compatible with the experimental measurement. Hence, in view of Eq. (3.34), κ_L^{NC} prefers positive values. Also, since the main contribution to ϵ_b is coming from κ_L^{NC} (for κ 's< 1), one finds that κ_L^{NC} is well constrained relative to κ_R^{NC} and κ_L^{CC} . The preference for $\kappa_R^{NC} \approx -\kappa_L^{CC}$ can be understood from the nonstandard contribution to ϵ_1 (see Eq. (3.33)). Since the experimental fit on ϵ_1 with its small uncertainty is compatible with the SM and because κ_L^{NC} is well constrained by ϵ_b , there is not much freedom in the sum $\kappa_R^{NC} + \kappa_L^{CC}$, i.e., $\kappa_R^{NC} + \kappa_L^{CC} \sim 0$.

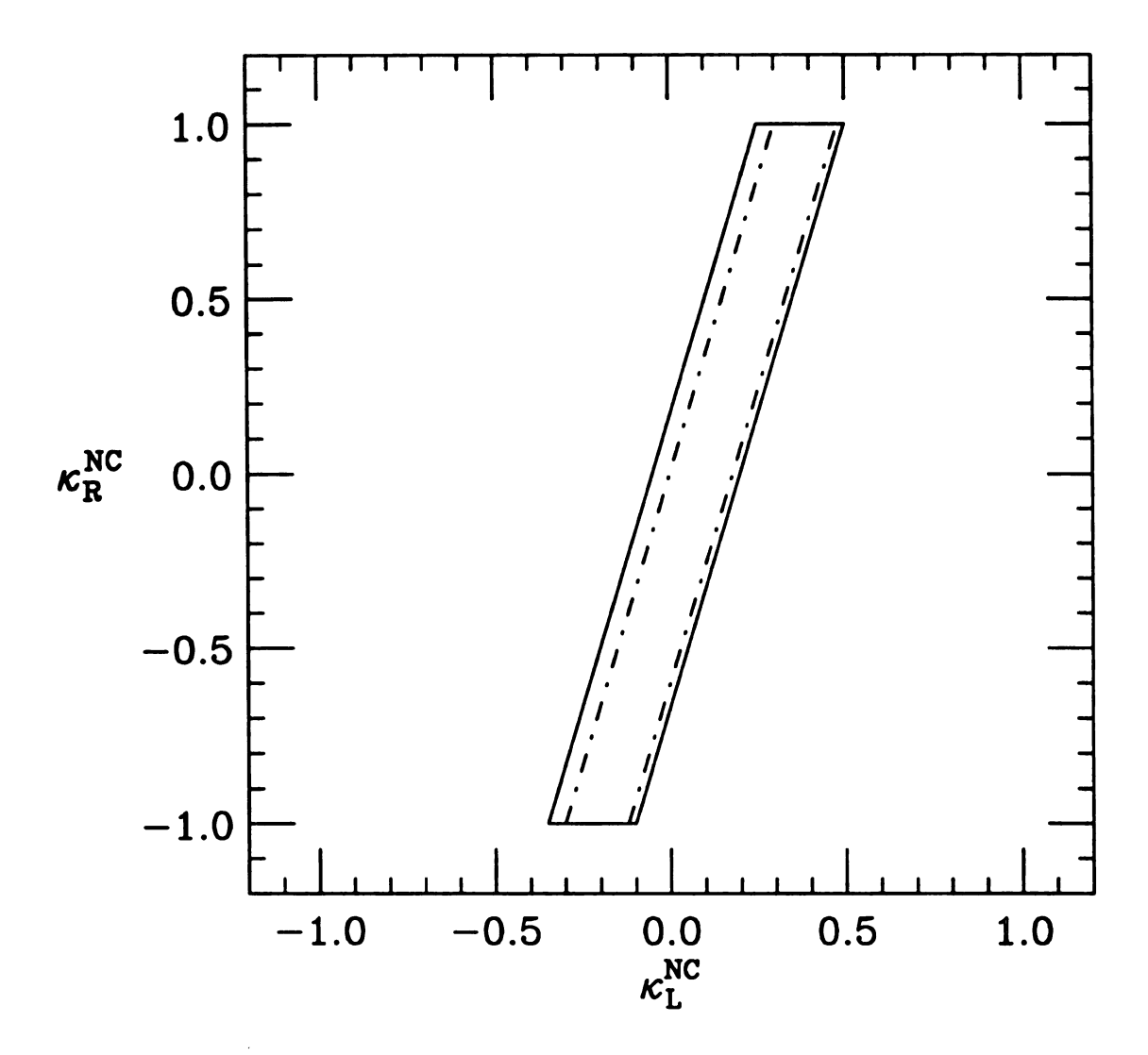


Figure 3.2: A two-dimensional projection in the plane of κ_L^{NC} and κ_R^{NC} , for $m_t = 160$ GeV (solid contour) and 180 GeV (dashed contour). The Higgs boson mass is fixed, $m_H = 65$ GeV.

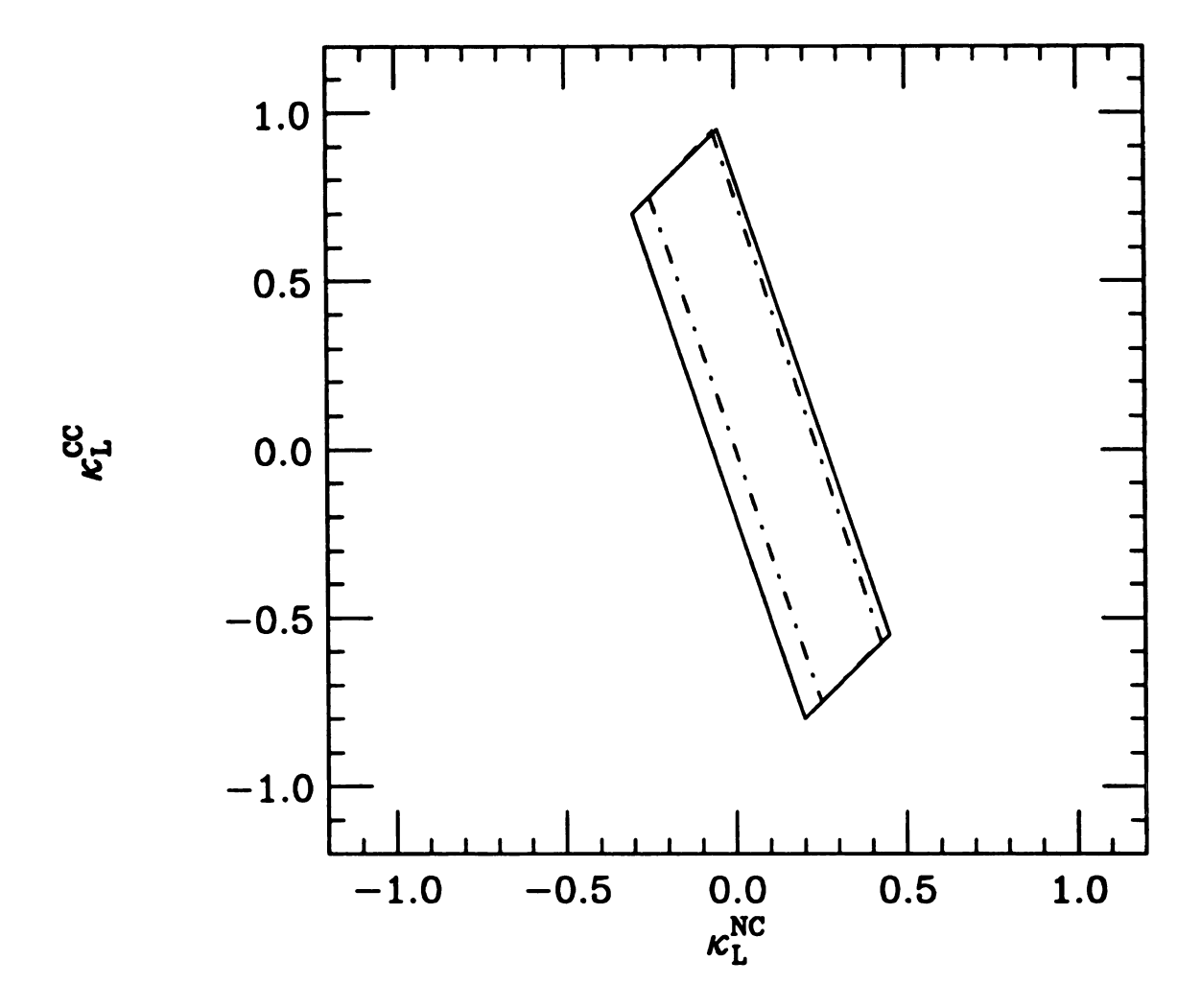


Figure 3.3: A two-dimensional projection in the plane of κ_L^{NC} and κ_L^{CC} , for $m_t = 160$ GeV (solid contour) and 180 GeV (dashed contour). The Higgs boson mass is fixed, $m_H = 65$ GeV.

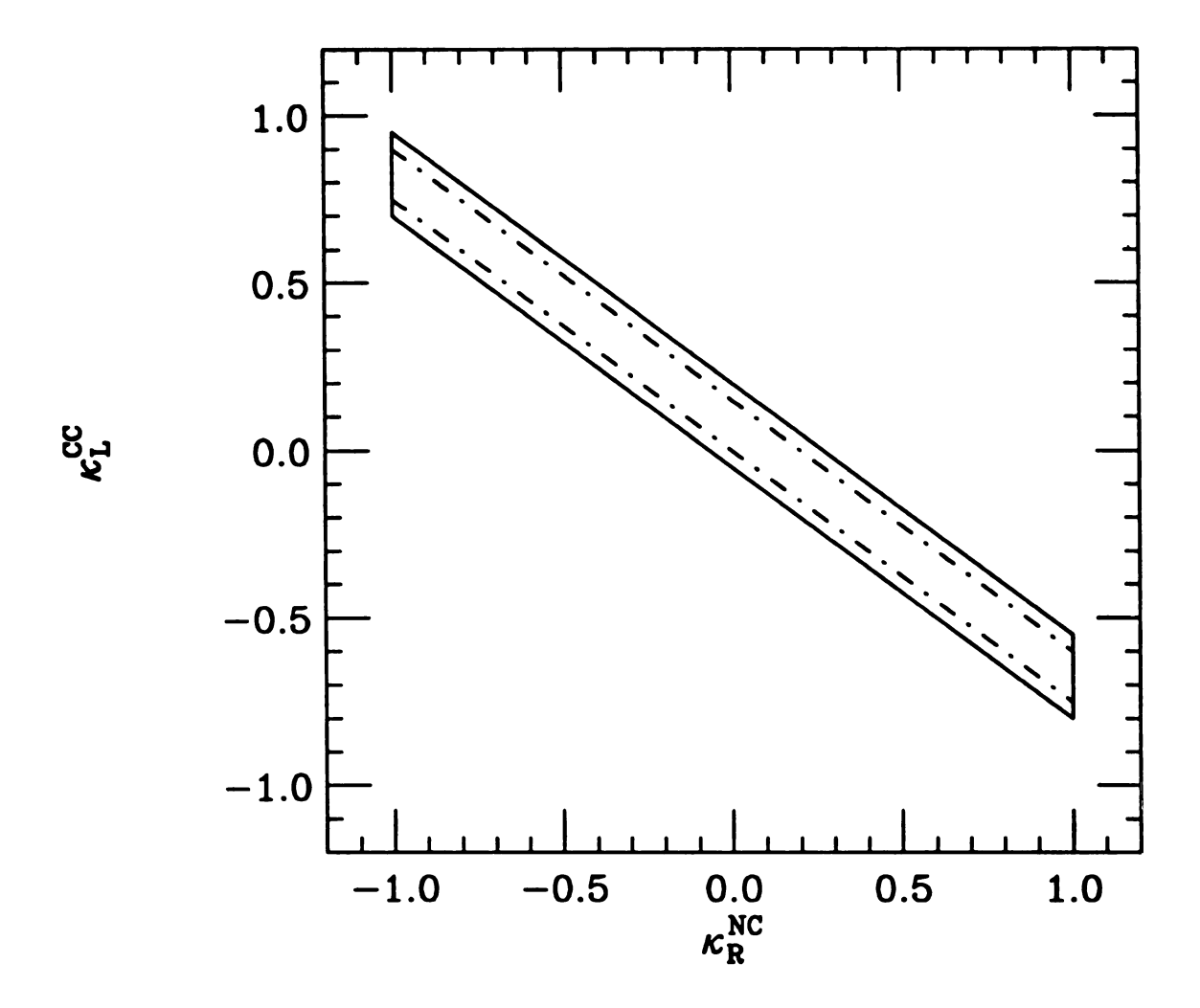


Figure 3.4: A two-dimensional projection in the plane of κ_R^{NC} and κ_L^{CC} , for $m_t=160$ GeV (solid contour) and 180 GeV (dashed contour). The Higgs boson mass is fixed, $m_H=65\,\mathrm{GeV}$.

Now, I comment on the heavy Higgs boson $(m_H > m_t)$ and the no-Higgs boson cases. A different Higgs boson mass does not have a large influence on the allowed parameter space. As discussed in section 1.5, ϵ_b is not sensitive to the Higgs boson mass at one-loop level, while ϵ_1 has at most, for a heavy Higgs boson, a logarithmic dependence on m_H . Since κ_L^{NC} is mostly constrained from ϵ_b one does not expect any noticeable effect on the allowed range of κ_L^{NC} as a function of the Higgs boson mass. Also, since the fit on ϵ_1 is compatible with a wide range of Higgs boson masses, the relation $\kappa_R^{NC} + \kappa_L^{CC} \sim 0$ is maintained. In Figure 3.5 I show the parameter space of κ_L^{NC} and κ_R^{NC} for the Higgs boson mass $m_H = 1000$ GeV and for two values of the top quark mass, $m_t = 160$ GeV(solid contour) and 180 GeV (dashed contour). One finds that for $\kappa_R^{NC} = 0$, κ_L^{NC} is constrained within -0.03 to 0.2 (0.0 to 0.2) for a 160 (180) GeV top quark.

Next, I consider the possibility of a new symmetry-breaking scenario without a fundamental scalar such as a SM Higgs boson. In this case, I simply subtract the Higgs boson contribution from the SM results obtained in Ref. [26]. In this case one expects to find no noticeable difference from the light Higgs boson case shown in Figures 3.2, 3.3, and 3.4. This is true because a light Higgs bosons has a smaller contribution to ϵ_1 than a heavy Higgs boson [21]. Therefore, the case of the no-Higgs boson scenario has a similar effect as the light Higgs boson case. In the next subsection, I will discuss the heavy Higgs boson and the no-Higgs boson cases in more detail.

In Ref. [95] a similar analysis has been carried out by Peccei et al. However, in their analysis they did not include the charged current contribution κ_L^{CC} and assumed only the vertex t-t-Z gives large nonstandard effects. The allowed region they found simply corresponds, in my analysis, to the region defined by the intersection of the allowed volume and the plane $\kappa_L^{CC} = 0$. This gives a small area confined in the

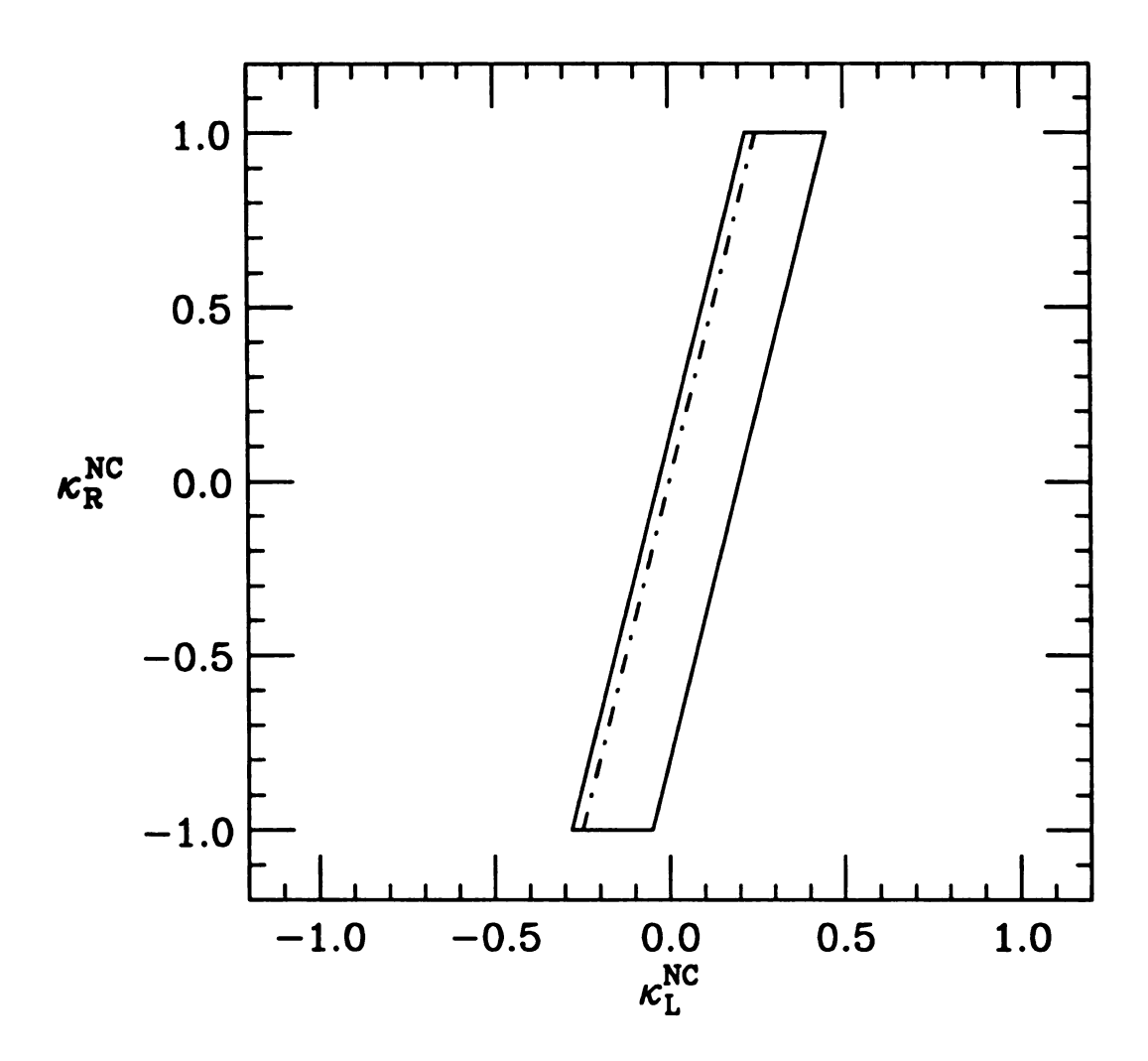


Figure 3.5: A two-dimensional projection in the plane of κ_L^{NC} and κ_R^{NC} , for $m_t=160$ GeV (solid contour) and 180 GeV (dashed contour), and for the heavy Higgs boson mass $m_H=1000$ GeV.

vicinity of the line $\kappa_L^{NC} = \kappa_R^{NC}$. This can be understood from the expression of ϵ_1 derived in Eq. (3.33). After setting $\kappa_L^{CC} = 0$, one finds

$$\epsilon_1 \propto \left(\kappa_R^{NC} - \kappa_L^{NC}\right)$$
 (3.42)

In this case one notes that the length of the allowed area is merely determined by the contribution from ϵ_b . I will elaborate on a more quantitative comparison in the second part of this section.

3.3.2 Special Case

The allowed region in the parameter space shown in Figures 3.2, 3.3, and 3.4 contains all possible new physics (to the order $m_t^2 \ln \Lambda^2$) which can modify the couplings of the top quark to gauge bosons as described by κ_L^{NC} , κ_R^{NC} , and κ_L^{CC} . In this subsection, I would like to examine a special class of models in which an approximate custodial symmetry is assumed as suggested by low energy data.

The SM has an additional (accidental) symmetry called the custodial symmetry which is responsible for the tree-level relation

$$\rho = \frac{M_W^2}{M_Z^2 c_\theta^2} = 1 \ , \tag{3.43}$$

where $c_{\theta}^2 = 1 - s_{\theta}^2$ and s_{θ}^2 is the weak mixing angle defined in the on-shell scheme (see appendix A). This symmetry is slightly broken at the quantum level by the SU(2) doublet fermion mass splitting and the hypercharge coupling g' [102]. Writing $\rho = 1 + \delta \rho$, $\delta \rho$ would vanish to all orders if this symmetry is exact. Low energy data indicate that $\delta \rho$ is very close to zero. In fact, low energy data constrains ρ to be 1 within about 0.1% accuracy [60]. Therefore, I will assume that the underlying theory has a global custodial symmetry. In other words, I require the global group $SU(2)_V$ associated with the custodial symmetry to be a subgroup of the full group

characterizing the full theory. I will assume that the custodial symmetry is broken by the same factors which break it in the SM, *i.e.*, by the fermion mass splitting and the hypercharge coupling g'.

In the chiral Lagrangian this assumption of a custodial symmetry sets $v_3 = v$, and forces the couplings of the top quark to gauge bosons W^a_μ to be equal after turning off the hypercharge and assuming $m_b = m_t$. If the dynamics of the symmetry breaking is such that the masses of the two SU(2) partners t and b remain degenerate then one expects new physics to contribute to the couplings of t-t-Z and t-b-W by the same amount. However, in reality, $m_b \ll m_t$; thus, the custodial symmetry has to be broken. I will discuss how this symmetry is broken shortly. Since I am mainly interested in the leading contribution enhanced by the top quark mass at the order $m_t^2 \ln \Lambda^2$, turning the hypercharge coupling on and off will not affect the final result up to this order.

I construct the two Hermitian operators J_L and J_R , which transform under G as

$$J_L^{\mu} = -i\Sigma D_{\mu} \Sigma^{\dagger} \to g_L J_L^{\mu} g_L^{\dagger} , \qquad (3.44)$$

$$J_R^{\mu} = i \Sigma^{\dagger} D_{\mu} \Sigma \to g_R J_R^{\mu} g_R^{\dagger} , \qquad (3.45)$$

where $g_L = \exp(i\alpha^a \frac{\tau^a}{2}) \in SU(2)_L$ and $g_R = \exp(iy\frac{\tau^3}{2})$. In fact, using either J_L or J_R will lead to the same result. Hence, from now on I will only consider J_R . The SM Lagrangian can be derived from

$$\mathcal{L}_{0} = \overline{\Psi_{L}} i \gamma^{\mu} D_{\mu}^{L} \Psi_{L} + \overline{\Psi_{R}} i \gamma^{\mu} D_{\mu}^{R} \Psi_{R} - (\overline{\Psi_{L}} \Sigma M \Psi_{R} + h.c.)$$

$$- \frac{1}{4} W_{\mu\nu}^{a} W^{\mu\nu a} - \frac{1}{4} B_{\mu\nu} B^{\mu\nu} + \frac{v^{2}}{4} \text{Tr}(J_{R}^{\mu} J_{R\mu}) , \qquad (3.46)$$

where M is a diagonal mass matrix. I have chosen the left-handed fermion fields to

be the ones defined in Eq. (2.13):

$$\Psi_L \equiv \Sigma \binom{t}{b}_L \,. \tag{3.47}$$

The fermion field Ψ_L transforms linearly under $G=SU(2)_L\times U(1)_Y$, i.e.,

$$\Psi_L \to \Psi'_L = g \, \Psi_L \,, \tag{3.48}$$

where $g \in SU(2)_L \times U(1)_Y$. The right-handed fermion fields t_R and b_R coincide with the original right-handed fields (see Eq. (2.18)). Also,

$$D^{L}_{\mu} = \partial_{\mu} - ig \frac{\tau^{a}}{2} W^{a}_{\mu} - ig' \frac{Y}{2} B_{\mu} , \qquad (3.49)$$

$$D_{\mu}^{R} = \partial_{\mu} - ig' \left(\frac{Y}{2} + \frac{\tau^{3}}{2} \right) B_{\mu} . \tag{3.50}$$

Note that in the nonlinear realized effective theories using either set of fields ($\Psi_{L,R}$ or $F_{L,R}$) to construct a chiral Lagrangian will lead to the same S matrix [66].

The Lagrangian \mathcal{L}_0 in Eq. (3.46) is not the most general Lagrangian one can construct based solely on the symmetry of G/H, for $G=SU(2)_L \times U(1)_Y$ and $H=U(1)_{em}$. Taking advantage of the chiral Lagrangian approach one can derive additional interaction terms which deviate from the SM. This is so because in this formalism the $SU(2)_L \times U(1)_Y$ symmetry is nonlinearly realized and only the $U(1)_{em}$ is linearly realized.

Because the SM is so successful one can think of the SM (without the top quark) as being the leading term in the expansion of the effective Lagrangian. Any possible deviation associated with the light fields can only come through higher dimensional operators in the Lagrangian. However, this assumption is neither necessary nor preferable when dealing with the top quark because no precise data are available to lead to

such a conclusion. I will include nonstandard dimension-four operators for the couplings of the top quark to gauge bosons. In fact this is all I will deal with and will not consider operators with dimension higher than four. Note that higher dimensional operators are naturally suppressed by powers of $1/\Lambda$.

One can rewrite J_R as

$$J_R^{\mu} = J_R^{\mu a} \frac{\tau^a}{2} \,, \tag{3.51}$$

with

$$J_R^{\mu a} = \text{Tr} \left(\tau^a J_R^{\mu} \right) = i \text{Tr} \left(\tau^a \Sigma^{\dagger} D^{\mu} \Sigma \right). \tag{3.52}$$

The full operator J_R posses an explicit custodial symmetry when g'=0 as can easily be checked by expanding it in powers of the Goldstone boson fields.

Consider first the left-handed sector. One can add additional interaction terms to the Lagrangian \mathcal{L}_0

$$\mathcal{L}_{1} = \kappa_{1} \overline{\Psi_{L}} \gamma_{\mu} \Sigma J_{R}^{\mu} \Sigma^{\dagger} \Psi_{L} + \kappa_{2} \overline{\Psi_{L}} \gamma_{\mu} \Sigma \tau^{3} J_{R}^{\mu} \Sigma^{\dagger} \Psi_{L} + \kappa_{2}^{\dagger} \overline{\Psi_{L}} \gamma_{\mu} \Sigma J_{R}^{\mu} \tau^{3} \Sigma^{\dagger} \Psi_{L}, \qquad (3.53)$$

where κ_1 is an arbitrary real parameter and κ_2 is an arbitrary complex parameter. Note that \mathcal{L}_1 still is not the most general Lagrangian one can write for the left-handed sector, as compared to Eq. (3.9). In fact, it is our insistence on using the fermion doublet form and the full operator J_R that lead us to this form. For shorthand, \mathcal{L}_1 can be further rewritten as

$$\mathcal{L}_{1} = \overline{\Psi_{L}} \gamma_{\mu} \Sigma K_{L} J_{R}^{\mu} \Sigma^{\dagger} \Psi_{L} + \overline{\Psi_{L}} \gamma_{\mu} \Sigma J_{R}^{\mu} K_{L}^{\dagger} \Sigma^{\dagger} \Psi_{L} , \qquad (3.54)$$

where K_L is a complex diagonal matrix with three real parameters.

These new terms can be generated either through some electroweak symmetrybreaking scenario or through some other new heavy physics effects. If $m_b = m_t$ and g'=0, then we require the effective Lagrangian to respect fully the custodial symmetry to all orders. In this limit, $\kappa_2=0$ in Eq. (3.53) and $K_L=\kappa_1 \mathbf{1}$, where $\mathbf{1}$ is the unit matrix and κ_1 is real.

Since $m_b \ll m_t$, one can think of κ_2 as generated through the evolution from $m_b = m_t$ to $m_b = 0$. In the matrix notation this implies K_L is not proportional to the unit matrix and can be parameterized by

$$K_L = \begin{pmatrix} \kappa_L^t & 0\\ 0 & \kappa_L^b \end{pmatrix} \,, \tag{3.55}$$

with

$$\kappa_L^t = \frac{\kappa_1}{2} + \kappa_2 \,, \tag{3.56}$$

and

$$\kappa_L^b = \frac{\kappa_1}{2} - \kappa_2 \,. \tag{3.57}$$

In the unitary gauge one gets the terms

$$+\frac{g}{2\cos\theta}2\operatorname{Re}(\kappa_{L}^{t})\overline{t_{L}}\gamma^{\mu}t_{L}Z_{\mu} + \frac{g}{\sqrt{2}}(\kappa_{L}^{t} + \kappa_{L}^{b}{}^{\dagger})\overline{t_{L}}\gamma^{\mu}b_{L}W_{\mu}^{+} + \frac{g}{\sqrt{2}}(\kappa_{L}^{b} + \kappa_{L}^{t}{}^{\dagger})\overline{b_{L}}\gamma^{\mu}t_{L}W_{\mu}^{-} - \frac{g}{2\cos\theta}2\operatorname{Re}(\kappa_{L}^{b})\overline{b_{L}}\gamma^{\mu}b_{L}Z_{\mu}.$$

$$(3.58)$$

As discussed in the previous section, I will assume that new physics effects will not modify the $b_L - \overline{b_L} - Z$ vertex. This can be achieved by choosing $\kappa_1 = 2\text{Re}(\kappa_2)$ such that $\text{Re}(\kappa_L^b)$ vanishes in Eq. (3.57). Later, in section 3.3, I will consider a specific model satisfying this assumption.

Since the imaginary parts of the couplings do not contribute, at one-loop level, to LEP physics of interest, I simply drop them hereafter. With this assumption one is left with one real parameter κ_L^t which will be denoted from now on by $\kappa_L/2$. The left-handed top quark couplings to the gauge bosons are

$$t_L - t_L - Z : \frac{g}{4c} \kappa_L \gamma_\mu (1 - \gamma_5),$$
 (3.59)

$$t_L - b_L - W: \frac{g}{2\sqrt{2}} \frac{\kappa_L}{2} \gamma_\mu (1 - \gamma_5)$$
 (3.60)

Notice the connection between the neutral and the charged current, as compared to Eq. (3.10):

$$\kappa_L^{NC} = 2\kappa_L^{CC} = \kappa_L \,. \tag{3.61}$$

This conclusion holds for any underlying theory with an approximate custodial symmetry such that the vertex $b_L - \overline{b_L} - Z$ is not modified as discussed above.

For the right-handed sector, the situation is different because the right-handed fermion fields are SU(2) singlet, hence the induced interactions do not see the full operator J_R but its components individually. Therefore, one cannot impose the previous connection between the neutral and charged current couplings.

The additional allowed interaction terms in the right-handed sector are given by

$$\mathcal{L}_{2} = \frac{g}{2c} \kappa_{R}^{t} {}^{NC} \overline{t_{R}} \gamma^{\mu} t_{R} J_{R_{\mu}}^{3} + \frac{g}{\sqrt{2}} \kappa_{R}^{CC} \overline{t_{R}} \gamma^{\mu} b_{R} J_{R_{\mu}}^{+}
+ \frac{g}{\sqrt{2}} \kappa_{R}^{CC} {}^{\dagger} \overline{b_{R}} \gamma^{\mu} t_{R} J_{R_{\mu}}^{-} - \frac{g}{2c} \kappa_{R}^{b} {}^{NC} \overline{b_{R}} \gamma^{\mu} b_{R} J_{R_{\mu}}^{3} ,$$
(3.62)

where $\kappa_R^{t \ NC}$ and $\kappa_R^{b \ NC}$ are two arbitrary real parameters and κ_R^{CC} is an arbitrary complex parameter. Note that in \mathcal{L}_2 we have one more additional coefficient than we have in \mathcal{L}_1 (in Eq. (3.53)), this is due to our previous assumption of using the full operator J_R in constructing the left-handed interactions. I assume that the $b_R - \overline{b_R} - Z$ vertex just as the $b_L - \overline{b_L} - Z$ vertex is not modified, then the coefficient $\kappa_R^{b \ NC}$ vanishes. Because κ_R^{CC} does not contribute to LEP physics in the limit of $m_b = 0$ and at the order $m_t^2 \ln \Lambda^2$ we are left with one real parameter $\kappa_R^{t \ NC}$ which will be denoted hereafter as κ_R . The right-handed top quark coupling to Z boson is

$$t_R - t_R - Z: \frac{g}{4c} \kappa_R \gamma_\mu (1 + \gamma_5) . \tag{3.63}$$

(As compared to Eq. (3.10), $\kappa_R = \kappa_R^{NC}$.)

In the rest of this section, I consider the models described by \mathcal{L}_1 and \mathcal{L}_2 with only two relevant parameters κ_L and κ_R . Performing the calculations as I discussed in the previous subsection one finds

$$\delta\epsilon_1 = \frac{G_F}{2\sqrt{2}\pi^2} 3m_t^2 \left(\kappa_R - \frac{\kappa_L}{2}\right) \ln(\frac{\Lambda^2}{m_t^2}) , \qquad (3.64)$$

$$\delta\epsilon_b = \frac{G_F}{2\sqrt{2}\pi^2} m_t^2 \left(-\frac{1}{4}\kappa_R + \kappa_L \right) \ln(\frac{\Lambda^2}{m_t^2}) . \tag{3.65}$$

These results simply correspond to those in Eqs. (3.33) and (3.34) after substituting $\kappa_L^{NC} = 2\kappa_L^{CC} = \kappa_L$ and $\kappa_R^{NC} = \kappa_R$.

The constraints on κ_L and κ_R for models with a light Higgs boson, a heavy Higgs boson, and without a Higgs boson are presented here in order. Let us first consider a light Higgs boson with $m_H=65$ GeV. I include the SM values for ϵ_1 and ϵ_b given in Ref. [26], the experimental fit on ϵ_1 and ϵ_b given in Eq. (3.35), and the nonstandard contribution given in Eqs. (3.64) and (3.65). I span the plane defined by κ_L and κ_R for a top quark mass of 170 GeV. Figure 3.6 shows the allowed range for those parameters within 95% C.L. As a general feature, one observes that the allowed range is a narrow area aligned close to the line $\kappa_L=2\kappa_R$ where for $m_t=170~{
m GeV}$ the maximum range for κ_L is between -0.03 and 0.23. In Table 3.1, I give the allowed range of the couplings κ_L and κ_R for different top quark masses. As the top quark mass increases this range shrinks and moves downward and to the right away form the origin $(\kappa_L, \kappa_R) = (0,0)$. This behavior can be understood if we notice that the width of the allowed area is controlled by ϵ_1 because of the small error in the value of $\epsilon_1^{\text{exp.}}$. Whereas, $\epsilon_b^{\text{exp.}}$ controls the length of the allowed region. As the top quark mass increases, the value of ϵ_1^{SM} increases. In order to be compatible with the experimental data, the nonstandard contribution to ϵ_1 prefers negative values, i.e., $2\kappa_R - \kappa_L \leq 0$.

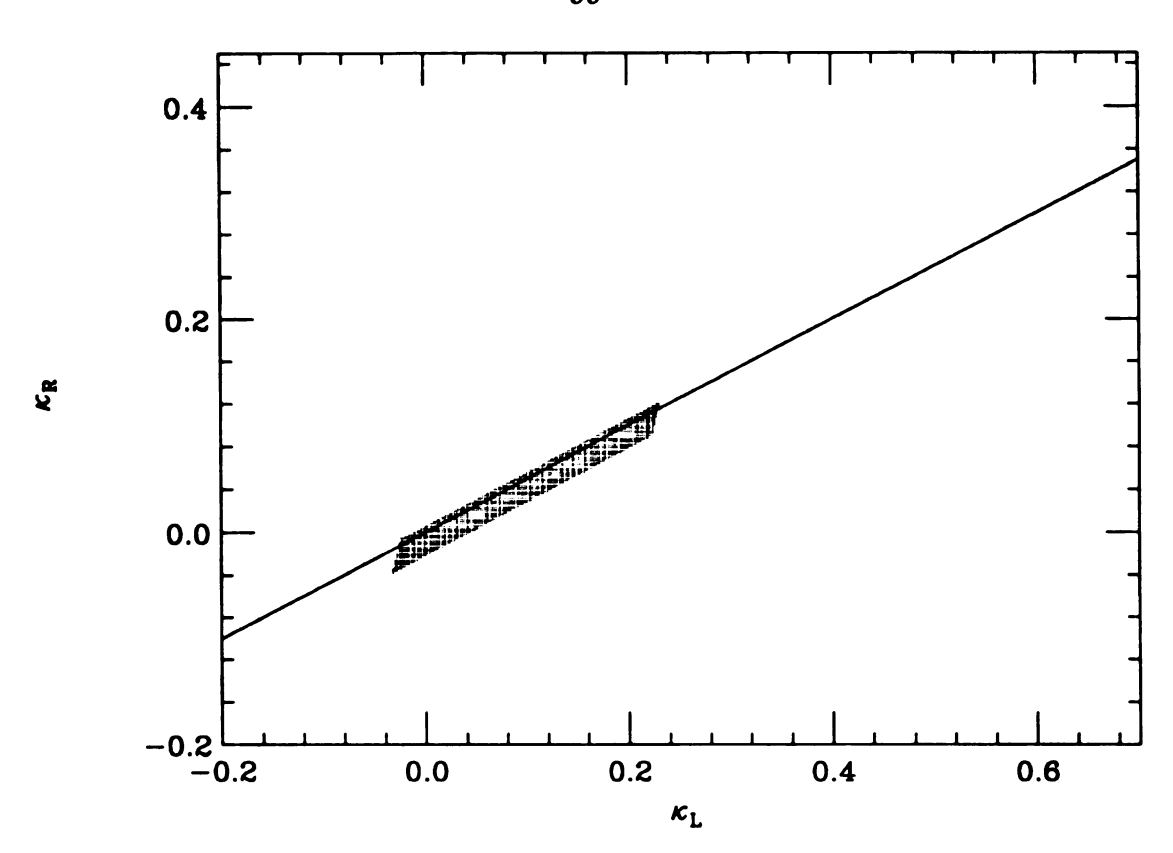


Figure 3.6: The allowed region of κ_L and κ_R , for $m_t = 170 \, \text{GeV}$, $m_H = 65 \, \text{GeV}$. (Note that $\kappa_L = \kappa_L^{NC} = 2\kappa_L^{CC}$ and $\kappa_R = \kappa_R^{CC}$.)

The observation that the allowed region shifts to the right, toward positive κ_L , as the top quark mass increases can be understood from the behavior of ϵ_b . As the top quark mass increases, the value of $\epsilon_b^{\rm SM}$ decreases forcing the nonstandard contribution to be more positive, *i.e.*, moving toward positive κ_L . The deviation from the relation $\kappa_L = 2\kappa_R$ for various top quark masses is given in Figure 3.7 by calculating $\kappa_L - 2\kappa_R$ as a function of m_t . Note that the SM has the solution $\kappa_L = \kappa_R = 0$, *i.e.*, the SM solution lies on the horizontal line shown in Figure 3.7. This solution ceases to exist for $m_t \geq 200$ GeV. The special relation $\kappa_L = 2\kappa_R$ is a consequence of the assumption of an approximate custodial symmetry which I imposed in connecting the left-handed neutral and charged currents.

As discussed above, the SM contribution to ϵ_b [26] is lower than the experimental

Table 3.1: The confined range of the couplings, κ_L and κ_R for various top quark masses and for $m_H=65$ GeV.

m_t (GeV)	κ_L	κ_R
120	-0.16 - 0.31	- 0.08 0.20
130	-0.12 - 0.28	- 0.07 0.17
140	-0.09 - 0.26	- 0.05 0.15
150	-0.07 - 0.25	- 0.05 0.14
160	-0.04 0.24	-0.03 0.13
170	-0.03 - 0.23	-0.03 - 0.12
180	-0.01 - 0.22	-0.02 - 0.11
190	0.00 0.21	-0.02 0.10
200	0.01 0.20	-0.02 - 0.09
210	0.02 0.20	-0.02 - 0.09
220	0.03 0.19	-0.01 0.08
230	0.04 0.19	- 0.01 - 0.07

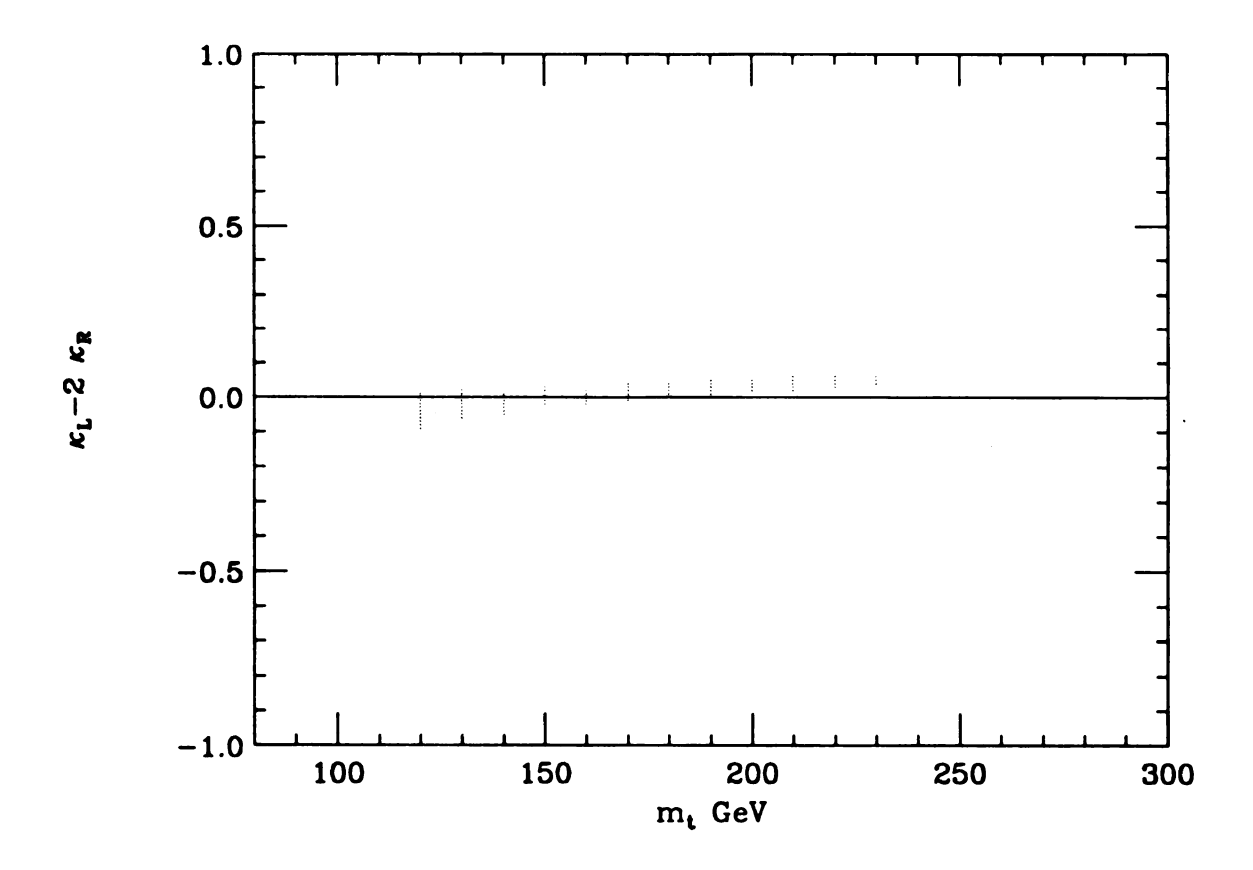


Figure 3.7: The allowed range of $(\kappa_L - 2\kappa_R)$ as a function of the mass of the top quark and for $m_H = 65$ GeV. (Note that $\kappa_L = \kappa_L^{NC} = 2\kappa_L^{CC}$ and $\kappa_R = \kappa_R^{CC}$.)

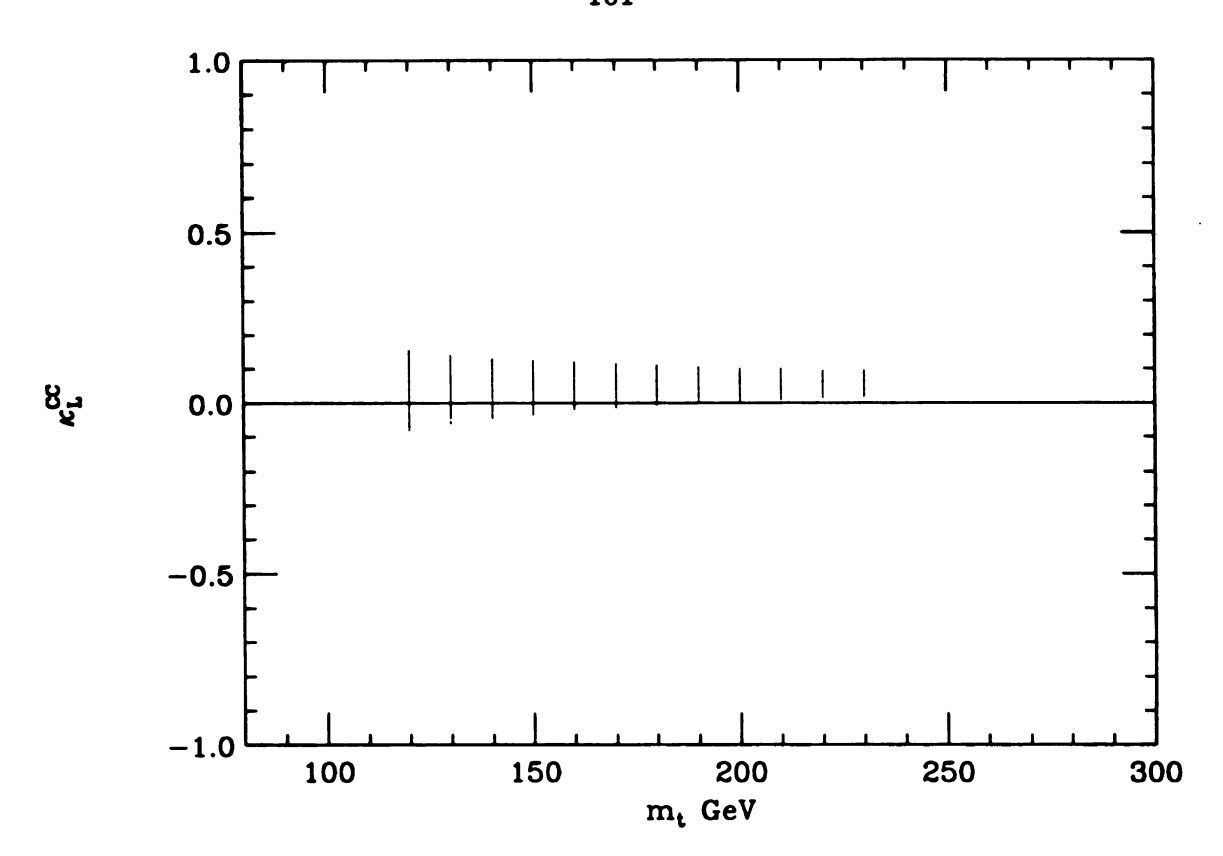


Figure 3.8: The allowed range of the coupling $\kappa_L^{CC} = \kappa_L^{NC}/2 = \kappa_L/2$ as a function of the mass of the top quark and for $m_H = 65$ GeV.

central value. This is reflected in the behavior of κ_L which prefers being positive to compensate this difference as can be seen from Eq. (3.65). This means that in models of electroweak symmetry-breaking with an approximate custodial symmetry, a positive κ_L is preferred. In Figure 3.8, I show the allowed values for $\kappa_L^{CC} = \kappa_L^{NC}/2 = \kappa_L/2$ as a function of m_t . With new physics effects ($\kappa_L \neq 0$) m_t can be as large as 300 GeV, although in the SM ($\kappa_L = 0$), as seen from Figure 3.8, m_t is bounded below 200 GeV.

Now, I would like to discuss the effect of the Higgs boson mass on the allowed range of these parameters. It is easy to anticipate the effect; since ϵ_b is not sensitive to the Higgs boson contribution up to one loop, the allowed range is only affected by the Higgs boson contribution to ϵ_1 which slightly affects its location relative to

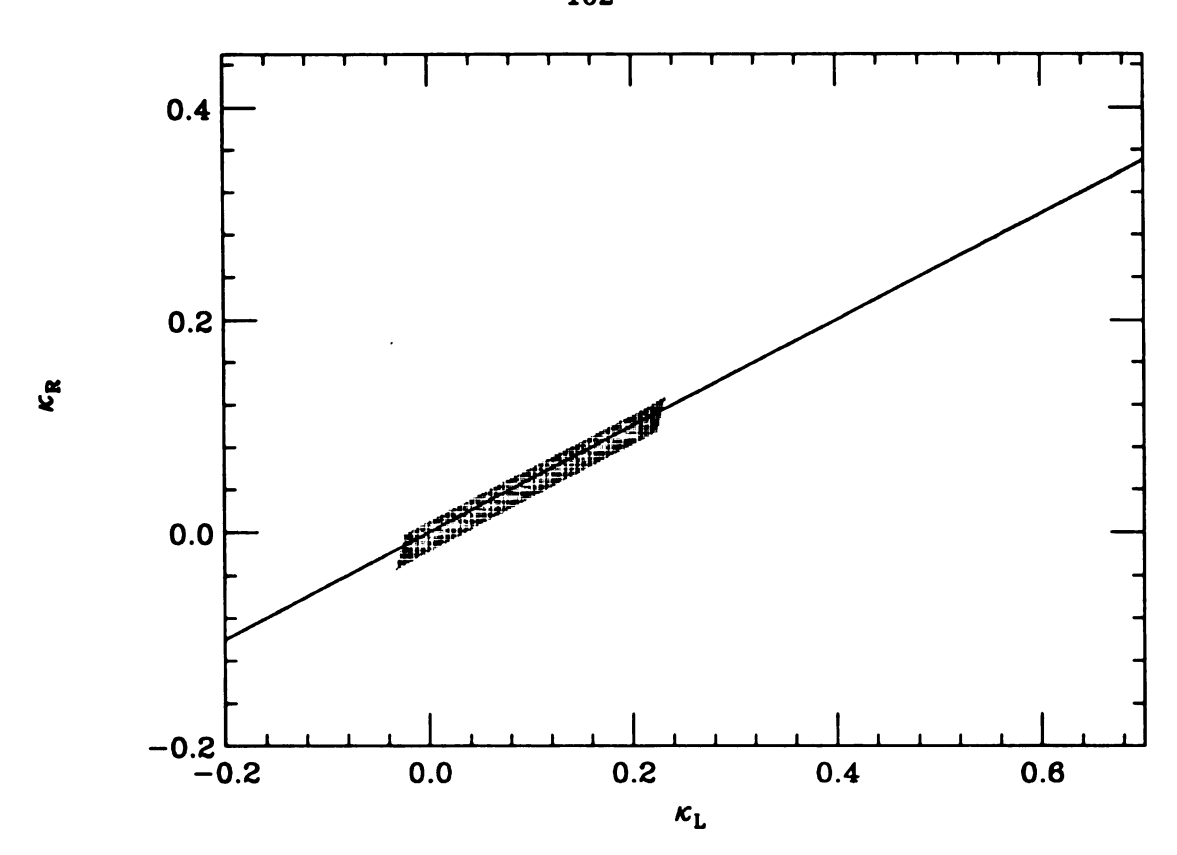


Figure 3.9: The allowed range of the coupling $\kappa_L^{CC} = \kappa_L^{NC}/2 = \kappa_L/2$ as a function of the mass of the top quark and for $m_H = 300$ GeV.

the line $\kappa_L = 2\kappa_R$. One expects that as the Higgs boson mass increases the allowed area moves upward. The reason simply lies in the fact that the standard Higgs boson contribution to ϵ_1 , up to one loop, becomes more negative for heavier Higgs boson (see section 1.5). Hence, $2\kappa_R$ prefers to be larger than κ_L to compensate this effect. However, this modification is not significant because ϵ_1 depends on the heavy Higgs boson mass only logarithmically. In Figures 3.9 and 3.10 I show the allowed range, within 95% C.L., for the parameters κ_L and κ_R for $m_t = 170$ GeV and for two choices of the heavy Higgs boson mass $m_H = 300$ GeV and $m_H = 1000$ GeV, respectively. Figures 3.9 and 3.10 are consistent with what one expects.

Now I consider the possibility of a new symmetry-breaking scenario without a fundamental scalar such as a SM Higgs boson. In this case, I simply subtract the

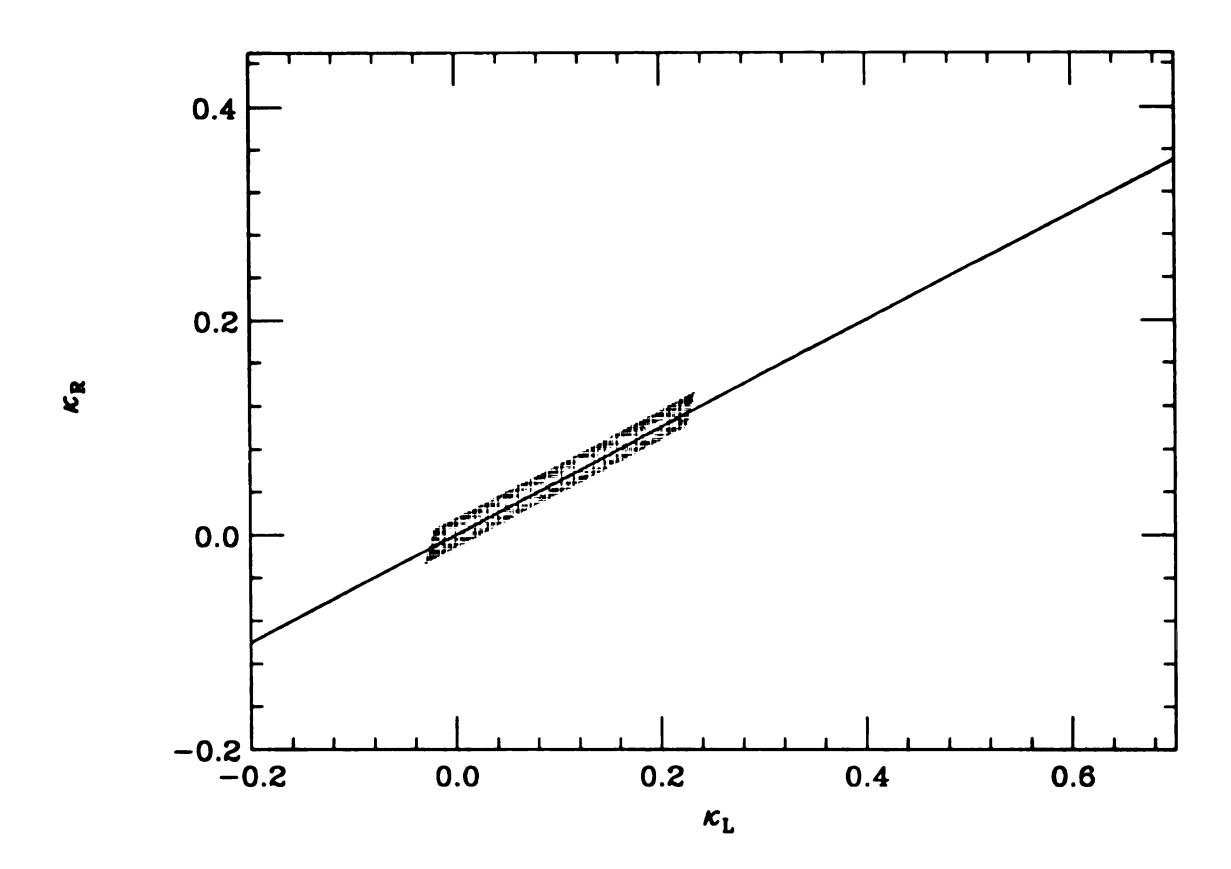


Figure 3.10: The allowed range of the coupling $\kappa_L^{CC} = \kappa_L^{NC}/2 = \kappa_L/2$ as a function of the mass of the top quark and for $m_H = 1000$ GeV.

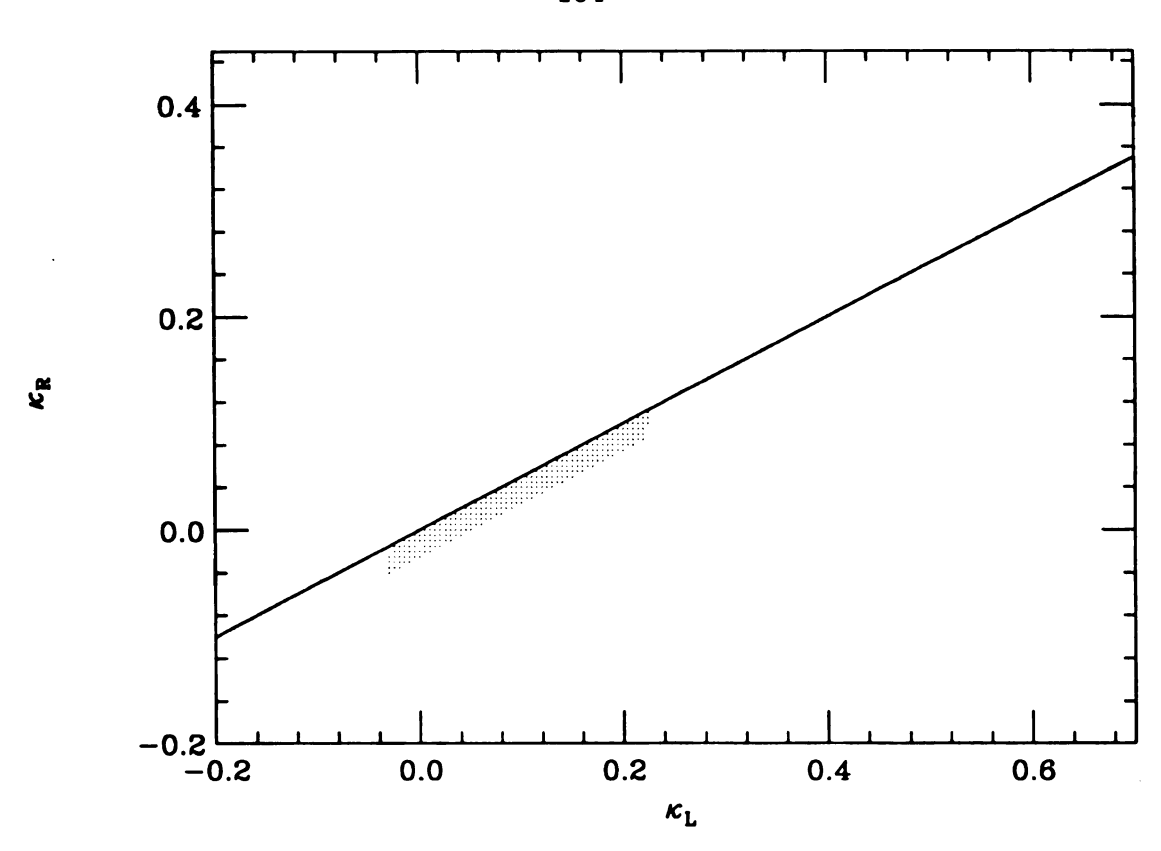


Figure 3.11: The allowed region of κ_L^{NC} and κ_R^{NC} , for models without a SM Higgs boson and for $m_t = 170$ GeV.

Higgs boson contribution from the SM results obtained in Ref. [26]. Figure 3.11 shows the allowed area in the κ_L and κ_R plane for a 170 GeV top quark in such models. In this case one expects to find no noticeable difference from the light Higgs boson case shown in Figure 3.6. This is true because a light Higgs bosons has a negligible contribution to ϵ_1 as compared to a heavy Higgs boson [21]. Therefore, the case of the no-Higgs boson scenario has a similar effect as the light Higgs case.

What we have learned is that to infer a bound on the Higgs boson mass from the measurement of the effective couplings of the top quark to gauge bosons, one needs a very precise measurement of the parameters κ_L and κ_R . However, from the correlations between the effective couplings (κ 's) of the top quark to the gauge bosons, one can infer if the symmetry-breaking sector is due to a Higgs boson or not, *i.e.*, we may be able to probe the symmetry-breaking mechanism in the top quark system. To illustrate this point, I would like to compare my results with those in Ref. [95]. Figure 3.12 shows the most general allowed region for the couplings κ_L^{NC} and κ_R^{NC} , i.e., without imposing any relation between κ_L^{NC} and κ_L^{CC} . This region is for a top quark mass of 170 GeV and covers the parameter space $-1.0 \le \kappa_L^{NC}$, $\kappa_R^{NC} \le 1.0$. One finds

$$-0.15 \le \kappa_L^{NC} \le 0.35$$
,

$$-1.0 \leq \kappa_R^{NC} \leq 1.0.$$

I also show on Figure 3.12 the allowed regions for our model $\left(\kappa_L^{CC} = 1/2\kappa_L^{NC}\right)$ and the model in Ref. [95] $\left(\kappa_L^{CC} = 0\right)$. The two regions overlap in the vicinity of the origin (0, 0) which corresponds to the SM case. Note that for $m_t \leq 200 \,\mathrm{GeV}$ the allowed region of κ 's in all models of symmetry-breaking should overlap near the origin because the SM is consistent with low energy data at the 95% C.L. For $\kappa_L^{NC} \geq 0.1$, these two regions diverge and become separable. One notices that the allowed range predicted in Ref. [95] lies along the line $\kappa_L^{NC} = \kappa_R^{NC}$ whereas in our case the slope is different $\kappa_L^{NC} = 2\kappa_R^{NC}$. This difference comes in because of the assumed dependence of κ_L^{CC} on the other two couplings κ_L^{NC} and κ_R^{NC} . In our case $\kappa_L^{CC} = \kappa_L^{NC}/2$, and in Ref. [95] $\kappa_L^{CC} = 0$.

If we imagine that any prescribed dependence between the couplings corresponds to a symmetry-breaking scenario, then, given the present status of low energy data, it is possible to distinguish between different scenarios if κ_L^{NC} , κ_R^{NC} and κ_L^{CC} are larger than 10%. Better future measurements of ϵ 's can further discriminate between different symmetry-breaking scenarios. Next, I will discuss how the SLC can contribute to the study of the nonstandard couplings.

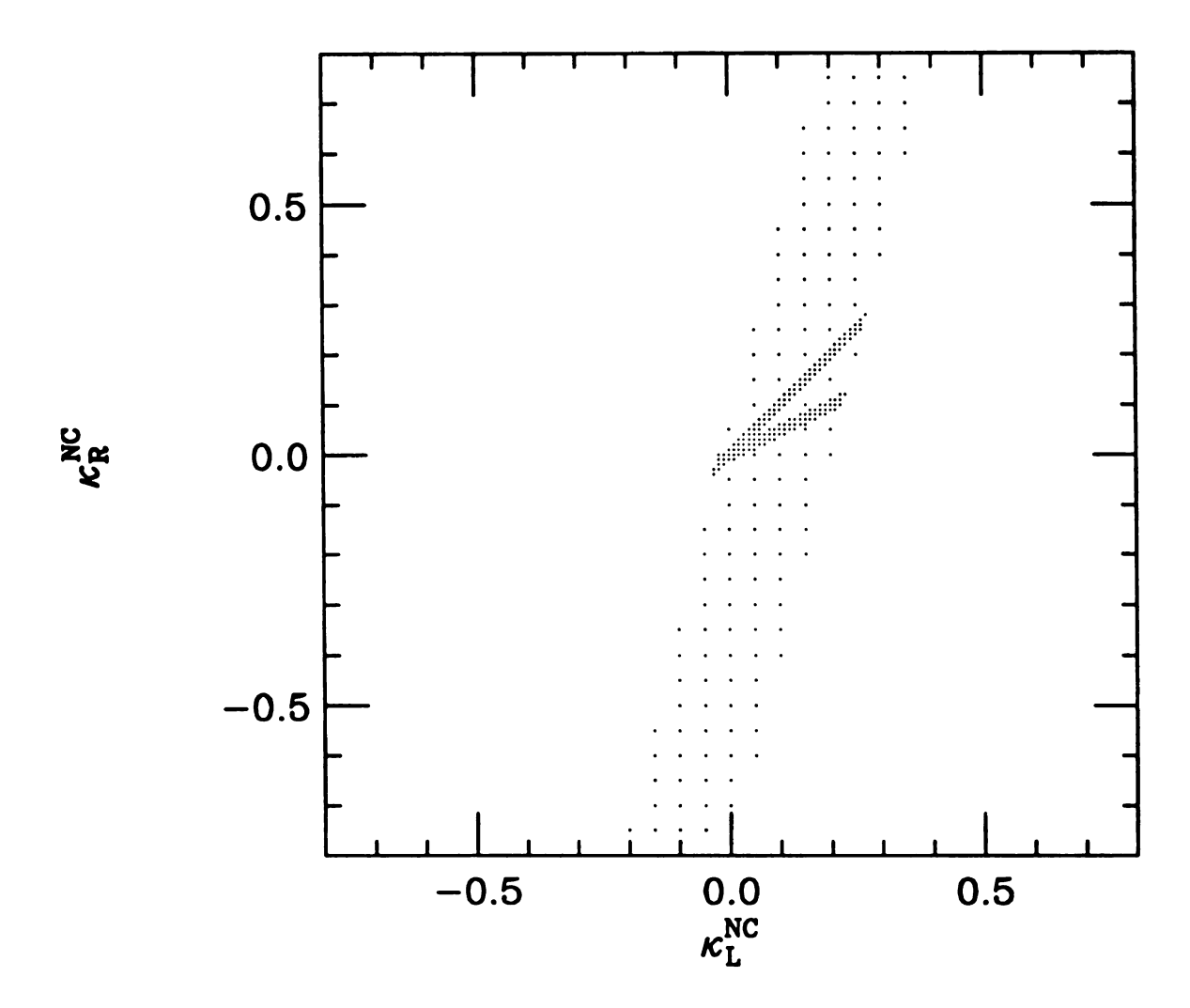


Figure 3.12: A comparison between our model and the model in Ref. [95]. The allowed regions in both models are shown on the plane of κ_L^{NC} and κ_R^{NC} , for $m_t=170$ GeV and $m_H=300$ GeV.

3.3.3 At the SLC

The measurement of the left-right cross section asymmetry A_{LR} in Z production with a longitudinally polarized electron beam at the SLC provides a further test of the SM and is sensitive to new physics. As I discussed in section 1.6, the reported measurement of A_{LR} [31] shows a deviation of about 2.8 σ from the SM prediction. By the SM prediction, I refer to the values in Table 1.2 with the reference masses $m_t = 175$ GeV and $m_H = 300$ GeV. In the previous discussion on the allowed space of the nonstandard couplings κ_L^{NC} , κ_R^{NC} , and κ_R^{CC} , I only concentrated on LEP data. It is interesting to investigate if our effective model can offer some explanation for the observed anomaly in A_{LR} . In section 1.4 we found that

$$A_{LR} = (A_{LR})|_{B} (1 + 17.3\epsilon_{1} - 22.5\epsilon_{3}) , \qquad (3.66)$$

where $(A_{LR})|_B$ is the improved Born value for A_{LR} .

In fact, as discussed below, the effect of the SLC measurement of A_{LR} on possible new physics in the top quark couplings depends on the way one incorporates A_{LR} with LEP data. There are two methods by which one can incorporate the SLC measurement of A_{LR} with the other existing low energy data at LEP. The first method is to combine and average A_{LR} with all LEP data. In this case, the anomaly in A_{LR} is washed away due to the large number of LEP measurements consistent with the SM. One finds that including the SLC measurement A_{LR} with all LEP data yields a new fit on the epsilon parameters with a slight decrease in the central value of ϵ_1 [38]

$$\epsilon_1^{\text{exp.}} = 3.5 \pm 1.5 \,, \tag{3.67}$$

while keeping the fit on ϵ_b the same. As discussed in the previous section, the non-standard coupling κ_L^{NC} is mostly constrained by ϵ_b . Therefore, no significant change

in the allowed range of κ_L^{NC} is expected. The effect of averaging the SLC and LEP data can be easily seen in the special model I discussed previously ($\kappa_L^{CC} = \kappa_L^{NC}/2$). In this case, the length of the allowed area is not affected since it is controlled by ϵ_b . Since the uncertainty in $\epsilon_1^{\text{exp.}}$ remains almost the same after including the A_{LR} measurement, the width of the allowed area is also hardly modified. The only effect will be to shift the allowed area slightly downward (toward $2\kappa_R < \kappa_L$). This conclusion is simply due to the preference for a more negative new physics contribution to accommodate the smaller value of $\epsilon_1^{\text{exp.}}$. It is interesting to note that the effect of including A_{LR} with the other LEP data is similar to the effect of a light Higgs boson.

The more interesting approach in dealing with the SLC measurement of A_{LR} is to ask whether our new effective model, checked against LEP data, can give some insight into the status of the SLC measurement of A_{LR} . In our effective model with nonstandard top quark couplings, the theoretical prediction for the observables A_e at LEP and A_{LR} at SLC are identical. Therefore, it is not possible to explain the anomaly in A_{LR} , at the 1σ level, without affecting the value of A_e which is in a very good agreement with the SM. However, at the 2σ level, one may be able to find a solution (notice that the SM is not a solution) which is compatible with both LEP and SLC measurements.

From Eq. (3.66) and using our effective model contribution to A_{LR} , one concludes that

$$A_{LR} = (A_{LR})|_{SM} (1 + 17.3\delta\epsilon_1) , \qquad (3.68)$$

where $\delta \epsilon_1$ is the nonstandard contribution to ϵ_1 , and

$$\delta\epsilon_1 = \frac{G_F}{2\sqrt{2}\pi^2} 3m_t^2 \left(-\kappa_L^{NC} + \kappa_R^{NC} + \kappa_L^{CC}\right) \ln\frac{\Lambda^2}{m_t^2} . \tag{3.69}$$

Since the reported measurement of A_{LR} is larger than the SM prediction as seen in

Table 1.2, the nonstandard contribution $\delta \epsilon_1$ prefers positive values, i.e., $\kappa_R^{NC} + \kappa_L^{CC} \geq \kappa_L^{NC}$. Therefore, the SLC measurement A_{LR} indicates a preference for that particular region of the parameter space.

It is much easier to appreciate the A_{LR} effect in dealing with the special model discussed in the previous section. In that special model with the approximate custodial symmetry, i.e., $\kappa_L^{NC} = 2\kappa_L^{CC} = \kappa_L$, the SLC A_{LR} measurement will have a significant effect on the allowed region in the κ_L and κ_R plane. In this case, one has

$$\delta\epsilon_1 = \frac{G_F}{4\sqrt{2}\pi^2} 3m_t^2 (-\kappa_L + 2\kappa_R) \ln \frac{\Lambda^2}{m_t^2} . \tag{3.70}$$

In Figure 3.13, I plot the allowed region for the parameters κ_L and κ_R using the SLC measurement of A_{LR} and ϵ_b extracted from the LEP data, for $m_t = 170$ GeV and $m_H = 300$ GeV at 95% C.L. From Figure 3.13 it is clear that the SLC measurement of A_{LR} indicates a preference for positive nonstandard contributions to $\delta\epsilon_1$, i.e., $\kappa_R \geq 2\kappa_L$. Also, one notices that the SM is excluded by the A_{LR} measurement at 95% C.L.

It is interesting to search for a solution which is compatible with the LEP and SLC data. In Figure 3.14, I plot the allowed region, the very narrow band, for $m_t = 170$ GeV and $m_H = 300$ GeV consistent with LEP data, at 95% C.L., and also compatible with the SLC measurement A_{LR} at the same level of accuracy. One can understand the result of Figure 3.14 as follows. First, as discussed before, there is no effect on the length of the allowed area since it is controlled by ϵ_b . Second, the measurement A_{LR} prefers positive values for $\delta\epsilon_1$, i.e., the region where $2\kappa_R > \kappa_L$. In other words it prefers the region above the line $2\kappa_R = \kappa_L$. This is the reason why we find the narrow band above the line $2\kappa_R = \kappa_L$. Obviously, in this case, the SM is excluded by the data for κ 's=0.

To understand the effect of the top quark mass m_t on the result let us concentrate

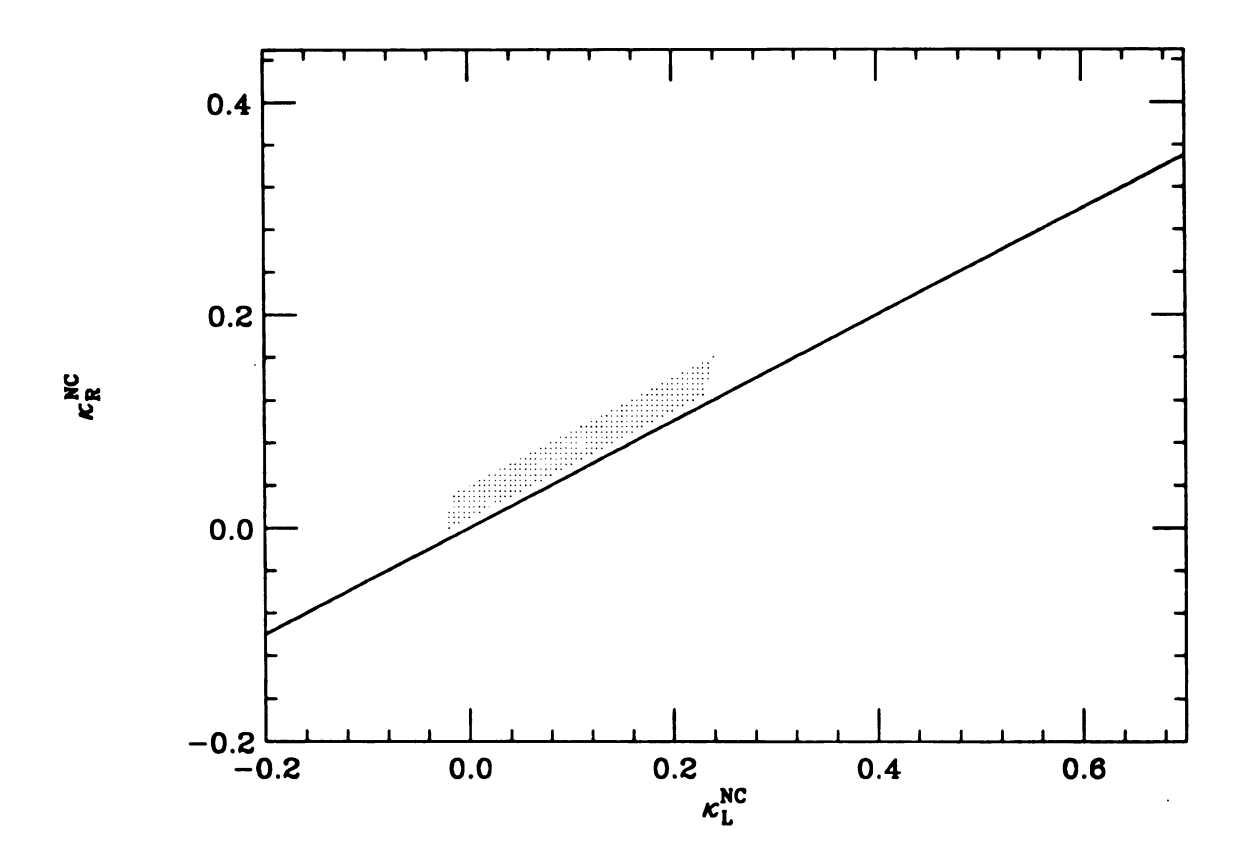


Figure 3.13: The allowed region of κ_L and κ_R , using the SLC measurement A_{LR} , for $m_t=170$ GeV and $m_H=300$ GeV.

on the two measurements: A_{ϵ} at LEP and A_{LR} at SLC. The two observables A_{ϵ} and A_{LR} have the same dependence on the quantity $\delta\epsilon_1$ [see Eq. (3.68)]. For a heavier top quark, the allowed band from the LEP fit shifts downward, this is because the SM prediction of A_{ϵ} increases. Similarly, the band consistent with A_{LR} also shifts downward, since the SM prediction of A_{LR} is identical to A_{ϵ} . Therefore, the two bands shift in the same direction. Furthermore, for a fixed κ_L , the difference between the central values of the experimental measurements, $\Delta = A_{LR}^{\exp} - A_{\epsilon}^{\exp}$, is proportional to the quantity

$$\Delta \propto m_t^2 (\kappa_R^{\rm SLC} - \kappa_R^{\rm LEP}) = m_t^2 \Delta_R, \tag{3.71}$$

where $\kappa_R^{\rm SLC}$ is the central value, for a fixed κ_L , of the allowed band extracted from the SLC measurement, similarly, for κ_R^{LEP} . Therefore, the difference Δ_R decreases as a function of the top quark mass. Nevertheless, the widths of the allowed bands decreases also as a function of the top quark mass. Thus, even though the two allowed bands from LEP and SLC move closer for a heavier top quark, their widths decrease rapidly such that the overlap in LEP and SLC data decreases as the top quark mass increases. In Figure 3.15 I plot the width of the overlapped region h, due to the measurements A_{ϵ} and A_{LR} , as a function of the top quark mass. Negative values of h indicates an overlap in the measurements while positive values indicates no overlap. One can see that the overlap |h| decreases as a function of the top quark mass. Nevertheless, a consistent solution for both measurements still exist for a wide range of m_t . The overlap does not depend on the Higgs boson mass m_H because the difference Δ_R is independent of m_H From Figure 3.14 it is clear that there will be no effect on the length of the allowed region which in our approximation is solely determined by ϵ_b . Hence, a more accurate measurement of ϵ_b , i.e., $\Gamma(Z \to b\bar{b})$, is needed to further confine the nonuniversal interactions of the top quark to gauge

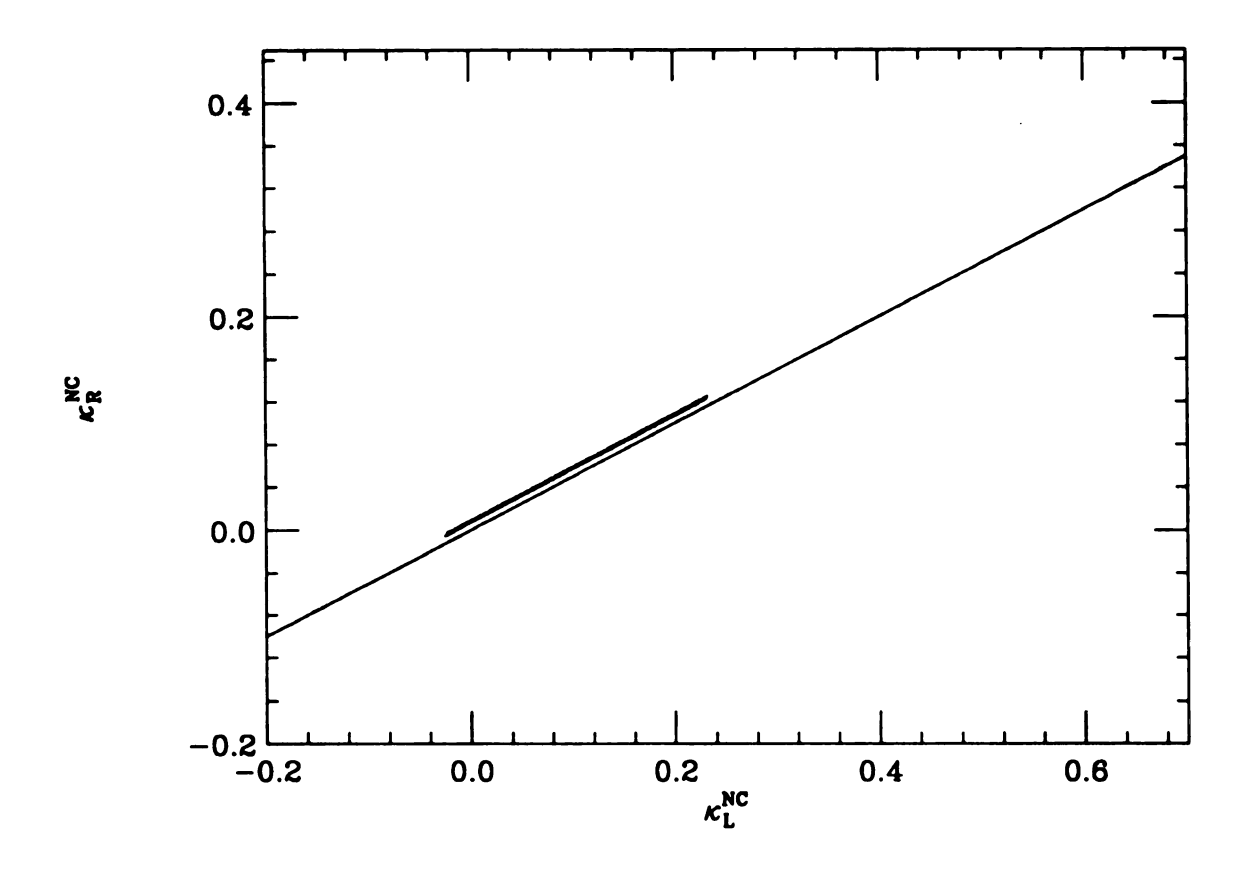


Figure 3.14: The allowed region of κ_L and κ_R , using LEP data and the SLC measurement of A_{LR} , for $m_t=170~{\rm GeV}$ and $m_H=300~{\rm GeV}$.

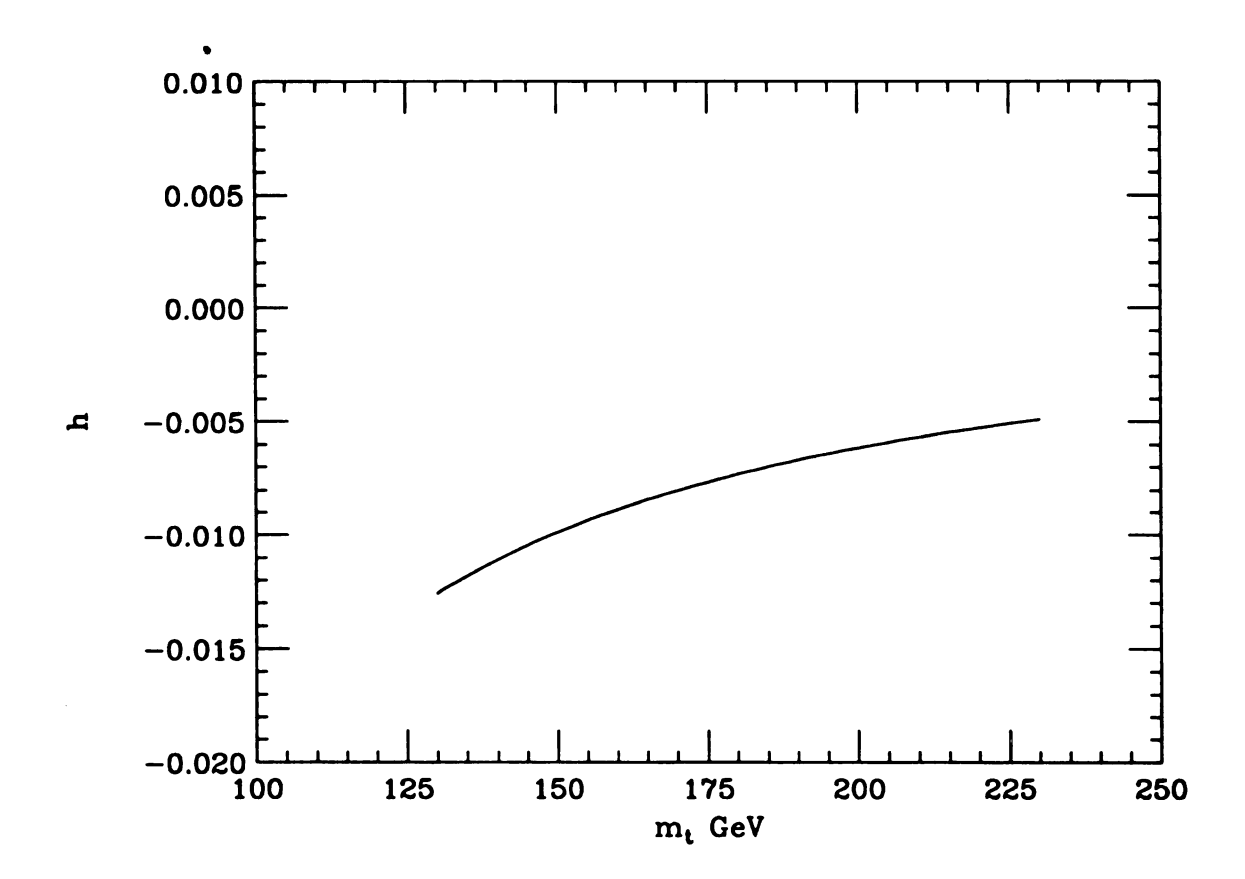


Figure 3.15: The overlapping of the two measurements A_e and A_{LR} as a function of the top quark mass. Negative values of h indicates overlapping, while positive values indicates no overlapping.

bosons to probe new physics.

3.4 Heavy Higgs Boson Limit in the SM

The goal of this study is to probe new physics effects, particularly the effects due to the symmetry-breaking sector, in the top quark system by examining the couplings of the top quark to the gauge bosons. To illustrate how a specific symmetry-breaking mechanism might affect these couplings, in this section I consider the Standard Model with a heavy Higgs boson $(m_H > m_t)$ as the full theory, and derive the effective couplings κ_L^{NC} , κ_R^{NC} , κ_L^{CC} , and κ_R^{CC} at the top quark mass scale in the effective Lagrangian after integrating out the heavy Higgs boson field.

Given the full theory (SM in this case), one can perform a matching between the underlying theory and the effective Lagrangian. In this case, the heavy Higgs boson mass acts as a regulator (cutoff) of the effective theory [103]. Figure 3.16 shows the Feynman diagrams needed to calculate the effective couplings of the top quark to the W and Z gauge bosons. While setting $m_b = 0$, and only keeping the leading terms of the order $m_t^2 \ln m_H^2$, I find the following effective couplings

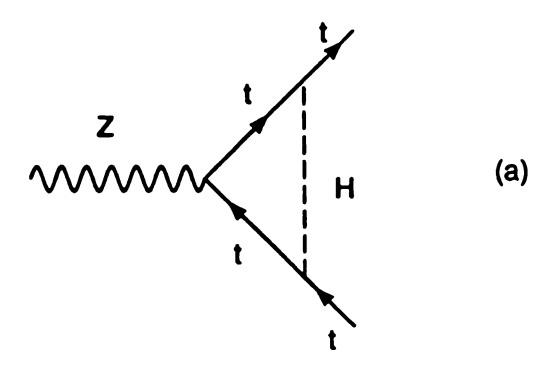
$$t - t - Z: \frac{g}{4c} \frac{G_F}{2\sqrt{2}\pi^2} \left(\frac{-1}{8} m_t^2 \gamma_\mu (1 - \gamma_5) + \frac{1}{8} m_t^2 \gamma_\mu (1 + \gamma_5) \right) \ln \left(\frac{m_H^2}{m_t^2} \right) , \qquad (3.72)$$

$$t - b - W: \frac{g}{2\sqrt{2}} \frac{G_F}{2\sqrt{2}\pi^2} \left(\frac{-1}{16}\right) m_t^2 \gamma_\mu (1 - \gamma_5) \ln \left(\frac{m_H^2}{m_t^2}\right). \tag{3.73}$$

From this result one concludes

$$\kappa_L^{\text{NC}} = 2\kappa_L^{\text{CC}} = \frac{G_F}{2\sqrt{2}\pi^2} \left(\frac{-1}{8}\right) m_t^2 \ln\left(\frac{m_H^2}{m_t^2}\right) , \qquad (3.74)$$

$$\kappa_R^{\rm NC} = \frac{G_F}{2\sqrt{2}\pi^2} \frac{1}{8} m_t^2 \ln\left(\frac{m_H^2}{m_t^2}\right) \,, \tag{3.75}$$



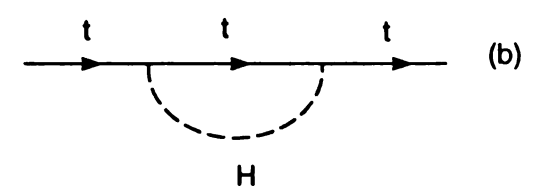


Figure 3.16: The Feynman diagrams needed to calculate the effective couplings of the top quark to the W and Z gauge bosons.

$$\kappa_R^{CC} = 0. ag{3.76}$$

Note that the relation between the left-handed currents ($\kappa_L^{NC} = 2\kappa_L^{CC}$) agree with our prediction because of the approximate custodial symmetry in the full theory (SM) and the fact that vertex b-b-Z is not modified. The right-handed currents κ_R^{CC} and κ_R^{NC} are not correlated, and κ_R^{CC} vanishes for a massless b. Also, note that an additional relation in the effective Lagrangian between the left- and right-handed effective couplings of the top quark to Z boson emerges, i.e.,

$$\kappa_L^{NC} = -\kappa_R^{NC} \,. \tag{3.77}$$

This means only the axial vector current of t-t-Z acquires a nonuniversal contribution while its vector current is not modified.

As discussed in Section 3.2, due to the Ward identities associated with the photon field there can be no nonuniversal contribution to either the b-b-A or t-t-A vertex after renormalizing the fine structure constant α . This can be explicitly checked in this model. Furthermore, up to the order of $m_t^2 \ln m_H^2$, the vertex b-b-Z is not modified which agrees with the assumption I made in Section 3.2 that there exists a dynamics of electroweak symmetry-breaking such that neither b_R - $\overline{b_R}$ -Z nor b_L - $\overline{b_L}$ -Z in the effective Lagrangian is modified at the scale of m_t .

From this example one learns that the effective couplings of the top quark to gauge bosons arising from a heavy Higgs boson are correlated in a specific way: namely,

$$\kappa_L^{NC} = 2\kappa_L^{CC} = -\kappa_R^{NC} \,. \tag{3.78}$$

can be arbitrary, and are not necessarily 1/2 and 1/4, respectively). In other words, if the couplings of a heavy top quark to the gauge bosons are measured and exhibit large deviations from these relations, then it is likely that the electroweak symmetry-breaking is not due to the standard Higgs mechanism which contains a fundamental heavy scalar boson. This illustrates how the symmetry-breaking sector can be probed by measuring the effective couplings of the top quark to gauge bosons.

Next, I study how the Tevatron, the LHC, and the LC can contribute to the measurements of the nonstandard couplings.

3.5 Direct Measurement of the Top Quark Couplings

In Section 3.2, I concluded that the precision LEP data can constrain the couplings κ_L^{NC} , κ_R^{NC} and κ_L^{CC} , but not κ_R^{CC} (the right-handed charged current). The nonstandard coupling κ_R^{CC} can be studied using the $b \to s\gamma$ measurement [98]. Also,

I discussed how the SLC measurement of A_{LR} can contribute to the study of the non-standard couplings κ_L^{NC} , κ_R^{NC} and κ_L^{CC} . The conclusion that the SM is not compatible with the combined LEP and SLC data may be an indirect evidence for the anomalous couplings of the top quark. In this section, I examine briefly how to improve our knowledge on these couplings at the other current and future colliders.

3.5.1 At the Tevatron and the LHC

In this section, I study how to constrain the nonstandard couplings of the top quark to the gauge bosons from direct detection of the top quark at hadron colliders.

At the Tevatron and the LHC, heavy top quarks are predominantly produced from the QCD process $gg, q\bar{q} \to t\bar{t}$ and the W-gluon fusion process $qg(Wg) \to t\bar{b}, \bar{t}b$. In the former process, one can probe κ_L^{CC} and κ_R^{CC} from the decay of the top quark to a bottom quark and a W boson. In the latter process, these nonstandard couplings can be measured by simply counting the production rates of signal events with a single t or t. More details can be found in Ref. [104].

To probe κ_L^{CC} and κ_R^{CC} from the decay of the top quark to a bottom quark and a W boson, one needs to measure the polarization of the W boson. For a massless b, the W boson from top quark decay can only be either longitudinally or left-handed polarized for a left-handed charged current ($\kappa_R^{CC} = 0$). For a right-handed charged current ($\kappa_L^{CC} = -1$) the W boson can only be either longitudinally or right-handed polarized. (Note that the handedness of the W boson is reversed for a massless \bar{b} from \bar{t} decays.) In all cases the fraction of longitudinal W from top quark decay is enhanced by $m_t^2/2M_W^2$ as compared to the fraction of transversely polarized W. Therefore, for a more massive top quark, it is more difficult to untangle the κ_L^{CC} and κ_R^{CC} contributions. The W polarization measurement can be done by measuring the

invariant mass $(m_{b\ell})$ of the bottom quark and the charged lepton from the decay of top quark [105]. We note that this method does not require knowing the longitudinal momentum (with two-fold ambiguity) of the neutrino from W decay to reconstruct the rest frame of the W boson in the rest frame of the top quark.

Consider the (upgraded) Tevatron as a $\bar{p}p$ collider at $\sqrt{s} = 2$ or 3.5 TeV, with an integrated luminosity of 1 or 10 fb⁻¹. Unless specified otherwise, we will give event numbers for a 175 GeV top quark and an integrated luminosity of 1 fb⁻¹.

The cross section of the QCD process $gg, q\bar{q} \to t\bar{t}$ is about 7 (29) pb at a $\sqrt{s}=2$ (3.5) TeV collider. In order to measure κ_L^{CC} and κ_R^{CC} we have to study the decay kinematics of the reconstructed t and/or \bar{t} . For simplicity, let us consider the $\ell^{\pm}+\geq$ 3 jet decay mode, whose branching ratio is $Br=2\frac{26}{9}\frac{8}{9}=\frac{8}{27}$, for $\ell^{+}=e^{+}$ or μ^{+} . We assume an experimental detection efficiency, which includes both the kinematic acceptance and the efficiency of b-tagging, of 15% for the $t\bar{t}$ event. We further assume that there is no ambiguity in picking up the right b (\bar{b}) to combine with the charged lepton ℓ^{+} (ℓ^{-}) to reconstruct t (\bar{t}). In total, there are 7 pb × 10³ pb⁻¹ × $\frac{8}{27}$ × 0.15 = 300 reconstructed $t\bar{t}$ events to be used in measuring κ_L^{CC} and κ_R^{CC} at $\sqrt{s}=2$ TeV. The same calculation at $\sqrt{s}=3.5$ TeV yields 1300 reconstructed $t\bar{t}$ events. Given the number of reconstructed top quark events, one can in principle fit the $m_{b\ell}$ distribution to measure κ_L^{CC} and κ_R^{CC} . We note that the polarization of the W boson can also be studied from the distribution of $\cos\theta_{\ell}^{*}$, where θ_{ℓ}^{*} is the polar angle of ℓ in the rest frame of the W boson whose z-axis is the W bosons moving direction in the rest frame of the top quark [105]. For a massless b, $\cos\theta_{\ell}^{*}$ is related to $m_{b\ell}^{2}$ by

$$\cos \theta_{\ell}^* \simeq \frac{2m_{b\ell}^2}{m_{\ell}^2 - M_W^2} - 1. \tag{3.79}$$

However, in reality, the momenta of the bottom quark and the charged lepton will be smeared by the detector effects and the most serious problem in this analysis is the identification of the right b to reconstruct t. There are two strategies to improve the efficiency of identifying the right b. One is to demand a large invariant mass of the $t\bar{t}$ system so that t is boosted and its decay products are collimated. Namely, the right b will be moving closer to the lepton from t decay. This can be easily enforced by demanding lepton ℓ with large transverse momentum. Another is to identify the nonisolated lepton from \bar{b} decay (with a branching ratio $Br(\bar{b} \to \mu^+ X) \sim 10\%$). Both of these methods will further reduce the reconstructed signal rate by an order of magnitude. How will these affect our conclusion on the determination of the nonuniversal couplings κ_L^{CC} and κ_R^{CC} ? This cannot be answered in the absence of detailed Monte Carlo studies.

Here I propose to probe the couplings κ_L^{CC} and κ_R^{CC} by measuring the production rate of the single-top quark events. A single-top quark event can be produced from either the W-gluon fusion process $qg\left(W^+g\right) \to t\bar{b}X$, or the Drell-Yan-type process $q\bar{q} \to W^* \to t\bar{b}$. Including both the single-t and single- \bar{t} events, for a 2 (3.5) TeV collider, the W-gluon fusion rate is 2 (16) pb; the Drell-Yan type rate is 0.6 (1.5) pb. The Drell-Yan-type event is easily separated from the W-gluon fusion event, therefore it will not be considered hereafter [106]. For the decay mode of $t \to bW^+ \to b\ell^+\nu$, with $\ell^+ = e^+$ or μ^+ , the branching ratio of interest is $Br = \frac{2}{9}$. The kinematic acceptance of this event at $\sqrt{s} = 2$ TeV is found to be 0.55 [106]. If the efficiency of b-tagging is 30%, there will be 2 pb \times 10³ pb⁻¹ \times $\frac{2}{9} \times$ 0.55 \times 0.3 = 75 single-top quark events reconstructed. At $\sqrt{s} = 3.5$ TeV the kinematic acceptance of this event is 0.50 which, from the above calculation yields about 530 reconstructed events. Based on statistical error alone, this corresponds to a 12% and 4% measurement on the single-top cross section. A factor of 10 increase in the luminosity of the collider can improve the measurement by a factor of 3 statistically.

Taking into account the theoretical uncertainties, we examine two scenarios: 20%

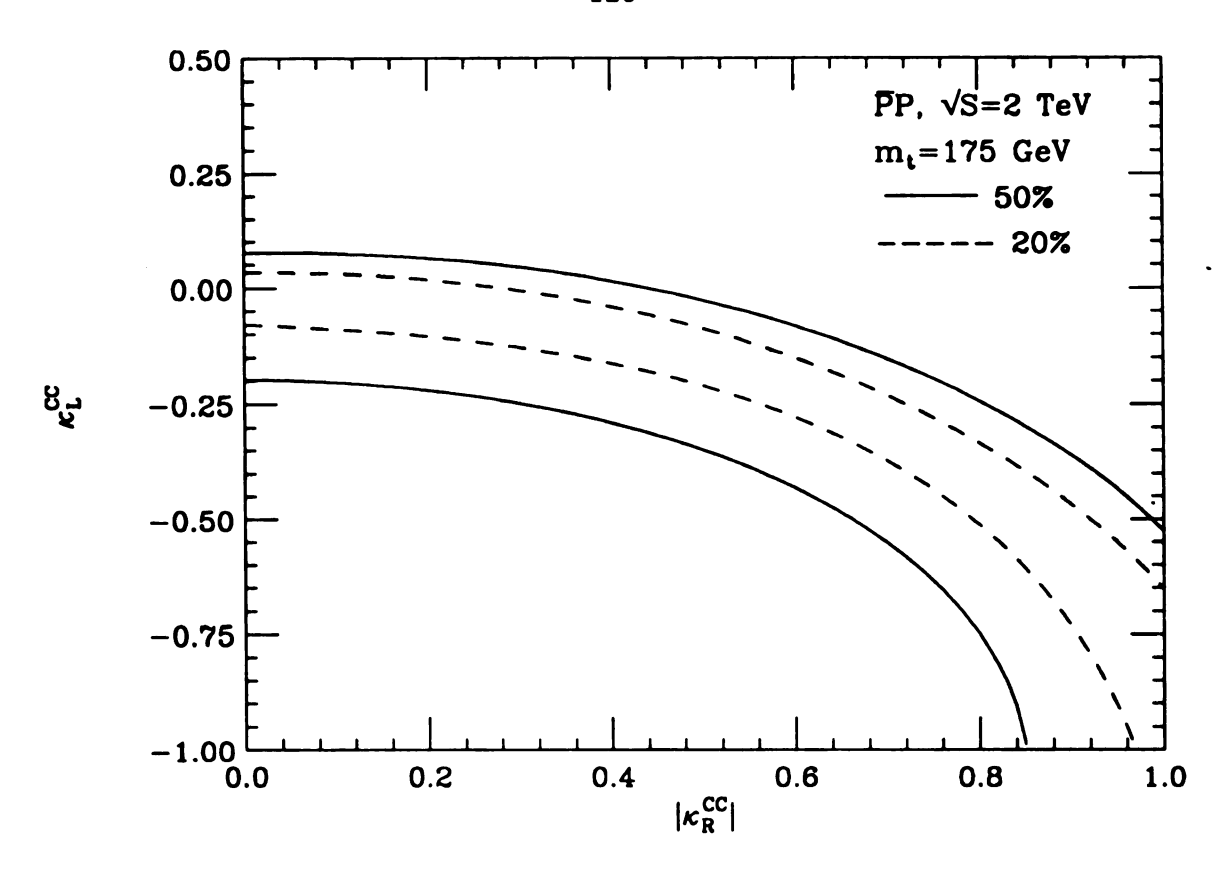


Figure 3.17: The allowed $|\kappa_R^{CC}|$ and κ_L^{CC} are bounded within the two dashed (solid) lines for a 20% (50%) error on the measurement of the single-top production rate, for a 175 GeV top quark.

and 50% error on the measurement of the single-top cross section, which depends on both κ_L^{CC} and κ_R^{CC} . (Here we assume the experimental data agrees with the SM prediction within 20% (50%).) We found that for a 175 GeV top quark κ_L^{CC} and κ_R^{CC} are well constrained inside the region bounded by two (approximate) ellipses, as shown in Figure 3.17. These results are not sensitive to the energies of the colliders considered here.

The top quark produced from the W-gluon fusion process is almost 100% left-handed (right-handed) polarized for a left-handed (right-handed) t-b-W vertex, therefore the charged lepton ℓ + from t decay has a harder momentum in a right-handed t-b-W coupling than in a left-handed coupling. (Note that the couplings

of light-fermions to W boson have been well tested from the low energy data to be left-handed as described in the SM.) This difference becomes smaller when the top quark is more massive because the W boson from the top quark decay tends to be more longitudinally polarized.

A right-handed charged current is absent in a linearly $SU(2)_L$ invariant gauge theory with a massless bottom quark. In this case $\kappa_R^{CC} = 0$, then κ_L^{CC} can be constrained to within about $-0.08 < \kappa_L^{CC} < 0.03$ ($-0.20 < \kappa_L^{CC} < 0.08$) with a 20% (50%) error on the measurement of the single-top quark production rate at the Tevatron. This means that if we interpret $(1 + \kappa_L^{CC})$ as the CKM matrix element V_{tb} , then V_{tb} can be bounded as $V_{tb} > 0.9$ (or 0.8) for a 20% (or 50%) error on the measurement of the single-top production rate. Recall that if there are more than three generations, within 90% C.L., V_{tb} can be anywhere between 0 and 0.9995 from low energy data [9]. This measurement can therefore provide useful information on possible additional fermion generations. Measuring the Drell-Yan-type single-top production rate can further improve the measurement of V_{tb} .

We expect the LHC can provide similar or better bounds on these nonstandard couplings when detailed analyses are available.

3.5.2 At the LC

The best place to probe κ_L^{NC} and κ_R^{NC} associated with the t-t-Z coupling is at the LC through $e^-e^+ \to A$, $Z \to t\bar{t}$. A detailed Monte Carlo study on the measurement of these couplings at the LC including detector effects and initial state radiation can be found in Ref. [107]. The bounds were obtained by studying the angular distribution and the polarization of the top quark produced in e^-e^+ collisions. Assuming a 50 fb⁻¹ luminosity at $\sqrt{s} = 500 \, \text{GeV}$, we concluded that within a 90% confidence level,

it should be possible to measure κ_L^{NC} to within about 8%, while κ_R^{NC} can be known to within about 18%. A 1 TeV machine can do better than a 500 GeV machine in determining κ_L^{NC} and κ_R^{NC} because the relative sizes of the $t_R(\bar{t})_R$ and $t_L(\bar{t})_L$ production rates become small and the polarization of the $t\bar{t}$ pair is purer. Namely, it is more likely to produce either a $t_L(\bar{t})_R$ or a $t_R(\bar{t})_L$ pair. A purer polarization of the $t\bar{t}$ pair makes κ_L^{NC} and κ_R^{NC} better determined. (The purity of the $t\bar{t}$ polarization can be further improved by polarizing the electron beam.) Furthermore, the top quark is boosted more in a 1 TeV machine thereby allowing a better determination of its polar angle in the $t\bar{t}$ system because it is easier to find the right b associated with the lepton to reconstruct the top quark moving direction.

Finally, we remark that at the LC κ_L^{CC} and κ_R^{CC} can be studied either from the decay of the top quark pair or from the single-top quark production process, W-photon fusion process $e^-e^+(W\gamma) \to tX$, or $e^-\gamma(W\gamma) \to \bar{t}X$, which is similar to the W-gluon fusion process in hadron collisions.

3.6 Discussion and Conclusions

In this chapter I have applied the electroweak chiral Lagrangian to probe new physics beyond the SM through studying the couplings of the top quark to gauge bosons. First, I examined the precision LEP data to extract the information on these couplings. Second, I discussed how the SLC measurement A_{LR} can contribute to the constraints on the nonstandard couplings κ_L^{NC} , κ_R^{NC} , and κ_L^{CC} . Third, I discussed how to improve our knowledge about the top quark nonstandard couplings at current and future colliders such as at the Tevatron, the LHC, and the LC.

Because of the non-renormalizability of the electroweak chiral Lagrangian one can only estimate the size of these nonstandard couplings by studying the contributions to LEP observables at the order of $m_t^2 \ln \Lambda^2$, where $\Lambda = 4\pi v \sim 3$ TeV is the cutoff scale of the effective Lagrangian. Already I found interesting constraints on these couplings.

Assuming b-b-Z vertex is not modified, I found that κ_L^{NC} is already constrained to be $-0.05 < \kappa_L^{NC} < 0.17$ (0.0 < $\kappa_L^{NC} < 0.15$) by LEP data at the 95% C.L. for a 160 (180) GeV top quark. Although κ_R^{NC} and κ_L^{CC} are allowed to be in the full range of ± 1 , the precision LEP data do impose some correlations among κ_L^{NC} , κ_R^{NC} , and κ_L^{CC} . (κ_R^{CC} does not contribute to the LEP observables of interest in the limit of $m_b = 0$.) In my calculations, these nonstandard couplings are only inserted once in loop diagrams using dimensional regularization.

Inspired by the experimental fact $\rho \approx 1$, reflecting the existence of an approximate custodial symmetry, I proposed an effective model to relate κ_L^{NC} and κ_L^{CC} . I found that the nonuniversal interactions of the top quark to gauge bosons parameterized by κ_L^{NC} , κ_R^{NC} , and κ_L^{CC} are well constrained by LEP data, within 95% C.L. The results are summarized in Table 3.1 (see also Figures 3.6–3.10). Also, the two parameters $\kappa_L = \kappa_L^{NC}$ and $\kappa_R = \kappa_R^{NC}$ are strongly correlated. In my model, $\kappa_L \sim 2\kappa_R$.

I note that the relations among κ 's can be used to test different models of electroweak symmetry-breaking. For instance, a heavy SM Higgs boson $(m_H > m_t)$ will modify the couplings t-t-Z and t-b-W of a heavy top quark at the scale m_t such that $\kappa_L^{NC} = 2\kappa_L^{CC}$, $\kappa_L^{NC} = -\kappa_R^{NC}$, and $\kappa_R^{CC} = 0$. Another example is the effective model discussed in Ref. [95] where, $\kappa_R^{CC} = \kappa_L^{CC} = 0$. In this model the low energy precision data impose the relation $\kappa_L^{NC} \sim \kappa_R^{NC}$. Also, the simple commuting extended technicolor model presented in Ref. [59] predicts that the nonstandard top quark couplings are of the same order as the nonstandard bottom quark couplings.

It is also interesting to note that the upper bound on the top quark mass can

be raised from the SM bound $m_t < 200$ GeV to as large as 300 GeV if new physics occurs. That is to say, if there is new physics associated with the top quark, it is possible that the top quark is heavier than what the SM predicts. However, for a SM top quark, m_t should be less than 200 GeV, as shown in Figures 3.7 and 3.8.

Also, I discussed how the present SLC measurement of A_{LR} can contribute to the constraints imposed on the nonstandard couplings κ_L^{NC} , κ_R^{NC} , and κ_L^{CC} at LEP. I found that if one uses the LEP constraints to predict the new physics contribution to the SLC measurement A_{LR} , then for the special model, $\kappa_L^{CC} = \kappa_L^{NC}/2$, it is possible to reconcile the LEP and SLC data at 95% C.L. for a wide range of the top quark mass. This is shown in Figure 3.15.

Undoubtedly, direct detection of the top quark at the Tevatron, the LHC, and the LC is crucial to measuring the couplings of t-b-W and t-t-Z. At hadron colliders, κ_L^{CC} and κ_R^{CC} can be measured by studying the polarization of the W boson from top quark decay in $t\bar{t}$ events. They can also be measured simply from the production rate of the single top quark event. The LC is the best machine to measure κ_L^{NC} and κ_R^{NC} which can be measured from studying the angular distribution and the polarization of the top quark produced in e^-e^+ collision. Details about these bounds were given in Section 3.5.

Chapter 4

Heavy Top Quark Effects and the Scalar Sector

4.1 Introduction

In chapter 3, I calculated the one-loop level quadratic contribution of the top quark mass m_t , i.e., $m_t^2 \ln \Lambda^2$, to the parameters ϵ_1 and ϵ_b . The calculation is based on the Lagrangian $\mathcal{L}_0 + \mathcal{L}_1$ (see Eqs. (2.29) and (3.9)). In general, in performing the one loop level calculation, one needs to consider a gauge invariant set of Feynman diagrams in which massive gauge bosons can appear as external and/or internal lines. However, at one-loop level, I found that to extract the $m_t^2 \ln \Lambda^2$ dependence of the low energy observables (equivalently, ϵ_1 and ϵ_b) one only needs to include the massive gauge bosons as external fields. Figure 3.1 shows the relevant Feynman diagrams needed to extract the m_t^2 dependence in a general R_ξ gauge. Only the Goldstone bosons and the top quark appear as internal (propagating) fields. The gauge bosons behave as classical (non-propagating) fields. This result is expected since extracting corrections in power of m_t is equivalent to a perturbative expansion in the Yukawa coupling $g_t = m_t/v$ which has nothing to do with the gauge structure [108]. This is true because the m_t^2 corrections are present even for vanishing gauge couplings ie g and $g' \to 0$. The m_t^2 corrections are a consequence of the symmetry-breaking mechanism

which controls the Yukawa interactions connecting the scalar fields and the fermion sector. This observation is important because one can generalize it to include the pure dependence on the top quark mass to all orders and not merely to the one-loop level. Furthermore, with the gauge couplings switched off in the Lagrangian, one can derive a set of Ward identities which relates the physical quantities, as discussed in the next section, to appropriate renormalization constants of the reduced Lagrangian (with gauge couplings switched off).

This observation was made for the SM case in Ref. [108], where explicit calculation of the two loop m_t^4 corrections to the low energy observables was performed for arbitrary values of the Higgs mass m_H . The calculation was performed by considering the Lagrangian of the SM in the limit of vanishing gauge coupling constants. The gauge bosons play the role of external sources and the relevant propagating fields are the top quark, the massless bottom quark, the Higgs boson field, and the charged and neutral Goldstone bosons ϕ^{\pm} , ϕ^3 . This reduced Lagrangian is called the Gaugeless Limit of the SM [108].

In this chapter, I develop a similar formalism to calculate, at one loop level, the contribution to ϵ_1 and ϵ_b that grows like m_t^2 in the chiral Lagrangian framework. The formalism holds for all contributions which do not vanish when setting the gauge couplings g and g' to be zero. Therefore, generalizing the result in Ref. [108] to incorporate a larger set of effective models. Similarly, I find that to extract the m_t^2 dependence in the chiral Lagrangian framework, one needs to concentrate only on the Goldstone bosons, the top quark, and the massless bottom quark. The calculation of m_t^2 dependence in the new formalism gives an identical result to the one I found in chapter 3.

Similar to the procedure in chapter 3, I consider an effective field theory describing the nonstandard top couplings to the gauge bosons. I show how to conveniently relate various radiative corrections important for testing the standard model (SM) in a rather elegant and clear way. More importantly, this approach is shown to clearly identify observables which are sensitive to the symmetry-breaking sector of the electroweak theories.

In section 2, I briefly review the Gaugeless limit of the SM [108]. In section 3, I present new formalism, in the chiral Lagrangian framework, to study the large top quark mass contribution (in powers of m_t) to low energy physics. I show that all large m_t effects enter through two quantities ρ and τ [108], which are, in this limit, equivalent to the quantities ϵ_1 and ϵ_b . Section 4 contains some of my conclusions.

4.2 Large m_t effects in the SM

In this section, I briefly review the analysis performed in Ref. [108] which is a study of the large m_t contributions to the low energy observables in the SM. In this case, one is interested in corrections in powers of the Yukawa coupling $g_t = m_t/v$, while, corrections in powers of the gauge coupling g are ignored. In other words, one is considering the perturbative expansion in the Yukawa coupling $g_t = m_t/v$ rather than the gauge coupling g. To fully extract the pure m_t corrections in a general R_{ξ} gauge, the massive gauge bosons do not appear in loops. Thus, gauge bosons can be treated as classical (non-propagating) sources. Consequently, there is no need to break the gauge invariance of the SM Lagrangian in order to perform the loop calculations. The exact gauge invariance of the Lagrangian (in the limit of ignoring corrections in power of the gauge coupling g) leads to a set of ward identities valid to all orders. These Ward identities relate the n-point functions of the gauge bosons to those of the scalar Goldstone bosons. Thus, by connecting the n-point functions of the gauge bosons to those of the Goldstone bosons, one can relate the physical

observables to the *n*-point functions of the Goldstone bosons. The Ward identities can be easily derived in the path integral formalism using the generating function technique.

As I discussed in chapter 1, all radiative corrections to low energy observables, under a few general assumptions, can be written in terms of the gauge boson vacuum polarization functions and the proper vertex correction of Z-b- \bar{b} . Thus, using the derived Ward identities, one can simply relate all physical radiative corrections to a set of corrections involving the Goldstone bosons and the fermion sector. The derived Ward identities relate the vacuum polarization functions of the gauge bosons to those of the Goldstone bosons [108] as follow

$$q^{\mu}q^{\nu}\Pi_{\mu\nu}(q) = \frac{g^{2}v^{2}}{4\cos^{2}\theta}\Pi(q),$$

$$q^{\mu}q^{\nu}\Pi^{\pm}_{\mu\nu}(q) = \frac{g^{2}v^{2}}{4}\Pi^{\pm}(q),$$
(4.1)

where $\Pi_{\mu\nu}(q)$ is the vacuum polarization of the Z boson, $\Pi^{\pm}_{\mu\nu}(q)$ is the vacuum polarization of the W^{\pm} boson, $\Pi(q)$ and $\Pi^{\pm}(q)$ are the self energy of the Goldstone bosons ϕ^3 and ϕ^{\pm} , respectively. Similarly, the Z-b- \bar{b} proper vertex correction Γ_{μ} can be related to the proper vertex ϕ^3 -b- \bar{b} correction Γ as follow

$$(p'^{\mu} - p^{\mu}) \Gamma_{\mu}(p', p) = i \frac{gv}{2\cos\theta} \Gamma +$$

$$\frac{g}{\cos\theta} \left(S_F^{-1}(p') (\frac{P_L}{2} - \frac{\sin^2\theta}{3}) - (\frac{P_R}{2} - \frac{\sin^2\theta}{3}) S_F^{-1}(p) \right)$$
(4.2)

where $P_{L,R} = (1 \mp \gamma_5)/2$ and $S_F^{-1}(p)$ is the self energy of the massless b quark with momentum p. $S_F^{-1}(p)$ is parameterized as

$$S_F^{-1}(p) = iZ^b \gamma_\mu p^\mu P_L + i\gamma_\mu p^\mu P_R. \tag{4.3}$$

At tree level, $Z^b = 1$. However, higher order corrections contribute to Z^b whereas the right handed self-energy of the massless b quark does not get modified. This is

true since the right-handed quark, b_R , is singlet under $SU(2)_L$ symmetry. Therefore, the right-handed quark, b_R , does not couple to the Goldstone bosons in the limit of vanishing b quark mass.

The 2-point functions of the W, Z gauge bosons, and the Goldstone bosons can be expanded in powers of q^2 since this is the only relevant low energy scale in the loop calculations after turning off the gauge couplings. In the limit $q^2 \to 0$ the 2-point functions are parameterized as

$$\Pi_{\mu\nu}(q) \approx \frac{g^2 v^2}{4 \cos^2 \theta} (Z - 1) g_{\mu\nu} ,$$
(4.4)

$$\Pi_{\mu\nu}^{\pm}(q) \approx \frac{g^2 v^2}{4} (Z^{\pm} - 1) g_{\mu\nu} .$$
(4.5)

$$\Pi(q) \approx (Z_2^3 - 1)q^2$$
, (4.6)

$$\Pi^{\pm}(q) \approx (Z_2^{\pm} - 1)q^2,$$
(4.7)

where at tree level $Z = Z^{\pm} = Z_2^3 = Z_2^{\pm} = 1$. The energy scale $q^2 = 0$ is the only relevant low energy scale in the loop calculations. The internal fields are the massless Goldstone bosons, the heavy top quark, and the Higgs boson. Therefore, there are only three mass scales in the calculations, a low energy scale $q^2 = 0$ and two high energy scales m_t and m_H .

Using the identities in Eq. (4.1), one obtains

$$Z = Z_2^3, (4.8)$$

$$Z^{\pm} = Z_2^{\pm} \,. \tag{4.9}$$

Since, as discussed in chapter 1, oblique corrections to physical observables can be written in terms of the quantities Z and Z^{\pm} , it is therefore possible to relate the

quantities Z_2^3 , Z_2^{\pm} to direct physical observables, or equivalently to the parameters $\delta \rho$, Δk , and Δr_W . The quantities Z_2^3 and Z_2^{\pm} are related to the quantities $A^{ZZ}(0)$ and $A^{WW}(0)$ defined in Eq. (1.49) as follows

$$A^{ZZ}(0) = \frac{g^2 v^2}{4 \cos^2 \theta} Z_2^3, \quad A^{WW}(0) = \frac{g^2 v^2}{4} Z_2^{\pm}. \tag{4.10}$$

I will discuss this connection in the next section after dealing with the chiral Lagrangian case.

The proper $Z-b-\bar{b}$ vertex, can be parameterized as [108]

$$\Gamma_{\mu}(p',p) = -\frac{ig}{2\cos\theta} \left((1 - \frac{2}{3}\sin^2\theta) Z_1 \gamma_{\mu} P_L - \frac{2}{3}\sin^2\theta \gamma_{\mu} P_R \right) , \qquad (4.11)$$

for $p'\approx p$, i.e., $q=p'-p\approx 0$. Similarly, for the proper ϕ^3 -b- \overline{b} vertex

$$\Gamma = Z_1^3 \gamma_\mu \frac{p'^\mu - p^\mu}{2v} P_L \,. \tag{4.12}$$

Therefore, using the Ward identity in Eq. (4.2) one finds

$$(1 - \frac{2}{3}\sin^2\theta)Z_1 = Z_1^3 + (1 - \frac{2}{3}\sin^2\theta)Z_2^b. \tag{4.13}$$

To get the physical $Z-b-\bar{b}$ vertex one needs to renormalize the left-handed b quark. Therefore, one finds the physical $Z-b-\bar{b}$ vertex to be

$$V_{\mu} = -\frac{ig}{2\cos\theta} \left[\left(1 - \frac{2}{3}\sin^2\theta + \frac{Z_1^3}{Z_2^b} \right) \gamma_{\mu} P_L - \frac{2}{3}\sin^2\theta P_R \right]. \tag{4.14}$$

The conclusion is that to calculate the pure m_t corrections to low energy data, one simply has to calculate the quantities Z_2^3 , Z_2^{\pm} , Z_1^3 , and Z_2^b which are calculated from a set of Feynman diagrams involving only fermions (top and bottom quarks) and scalar bosons (Goldstone bosons and the Higgs boson) but not gauge bosons.

Thus, in extracting the large m_t corrections to low energy observables in the SM, one starts with the tree-level Lagrangian, involving the Higgs doublet Φ , the third

generation left-handed quark doublet $\psi_L = (t_L, b_L)$ and the right-handed top quark field t_R

$$\mathcal{L} = (\partial_{\mu}\Phi)^{\dagger}(\partial^{\mu}\Phi) - \frac{\lambda}{2} \left((\Phi^{\dagger}\Phi)^{2} - \frac{v^{2}}{2} \right)^{2} +$$

$$\overline{\Psi_{L}}i\gamma^{\mu}\partial_{\mu}\Psi_{L} + \overline{t_{R}}i\gamma^{\mu}\partial_{\mu}t_{R} + \frac{\sqrt{2}m_{t}}{v} (\overline{t_{L}}\ \overline{b}_{L}) \Phi t_{R} + h.c. \tag{4.15}$$

From which one calculates the needed quantities Z_2^3 , Z_2^{\pm} , Z_1^3 , and Z_2^b .

4.3 Large m_t Effects In the Chiral Lagrangian

In this section, I am interested in the chiral Lagrangian formulated electroweak theories in which the gauge symmetry $SU(2)_L \times U(1)_Y$ is nonlinearly realized. A mentioned in chapter 3, the chiral Lagrangian can be constructed solely based upon the broken symmetry of the theory, and it is not necessary to specify the detailed dynamics of the actual breaking mechanism. Hence, it is the most general effective Lagrangian that can accommodate any underlying theory with that pattern of symmetry-breaking at the low energy scale.

In this section, as a matter of convenience, I define the composite fields in a slightly different way from the ones I defined in chapter 3. I define

$$W_{\mu}^{a} = -i \text{Tr}(\tau^{a} \Sigma^{\dagger} D_{\mu} \Sigma) \tag{4.16}$$

and

$$\mathcal{B}_{\mu} = g' B_{\mu} , \qquad (4.17)$$

where I define the quantity

$$D_{\mu}\Sigma = \left(\partial_{\mu} - ig\frac{\tau^a}{2}W_{\mu}^a\right)\Sigma \quad . \tag{4.18}$$

The quantity $D_{\mu}\Sigma$ as defined above is not a covariant derivative. Its transformation under $SU(2)_L \times U(1)_Y$ can be checked using the W and Σ field transformations (see appendix D). In my notation W^a_{μ} and B_{μ} are the gauge bosons associated with the $SU(2)_L$ and $U(1)_Y$ groups, respectively. Also, g and g' are the corresponding gauge couplings. The composite fields transform under $SU(2)_L \times U(1)_Y$ as

$$\mathcal{W}_{\mu}^{3} \to \mathcal{W}_{\mu}^{\prime 3} = \mathcal{W}_{\mu}^{3} - \partial_{\mu} y \,, \tag{4.19}$$

$$\mathcal{W}_{\mu}^{\pm} \to \mathcal{W}_{\mu}^{\prime \pm} = e^{\pm iy} \mathcal{W}_{\mu}^{\pm} \,, \tag{4.20}$$

$$\mathcal{B}_{\mu} \to \mathcal{B}'_{\mu} = \mathcal{B}_{\mu} + \partial_{\mu} y , \qquad (4.21)$$

where

$$\mathcal{W}^{\pm}_{\mu} = \frac{\mathcal{W}^1_{\mu} \mp i \mathcal{W}^2_{\mu}}{\sqrt{2}} \,. \tag{4.22}$$

I also introduce the composite fields \mathcal{Z}_{μ} and \mathcal{A}_{μ} as

$$\mathcal{Z}_{\mu} = \mathcal{W}_{\mu}^3 + \mathcal{B}_{\mu} , \qquad (4.23)$$

$$s^2 \mathcal{A}_{\mu} = s^2 \mathcal{W}_{\mu}^3 - c^2 \mathcal{B}_{\mu} \,, \tag{4.24}$$

where $s^2 \equiv \sin^2 \theta$, and $c^2 = 1 - s^2$. In the unitary gauge $(\Sigma = 1)$

$$\mathcal{W}^a_\mu = -gW^a_\mu \ , \tag{4.25}$$

$$\mathcal{Z}_{\mu} = -\frac{g}{c} Z_{\mu} , \qquad (4.26)$$

$$\mathcal{A}_{\mu} = -\frac{e}{s^2} A_{\mu} , \qquad (4.27)$$

where I have used the relations e=gs=g'c, $W_{\mu}^{3}=cZ_{\mu}+sA_{\mu}$, and $B_{\mu}=-sZ_{\mu}+cA_{\mu}$. The transformations of \mathcal{Z}_{μ} and \mathcal{A}_{μ} under $SU(2)_{L}\times U(1)_{Y}$ are

$$\mathcal{Z}_{\mu} \to \mathcal{Z}'_{\mu} = \mathcal{Z}_{\mu} , \qquad (4.28)$$

$$\mathcal{A}_{\mu} \to \mathcal{A}'_{\mu} = \mathcal{A}_{\mu} - \frac{1}{s^2} \partial_{\mu} y \ . \tag{4.29}$$

Hence, under $SU(2)_L \times U(1)_Y$ the fields \mathcal{W}^{\pm}_{μ} and \mathcal{Z}_{μ} transform as vector fields, but \mathcal{A}_{μ} transforms as a gauge boson field which plays the role of the photon field A_{μ} .

Using the fields defined as above, one may construct the $SU(2)_L \times U(1)_Y$ gauge invariant interaction terms in the chiral Lagrangian

$$\mathcal{L}_{B} = -\frac{1}{4g^{2}} \mathcal{W}_{\mu\nu}^{a} \mathcal{W}^{a\mu\nu} - \frac{1}{4g'^{2}} \mathcal{B}_{\mu\nu} \mathcal{B}^{\mu\nu} + \frac{v^{2}}{4} \mathcal{W}_{\mu}^{+} \mathcal{W}^{-\mu} + \frac{v^{2}}{8} \mathcal{Z}_{\mu} \mathcal{Z}^{\mu} + \dots,$$

$$(4.30)$$

where

$$\mathcal{W}^{a}_{\mu\nu} = \partial_{\mu}\mathcal{W}^{a}_{\nu} - \partial_{\nu}\mathcal{W}^{a}_{\mu} + \epsilon^{abc}\mathcal{W}^{b}_{\mu}\mathcal{W}^{c}_{\nu} , \qquad (4.31)$$

$$\mathcal{B}_{\mu\nu} = \partial_{\mu}\mathcal{B}_{\nu} - \partial_{\nu}\mathcal{B}_{\mu} , \qquad (4.32)$$

and where ... denotes other possible four- or higher- dimensional operators [78, 72].

It is easy to show that1

$$\mathcal{W}^{a}_{\mu\nu}\tau^{a} = -g\Sigma^{\dagger}W^{a}_{\mu\nu}\tau^{a}\Sigma \tag{4.33}$$

and

$$W^{a}_{\mu\nu}W^{a\mu\nu} = g^2 W^{a}_{\mu\nu}W^{a\mu\nu} \ . \tag{4.34}$$

¹Use $W_{\mu}^{a} \tau^{a} = -2i\Sigma^{\dagger} D_{\mu} \Sigma$, and $[\tau^{a}, \tau^{b}] = 2i\epsilon^{abc} \tau^{c}$.

This simply reflects the fact that the kinetic term is not related to the Goldstone bosons sector, i.e., it does not originate from the symmetry-breaking sector.

The mass terms in Eq. (4.30) can be expanded as

$$\frac{v^{2}}{4}W_{\mu}^{+}W^{-\mu} + \frac{v^{2}}{8}Z_{\mu}Z^{\mu} = \partial_{\mu}\phi^{+}\partial^{\mu}\phi^{-} + \frac{1}{2}\partial_{\mu}\phi^{3}\partial^{\mu}\phi^{3} + \frac{g^{2}v^{2}}{4}W_{\mu}^{+}W^{\mu-} + \frac{g^{2}v^{2}}{8c^{2}}Z_{\mu}Z^{\mu} + \dots$$
(4.35)

At the tree level, the mass of W^{\pm} boson is $M_W = gv/2$ and the mass of Z boson is $M_Z = gv/2c$. The above identity implies that the radiative corrections to the mass of the gauge bosons can be related to the wave function renormalization of the Goldstone bosons, cf. Eq. (4.51), and therefore sensitive to the symmetry-breaking sector.

Fermions can be included in this context by assuming that each flavor transforms under $SU(2)_L \times U(1)_Y$ as [74]

$$f \to f' = e^{iyQ_f} f \,, \tag{4.36}$$

where Q_f is the electric charge of f.

My goal is to study the large Yukawa corrections to the low energy data from the chiral Lagrangian formulated electroweak theories. I will separate the radiative corrections as an expansion in both the Yukawa coupling g_t and the weak coupling g_t ($g_t = m_t/v$, where m_t is the mass of the top quark.) With this separation one can then consider the case where corrections of the order g_t are ignored compared to those of g_t . This case is similar to the analysis in Ref. [108] where the gauge bosons were considered as classical fields so that the full gauge invariance of the SM Lagrangian was maintained, and a set of Ward identities was derived to relate the Green's functions of the Goldstone bosons and the gauge bosons. Hence, large g_t

corrections can be easily obtained from calculating Feynman diagrams involving only fermions (top and bottom quarks) and scalar bosons (e.g., Goldstone bosons and possibly the Higgs boson) but not gauge bosons. The same conclusion can be drawn using the chiral Lagrangian approach in a far more elegant and clear way, as shown below in this section.

Why is the chiral Lagrangian formulation useful in finding large g_t corrections beyond the tree-level? In general to perform a loop calculation, one needs to fix a gauge and therefore explicitly destroys the gauge invariance $[SU(2)_L \times U(1)_Y]$ of the Lagrangian. However, to find the large g_t corrections one does not need to include gauge bosons in loops [108]. Thus, there is no need to fix a gauge and the full gauge invariance of the effective Lagrangian is maintained. Because the chiral Lagrangian possesses the $SU(2)_L \times U(1)_Y$ invariance (nonlinearly) and the $U(1)_{em}$ invariance (linearly) at any given order of the perturbative expansions, and all the loop corrections can be reorganized using the composite fields \mathcal{W}^{\pm}_{μ} , \mathcal{Z}_{μ} , and \mathcal{A}_{μ} in a gauge invariant form, therefore, it is the most convenient and elegant way to find g_t corrections beyond the tree-level. This is obvious because the leading radiative corrections (in powers of m_t) are products of the spontaneous symmetry breaking (SSB) and therefore independent of the weak gauge coupling g. One notes that in the expansion of the field

$$\mathcal{Z}_{\mu} = \frac{2}{v}\partial_{\mu}\phi^3 - \frac{g}{c}Z_{\mu} + \dots, \tag{4.37}$$

there is always a factor g associated with a weak gauge boson field. Hence, loop corrections independent of the gauge coupling g can be obtained by simply considering the scalar and the fermionic sectors in the theory. In the following discussion, I will show how this is done.

4.3.1 Effective Lagrangian

To obtain the large contributions of the top quark mass (in powers of m_t) to low energy data, one needs only to concentrate on the top-bottom fermionic sector ($f_1 = t$ and $f_2 = b$) in addition to the bosonic sector. The most general gauge invariant chiral Lagrangian can be written as

$$\mathcal{L}_{0} = i\bar{t}\gamma^{\mu} \left(\partial_{\mu} + i\frac{2s_{0}^{2}}{3}\mathcal{A}_{\mu}\right) t + i\bar{b}\gamma^{\mu} \left(\partial_{\mu} - i\frac{s_{0}^{2}}{3}\mathcal{A}_{\mu}\right) b$$

$$- \left(\frac{1}{2} - \frac{2s_{0}^{2}}{3} + \kappa_{L}^{NC}\right) \bar{t}_{L}\gamma^{\mu} t_{L} \mathcal{Z}_{\mu} - \left(\frac{-2s_{0}^{2}}{3} + \kappa_{R}^{NC}\right) \bar{t}_{R}\gamma^{\mu} t_{R} \mathcal{Z}_{\mu}$$

$$- \left(\frac{-1}{2} + \frac{s_{0}^{2}}{3}\right) \bar{b}_{L}\gamma^{\mu} b_{L} \mathcal{Z}_{\mu} - \frac{s_{0}^{2}}{3} \bar{b}_{R}\gamma^{\mu} b_{R} \mathcal{Z}_{\mu}$$

$$- \frac{1}{\sqrt{2}} \left(1 + \kappa_{L}^{CC}\right) \bar{t}_{L}\gamma^{\mu} b_{L} \mathcal{W}_{\mu}^{+} - \frac{1}{\sqrt{2}} \left(1 + \kappa_{L}^{CC^{\dagger}}\right) \bar{b}_{L}\gamma^{\mu} t_{L} \mathcal{W}_{\mu}^{-}$$

$$- \frac{1}{\sqrt{2}} \kappa_{R}^{CC} \bar{t}_{R} \gamma^{\mu} b_{R} \mathcal{W}_{\mu}^{+} - \frac{1}{\sqrt{2}} \kappa_{R}^{CC^{\dagger}} \bar{b}_{R} \gamma^{\mu} t_{R} \mathcal{W}_{\mu}^{-}$$

$$- m_{t} \bar{t}t + \dots, \qquad (4.38)$$

where $\kappa_L^{\rm NC}$, $\kappa_R^{\rm NC}$, $\kappa_L^{\rm CC}$, and $\kappa_R^{\rm CC}$ parameterize possible deviations from the SM predictions, and ... indicates possible Higgs boson interactions and other higher dimensional operators. Here I have assumed that new physics from the SSB modify the interactions of the top quark to the electroweak gauge bosons. On the other hand, the bare b-b-Z couplings are not modified in the limit of ignoring the mass of the bottom quark. The subscript 0 denotes bare quantities and all the fields in the Lagrangian \mathcal{L}_0 , Eq. (4.38), are bare fields.

Needless to say, the composite fields are only used to organize the radiative corrections in the chiral Lagrangian. To actually calculate loop corrections one should expand these operators in terms of the Goldstone boson and the gauge boson fields. The gauge invariant result of loop calculations can be written in an effective La-

grangian with a form similar to Eq. (4.38). Denoting the fermionic part of this effective Lagrangian as \mathcal{L}_{eff} , then

$$\mathcal{L}_{eff} = iZ_b^L \overline{b_L} \gamma_\mu \partial^\mu b_L + Z_1 \frac{s_0^2}{3} \overline{b_L} \gamma_\mu b_L \mathcal{A}^\mu + \frac{1}{2} \left(Z_v^L - Z_2 \frac{2s_0^2}{3} \right) \overline{b_L} \gamma_\mu b_L \mathcal{Z}^\mu$$

$$+ iZ_b^R \overline{b_R} \gamma_\mu \partial^\mu b_R + Z_3 \frac{s_0^2}{3} \overline{b_R} \gamma_\mu b_R \mathcal{A}^\mu - Z_4 \frac{s_0^2}{3} \overline{b_R} \gamma_\mu b_R \mathcal{Z}^\mu + \dots,$$

$$(4.39)$$

in which the coefficient functions Z_1 , Z_2 , Z_3 , Z_4 , Z_b^L , Z_b^R , and Z_v^L contain all the loop corrections, and all the fields in \mathcal{L}_{eff} are bare fields.

Since the gauge invariance is maintained one can write \mathcal{L}_{eff} in a from similar to Eq. (2.29), i.e., in terms of the B gauge boson field rather than the composite field \mathcal{A} . Explicitly, \mathcal{L}_{eff} can written as

$$\mathcal{L}_{eff} = iZ_b^L \overline{b_L} \gamma_\mu \partial^\mu b_L - Z_1 \frac{1}{3} \overline{b_L} \gamma_\mu b_L \mathcal{B}^\mu + \frac{1}{2} Z_v^L \overline{b_L} \gamma_\mu b_L \mathcal{Z}^\mu + iZ_b^R \overline{b_R} \gamma_\mu \partial^\mu b_R - Z_3 \frac{1}{3} \overline{b_R} \gamma_\mu b_R \mathcal{B}^\mu + \dots,$$

$$(4.40)$$

where

$$\mathcal{B}_{\mu} = s_0^2 (\mathcal{Z}_{\mu} - \mathcal{A}_{\mu}) , \qquad (4.41)$$

derived from Eqs. (4.23) and (4.24). Note that as shown in Eqs. (4.17) and (4.21) the field \mathcal{B}_{μ} is not composite and transforms exactly like B_{μ} . Comparing Eq. (4.39) with (4.40), one conclude that the coefficient functions Z_1 , Z_2 , Z_3 , and Z_4 must be related and

$$Z_2 = Z_1$$
, (4.42)

$$Z_4 = Z_3$$
 (4.43)

All the radiative corrections to the vertex b-b- ϕ^3 in powers of m_t are summarized by the coefficient function Z_v^L because, from Eq. (4.37),

$$\frac{1}{2}Z_v^L \overline{b_L} \gamma_\mu b_L \mathcal{Z}^\mu = Z_v^L \frac{1}{v} \overline{b_L} \gamma_\mu b_L \partial^\mu \phi^3 + \dots$$
(4.44)

Since the effective Lagrangian \mathcal{L}_{eff} possesses an explicit $U(1)_{em}$ symmetry and under G the field \mathcal{A}_{μ} transforms as a gauge boson field and \mathcal{Z}_{μ} as a neutral vector boson field, therefore, based upon the Ward identities in QED one concludes that in Eq. (4.39)

$$Z_1 = Z_b^L (4.45)$$

and

$$Z_3 = Z_b^R (4.46)$$

Hence, the effective Lagrangian \mathcal{L}_{eff} can be rewritten as

$$\mathcal{L}_{eff} = iZ_b^L \overline{b_L} \gamma^{\mu} \left(\partial_{\mu} - i \frac{s_0^2}{3} \mathcal{A}_{\mu} \right) b_L + iZ_b^R \overline{b_R} \gamma^{\mu} \left(\partial_{\mu} - i \frac{s_0^2}{3} \mathcal{A}_{\mu} \right) b_R$$

$$+ \frac{1}{2} \left(Z_v^L - Z_b^L \frac{2s_0^2}{3} \right) \overline{b_L} \gamma_{\mu} b_L \mathcal{Z}^{\mu} - Z_b^R \frac{s_0^2}{3} \overline{b_R} \gamma_{\mu} b_R \mathcal{Z}^{\mu} + \dots$$

$$(4.47)$$

This effective Lagrangian summarizes all the loop corrections in powers of m_t in the coefficient functions Z_b^L , Z_b^R , and Z_v^L . Recall that up to now all the fields in \mathcal{L}_{eff} are bare fields. To compare with the low energy data I prefer to express \mathcal{L}_{eff} in terms of the renormalized fields. In Eq. (4.47), the kinetic terms of the b_L and b_R fields can be properly normalized after redefining (renormalizing) the fields b_L and b_R by $(Z_b^L)^{\frac{-1}{2}}b_L$ and $(Z_b^R)^{\frac{-1}{2}}b_R$, respectively. In terms of the renormalized fields b_L and b_R , \mathcal{L}_{eff} can be rewritten as

$$\mathcal{L}_{eff} = \overline{b_L} i \gamma^{\mu} \left(\partial_{\mu} - i \frac{s_0^2}{3} \mathcal{A}_{\mu} \right) b_L + \overline{b_R} i \gamma^{\mu} \left(\partial_{\mu} - i \frac{s_0^2}{3} \mathcal{A}_{\mu} \right) b_R$$

$$+ \frac{1}{2} \left(\frac{Z_v^L}{Z_b^L} - \frac{2s_0^2}{3} \right) \overline{b_L} \gamma_{\mu} b_L \mathcal{Z}^{\mu} - \frac{s_0^2}{3} \overline{b_R} \gamma_{\mu} b_R \mathcal{Z}^{\mu} + \dots$$

$$(4.48)$$

Before considering the physical observables at low energy let us first examine the bosonic sector. Similar to our previous discussions, loop corrections to the bosonic

sector can be organized using the effective Lagrangian

$$\mathcal{L}_{eff}^{B} = -\frac{1}{4g_{0}^{2}} \mathcal{W}_{\mu\nu}^{a} \mathcal{W}^{\mu\nu a} - \frac{1}{4g_{0}^{\prime 2}} \mathcal{B}_{\mu\nu} \mathcal{B}^{\mu\nu} + Z^{\phi} \frac{v_{0}^{2}}{4} \mathcal{W}_{\mu}^{+} \mathcal{W}^{-\mu} + Z^{\chi} \frac{v_{0}^{2}}{8} \mathcal{Z}_{\mu} \mathcal{Z}^{\mu} + \dots$$

$$(4.49)$$

Note that in the above equation I have explicitly used the subscript 0 to indicate bare quantities. The bosonic Lagrangian in Eq. (4.30) and the identity in Eq. (4.34) imply that the Yang-Mills terms (the first two terms in \mathcal{L}_B) are not directly related to the SSB sector. Hence, any radiative corrections to the field $W^a_{\mu\nu}$ must know about the weak coupling g, i.e., suppressed by g in our point of view. This also holds for operators, of dimension four or higher, which include $W^a_{\mu\nu}$ in the chiral Lagrangian where all these gauge invariant terms are suppressed by the weak coupling g [72, 78]. (The same conclusion applies to $B_{\mu\nu}$.) Therefore we conclude that the fields \mathcal{W}^{\pm}_{μ} , \mathcal{Z}_{μ} , and \mathcal{A}_{μ} in \mathcal{L}_{eff} and \mathcal{L}_{eff}^B do not get wave function corrections (renormalization) in the limit of ignoring corrections of the order g, namely the renormalized fields and the bare fields are identical in this limit.

Expanding the mass terms in Eq. (4.49) we find

$$Z^{\phi} \frac{v_0^2}{4} W_{\mu}^{+} W^{-\mu} + Z^{\chi} \frac{v_0^2}{8} Z_{\mu} Z^{\mu} = Z^{\phi} \partial_{\mu} \phi^{+} \partial^{\mu} \phi^{-} + \frac{1}{2} Z^{\chi} \partial_{\mu} \phi^{3} \partial^{\mu} \phi^{3} + Z^{\phi} \frac{g_0^2 v_0^2}{4} W_{\mu}^{+} W^{-\mu} + Z^{\chi} \frac{g_0^2 v_0^2}{8c_0^2} Z_{\mu} Z^{\mu} + \dots$$
(4.50)

It is clear that Z^{ϕ} denotes the self energy correction of the charged Goldstone boson ϕ^{\pm} , and Z^{χ} denotes the self energy correction of the neutral Goldstone boson ϕ^{3} . Since W^{\pm}_{μ} and Z_{μ} do not get wave function correction in powers of m_{t} , therefore the gauge boson masses are

$$M_W^2 = Z^{\phi} \frac{g_0^2 v_0^2}{4} = Z^{\phi} M_{W0}^2 ,$$

$$M_Z^2 = Z^{\chi} \frac{g_0^2 v_0^2}{4c_{\pi}^2} = Z^{\chi} M_{Z0}^2 . \tag{4.51}$$

In summary, all the loop corrections in powers of m_t to low energy data can be organized in the sum of \mathcal{L}_{eff} [in Eq. (4.48)] and \mathcal{L}_{eff}^B [in Eq. (4.49)]. Comparing them to the bare Lagrangian \mathcal{L}_0 in Eq. (4.38), we find that in the limit of taking $g \to 0$ the chiral Lagrangian \mathcal{L}_0 behaves as a renormalizable theory although in general a chiral Lagrangian is nonrenormalizable. In other words, no higher dimensional operators (counterterms) are needed to renormalize the theory in this limit. The same feature was also found in another application of a chiral Lagrangian with 1/N expansion [109].

4.3.2 Renormalization

Now we are ready to consider the large m_t corrections to low energy data. I choose the renormalization scheme to be the α , G_F , and M_Z scheme (the Z-pole scheme). With

$$g_0^2 = \frac{4\pi\alpha_0}{s_0^2} \tag{4.52}$$

and

$$s_0^2 c_0^2 = \frac{\pi \alpha_0}{\sqrt{2} G_{F0} M_{Z0}^2} , \qquad (4.53)$$

or,

$$s_0^2 = \frac{1}{2} \left[1 - \left(1 - \frac{4\pi\alpha_0}{\sqrt{2}G_{F0}M_{Z0}^2} \right)^{1/2} \right] . \tag{4.54}$$

Define the counterterms as

$$\alpha = \alpha_0 + \delta \alpha ,$$
 $G_F = G_{F0} + \delta G_F ,$
 $M_Z^2 = M_{Z0}^2 + \delta M_Z^2 ,$

(4.55)

and

$$s^{2} = s_{0}^{2} + \delta s^{2} = s_{0}^{2} - \delta c^{2} ,$$

$$c^{2} = c_{0}^{2} + \delta c^{2} ,$$

$$(4.56)$$

then

$$s^{2}c^{2} + (c^{2} - s^{2}) \delta c^{2} = \frac{\pi \alpha}{\sqrt{2}G_{F}M_{Z}^{2}} \left(1 - \frac{\delta \alpha}{\alpha} + \frac{\delta G_{F}}{G_{F}} + \frac{\delta M_{Z}^{2}}{M_{Z}^{2}} \right) . \tag{4.57}$$

As shown in the above equation, even after the counterterms $\delta \alpha$, δG_F , and δM_Z^2 are fixed by data [e.g., the electron (g-2), muon lifetime, and the mass of the Z boson], I still have the freedom to choose δc^2 by using a different definition of the renormalized quantity s^2c^2 . In this case, I will choose the definition of the renormalized s^2 such that there will be no large top quark mass dependence (in powers of m_t) in the counterterm δc^2 . I will show later that for this purpose the renormalized s^2 satisfies s^2

$$s^2 c^2 = \frac{\pi \alpha}{\sqrt{2} G_F M_Z^2 \rho} \,\,\,(4.58)$$

where ρ is defined from the partial width of Z into lepton pairs, cf. Eq. (4.75). With this choice of s^2 and the definition of the renormalized weak coupling

$$g^2 = \frac{4\pi\alpha}{s^2} \ , \tag{4.59}$$

one can easily show that the counterterm δg^2 (= $g^2 - g_0^2$) does not contain large m_t dependence. (Obviously, $\delta \alpha$ will not have contributions purely in powers of m_t .) Namely, in this renormalization scheme, α , g, and s^2 do not get renormalized after ignoring all the contributions of the order g. Hence, all the bare couplings g_0 , g_0' , and s_0^2 in the effective Lagrangians \mathcal{L}_{eff} and \mathcal{L}_{eff}^B do not get corrected when considering the contributions which do not vanish in the limit of $g \to 0$. The only non-vanishing

²If one defines $s'^2c'^2 = \pi\alpha/\sqrt{2}G_FM_Z^2$, then $s^2 = s'^2(1 + \Delta\kappa')$ with $\Delta\kappa' = -c'^2\delta\rho/(c'^2 - s'^2)$, and the counterterm of s'^2 will contain contributions in powers of m_t .

counterterm needs to be considered in Eq. (4.49) is δv^2 (= $v^2 - v_0^2$). From Eq. (4.51) and $M_W = gv/2$, one finds

$$Z^{\phi}v_0^2 = v^2 \ , \tag{4.60}$$

because neither g nor \mathcal{W}^{\pm} (or W^{\pm}) gets renormalized. Thus,

$$G_{F0} = \frac{1}{\sqrt{2}v_0^2} = Z^{\phi} \frac{1}{\sqrt{2}v^2} = Z^{\phi}G_F . \tag{4.61}$$

Consequently,

$$\frac{g_0^2}{c_0^2} = \frac{8G_{F0}M_{Z0}^2}{\sqrt{2}} = \frac{8G_FM_Z^2}{\sqrt{2}}\frac{Z^\phi}{Z^\chi} , \qquad (4.62)$$

and the effective Z-b-b coupling is

$$-\frac{g_0}{2c_0}\gamma^{\mu} \left[\left(\frac{Z_v^L}{Z_b^L} - \frac{2s_0^2}{3} \right) P_L - \frac{2s_0^2}{3} P_R \right] =$$

$$-\sqrt{\frac{G_F M_Z^2}{2\sqrt{2}}} \frac{Z^{\phi}}{Z^{\chi}} \gamma^{\mu} \left[\left(\frac{Z_v^L}{Z_b^L} - \frac{4s^2}{3} \right) - \frac{Z_v^L}{Z_b^L} \gamma_5 \right] , \qquad (4.63)$$

where $P_{L,R} = (1 \mp \gamma_5)/2$.

4.3.3 Low Energy Observables

A discussed in chapter 1, all the radiative corrections to low energy data can be categorized in a model independent way into four parameters: ϵ_1 , ϵ_2 , ϵ_3 , and ϵ_b [16, 22, 23] or equivalently, the S, T, U, ... [24] (see appendix B). The parameters ϵ_1 , ϵ_2 , ϵ_3 , and ϵ_b can be derived from four basic measured observables, such as Γ_{μ} (the partial decay width of Z into a μ pair), A^{μ}_{FB} (the forward-backward asymmetry at the Z peak for the μ lepton), M_W/M_Z (the ratio of W^{\pm} and Z masses), and Γ_b (the partial decay width of Z into a $b\bar{b}$ pair). The expressions of these observables in terms of ϵ 's can be found in chapter 1.

In this section, I only give the relevant terms in ϵ 's that might contain the leading effects in powers of m_t from new physics. Denote the vacuum polarization for the W^1 , W^2 , W^3 , and B gauge bosons as

$$\Pi^{ij}_{\mu\nu}(q) = -ig_{\mu\nu} \left[A^{ij}(0) + q^2 F^{ij}(q^2) \right] + q_{\mu}q_{\nu} \text{ terms}, \qquad (4.64)$$

where $i, j = W, Z, \gamma$, respectively. Then,

$$\epsilon_1 = e_1 - e_5 \,, \tag{4.65}$$

$$\epsilon_2 = e_2 - \cos^2 \theta^2 e_5 \,, \tag{4.66}$$

$$\epsilon_3 = e_3 - \cos^2 \theta^2 e_5 \,, \tag{4.67}$$

$$\epsilon_b = e_b \,, \tag{4.68}$$

where

$$e_1 = \frac{A^{ZZ}(0)}{M_Z^2} - \frac{A^{WW}(0)}{M_W^2} \,, \tag{4.69}$$

$$e_2 = F^{WW}(M_W^2) - F^{33}(M_Z^2), (4.70)$$

$$e_3 = \frac{\cos \theta}{\sin \theta} F^{30}(M_Z^2) \,, \tag{4.71}$$

$$e_5 = M_Z^2 \frac{dF^{ZZ}}{dq^2} (M_Z^2) , (4.72)$$

and e_b is defined through the vertex corrections to $Z\to b\overline{b}$

$$V_{\mu}\left(Z \to b\bar{b}\right) = -\frac{g}{2c}e_{b}\gamma_{\mu}\frac{1-\gamma_{5}}{2}.$$
(4.73)

Both ϵ_1 and ϵ_b gain corrections in powers of m_t , and are sensitive to new physics coming through the top quark. On the contrary, ϵ_2 and ϵ_3 do not play any significant

role in our analysis because their dependence on the top mass is only logarithmic. Hence,

 $\epsilon_1 = \delta \rho + \text{corrections of the order } g$,

 $\epsilon_b = \tau + \text{corrections of the order } g$,

 ϵ_2 = corrections of the order g,

$$\epsilon_3$$
 = corrections of the order g , (4.74)

where $\delta \rho = \rho - 1$. The parameters ρ and τ are defined by

$$\Gamma_{\mu} \equiv \Gamma(Z \to \mu^{+}\mu^{-}) = \rho \frac{G_{F}M_{Z}^{3}}{6\pi\sqrt{2}} \left(g_{\mu V}^{2} + g_{\mu A}^{2}\right) ,$$

$$\Gamma_b \equiv \Gamma(Z \to \bar{b}b) = \rho \frac{G_F M_Z^3}{2\pi\sqrt{2}} \left(g_{bV}^2 + g_{bA}^2\right) , \qquad (4.75)$$

where

$$g_{\mu V} = -\frac{1}{2} \left(1 - 4s^2 \right), \quad g_{\mu A} = -\frac{1}{2} ,$$

$$g_{bV} = -\frac{1}{2} \left(1 - \frac{4}{3}s^2 + \tau \right), \quad g_{bA} = -\frac{1}{2} \left(1 + \tau \right) . \tag{4.76}$$

Hence, comparing to Eq. (4.63) we conclude

$$\delta \rho = \frac{Z^{\phi}}{Z^{\chi}} - 1 ,$$

$$\tau = \frac{Z_{v}^{L}}{Z_{b}^{L}} - 1 .$$

$$(4.77)$$

4.4 One Loop Corrections in the SM

The SM, being a linearly realized $SU(2)_L \times U(1)_Y$ gauge theory, can be formulated as a chiral Lagrangian after nonlinearly transforming the fields (see chapter 2). Applying the previous formalism, I calculate the one-loop corrections of order m_t^2 to ρ and τ for the SM by taking $\kappa_L^{\rm NC} = \kappa_R^{\rm NC} = \kappa_L^{\rm CC} = 0$ in Eq. (4.38). These

loop corrections can be summarized by the coefficient functions Z^{χ} , Z^{ϕ} , Z^{L}_{b} , and Z^{L}_{v} which are calculated from the Feynman diagrams shown in Figure 4.1(a), 1(b), 1(c), and the sum of 1(d) and 1(e), respectively. I find

$$Z^{\chi} = 1 + \frac{6m_t^2}{16\pi^2 v^2} \left(\Delta - \ln m_t^2\right) ,$$

$$Z^{\phi} = 1 + \frac{6m_t^2}{16\pi^2 v^2} \left(\Delta + \frac{1}{2} - \ln m_t^2\right) ,$$

$$Z_b^L = 1 + \frac{3m_t^2}{16\pi^2 v^2} \left(-\Delta + \ln m_t^2 - \frac{5}{6}\right) ,$$

$$Z_v^L = 1 + \frac{3m_t^2}{16\pi^2 v^2} \left(-\Delta + \ln m_t^2 - \frac{3}{2}\right) .$$

$$(4.78)$$

One notes that Figure 4.1(e) arises from the nonlinear realization of the gauge symmetry in the chiral Lagrangian approach. Substituting the above results into Eq. (4.77), one obtains

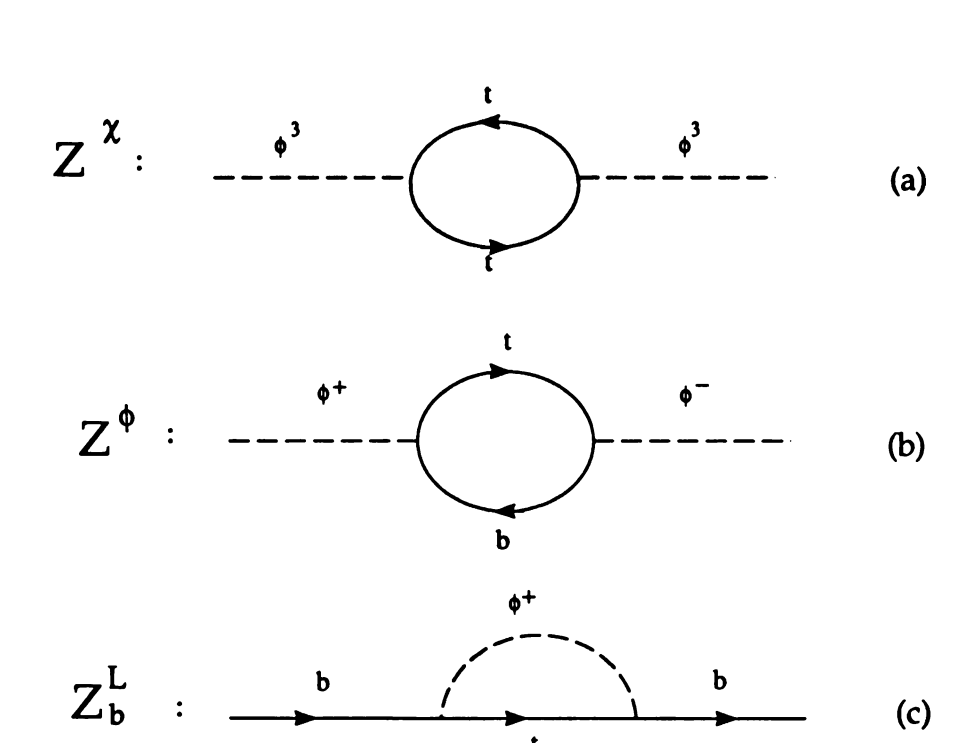
$$\delta \rho = \frac{3G_F m_t^2}{8\sqrt{2}\pi^2} ,$$

$$\tau = -\frac{G_F m_t^2}{4\sqrt{2}\pi^2} ,$$
(4.79)

which are the established results (see section 1.5).

4.5 One Loop Corrections with Nonstandard Top Quark Couplings

In chapter 3, I calculated the one-loop corrections (of order $m_t^2 \ln \Lambda^2$) to ρ and τ due to the nonstandard couplings of the top quark to the electroweak gauge bosons. The set of Feynman diagrams we considered contained external massive gauge bosons lines. In this section, I show how to reproduce those results by considering a set of Feynman diagrams which contains only the pure Goldstone bosons, the top quark, and the bottom quark lines, as described in Section 4.3.



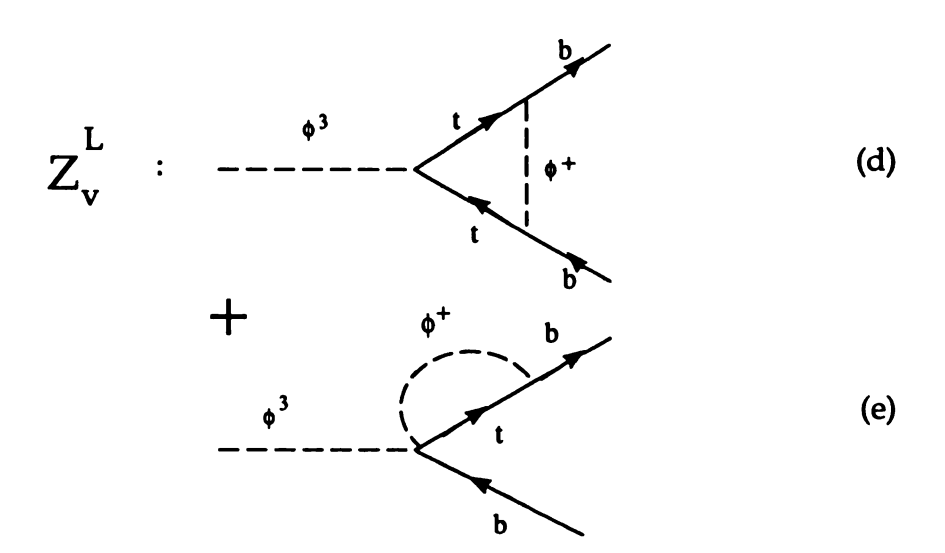


Figure 4.1: The Feynman diagrams which contribute to ρ and τ to the order $\mathcal{O}(m_t^2 \ln \Lambda^2)$.

Non-renormalizability of the effective Lagrangian presents a major problem on how to find a scheme to handle both the divergent and the finite pieces in loop calculations [99]. Such a problem arises because the underlying theory is not yet known, so it is not possible to apply the exact matching conditions to find the correct scheme to be used in the effective Lagrangian [61]. One approach is to associate the divergent piece in loop calculations with a physical cutoff Λ , the upper scale at which the effective Lagrangian is valid [74]. In the chiral Lagrangian approach this cutoff Λ is taken to be $4\pi v \sim 3 \text{ TeV}$ [61].³ For the finite piece no completely satisfactory approach is available [99].

To perform loop calculations using the chiral Lagrangian, one should arrange the corrections in powers of $1/4\pi v$ and include all the Feynman diagrams up to the desired order. Figure 4.1 contains all the Feynman diagrams needed for our study. I calculate the leading contribution to ρ and τ due to the new interaction terms in the chiral Lagrangian using the dimensional regularization scheme and taking the bottom quark mass to be zero. At the end of the calculation, I replace the divergent piece $1/\epsilon$ by $\ln(\Lambda^2/m_t^2)$ for $\epsilon = (4-n)/2$, where n is the space-time dimension. Effectively, I have assumed that the underlying full theory is renormalizable. The cutoff scale Λ serves as the infrared cutoff of the operators in the effective Lagrangian. Due to the renormalizability of the full theory, from renormalization group analysis, I conclude that the same cutoff Λ should also serve as the ultraviolet cutoff of the effective Lagrangian in calculating Wilson coefficients. Hence, in the dimensional regularization scheme, $1/\epsilon$ is replaced by $\ln(\Lambda^2/\mu^2)$. Furthermore, the renormalization scale μ is set to be m_t , the heaviest mass scale in the effective Lagrangian of interest. Since I am mainly interested in new physics associated with the top quark couplings to gauge bosons, I will restrict myself to the leading contribution enhanced by the

³This scale, $4\pi v \sim 3 \text{ TeV}$, is only meant to indicate the typical cutoff scale. It is equally probable to have, say, $\Lambda = 1 \text{ TeV}$.

top quark mass, i.e., of the order of $(m_t^2 \ln \Lambda^2)$.

Inserting these nonstandard couplings in loop diagrams and keeping only the linear terms in κ 's, one finds

$$Z^{\chi} = 1 + \frac{6m_t^2}{16\pi^2 v^2} \left(2\kappa_L^{\text{NC}} - 2\kappa_R^{\text{NC}} \right) \ln \frac{\Lambda^2}{m_t^2} ,$$

$$Z^{\phi} = 1 + \frac{12m_t^2}{16\pi^2 v^2} \kappa_L^{\text{CC}} \ln \frac{\Lambda^2}{m_t^2} ,$$

$$Z_b^L = 1 - \frac{6m_t^2}{16\pi^2 v^2} \kappa_L^{\text{CC}} \ln \frac{\Lambda^2}{m_t^2} ,$$

$$Z_v^L = 1 - \frac{m_t^2}{16\pi^2 v^2} \left(6\kappa_L^{\text{CC}} - 4\kappa_L^{\text{NC}} + \kappa_R^{\text{NC}} \right) \ln \frac{\Lambda^2}{m_t^2} .$$

$$(4.80)$$

Thus the nonstandard contributions to ρ and τ are

$$\delta \rho = \frac{3G_F m_t^2}{2\sqrt{2}\pi^2} \left(\kappa_L^{\text{CC}} - \kappa_L^{\text{NC}} + \kappa_R^{\text{NC}} \right) \ln \frac{\Lambda^2}{m_t^2} ,$$

$$\tau = \frac{G_F m_t^2}{2\sqrt{2}\pi^2} \left(-\frac{1}{4} \kappa_R^{\text{NC}} + \kappa_L^{\text{NC}} \right) \ln \frac{\Lambda^2}{m_t^2} ,$$
(4.81)

which agree with my previous results obtained in chapter 3.

4.6 Conclusions

In chapter 3, I performed a one-loop level calculation of the leading quadratic m_t corrections by considering a set of Feynman diagrams, derived form the nonlinear chiral Lagrangian, whose external lines were the massive gauge boson lines. The leading corrections (in power of m_t) to the low energy observables were found not to vanish in the limit of vanishing g (the weak coupling) because they originate from strong couplings to the SSB sector, e.g., through large Yukawa coupling g_t . Therefore, the result in chapter 3 should in principle be reproduced by considering an effective Lagrangian which involves only the scalar (the unphysical Goldstone bosons and

probably the Higgs boson) and the top-bottom fermionic sectors. This was shown in Section 4.3. I discussed how to relate the two corresponding sets of Green's functions for the low energy observables of interest. I showed that by considering a completely different set of Green's functions (without involving any external gauge boson line) from that discussed in chapter 3, I obtained exactly the same results. My result for τ is different from that given in Ref. [101] where the wave function correction to the bottom quark was not included.

Chapter 5

A Model of Strong Flavor Dynamics for the Top Quark

5.1 Introduction

In chapter 3, I discussed a phenomenological model in which new physics appears in the top quark interaction with the gauge bosons. In that phenomenological model I did not specify an explicit dynamics which triggers the top quark nonstandard couplings. In general, these couplings could be due to different dynamical models, e.g., extended technicolor models, models with extra gauge bosons, etc. In this chapter, I construct a specific model which triggers the top quark nonstandard couplings. It also leads to other interesting physics at low energy. Therefore, one has to study all of the aspects and effects of the model at low energy.

The construction of this model is based on the theoretical observation of the hierarchy of the fermion mass spectrum. The relatively large mass of the third generation of fermions may suggest a dynamical behavior for the third generation different from that of the first two generations. In this model, the third generation undergoes a different flavor dynamics from the usual weak interaction proposed in the SM. I assume this flavor dynamics to be associated with a new SU(2) gauged symmetry. Therefore, a new spectrum of gauge bosons emerges in this model. No modifications to QCD

interactions are considered here; this case has been discussed elsewhere [110].

5.2 The Model

The model is based on the flavor symmetry $G = SU(2)_l \times SU(2)_h \times U(1)_Y$. Where the third generation of matter (top quark, t, bottom quark, b, tau lepton, τ , and its neutrino, ν_{τ}) experience a strong flavor interaction, instead of the weak interaction advocated by the SM. On the contrary the first and second generations only feel the weak interaction supposedly equivalent to the SM case. The strong flavor dynamics is attributed to the $SU(2)_h$ symmetry under which the left-handed fermions of the third generation transform in the fundamental representation (doublets), while they remain to be singlets under the $SU(2)_l$ symmetry. On the other hand, the left-handed fermions of the first and second generation transform as doublets under the $SU(2)_l$ group and singlets under the $SU(2)_h$ group. The $U(1)_Y$ group is the SM hypercharge group. The right-handed fermions only transform under the $U(1)_Y$ group as assigned by the SM. Finally the QCD interactions and the color symmetry $SU(3)_C$ are the same as in the SM.

The symmetry breaking of the Lie group G into the electromagnetic group $U(1)_{em}$, is a two stage mechanism, first $SU(2)_l \times SU(2)_h \times U(1)_Y$ breaks down into $SU(2)_L \times U(1)_Y$ $U(1)_Y$ at some large mass scale. The second stage is where $SU(2)_L \times U(1)_Y$ breaks down into $U(1)_{em}$ at a scale of the order of the SM electroweak symmetry-breaking scale. The spontaneous symmetry-breaking of the group $SU(2)_l \times SU(2)_h \times U(1)_Y$ is accomplished by introducing two scalar matrix fields $\Sigma = \sigma + i \pi^a \tau^{a-1}$ and Φ with the transformations

i.e., the Σ field transforms as a doublet under both $SU(2)_l$ and $SU(2)_h$ and as a singlet under $U(1)_Y$. On the other hand the Φ field transforms as a doublet under $SU(2)_l$, as a singlet under $SU(2)_h$, and has a hypercharge quantum number Y=1. Thus, the scalar doublet Φ is equivalent to the SM Higgs doublet. However, as to be shown later, the Yukawa sector is different.

As a realization of the symmetry I define the field transformations as

$$\Sigma \to g_1 \Sigma g_2^{\dagger} , \qquad \Phi \to g_1 g_Y \Phi , \qquad (5.2)$$

where $g_1 \in SU(2)_l$, $g_2 \in SU(2)_h$, and $g_Y \in U(1)_Y$. In this section I discuss fully the structure of this model.

5.2.1 The Bosonic Sector

Under the gauged $SU(2)_l \times SU(2)_h \times U(1)_Y$, I introduce the covariant derivatives of the scalar fields,

$$D^{\mu}\Sigma = \partial^{\mu}\Sigma + ig_{l}W_{l}^{\mu}\Sigma - ig_{h}\Sigma W_{h}^{\mu} , \qquad (5.3)$$

$$D^{\mu}\Phi = \partial^{\mu}\Phi + ig_l W_l^{\mu}\Phi + \frac{i}{2}g'B^{\mu}\Phi , \qquad (5.4)$$

where the gauge boson fields $W_l \equiv W_l^a \tau^a/2$ and $W_h \equiv W_h^a \tau^a/2$ corresponds to the gauged groups $SU(2)_l$ and $SU(2)_h$, respectively. The gauge coupling g_h is assumed to be larger than g_l even though I will restrict myself to the region where the perturbative calculation still holds.

With these definitions, the gauge invariant bosonic Lagrangian is

$$\mathcal{L}_{B} = \frac{1}{2} D_{\mu} \Phi^{\dagger} D^{\mu} \Phi + \frac{1}{4} \text{Tr} (D_{\mu} \Sigma^{\dagger} D^{\mu} \Sigma) + V(\Phi, \Sigma) - \frac{1}{4} W_{l \mu}^{a} W_{l}^{a\mu} - \frac{1}{4} W_{h \mu}^{a} W_{h}^{a\mu} - \frac{1}{4} B_{\mu} B^{\mu} , \qquad (5.5)$$

where $V(\Phi, \Sigma)$ is the scalar potential. I assume that the first stage of symmetry breaking is accomplished through the Σ field, i.e. by acquiring a vacuum expectation value u,

$$\langle \Sigma \rangle = \begin{pmatrix} u & 0 \\ 0 & u \end{pmatrix} . \tag{5.6}$$

Hence the symmetry $SU(2)_l \times SU(2)_h \times U(1)_Y$ is broken into the diagonal group $SU(2)_L \times U(1)_Y$, and the symmetry-breaking scale is set by the vacuum expectation value u. The next step is to break the $SU(2)_L \times U(1)_Y$ symmetry into the $U(1)_{\rm em}$ symmetry through the scalar Φ field, i.e. by acquiring a vacuum expectation value v.

$$\langle \Phi \rangle = \begin{pmatrix} 0 \\ v \end{pmatrix} \,, \tag{5.7}$$

where v, as we will see later, is of the order of the SM symmetry-breaking scale. Because of this pattern of symmetry breaking, the gauge couplings are related to the $U(1)_{em}$ gauge coupling e by the relation

$$\frac{1}{e^2} = \frac{1}{g_l^2} + \frac{1}{g_h^2} + \frac{1}{g'^2} \ . \tag{5.8}$$

Here I define

$$g_l = \frac{e}{\sin \theta \cos \phi}, \qquad g_h = \frac{e}{\sin \theta \sin \phi}, \qquad g' = \frac{e}{\cos \theta},$$
 (5.9)

where θ is the usual weak mixing angle and ϕ is a new parameter in this model. The scalar fields, except $\text{Re}(\phi^0)$ from the Φ doublet and σ from the Σ matrix field, become the longitudinal components of the physical gauge bosons. The surviving $\text{Re}(\phi^0)$ field behaves similar to the SM Higgs boson except that it does not have the usual Yukawa couplings to the third generation.

To get the gauge boson mass eigenstates, I first concentrate on the charged gauge bosons. As a first step I rotate the gauge fields by the angle ϕ .

$$W_{1\ \mu}^{\pm} = \cos\phi W_{l\ \mu}^{\pm} + \sin\phi W_{h\ \mu}^{\pm}, \qquad W_{2\ \mu}^{\pm} = -\sin\phi W_{l\ \mu}^{\pm} + \cos\phi W_{h\ \mu}^{\pm}, \qquad (5.10)$$

where $W_{l\ \mu}^{\pm}=(W_{l\ \mu}^{1}\mp iW_{l\ \mu}^{2})/\sqrt{2}$, and similarly for $W_{h\ \mu}^{\pm}$. The mass matrix reduces to

$$M_W^2 = M_0^2 \begin{pmatrix} 1 & -\tan\phi \\ -\tan\phi & \frac{x}{\sin^2\phi\cos^2\phi} + \tan^2\phi \end{pmatrix} , \qquad (5.11)$$

where

$$M_0^2 \equiv \frac{e^2 v^2}{4 \sin^2 \theta} \,, \qquad x \equiv \frac{u^2}{v^2} \,.$$
 (5.12)

Next I consider the neutral sector $W_{l_{\mu}}^{3}$, $W_{h_{\mu}}^{3}$, and B_{μ} . Define

$$W_{1\mu}^{3} = \cos\theta(\cos\phi W_{l\mu}^{3} + \sin\phi W_{h\mu}^{3}) - \sin\theta B_{\mu}, \qquad (5.13)$$

$$A_{\mu} = \sin \theta (\cos \phi W_{l \mu}^{3} + \sin \phi W_{h \mu}^{3}) + \cos \theta B_{\mu}, \qquad (5.14)$$

and

$$W_{2\mu}^3 = -\sin\phi W_{l\mu}^3 + \cos\phi W_{h\mu}^3. \tag{5.15}$$

The gauge field A_{μ} is massless, corresponding to the physical photon field, while the remaining fields have the mass matrix

$$M_Z^2 = \frac{M_0^2}{\cos^2 \theta} \left(-\cos \theta \tan \phi - \cos \theta \tan \phi - \cos^2 \theta \tan^2 \phi \right). \tag{5.16}$$

To get the mass eigenstates and the physical masses of the gauge bosons, I further diagonalize the mass matrices M_W^2 and M_Z^2 . In this model, I am concentrating on the case where $g_h > g_l$, (equivalently $\tan \phi < 1$) but with $g_h^2 \le 4\pi$ (which implies $\sin^2 \phi \ge g^2/(4\pi) \sim 1/30$) so that the perturbation theory is valid. Similarly, for $g_h < g_l$, we require $\sin^2 \phi \le 0.96$. Furthermore, I focus on the region where $x \gg 1$,

though another region of interest could be $x \sim 1$ ($u \sim v$), but in this case the one-loop level contributions due to the heavy gauge bosons should also be included because they are of the same order as the SM one-loop contributions. In the limit $x \gg 1$, I expand terms only up to the leading order in 1/x. Thus, in dealing with this limit one can ignore all higher order corrections, since they are suppressed by higher powers of 1/x. To the order 1/x, the eigenstates of the light gauge bosons are

$$W_{\mu}^{\pm} = W_{1\ \mu}^{\pm} + \frac{\sin^3 \phi \cos \phi}{x} W_{2\ \mu}^{\pm}, \tag{5.17}$$

$$Z_{\mu} = Z_{1\mu} + \frac{\sin^3 \phi \cos \phi}{x \cos \theta} Z_{2\mu} \,. \tag{5.18}$$

While for the heavy gauge bosons one finds

$$W_{\mu}^{\prime \pm} = -\frac{\sin^3 \phi \cos \phi}{x} W_{1\ \mu}^{\pm} + W_{2\ \mu}^{\pm}, \tag{5.19}$$

$$Z'_{\mu} = -\frac{\sin^3 \phi \cos \phi}{x \cos \theta} Z_{1\mu} + Z_{2\mu} \,. \tag{5.20}$$

To the same order, the gauge boson masses are

$$M_{W^{\pm}}^2 = M_0^2 (1 - \frac{\sin^4 \phi}{x}), \qquad (5.21)$$

$$M_Z^2 = \frac{M_0^2}{\cos^2 \theta} \left(1 - \frac{\sin^4 \phi}{x}\right). \tag{5.22}$$

While for the heavy gauge bosons one finds

$$M_{W'^{\pm}}^{2} = M_{0}^{2} \left(\frac{x}{\sin^{2} \phi \cos^{2} \phi} + \frac{\sin^{2} \phi}{\cos^{2} \phi} \right) , \qquad (5.23)$$

$$M_{Z'}^2 = M_0^2 \left(\frac{x}{\sin^2 \phi \cos^2 \phi} + \frac{\sin^2 \phi}{\cos^2 \phi} \right) . \tag{5.24}$$

It is interesting to notice that the heavy gauge bosons are degenerate up to this order, i.e., $M'_Z = M_{W'^{\pm}}$. This is due to the fact that the heavy gauge bosons do not mix with the hypercharge gauge boson field, B_{μ} .

5.2.2 The Fermion Sector

Now I focus my attention on the fermionic sector. The quarks transform under the usual color $SU(3)_c$ gauge group as in the SM. As discussed before, only the third generation interacts with the $SU(2)_h$ gauge bosons. The first and second generations only interact with the $SU(2)_l$ gauge bosons. Explicitly, under the $SU(2)_l \times SU(2)_h \times U(1)_Y$ symmetry, the transformation of the first and second generation is as follows

Left-handed quarks: $(2,1)_{1/3}$, Left-handed leptons: $(2,1)_{-1}$.

For the third generation, we have

Left-handed quarks: $(1,2)_{1/3}$, Left-handed leptons: $(1,2)_{-1}$.

For all the right-handed fermions, we have

Right-handed quarks and leptons: $(1,1)_Q$,

where Q is the electric charge of the right-handed fermions. Because of this assignment, the model is anomaly free since cancelation of anomalies are satisfied family by family. I denote left-handed doublets of the first and second generation by $\Psi_L^{(1,2)}$, and right-handed singlets by $\Psi_R^{(1,2)}$. On the other hand, I denote the left-handed doublets of the third generation by Ψ_L^3 and right-handed singlets by Ψ_R^3 . The fermionic Lagrangian is

$$\mathcal{L}_{f} = \overline{\Psi_{L}}^{(1,2)} i \gamma^{\mu} D_{\mu} \Psi_{L}^{(1,2)} + \overline{\Psi_{R}}^{(1,2)} i \gamma^{\mu} D_{\mu} \Psi_{R}^{(1,2)} + \overline{\Psi_{L}}^{3} i \gamma^{\mu} D_{\mu} \Psi_{L}^{3} + \overline{\Psi_{R}}^{3} i \gamma^{\mu} D_{\mu} \Psi_{R}^{3}, \qquad (5.25)$$

with

$$D_{\mu}\Psi_{L}^{(1,2)} = \left(\partial_{\mu} - ig_{l}\frac{\tau^{a}}{2}W_{l\mu}^{a} - ig'\frac{Y}{2}B_{\mu}\right)\Psi_{L}^{(1,2)}, \qquad (5.26)$$

$$D_{\mu}\Psi_{R}^{(1,2)} = (\partial_{\mu} + ig'QB_{\mu})\Psi_{R}^{(1,2)}, \qquad (5.27)$$

$$D_{\mu}\Psi_{L}^{3} = \left(\partial_{\mu} + ig_{h}\frac{\tau^{a}}{2}W_{h\mu}^{a} + ig'\frac{Y}{2}B_{\mu}\right)\Psi_{L}^{3}, \qquad (5.28)$$

$$D_{\mu}\Psi_{R}^{3} = (\partial_{\mu} + ig'QB_{\mu})\Psi_{R}^{3}, \tag{5.29}$$

where Y is the hypercharge generator of the $U(1)_Y$ group, and the relation

$$Q = T_l^3 + T_h^3 + \frac{Y}{2} (5.30)$$

is satisfied, where $T_{l(h)}^3$ is the third isospin component of $SU(2)_{l(h)}$.

In terms of the mass eigenstates of the gauge bosons W_{μ}^{\pm} , Z_{μ} , W_{μ}^{\prime} , and Z_{μ}^{\prime} the interaction Lagrangian is

$$\mathcal{L}_{f}^{int} = \frac{e}{\sin\theta} \overline{\Psi_{L}}^{(1,2)} \gamma^{\mu} \left[T_{l}^{\pm} + T_{h}^{\pm} + \frac{\sin^{2}\phi}{x} \left(T_{h}^{\pm} \cos^{2}\phi - T_{l}^{\pm} \sin^{2}\phi \right) \right] \Psi_{L}^{(1,2)} W_{\mu}^{\pm} + \frac{e}{\sin\theta \cos\theta} \overline{\Psi_{L}}^{(1,2)} \gamma^{\mu} \left[T_{l}^{3} + T_{h}^{3} - Q \sin^{2}\theta + \frac{\sin^{2}\phi}{x} \left(\cos^{2}\phi T_{h}^{\pm} - \sin^{2}\phi T_{l}^{\pm} \right) \right] \Psi_{L}^{(1,2)} Z_{\mu} + \frac{e}{\sin\theta} \overline{\Psi_{L}}^{3} \gamma^{\mu} \left[-\frac{\sin\phi}{\cos\phi} T_{l}^{\pm} + \frac{\cos\phi}{\sin\phi} T_{h}^{\pm} - \frac{\sin^{3}\phi\cos\phi}{x\cos^{2}\theta} \left(T_{h}^{\pm} + T_{l}^{\pm} \right) \right] \Psi_{L}^{3} W_{\mu}^{\prime \pm} + \frac{e}{\sin\theta} \overline{\Psi_{L}}^{3} \gamma^{\mu} \left[-\frac{\sin\phi}{\cos\phi} T_{l}^{3} + \frac{\cos\phi}{\sin\phi} T_{h}^{3} - \frac{\sin^{3}\phi\cos\phi}{x\cos^{2}\theta} \left(T_{h}^{3} + T_{l}^{3} - Q \sin^{2}\theta \right) \right] \Psi_{L}^{3} Z_{\mu}^{\prime} + eQ\overline{f}^{i} \gamma^{\mu} f^{i} A_{\mu} - \frac{eQ \sin^{2}\theta}{\sin\theta\cos\theta} \overline{f_{R}}^{i} \gamma^{\mu} f_{R}^{i} \left(Z_{\mu} - \frac{\sin^{3}\phi\cos\phi}{x\cos\theta} Z_{\mu}^{\prime} \right). \tag{5.31}$$

Now I consider fermion mass generation and mixing. The first and second generations acquire their masses through the Yukawa interactions to the Φ doublet field,

with $\langle \Phi \rangle = v$. The Yukawa Lagrangian is

$$\mathcal{L}_{\text{Yukawa}} = \overline{\Psi_L}^1 \Phi \left[g_{11}^e e_R + g_{12}^e \mu_R + g_{13}^e \tau_R \right] + \overline{\Psi_L}^2 \Phi \left[g_{21}^e e_R + g_{22}^e \mu_R + g_{23}^e \tau_R \right] + h.c.$$
 (5.32)

For the third generation one can not generate the fermion masses through the usual Yukawa terms (dimension four operators), as it is not allowed by gauge invariance. It is only through higher dimension operators that one can generate these fermion masses. This characteristic of this model may be significant in understanding the fermion mass generation problem especially in understanding the observed mass hierarchy. Thus, although the masses of the first and second generations are generated through the Yukawa interactions as in the SM. The mass spectrum of third generation must be generated by a different mechanism. This conclusion may be attributed, in this model, to the strong flavor dynamics which may be evident at adequate high energy. At high energy where the interactions are strong enough, the masses of the third fermion generation are assumed to be generated possibly within some dynamical framework. I do not offer an explicit scenario for such a picture, however, an extended technicolor scenario may offer such a solution. The conclusion is that the strong flavor dynamics may be an essential player in the mass generation mechanism and an understanding of the strong dynamics at the high energy scale is required to solve the mass generation issue. Also, the strong dynamics may be responsible for the large masses of the third generation as compared to the first and second generations. In this discussion, I limit my self to the region where the strong flavor interaction is being under a perturbative control. Effectively, one can generate the third generation masses using dimension five operators, e.g., for the τ lepton one can generate its mass through the following mass terms

$$\frac{1}{\Lambda} \overline{\Psi_L}^3 \Sigma^{\dagger} \Phi \left[g_{31} e_R + g_{32} \mu_R + g_{33} \tau_R \right] + h.c., \tag{5.33}$$

where $\Psi_L^3 = \binom{\nu_r}{\tau}_L$, and Λ characterizes some large mass scale associated with the strong flavor interaction. It is reasonable to assume that $\Lambda \sim u \gg v$, and thus g_{33} is of order 1. An early version of the model Ref. [111] with an additional scalar doublet couples only to the third generation through the usual Yukawa interactions is another scenario for generating the third family masses.

With the fermion mass matrices being generated, one can obtain their physical masses by diagonalizing the mass matrices using bilinear unitary transformations. For example, for the lepton sector, the lepton mass matrix M_e can be read out from the mass Lagrangian written above in Eqs. (5.32) and (5.33). I introduce the rotational unitary matrices L_e , and R_e with the transformations,

$$e_L^i \to L_e^{ij} e_L^j$$
, $e_R^i \to R_e^{ij} e_R^j$. (5.34)

Hence, the physical mass matrix is given by

$$M_e^{\text{diag.}} = L_e^{\dagger} M_e R_e \,. \tag{5.35}$$

Because the third family interacts differently form the first and second generation, I expect in general Flavor Changing Neutral Currents (FCNC) may occur at tree level. For example, in terms of the leptonic weak eigenstates the left-handed neutral and charged currents are given by

$$\frac{e}{2\sin\theta\cos\theta}\left(\overline{e_L}\ \overline{\mu_L}\ \overline{\tau_L}\right)\gamma^{\mu}\left[-1+2\sin^2\theta+\frac{\sin^4\phi}{x}-\frac{\sin^2\phi}{x}G\right]\left(\frac{e_L}{\mu_L}\right)Z_{\mu},\,(5.36)$$

and

$$\frac{e}{\sqrt{2}\sin\theta} \left(\overline{e_L} \ \overline{\mu_L} \ \overline{\tau_L} \right) \gamma^{\mu} \left[1 - \frac{\sin^4\phi}{x} + \frac{\sin^2\phi}{x} G \right] \begin{pmatrix} \nu_{eL} \\ \nu_{\mu_L} \\ \nu_{\tau_L} \end{pmatrix} W_{\mu}^{\pm}, \tag{5.37}$$

where

$$G = \begin{pmatrix} 0 & 0 & 0 \\ 0 & 0 & 0 \\ 0 & 0 & 1 \end{pmatrix} . \tag{5.38}$$

In terms of the fermion mass eigenstates it follows that the left-handed neutral current interactions are

$$\frac{e}{2\sin\theta\cos\theta} \left(\overline{e_L} \ \overline{\mu_L} \ \overline{\tau_L} \right) \gamma^{\mu} \left[-1 + 2\sin^2\theta + \frac{\sin^4\phi}{x} - \frac{\sin^2\phi}{x} L_e^{\dagger} G L_e \right] \begin{pmatrix} e_L \\ \mu_L \\ \tau_L \end{pmatrix} Z_{\mu} . \tag{5.39}$$

For the left-handed charged current interactions, one has

$$\frac{e}{\sqrt{2}\sin\theta} \left(\overline{e_L} \ \overline{\mu_L} \ \overline{\tau_L} \right) \gamma^{\mu} \left[1 - \frac{\sin^4\phi}{x} + \frac{\sin^2\phi}{x} L_{\epsilon}^{\dagger} G L_{\epsilon} \right] \begin{pmatrix} \nu_{\epsilon L} \\ \nu_{\mu L} \\ \nu_{\tau L} \end{pmatrix} W_{\mu}^{-} + h.c. \quad (5.40)$$

For the neutrino sector, the neutral currents are

$$\frac{e}{2\sin\theta\cos\theta} \left(\overline{\nu_{eL}} \ \overline{\nu_{\mu_L}} \ \overline{\nu_{\tau_L}} \right) \gamma^{\mu} \left[1 - \frac{\sin^4\phi}{x} + \frac{\sin^2\phi}{x} L_e^{\dagger} G L_e \right] \begin{pmatrix} \nu_{eL} \\ \nu_{\mu_L} \\ \nu_{\tau_L} \end{pmatrix} Z_{\mu} . \tag{5.41}$$

Similarly, for the quark sector I introduce the unitary matrices L_{μ} and L_{d} , in terms of the mass eigenstates one finds the following interaction terms:

$$\frac{e}{2\sin\theta\cos\theta} \left(\overline{u_L} \ \overline{c_L} \ \overline{t_L} \right) \gamma^{\mu} \left[1 - \frac{4}{3}\sin^2\theta - \frac{\sin^4\phi}{x} + \frac{\sin^2\phi}{x} L_u^{\dagger} G L_u \right] \begin{pmatrix} u_L \\ c_L \\ t_L \end{pmatrix} Z_{\mu} , \tag{5.42}$$

$$\frac{e}{\sqrt{2}\sin\theta} \left(\overline{u_L} \overline{c_L} \overline{t_L} \right) \gamma^{\mu} \left[(1 - \frac{\sin^4\phi}{x}) L_u^{\dagger} L_d + \frac{\sin^2\phi}{x} L_u^{\dagger} G L_d \right] \begin{pmatrix} d_L \\ s_L \\ b_L \end{pmatrix} W_{\mu}^{-} + h.c., \tag{5.43}$$

and

$$\frac{e}{2\sin\theta\cos\theta} \left(\overline{d_L} \ \overline{s_L} \ \overline{b_L} \right) \gamma^{\mu} \left[-1 + \frac{2}{3}\sin^2\theta + \frac{\sin^4\phi}{x} - \frac{\sin^2\phi}{x} L_d^{\dagger} G L_d \right] \begin{pmatrix} d_L \\ s_L \\ b_L \end{pmatrix} Z_{\mu} . \tag{5.44}$$

The right-handed fermion couplings to the neutral gauge bosons Z and Z' are, respectively,

$$\frac{e}{\sin\theta\cos\theta}\left(-Q\sin^2\theta\right),\tag{5.45}$$

and

$$\frac{e}{\sin\theta} \left(Q \sin^2\theta \frac{\sin^3\phi \cos\phi}{x \cos^2\theta} \right). \tag{5.46}$$

The fermion couplings to the photon are the usual electromagnetic couplings. As shown above, if $g_h > g_l$ then the heavy gauge bosons would couple strongly to the third generation and weakly to the first two generations, and vice versa.

For the charged-current interactions in the quark sector, one observes that in the case of ignoring the new physics effect, the quark mixing is described by the unitary matrix $V = L_u^{\dagger} L_d$ which is identified as the usual Cabibbo-kobayashi-Maskawa (CKM) mixing matrix. When new physics are turned on, the mixing acquires an additional contribution proportional to $\sin^2 \phi/x$. Since the off-diagonal elements in the CKM matrix are small, one can approximate the quark mixing as

$$L_u^{\dagger} \left(1 - \frac{\sin^4 \phi}{x} + \frac{\sin^2 \phi}{x} G \right) L_d \simeq L_u^{\dagger} L_d - \frac{\sin^4 \phi}{x} + \frac{\sin^2 \phi}{x} G$$

$$= V - \frac{\sin^4 \phi}{x} + \frac{\sin^2 \phi}{x} G. \tag{5.47}$$

Interesting new features emerge in this model, e.g., lepton mixing is an exciting possibility. In addition to that, neutrinos can mix through their weak interactions,

making it an exciting feature that may be connected to the solar neutrino problem. Quark mixing also has interesting features, e.g., FCNC are a possibility in the model which could be investigated. However, the quark sector has more free parameters (to describe the mixing) than the lepton sector which makes the analysis more tedious and less predictive. Hence, I will not consider FCNC in the quark sector. For the lepton sector, there are already significant constraints on lepton universality and lepton number violation from the low energy data that one has to check against from the start. First, one must examine the already existed data on lepton number violation to see if such mixings are allowed. As an example is the almost vanishing branching ratio of the process $\Gamma_{\mu^-\to e^-e^+e^-}$ which forbids any mixing between the first and second generation. Other lepton number violation processes, especially those involving the third family, are not as severe as $\Gamma_{\mu^-\to e^-e^+e^-}$. In the next section, I will discuss in more details the constraints imposed by the low energy data.

5.3 Low Energy Constraints

As discussed in chapter 1, the input parameters of the SM α , G_F , and M_Z are defined through three experimental measurements, e.g., through the e-p scattering, the μ decay, and the Z peak at LEP. Similarly, one needs to fix the input parameters in the proposed model. The input parameters can be chosen as α , G_F , M_Z , $\sin \phi$, and x. I fix the first three parameters in a similar way to the SM case. The last two parameters will be treated as free parameters to be constrained through the low energy data. It is advantageous to express the input parameters in this model in terms of their corresponding SM ones. In the case of the electromagnetic coupling both values coincide, i.e., $\alpha = \alpha^{\rm SM}$. In the case of weak coupling constant I use the μ decay to define G_F . I calculate the μ -decay width as predicted in this model and

including the W and W' contributions. I find that $G_F = G_F^{\rm SM}$ (equivalently $v = v^{\rm SM}$) as long as one demands no mixings between the first and second lepton families (see below). Finally, I define M_Z using the Z peak at LEP, i.e., $M_Z = M_Z^{\rm SM}$.

Now, one can write other bare parameters in the proposed model in terms of the input parameters. For example consider Eq. (5.22)

$$M_Z = \frac{ev}{2\sin\theta\cos\theta} \left(1 - \frac{\sin^4\phi}{2x} \right) \,. \tag{5.48}$$

In the SM, M_Z can be written as

$$M_Z = \frac{ev}{2\sin\theta_{\rm SM}\cos\theta_{\rm SM}}\,,\tag{5.49}$$

where $\sin \theta_{\rm SM}$ is the SM weak mixing angle. Since M_Z is defined in both the SM and the proposed model through the Z peak at LEP, one concludes that

$$\frac{ev}{2\sin\theta\cos\theta}\left(1 - \frac{\sin^4\phi}{2x}\right) = \frac{ev}{2\sin\theta_{\rm SM}\cos\theta_{\rm SM}} \ . \tag{5.50}$$

One finds that

$$2\sin\theta\cos\theta = 2\sin\theta_{\rm SM}\cos\theta_{\rm SM}\left(1 - \frac{\sin^4\phi}{2x}\right) . \tag{5.51}$$

Hence, solving for $\sin^2\theta = 1 - \cos^2\theta$ in terms of $\sin^2\theta_{\rm SM}$, one finds that

$$\sin^2 \theta = \sin^2 \theta_{\rm SM} \left[1 - \left(\frac{\cos^2 \theta}{\cos 2\theta} \right)_{\rm SM} \frac{\sin^4 \phi}{x} \right]. \tag{5.52}$$

Therefore, observables can be predicted in the proposed model using the the input quantities α , G_F , M_Z , and $\sin^2\theta_{\rm SM}$. (The values of these quantities are given in chapter 1.) In addition to those quantities one has two additional free parameters $\sin^2\phi$ and x.

As previously discussed, lepton mixing is an interesting consequence of this model. However, the almost null measurement of $\mu \to e^-e^+e^-$ forbids any mixing between

the first and second lepton families. Still mixing may be allowed to exist between the third family and either the first or the second one. It is natural to assume that the mixing strength between leptons may be directly related to the lepton masses. If so, one would expect the mixing between the second and the third families to be more significant than the first and the third families. In the following discussion, I will assume that in the case of leptons, mixing will be only between the second and the third families. Because the mixing matrix is of the form $L_e^{\dagger}GL_e$, where the matrix G is given in Eq. (5.38). One finds that the mixing matrix for the second and third lepton families can be expressed by one free parameter. The 2×2 mixing matrix can be written as

$$\begin{pmatrix} \sin^2 \beta & \cos \beta \sin \beta \\ \cos \beta \sin \beta & \cos^2 \beta \end{pmatrix}, \tag{5.53}$$

where $\sin \beta$ is a free parameter of the model for describing the mixing between the second and third lepton families.

To test this model by the low energy constraints on lepton mixing and FCNC processes, it is necessary to understand the form of the four-fermion current-current interactions at zero momentum transfer. The four-fermion charged-current weak interactions are [112]

$$\frac{2}{v^2}(j_l+j_h)^2+\frac{2}{u^2}j_h^2\,, (5.54)$$

and the neutral current four-fermion interactions are

$$\frac{2}{v^2}(j_l^3 + j_h^3 - \sin^2\theta j_{\rm em})^2 + \frac{2}{u^2}(j_h^3 - \sin^2\phi \sin^2\theta j_{\rm em})^2, \qquad (5.55)$$

where $j_{l,h}$ are the left-handed charged currents corresponding to the first two generations and the third generation, respectively. Similarly, $j_{l,h}^3$ refers to the left-handed T^3 currents, while j_{em} represents the full electromagnetic current of the three families. I

conclude that if there is no mixing in the lepton families then all leptonic decays are identical to the SM, e.g., the τ lifetime can not furnish any new information about this model. (This also explains why $G_F = G_F^{\rm SM}$ from the μ -decay if there is no mixing between the first and second lepton families.) However, it is more general to allow mixing in the leptonic families, so I will investigate this possibility more carefully. Because of the almost vanishing branching ratio of the decay $\Gamma_{(\mu^- \to e^- e^+ e^-)}$, $BR \leq 10^{-12}$ [9], I will only allow mixing of τ and μ and their neutrinos. This mixing will modify the lifetime of the τ lepton, which depends on one free parameter, $\sin^2 \beta$. The constraints on $\sin^2 \beta$ come from: the ALEPH measurement (in terms of the effective couplings ratio g_τ/g_μ , cf. Table 5.1) of the branching fraction for τ decay into μ and the determination of the τ lifetime [113], the lepton number violation decay of $\tau \to \mu\mu\mu$, with a branching ratio $BR < 4.3 \times 10^{-6}$ (at 90% C.L.) [9], and the FCNC search at LEP with $BR(Z \to \mu^{\pm} \tau^{\mp}) < 1.7 \times 10^{-5}$ (at 95% C.L.) [114]. Figure 5.1 shows the Feynman diagrams for the process $\tau \to \mu\mu\mu$. At zero momentum transfer both diagrams are of equal importance. One finds that

$$\Gamma_{(\tau^- \to \mu^- \mu^- \mu^+)} = \Gamma_{(\tau^- \to \mu^- \nu_\tau \overline{\nu}_\mu)} \frac{\sin^2 \beta \cos^2 \beta}{4x^2} \left(\sin \beta^2 - 4 \sin^2 \theta \sin^2 \phi \right)^2 . \tag{5.56}$$

All other fermionic processes at zero momentum transfer, such as the μ decay, $K-\overline{K}$ mixing, and $B-\overline{B}$ mixing, are identical to the SM predictions.

In this model, the low energy predictions depend on the values of 1/x, $\sin^2 \phi$, and $\sin^2 \beta$ in addition to the measured values of $\alpha(M_Z)$, G_F , and M_Z . Using the most recent LEP measurements [12] (the total width of the Z boson, R_e , R_μ , R_τ , the vector g_V and axial-vector g_A couplings of e, the ratios $g_V(\mu,\tau)/g_V(e)$, $g_A(\mu,\tau)/g_A(e)$, the lepton forward-backward asymmetries, the τ and e polarization asymmetry, the hadronic pole cross section σ_h^0 , and the ALEPH measurement of g_τ/g_μ [113]) combined with the FCNC measurements of $\tau^- \to \mu^- \mu^- \mu^+$ and $Z \to \mu^- \tau^+$, I determine the

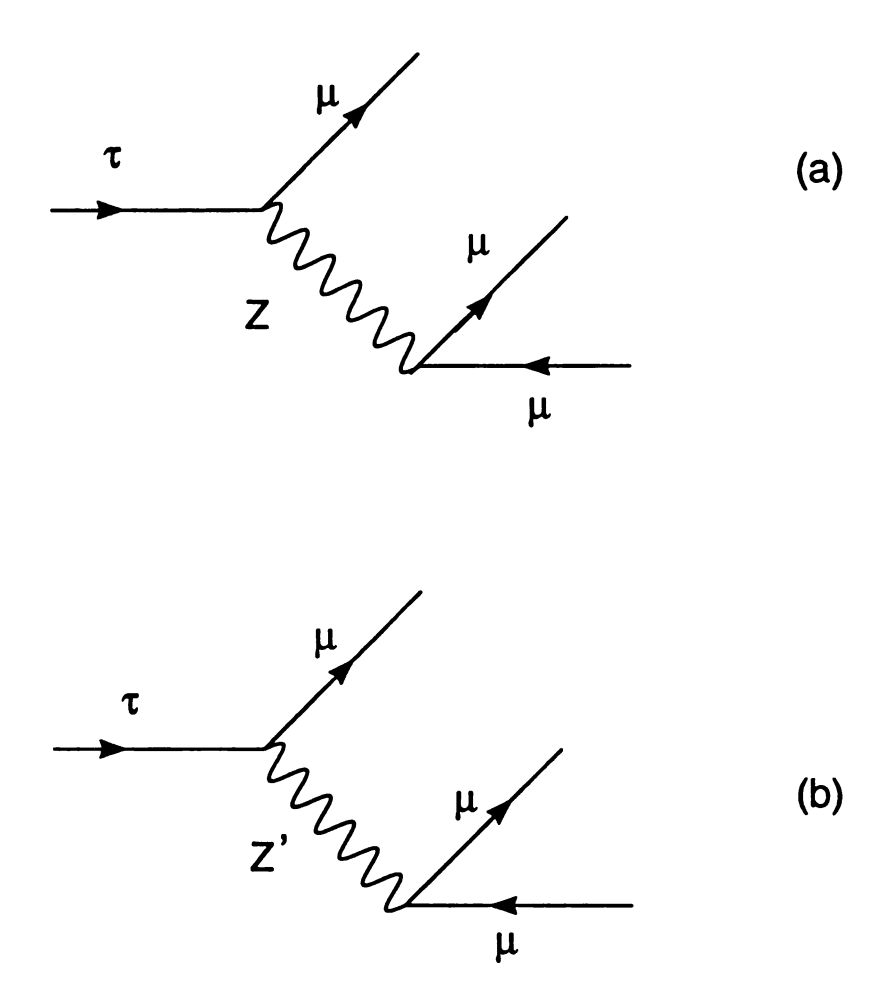


Figure 5.1: The Feynman diagrams for the process $\tau \to \mu \mu \mu$.

allowed values of $\sin^2 \phi$, $\sin^2 \beta$, and $M_{Z'}$. I do not include the controversial observables R_b and R_c as a part of the fit. Instead, I treat them as a prediction and discuss later whether the proposed model is able to explain the anomaly in these measurements. The experimental values of the electroweak observables [12] and their SM prediction [30] are given in Table 5.1.

I calculate the changes in the relevant physical observables relative to their SM values to leading order in 1/x, *i.e.*,

$$O = O^{SM} \left(1 + \delta O \right) \,, \tag{5.57}$$

where O^{SM} is the SM value for the observable O including the one-loop SM correction, and δO represents the new physics effect to leading order in 1/x. I list the calculated observables as follows,

$$\Gamma_Z = \Gamma_Z^{\text{SM}} \left(1 + \frac{1}{x} \left[-0.896 \sin^4 \phi + 0.588 \sin^2 \phi \right] \right) ,$$
 (5.58)

$$R_{\epsilon} = R_{\epsilon}^{\text{SM}} \left(1 + \frac{1}{x} \left[0.0794 \sin^4 \phi + 0.549 \sin^2 \phi \right] \right) , \qquad (5.59)$$

$$R_{\mu} = R_{\mu}^{\text{SM}} \left(1 + \frac{1}{x} \left[0.0794 \sin^4 \phi + 0.549 \sin^2 \phi - 2.139 \sin^2 \beta \sin^2 \phi \right] \right) , \qquad (5.60)$$

$$R_{\tau} = R_{\tau}^{\text{SM}} \left(1 + \frac{1}{x} \left[0.0794 \sin^4 \phi + 0.549 \sin^2 \phi - 2.139 \cos^2 \beta \sin^2 \phi \right] \right) , \qquad (5.61)$$

$$A_{FB}^{e} = (A_{FB}^{e})^{SM} \left(1 + \frac{1}{x} \left[10.44 \sin^{4} \phi \right] \right) ,$$
 (5.62)

$$A_{FB}^{\mu} = (A_{FB}^{\mu})^{SM} \left(1 + \frac{1}{x} \left[10.44 \sin^4 \phi + 12.14 \sin^2 \beta \sin^2 \phi \right] \right) , \qquad (5.63)$$

$$A_{FB}^{\tau} = (A_{FB}^{\tau})^{SM} \left(1 + \frac{1}{x} \left[10.44 \sin^4 \phi + 12.14 \cos^2 \beta \sin^2 \phi \right] \right) , \qquad (5.64)$$

$$A_{\epsilon} = A_{\epsilon}^{\text{SM}} \left(1 + \frac{1}{x} \left[5.22 \sin^4 \phi \right] \right) , \qquad (5.65)$$

$$A_{\tau} = A_{\tau}^{\text{SM}} \left(1 + \frac{1}{x} \left[5.22 \sin^4 \phi + 12.14 \cos^2 \beta \sin^2 \phi \right] \right) , \qquad (5.66)$$

$$\sigma_h^0 = (\sigma_h^0)^{\text{SM}} \left(1 + \frac{1}{x} \left[-0.01 \sin^4 \phi - 0.628 \sin^2 \phi \right] \right) , \qquad (5.67)$$

$$M_W = M_W^{\rm SM} \left(1 + \frac{1}{x} \left[1 + 0.215 \sin^4 \phi \right] \right) , \tag{5.68}$$

$$\frac{g_{\tau}}{g_{\mu}} = \left(\frac{g_{\tau}}{g_{\mu}}\right)^{\text{SM}} \left(1 + \frac{1}{x} \left[0.50 \sin^2 \beta \cos^2 \beta\right]\right) , \qquad (5.69)$$

$$BR(\tau^- \to \mu^- \mu^- \mu^+) = 0.045 \frac{\sin^2 \beta \cos^2 \beta}{x^2} \left(\sin^2 \beta - 4\sin^2 \theta \sin^2 \phi\right)^2, \tag{5.70}$$

$$\Gamma_{(Z \to \mu^- \tau^+)} = 0.167 \,\text{GeV} \left(\frac{\sin^2 \phi \sin \beta \cos \beta}{x}\right)^2. \tag{5.71}$$

In Figure 5.2 I show the fit result, at the 3σ level, of the Z' mass as a function of $\sin^2\phi$, for $\alpha_s=0.125$ and for three values of the mixing parameter $\sin^2\beta=0$ (dashed line), 0.5 (dot-dashed line) and 1 (solid line). In the case of $\sin^2\beta=0$, I find a lower bound on $M_{Z'}$ approximately 1.1 TeV. For $\sin^2\beta=1$, $M_{Z'}$ is approximately 1.4 TeV. For $\sin^2\beta=0.5$, $M_{Z'}$ is required to be larger for smaller $\sin^2\phi$ (< 0.1) due to the strong constraint from the lepton number violating process $\tau\to\mu\mu\mu$ (see Eq. (5.70)). As shown in Figure 5.2, as $\sin^2\phi$ increases the lower bound on $M_{Z'}$ increases, and increase in $M_{Z'}$ is slow for $\sin^2\phi<0.5$ and fast in the other case. This indicates that, a relatively light Z' prefers strong interactions with the third family fermions. If I consider a 2σ fit, then the lower bound on $M_{Z'}$ is about 1.4 TeV for $\sin^2\beta=0$ and 1.8 TeV for $\sin^2\beta=1$. In Figure 5.3 I show the fit result, at the 3σ level, For $\alpha_s=0.115$ I find that $M_{Z'}\geq 1.3$ TeV for $\sin^2\beta=0$ and $M_{Z'}\geq 2.2$ TeV for $\sin^2\beta=1$. In Tables 5.1 and 5.2 I calculate the low energy predictions in the model understudy for different choices of $\sin^2\phi$, x, $\sin^2\beta=1$, and for two values of α_s , 0.125 and 0.115, respectively.

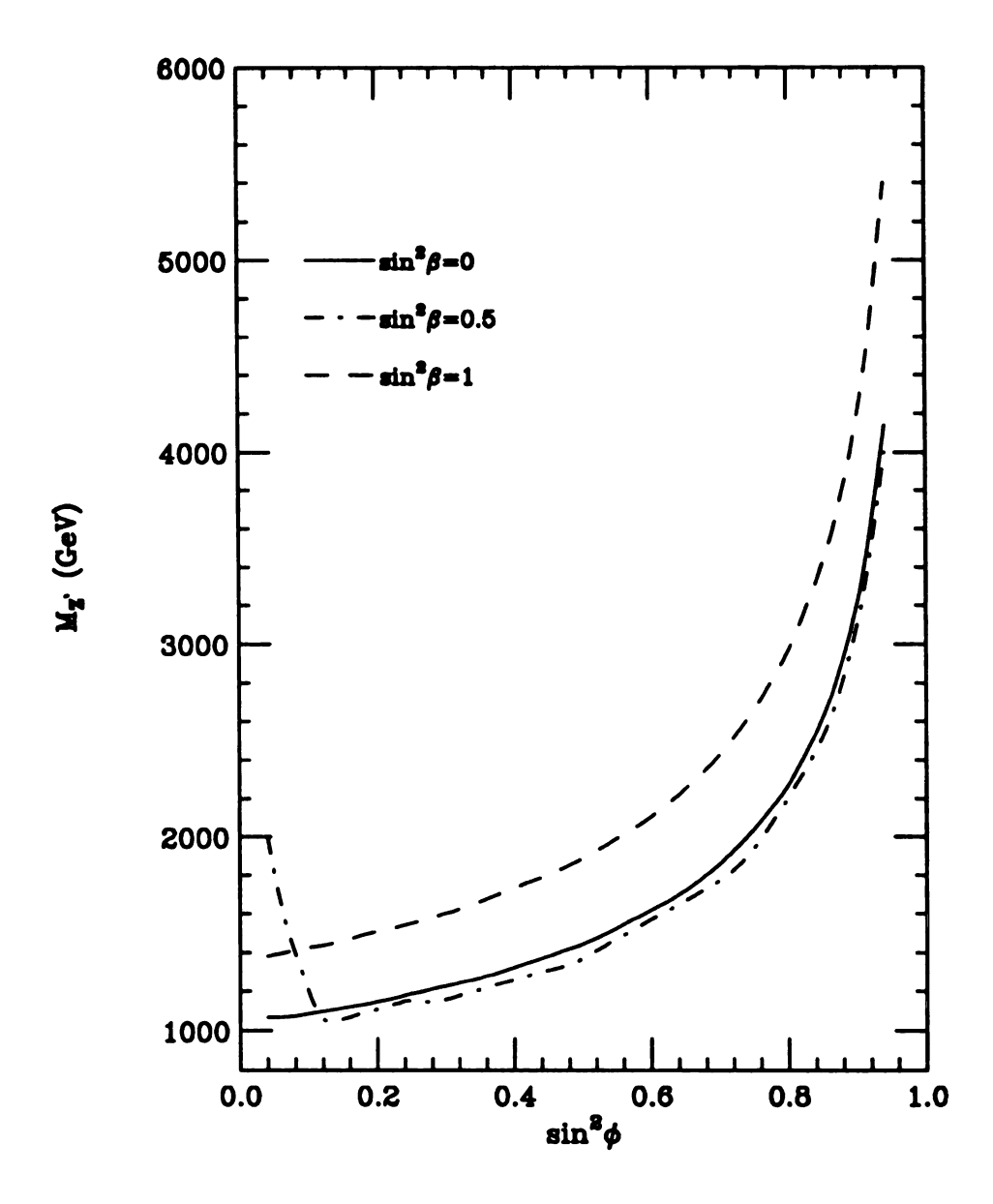


Figure 5.2: The lower bound on the heavy Z' mass as a function of $\sin^2 \phi$ for 3σ , $\sin^2 \beta = 0$ (solid) and $\sin^2 \beta = 1$ (dashed) and $\alpha_s = 0.125$

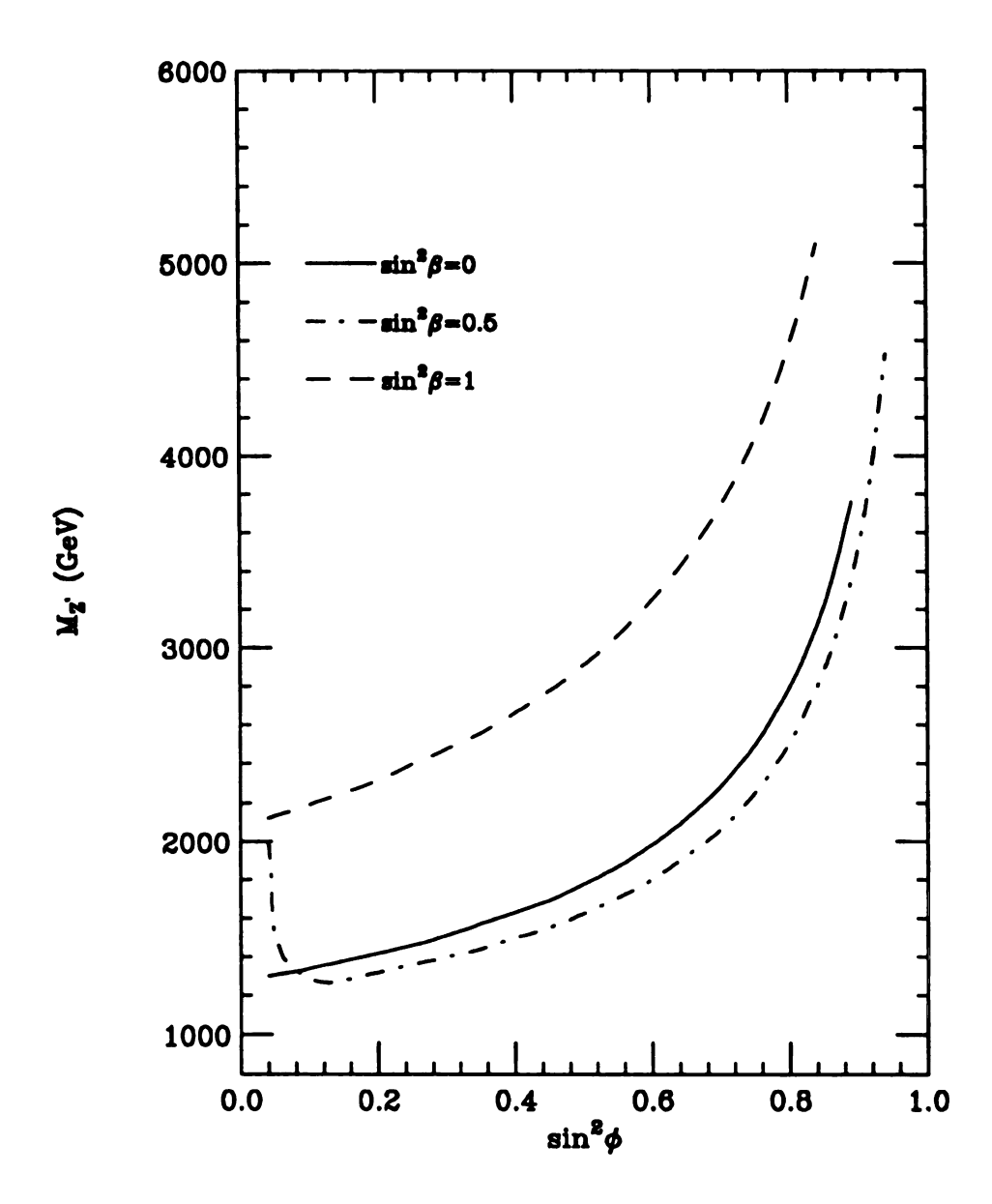


Figure 5.3: The lower bound on the heavy Z' mass as a function of $\sin^2 \phi$ for 3σ , $\sin^2 \beta = 0$ (solid) and $\sin^2 \beta = 1$ (dashed) and $\alpha_s = 0.115$.

As discussed in chapter 1, the LEP measured quantities $R_b = \Gamma_b/\Gamma_h$ and $R_c = \Gamma_c/\Gamma_h$ are not consistent with the SM prediction. One possibility to explain the anomaly in these quantities is to consider new physics which can affect the b and c quarks' couplings to the Z boson. The question now is whether this model is able to give any insight regarding these measurements. The observed value $R_b^{\rm exp.} = 0.2219 \pm 0.0017$ [12] is higher than the SM value $R_b^{\rm SM} = 0.2157$ [30] by about 3.5 σ . On the other hand, $R_c^{\rm exp.} = 0.1543 \pm 0.0074$ is smaller than the SM value $R_c^{\rm SM} = 0.1721$ by about 2.5 σ . With the allowed region of the parameter space being determined, I investigate which part of the allowed space is able to explain the anomaly in R_b . Because the measured value of R_b is different from the SM value by more than 3σ , I expect to be able to constrain the smallest and largest Z' mass by requiring that the new physics effect shifts the theoretical value of R_b to be within the 3σ range of the measured value. In this model, R_b is given by

$$R_b = R_b^{\text{SM}} \left(1 + \frac{1}{x} \left[-0.0149 \sin^4 \phi + 1.739 \sin^2 \phi \right] \right) . \tag{5.72}$$

Ignoring the negligible $\sin^4 \phi$ term, one finds

$$\frac{R_b - R_b^{\text{SM}}}{R_b^{\text{SM}}} = \left(1.739 \frac{\sin^2 \phi}{x}\right). \tag{5.73}$$

Since $M_{Z'}^2 \approx M_{W \frac{z}{\sin^2 \phi \cos^2 \phi}}^2$, the Z' mass can be constrained to be

$$462 < M_{Z'} \cos \phi < 1481 \text{ GeV}. \tag{5.74}$$

Thus, if I assume the anomaly in R_b is mainly due to this type of new physics, then there is an upper bound on $M_{Z'}$ which depends on the gauge coupling (equivalently $\sin \phi$). For example, for $\sin^2 \phi = 0.04$, the upper bound (which is independent of $\sin^2 \beta$) on $M_{Z'}$ obtained from R_b is ~ 1.5 TeV.

For R_c I find that the new modification to the SM model shifts R_c in the correct direction, i.e. it decreases the theoretical value as desired. I find

$$R_c = R_c^{SM} \left(1 + \frac{1}{x} \left[0.038 \sin^4 \phi - 0.549 \sin^2 \phi \right] \right). \tag{5.75}$$

However, the amount of shift is very small to account for its anomaly, e.g., with the lower bound on the heavy mass coming from 1.1 TeV, I find that the theoretical value of R_c is still outside the 2σ range of the measured value.

From these results I conclude that this model can account for the deviation in R_b from the SM at the 3σ level. Even though R_c is shifted in the needed direction, the predicted value is still outside the 2σ range of the data. Therefore, one cannot explain the anomaly in R_c entirely based on the proposed model. Also, in this model the prediction of the observable $A_{\rm LR}$ is identical to that of the observable A_c . Thus, this model cannot explain the discrepancy between the the SLC measurement $A_{\rm LR} = 0.1551 \pm 0.0040$ and the LEP measurement A_c [30].

5.4 High Energy Experiments

LEP was operating at the Z-pole with large production rates, it is therefore unlikely to better test this model at other high energy colliders at the scale of M_Z . I have checked that the allowed parameters in Figures 5.2 and 5.3 do not upset the measurements of W^{\pm} and Z properties at the Tevatron by CDF and DØ groups [115]. To study the possible effects due to the heavy W' and Z' bosons, I will concentrate on physics at energy scales larger than M_Z . In this study, the interference effects from A (photon), Z and Z' in neutral channels and the interference of W and W' in charged channels are all included. To simplify the discussion, I will consider two sets of parameters for $(x, \sin^2 \phi, \sin^2 \beta)$: (7,0.04,0) and (20.6,0.14,0.5) which correspond to $(M_{Z'}, \Gamma_{Z'})$ equal to (1083,291) GeV and (1050,76) GeV, respectively. The

conclusions, however, will not significantly depend on the details of the parameters chosen from Figures 5.2 and 5.3.

At the Tevatron, it is possible to reach the high energy region where the W' or Z' effects can be important. CDF has reported the result of searching for new gauge bosons by measuring the number of excess di-lepton events with large transverse mass [116] or invariant mass [117]. I find that those results do not further constrain the parameters shown in Figures 5.2 and 5.3. For the Tevatron with Main Injector (a $\bar{p}p$ collider at $\sqrt{s} = 2$ TeV with a 2 fb⁻¹ luminosity), the excess in the e^-e^+ or $e^+\nu_e$ rates from this model is generally not big enough to be easily observed. Since the third family leptons can strongly couple to the new gauge bosons, the rate of τ lepton production can in principle be quite different from that of e or μ . Furthermore, if $\sin \beta$ is not zero, the production rates of $\bar{p}p \to W, W' \to \ell \nu_{\ell}$ or $\bar{p}p \to \gamma, Z, Z' \to \ell \bar{\ell}$ will be different for $\ell = e$ and μ . However, even with the maximal mixing between τ and μ (i.e., $\sin \beta = 1$) this difference at the Tevatron can only exceed a 3σ effect for a $10\,\mathrm{fb^{-1}}$ of integrated luminosity. At the LHC (a pp collider with $\sqrt{s}=10\,\mathrm{TeV}$ and a luminosity of 100 fb⁻¹), this excess cannot be mistaken. Furthermore, at the LHC, the excess in the production rates of the $\ell\nu_{\ell}$ and the $\ell^+\ell^-$ events can also be individually tested. Thus, it is much easier to either find such new effects or constrain parameters of the model at the LHC than at the Tevatron. I note that this conclusion holds for either a small or large $\sin^2 \phi$. Although with a large $\sin^2 \phi$, the new physics effects to light family fermions will be large, because of the large W' and Z' masses, the net effect of the new physics to the production of di-lepton pairs does not significantly depend on $\sin^2 \phi$.

Another signature of the model is an excess in the top quark production, however, this excess cannot be observed at the Tevatron because of large background from the QCD processes $q\bar{q}, gg \to t\bar{t}$. At the LHC, the excess in the $t\bar{t}$ pair productions can

easily be seen in the invariant mass distributions. The extra gauge bosons can produce an excess of di-jet events in the large invariant mass region, but the parameter space remaining after imposing low energy constraints does not allow a big enough effect to explain the results reported by CDF [32].

Another possible interesting signature is the production of $\mu^{\pm}\tau^{\mp}$ pairs, which is unconstrained by current LEP data. At the Tevatron for $(x, \sin^2\phi, \sin^2\beta)$ equal to (20.6,0.14,0.5), the most favorable scenario for observing this signal, I find a total of about 20 events for $2 \, \text{fb}^{-1}$ of integrated luminosity, assuming no cuts are imposed. It is interesting to notice that this implies that the upgraded Tevatron can provide a better constraint on this FCNC type of event than LEP can. At the LHC, the cross section is 170 fb for this choice of parameters.

At high energy electron colliders, the detection of the above new signatures becomes much easier as long as there are enough of them produced in the collisions. In this model, neither LEP140 or LEP-II can see them, so I will concentrate on the future high energy Linear Collider (LC) [118]. Consider the proposed e^+e^- LC at center of mass (CM) energy $\sqrt{s} = 500$ GeV with an integrated luminosity of 50 fb⁻¹. For $m_t = 175$ GeV the SM production rate $\sigma^{SM}_{(e^+e^- \to t\bar{t})}$ is 558 fb. Thus, a large number of $t\!-\bar{t}$ pairs is expected at the LC. Considering the set of parameters $(x,\sin^2\phi,\sin^2\beta) = (7.0,0.04,0.0)$, I find that $\sigma_{(e^+e^- \to t\bar{t})} = 709$ fb, i.e. there is about 27% increase in the total production rate compared to the SM. At the LC it is expected to measure the $t\!-\bar{t}$ cross section, for ℓ + jets decay modes, to within a few percent. With the assumption that the expected measurement is within 3 standard deviation from the SM, one can constrain the parameters to those which produce $M_{Z'} \geq 2.3$ TeV. I note that the same constraints hold for different choices of $\sin^2\phi$ and x but with almost the same ratio $\sin^2\phi/x$, especially for small $\sin\phi$, since in the cross section the two parameters enter as a ratio. Because only the left-handed couplings of the top quark

are significantly modified in this model, measuring the angular distribution of t in the $t-\bar{t}$ CM frame can further improve these bounds if no new signal is found.

Although the e^+e^- LC is suitable to probe the model under study, I notice that the $\mu^+\mu^-$ collider is also interesting because of the possible mixing between μ and τ leptons. For small mixing the e^+e^- and the $\mu^+\mu^-$ colliders lead to similar production rates as expected. For large $\sin\beta$ the total production rate of $\sigma_{(\mu^+\mu^-\to t\bar{t})}$ becomes smaller than the SM rate which shows the opposite effect to the production of the $e^+e^-\to t\bar{t}$ events predicted by this model. For the same reason, if $\sin^2\beta=1.0$, then it is easy to observe the difference in the production rates of e^-e^+ and $\mu^-\mu^+$ (or $\tau^+\tau^-$) pairs at the LC. Furthermore, at the LC, if the FCNC event $e^-e^+\to \mu^\pm\tau^\mp$ occurs, it can be unmistakably identified. For a 500 GeV LC with a 50 fb⁻¹ luminosity, I expect an order of 300 such events to be observed for $(x,\sin^2\phi,\sin^2\beta)$ equal to (20.6,0.14,0.5). Figure 5.4 shows the FCNC event numbers at the LC for a few choices of parameters, assuming no cuts are imposed.

In summary, I find that due to the strong constraints to this model implied from low energy data (including Z-pole data) it is not easy to find events with new signatures predicted for Tevatron or LEP-II. However, at the LHC and the LC, it becomes easy to detect deviations from the SM in the productions of the third family or second family (in case of large mixing between τ and μ lepton) fermions. I have also checked the possible excess in the W^+W^- or the $W^\pm Z$ productions at future high energy colliders. It turns out that the branching ratios for Z' or W' to the pure gauge boson modes are always small. One finds

$$\Gamma(Z' \to W^+ W^-) \approx \frac{e^2 M_{Z'}}{192\pi \sin^2 \theta} \frac{\sin^6 \phi \cos^2 \phi}{x^2} \frac{M_{Z'}^4}{M_W^4}$$
 (5.76)

Therefore, the gauge boson pair productions are not good channels for testing this model.

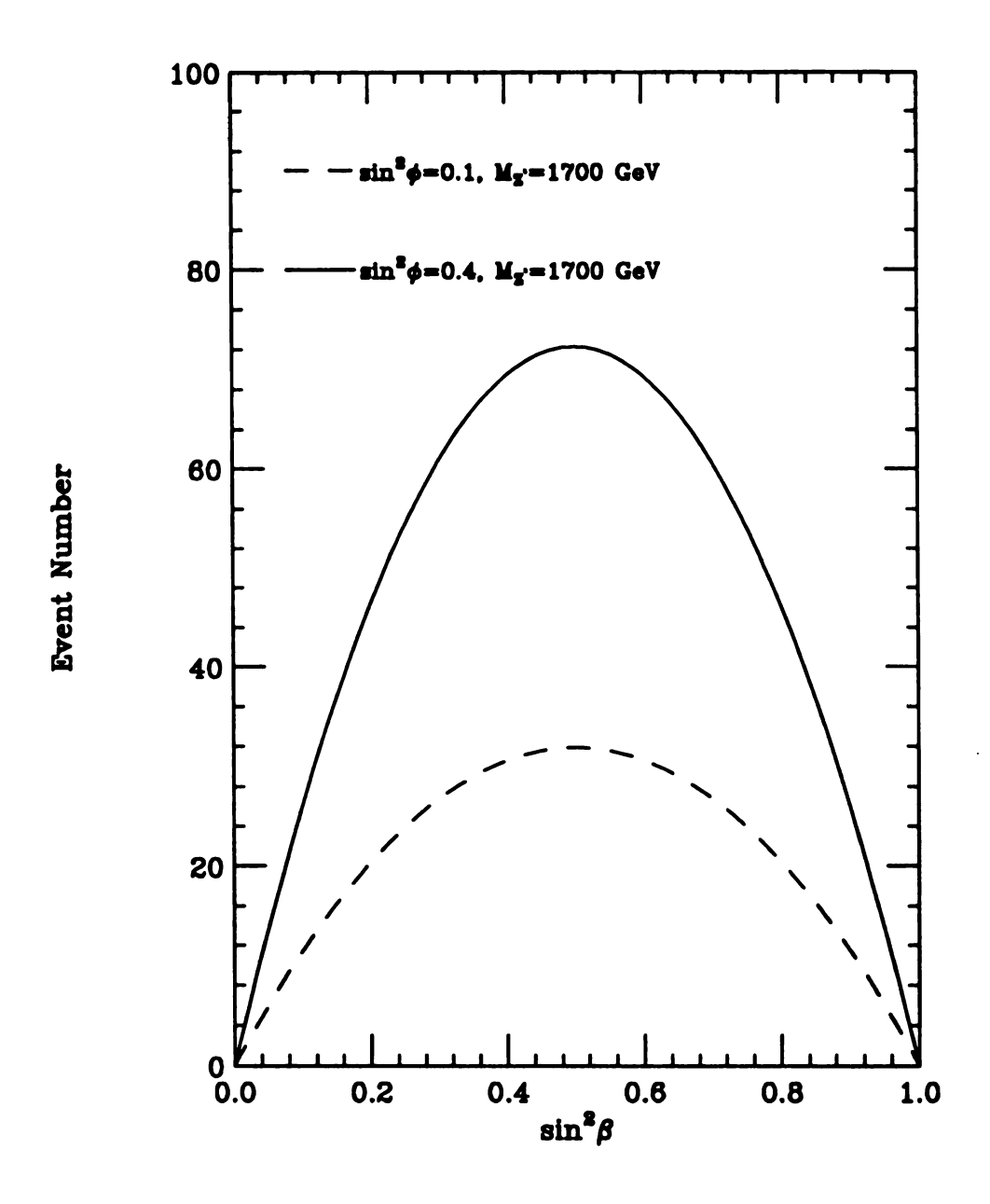


Figure 5.4: The event number of $\mu^{\pm}\tau^{\mp}$ produced at the LC, with a c.m. energy of 500 GeV, and for two choices of parameters.

In the process of preparing for this paper, I noticed that another similar work appears in Ref. [42]. My conclusions on the allowed parameters of the model and the predictions on the event yields for electron or hadron colliders are different from theirs. Also, I became aware of a work done in Ref. [43], in which a similar model was proposed and studied using the low energy data.

Table 5.1: Experimental and predicted values of electroweak observables for the SM and the proposed model (with different choices of parameters) for $\alpha_s = 0.125$ with $m_t = 175 \text{ GeV}$ and $m_H = 300 \text{ GeV}$.

a: $\sin^2 \beta = 0$, $\sin^2 \phi = 0.04$, $M_Z' = 1.1$ TeV, $\Gamma_Z' = 288$ GeV. b: $\sin^2 \beta = 1$, $\sin^2 \phi = 0.04$, $M_Z' = 1.4$ TeV, $\Gamma_Z' = 370$ GeV. c: $\sin^2 \beta = 0$, $\sin^2 \phi = 0.80$, $M_Z' = 3.0$ TeV, $\Gamma_Z' = 287$ GeV. d: $\sin^2 \beta = 1$, $\sin^2 \phi = 0.80$, $M_Z' = 3.3$ TeV, $\Gamma_Z' = 316$ GeV.

Observables	Experimental data	SM	The model			
			a	b	С	d
$g_V(e)$	-0.0368 ± 0.0017	-0.0367	-0.0367	-0.0367	-0.0372	-0.0371
$g_A(e)$	-0.50115 ± 0.00052	-0.5012	-0.5012	-0.5012	-0.5005	-0.5006
$g_V(\mu)/g_V(e)$	1.01 ± 0.14	1.00	1.00	1.05	1.00	1.04
$g_A(\mu)/g_A(e)$	1.0000 ± 0.0018	1.0000	1.0000	1.0034	1.0000	1.0030
$g_V(au)/g_V(e)$	1.008 ± 0.071	1.000	1.073	1.000	1.047	1.000
$g_A(au)/g_A(e)$	1.0007 ± 0.0020	1.0000	1.0055	1.0000	1.0036	1.0000
Γ_{Z}	2.4963 ± 0.0032	2.4978	2.5054	2.5025	2.4967	2.4969
R_e	20.797 ± 0.058	20.784	20.848	20.823	20.830	20.822
R_{μ}	20.796 ± 0.043	20.784	20.848	20.671	20.830	20.690
$R_{ au}$	20.813 ± 0.061	20.831	20.648	20.870	20.717	20.869
σ_h^0	41.488 ± 0.078	41.437	41.293	41.348	41.343	41.359
A_{e}	0.139 ± 0.0089	0.1439	0.1441	0.1440	0.1461	0.1457
$A_{ au}$	0.1418 ± 0.0075	0.1439	0.1537	0.1440	0.1523	0.1457
A_{e}^{FB}	0.0157 ± 0.0028	0.0157	0.0157	0.0157	0.0162	0.0161
A_{μ}^{FB}	0.0163 ± 0.0016	0.0157	0.0157	0.0164	0.0162	0.0167
$A_e^{FB} \ A_\mu^{FB} \ A_ au^{FB}$	0.0206 ± 0.0023	0.0157	0.0168	0.0157	0.0169	0.0161
$g_ au/g_\mu$	0.9943 ± 0.0065	1.0000	1.0000	1.0000	1.0000	1.0000
R_b	0.2219 ± 0.0017	0.2157	0.2178	0.2170	0.2170	0.2168
R_c	0.1543 ± 0.0074	0.1721	0.1716	0.1718	0.1718	0.1718
M_{W}	80.26 ± 0.16	80.32	80.32	80.32	80.37	80.36
A_{LR}	0.1551 ± 0.0040	0.1439	0.1441	0.1440	0.1461	0.1457

Table 5.2: Experimental and predicted values of electroweak observables for the SM and the proposed model (with different choices of parameters) for $\alpha_s = 0.115$ with $m_t = 175$ GeV and $m_H = 300$ GeV.

 $m_t = 175 \text{ GeV and } m_H = 300 \text{ GeV.}$ a: $\sin^2 \beta = 0$, $\sin^2 \phi = 0.04$, $M_Z' = 1.3 \text{ TeV}$, $\Gamma_Z' = 343 \text{ GeV.}$ b: $\sin^2 \beta = 1$, $\sin^2 \phi = 0.04$, $M_Z' = 2.1 \text{ TeV}$, $\Gamma_Z' = 562 \text{ GeV.}$ c: $\sin^2 \beta = 0$, $\sin^2 \phi = 0.80$, $M_Z' = 3.0 \text{ TeV}$, $\Gamma_Z' = 287 \text{ GeV.}$ d: $\sin^2 \beta = 1$, $\sin^2 \phi = 0.80$, $M_Z' = 4.5 \text{ TeV}$, $\Gamma_Z' = 430 \text{ GeV.}$

Observables	Experimental data	SM	The model			
			a	b	С	d
$g_V(e)$	-0.0368 ± 0.0017	-0.0367	-0.0367	-0.0367	-0.0372	-0.0369
$g_A(e)$	-0.50115 ± 0.00052	-0.5009	-0.5012	-0.5012	-0.5005	-0.5009
$\int g_V(\mu)/g_V(e)$	1.01 ± 0.14	1.00	1.00	1.02	1.00	1.02
$\int g_A(\mu)/g_A(e)$	1.0000 ± 0.0018	1.0000	1.0000	1.0015	1.0000	1.0016
$g_V(\tau)/g_V(e)$	1.008 ± 0.071	1.000	1.053	1.000	1.047	1.000
$\int g_A(\tau)/g_A(e)$	1.0007 ± 0.0020	1.0000	1.0040	1.0000	1.0036	1.0000
$\Gamma_{\mathbf{Z}}$	2.4963 ± 0.0032	2.4922	2.4977	2.4943	2.4911	2.4917
\setminus R _e	20.797 ± 0.058	20.716	20.761	20.733	20.762	20.736
$\setminus R_{\mu}$	20.796 ± 0.043	20.716	20.761	20.666	20.762	20.666
$R_{ au}$	20.813 ± 0.061	20.762	20.631	20.779	20.649	20.782
$\setminus \qquad \sigma_h^0$	41.488 ± 0.078	41.490	41.387	41.450	41.395	41.448
A_e	0.139 ± 0.0089	0.1439	0.1440	0.1440	0.1461	0.1449
$\setminus A_{ au}$	0.1418 ± 0.0075	0.1449	0.1510	0.1440	0.1523	0.1449
A_e^{FB}	0.0157 ± 0.0028	0.0157	0.0157	0.0157	0.0162	0.0159
$A_{\mu}^{FB} A_{ au}^{FB}$	0.0163 ± 0.0016	0.0157	0.0157	0.0160	0.0162	0.0162
A_{τ}^{FB}	0.0206 ± 0.0023	0.0157	0.0165	0.0157	0.0169	0.0159
$g_{ au}/g_{\mu}$	0.9943 ± 0.0065	1.0000	1.0000	1.0000	1.0000	1.0000
R_b	0.2219 ± 0.0017	0.2157	0.2172	0.2163	0.2170	0.2163
R_c	0.1543 ± 0.0074	0.1721	0.1717	0.1720	0.1718	0.1720
$\setminus M_W$	80.26 ± 0.16	80.32	80.32	80.32	80.37	80.34

Chapter 6

Discussions and Conclusions

Since the top quark is heavy, the top quark can be a window for new physics, either from top quark decays to new objects, or from large radiative corrections. Because of the heavy top quark mass, new physics will feel its presence easily and eventually may show up in the effective top quark couplings to the gauge bosons. Furthermore, since the top quark mass is of the order of the symmetry-breaking scale, the top quark is likely to provide useful hints about the symmetry-breaking mechanism responsible for generating the gauge boson masses and at least connected with the fermion mass generation mechanism.

The main goal of this work is to browse through the low energy precision data from LEP and SLC searching for possible new physics effects dominantly in conjunction with the top quark couplings to the gauge bosons. Constraining the nonstandard couplings of the top quark provides an estimate for possible deviation in the gauge universality advocated in the SM. Furthermore, if the deviation in the gauge universality for the top quark case is due to the symmetry-breaking mechanism, then the measurement of and the correlation among the nonstandard couplings can be a direct probe to the symmetry-breaking mechanism.

In chapter 3, I have applied the electroweak chiral Lagrangian to probe the non-

standard couplings of the top quark to the gauge bosons using precision LEP data. Assuming b-b-Z vertex is not modified, I found that κ_L^{NC} is already constrained to be $-0.05 < \kappa_L^{NC} < 0.17 \; (0.0 < \kappa_L^{NC} < 0.15)$ at the 95% C.L. for a 160 (180) GeV top quark. Although κ_R^{NC} and κ_L^{CC} are allowed to be in the full range of ± 1 , precision LEP data do impose some correlations among κ_L^{NC} , κ_R^{NC} , and κ_L^{CC} . (κ_R^{CC} does not contribute to the LEP observables of interest in the limit of $m_b = 0$.)

Inspired by the experimental fact $\rho \approx 1$, reflecting the existence of an approximate custodial symmetry, I proposed an effective model to relate κ_L^{NC} and κ_L^{CC} . I found that the nonuniversal interactions of the top quark to the gauge bosons are well constrained by LEP data, within 95% C.L. The constraints are summarized in Table 3.1 (see also Figures 3.6–3.10). Also, the two parameters $\kappa_L = \kappa_L^{NC}$ and $\kappa_R = \kappa_R^{NC}$ are strongly correlated where $\kappa_L \sim 2\kappa_R$.

I note that the relations among κ 's can be used to test different models of electroweak symmetry-breaking. For instance, a heavy SM Higgs boson $(m_H > m_t)$ will modify the couplings t-t-Z and t-b-W of a heavy top quark at the scale m_t such that $\kappa_L^{NC} = 2\kappa_L^{CC}$, $\kappa_L^{NC} = -\kappa_R^{NC}$, and $\kappa_R^{CC} = 0$. Another example is the effective model discussed in Ref. [95] where, $\kappa_R^{CC} = \kappa_L^{CC} = 0$. In this model the low energy precision data impose the relation $\kappa_L^{NC} \sim \kappa_R^{NC}$. Also, the simple commuting extended technicolor model presented in Ref. [59] predicts that the nonstandard top quark couplings are of the same order as the nonstandard bottom quark couplings.

It is also interesting to note that the upper bound on the top quark mass can be raised from the SM bound $m_t < 200 \,\text{GeV}$ to as large as 300 GeV if new physics occurs. That is to say, if there is new physics associated with the top quark, it is possible that the top quark is heavier than what the SM predicts.

Also, in chapter 3, I discussed how the present SLC measurement of A_{LR} can

contribute to the constraints imposed on the nonstandard couplings κ_L^{NC} , κ_R^{NC} , and κ_L^{CC} at LEP. I found that if one uses the LEP constraints to predict the new physics contribution to the SLC measurement of A_{LR} , then for the special model, $\kappa_L^{CC} = \kappa_L^{NC}/2$, it is possible to reconcile the LEP and SLC data at 95% C.L.

Undoubtedly, direct detection of the top quark at the Tevatron, the LHC, and the LC is crucial to measuring the couplings of t-b-W and t-t-Z. At hadron colliders, κ_L^{CC} and κ_R^{CC} can be measured by studying the polarization of the W boson from top quark decay in $t\bar{t}$ events. They can also be measured simply from the production rate of the single top quark event. The LC is the best machine to measure κ_L^{NC} and κ_R^{NC} which can be measured from studying the angular distribution and the polarization of the top quark produced in e^-e^+ collision. Details about these bounds were given in section 3.5.

In chapter 4, I present a theoretical frame work to extract the pure m_t corrections to low energy data in the chiral Lagrangian approach. I reproduced the results in chapter 3 by considering an effective Lagrangian which involves only the scalar sector (the unphysical Goldstone bosons and probably the Higgs boson), and the top and bottom quarks. I discussed how to relate the two different approaches presented in chapters 3 and 4. I showed that by considering a completely different set of Green's functions (without involving any external gauge boson line) from that discussed in chapter 3, I recovered exactly the same result. The new frame work is useful and interesting because first, it simplifies the whole process of calculating radiative corrections, as it is much easier to work with scalers than with vector bosons. Also, this approach is shown to clearly identify observables which are sensitive to the symmetry-breaking sector of the electroweak theory. This is clear since only contributions independent of the gauge structure survives.

In chapter 5, I present a self-contained model which demonstrates how the non-

standard top quark couplings to gauge bosons can be generated. The model has a very rich structure and significant implications at low and high energy scales. Using the low energy data I discuss the possible constraints on the model. On the other hand, the high energy colliders will provide further tests and demonstrate possible new physics especially interesting FCNC processes.

Appendix A

Renormalization Schemes

In chapter 1, I discuss in details the Z-pole renormalization scheme and very briefly mention few other schemes. In this appendix, I discuss to some extent different renormalization schemes and possible relations among these schemes. As discussed in chapter 1, to fix the low energy part of the SM one needs to specify three input quantities, the light fermion masses, and quark mixing. Different choices correspond to different renormalization schemes. The most common used renormalization schemes include, the Z-pole scheme, the on-shell scheme, and the $\overline{\rm MS}$ scheme.

At tree level the weak mixing angle can be written in different equivalent ways,

$$\sin^2 \theta_0 = \frac{1}{2} \left(1 - \left[1 - \frac{4\pi\alpha_0}{\sqrt{2}G_{F0}M_{Z0}^2} \right]^{1/2} \right) = 1 - \frac{M_{W0}^2}{M_{Z0}^2} = \frac{g_0^{\prime 2}}{g_0^{\prime 2} + g_0^2} . \tag{A.1}$$

Once radiative corrections are included all these definitions are are not satisfied simultaneously. One has to pick one of these definition for any specific renormalization scheme.

- The Z-pole scheme.
 - In this scheme, the input observables are chosen to be:
 - The electromagnetic coupling $\alpha=e^2/4\pi$ measured from electron-proton

(e-p) scattering in the limit of zero momentum transfer $q^2 \to 0$ (Thomson limit) [9]

$$\alpha^{-1} = 137.0359895(61). (A.2)$$

- The Fermi coupling constant G_F measured from the muon lifetime τ_{μ} [9]

$$G_F = 1.166389(22) \times 10^{-5} \text{ GeV}^{-2}$$
 (A.3)

- The Z mass [12]

$$M_Z = 91.1885 \pm 0.0022 \text{ GeV}$$
 (A.4)

The Z-pole scheme is simple and precise because the input parameters are measured very well. This scheme is suitable in studying physical observables at the Z pole. As discussed in chapter 1, in analysing the Z-pole physics the pure QED corrections are treated separately from the weak corrections. In particular, the light fermions contributions to the photon vacuum polarization function are absorbed in defining the running coupling $\alpha(M_Z^2)$ at the M_Z scale. In chapter 1, we found

$$\alpha(M_Z^2) = \frac{\alpha}{1 - \Delta\alpha(M_Z^2)} \ . \tag{A.5}$$

where, $\Delta \alpha(M_Z^2)$ is defined as

$$\Delta\alpha(M_Z^2) = -F^{\gamma\gamma}(M_Z^2) + F^{\gamma\gamma}(0). \tag{A.6}$$

Currently, there is a lively debate on what value of $\alpha(M_Z^2)$ to use. I quote the value [18]

$$\alpha^{-1}(M_Z^2) = 128.89 \pm 0.09$$
, (A.7)

In this scheme, the main theoretical error propagating into the definitions of the SM parameters is coming from the error in determining $\alpha(M_Z^2)$. In this scheme, the weak mixing angle is defined to all orders by the relation

$$\sin^2 \theta = 1 - \cos^2 \theta \equiv \frac{1}{2} \left(1 - \left[1 - \frac{4\pi\alpha(M_Z^2)}{\sqrt{2}G_F M_Z^2} \right]^{1/2} \right) . \tag{A.8}$$

The weak mixing angle $\sin^2 \theta$ is well determined theoretically [60],

$$\sin^2\theta = 0.2312 \pm 0.0003. \tag{A.9}$$

The main theoretical error in $\sin^2\theta$ is coming from the theoretical error in determining the running coupling $\alpha(M_Z^2)$. In fact by only considering the error in $\alpha(M_Z^2)$, there is an induced error in $\delta \sin^2\theta$

$$\frac{\delta \sin^2 \theta}{\sin^2 \theta} \sim 0.1\% \,, \tag{A.10}$$

which amounts to most of the error in $\sin^2 \theta$.

The Z-pole scheme is defined such that all top quark and Higgs boson contributions are removed from the parameters $\alpha(M_Z^2)$ and $\sin^2\theta$. The top quark and Higgs boson contributions enter when considering other predicted observables (see chapter 1), e.g., the W mass, the partial decay widths, etc.

• The on-shell scheme.

In this scheme, the input observables are taken to be α , M_Z , and M_W . In the on-shell scheme, the weak mixing angle has a simple definition. To distinguish different schemes I will denote $\sin^2\theta$ in the on-shell scheme by s_{θ}^2 where, s_{θ}^2 is defined to all orders by the relation

$$s_{\theta}^2 = 1 - \frac{M_W^2}{M_Z^2} \,. \tag{A.11}$$

Unfortunately, the W mass is not determined precisely as M_Z [13]

$$M_W = 80.26 \pm 0.16 \text{ GeV}$$
 (A.12)

The large error in the measurement of M_W induces a large error in calculating s_{θ}^2 using the defining relation [29],

$$\left(\frac{\delta s_{\theta}^2}{s_{\theta}^2}\right)_{\text{exp}} \approx -\frac{c_{\theta}^2}{s_{\theta}^2} \left(\frac{\delta M_W^2}{M_W^2}\right)_{\text{exp}} \approx 1.6\%,$$
(A.13)

where I ignored the small error in M_Z . Therefore, one does not rely to the measurement of M_W to extract s_{θ}^2 . The usual approach is to use the measurement of the μ decay and the theoretical formula

$$\frac{1}{\tau_{\mu}} = \frac{G_F^2 m_{\mu}^5}{192\pi^3} \left(1 - 8 \frac{m_e^2}{m_{\mu}^2} \right) \left(1 + \frac{\alpha}{\pi} \left(\frac{25}{4} - \pi^2 \right) \right) \left(1 + \frac{2\alpha}{3\pi} \ln \frac{m_{\mu}}{m_e} \right) , \tag{A.14}$$

where QED corrections to the four-fermion interaction includes one loop correction and the leading correction in α^2 . Performing the 1-loop radiative corrections to the μ decay (see Figure 1.4b) one finds that $G_F/\sqrt{2}$ coincides with the expression [14]

$$\frac{G_F}{\sqrt{2}} = \frac{\pi \alpha_0}{2s_{\theta 0}^2 M_{W0}^2} \left[1 + \frac{A^{WW}(0)}{M_W^2} + (\text{vertex, box}) \right], \tag{A.15}$$

where I used the bare parameters in the above equation and the term (vertex,box) denote corrections other than the W-self energy, *i.e.*, due to vertex, box, and fermion self energy diagrams. In fact these corrections are in correspondence with what I called $\delta G_{V,B}$ in chapter 1,

$$\frac{\delta G_{V,B}}{\sqrt{2}} = \frac{\pi \alpha_0}{2s_{\theta 0}^2 M_{W0}^2} (\text{vertex, box}). \tag{A.16}$$

The bare quantities can be written in terms of the renormalized quantities as follow

$$\alpha_0 = \alpha - \delta \alpha \,, \tag{A.17}$$

$$M_{Z0}^2 = M_Z^2 - \delta M_Z^2 \,, \tag{A.18}$$

$$M_{W0}^2 = M_W^2 - \delta M_W^2 \,. \tag{A.19}$$

Therefore, one finds

$$s_{\theta 0}^2 = 1 - \frac{M_{W0}^2}{M_{Z0}^2} = s_{\theta}^2 - c_{\theta}^2 \left(\frac{\delta M_Z^2}{M_Z^2} - \frac{\delta M_W^2}{M_W^2} \right) , \qquad (A.20)$$

where to all orders we have

$$s_{\theta}^2 = 1 - c_{\theta}^2 \equiv 1 - \frac{M_W^2}{M_Z^2}$$
 (A.21)

Thus, one finds

$$\frac{G_F}{\sqrt{2}} = \frac{\pi \alpha}{2s_\theta^2 M_W^2} \left[1 - \frac{\delta \alpha}{\alpha} + \frac{c_\theta^2}{s_\theta^2} \left(\frac{\delta M_Z^2}{M_Z^2} - \frac{\delta M_W^2}{M_W^2} \right) + \frac{\delta M_W^2 + A^{WW}(0)}{M_W^2} + (\text{vertex, box}) \right]$$

$$\equiv \frac{\pi \alpha}{2s_\theta^2 c_\theta^2 M_Z^2} (1 + \Delta r) , \qquad (A.22)$$

where, Δr is a finite combination of one-loop diagrams and counterterms. It is clear that Δr depends on the top quark mass m_t and the Higgs boson mass m_H . By including and summation of higher order corrections [14], one can write the above relation as

$$s_{\theta}^{2}c_{\theta}^{2} = \left(1 - \frac{M_{W}^{2}}{M_{Z}^{2}}\right)\frac{M_{W}^{2}}{M_{Z}^{2}} = \frac{\pi\alpha}{\sqrt{2}G_{F}M_{Z}^{2}(1 - \Delta r)}.$$
(A.23)

One should recognize that the quantity Δr is different in two aspects from the quantity Δr_W I defined in chapter 1. First, in calculating Δr one should use the on-shell quantities s_{θ}^2 and c_{θ}^2 rather than $\sin^2\theta$ and $\cos^2\theta$ defined in the Z-pole scheme. Second, in Δr , the electromagnetic α is still defined at $q^2=0$ rather than at $q^2=M_Z^2$. Thus, Δr contains QED corrections from the light fermions,

 $\Delta \alpha(M_Z^2)$ as discussed in section 1.2. In fact, for the case of Δr one can absorb the quantity $\Delta \alpha(M_Z^2)$ in defining $\alpha(M_Z^2)$ as we did for the Z-pole scheme.

One can split the different contributions to Δr at one loop and write Δr as [14]

$$\Delta r = \Delta \alpha(M_Z^2) - \frac{c_\theta^2}{s_\theta^2} \Delta \rho + (\Delta r)_{\text{remainder}}, \qquad (A.24)$$

where by $\Delta \rho$ I mean the leading contributions of the top quark mass (quadratic in m_t). Therefore, this $\Delta \rho$ coincide with the quantity $\Delta \rho$ I defined in chapter 1, as long as one only concentrates on the quadratic terms in m_t . The term $(\Delta r)_{\text{remainder}}$ includes the remaining contributions, e.g., the logarithmic dependence in m_t and m_H , gauge bosons contributions, etc. The typical sizes of $\Delta \alpha(M_Z^2)$, $\Delta \rho$, and $(\Delta r)_{\text{remainder}}$ are ~ 0.06 , 0.03-0.05, and 0.01, respectively [14].

The measurement of s_{θ}^2 is usually extracted using the measured ratio M_W^2/M_Z^2 from low energy experiments like the neutrino-electron scattering. The present world average on s_{θ}^2 from experimental data is [14]

$$s_{\theta}^2 = 1 - \frac{M_W^2}{M_Z^2} = 0.2253 \pm 0.0047$$
 (A.25)

Despite the simple definition of s_{θ}^2 in the on-shell renormalization scheme, the weak mixing angle s_{θ}^2 has a strong dependence on the top quark mass m_t . Hence, using this scheme in any analysis requires a precise knowledge of the top quark mass.

• The \overline{MS} scheme.

The $\overline{\rm MS}$ scheme, also known as the modified minimal subtraction scheme, is a well-known scheme in QCD physics. In this scheme, one simply, in doing the radiative corrections, only requires that the counterterms contain the divergent pieces needed to cancel divergencies arising from loop calculations. In

other words, one only absorbs the loop divergencies in the counterterms. In dimensional regularization one simply cancels the quantity

$$\Delta = -\frac{2}{n-4} - \gamma - \ln 4\pi \,, \tag{A.26}$$

from the loop calculations, where n is the space-time dimension and $\gamma = 0.577...$ is the Euler's constant.

Therefore, masses and couplings calculated in the \overline{MS} scheme have a dependence on the renormalization scale μ . Consequently masses in the \overline{MS} scheme (running masses) have no direct physical meaning. To distinguish the \overline{MS} quantities I will use a bar over the quantities. The bare quantities can be written as

$$\alpha_0 = \overline{\alpha} - \delta \overline{\alpha} \,, \tag{A.27}$$

$$M_{Z0}^2 = \overline{M_Z^2} - \delta \overline{M_Z^2} \,, \tag{A.28}$$

$$M_{W0}^2 = \overline{M_W^2} - \delta \overline{M_W^2} \,, \tag{A.29}$$

The coupling $\overline{\alpha}$ is defined using the e-p scattering at $q^2 = 0$. From the result in chapter 1 we know that the quantity α is given by

$$\alpha = \alpha_0 \left[1 - F^{\gamma\gamma}(0) - \frac{2\sin\theta}{\cos\theta} \frac{A^{\gamma Z}(0)}{M_Z^2} \right]. \tag{A.30}$$

Writing α_0 in terms of the \overline{MS} renormalized quantity we find

$$\alpha = \overline{\alpha} \left[1 - F_{\overline{MS}}^{\gamma\gamma}(0) - \frac{2\overline{s}_{\theta}}{\overline{c}_{\theta}} \frac{A_{\overline{MS}}^{\gamma Z}(0)}{M_Z^2} \right] , \qquad (A.31)$$

where $F_{\overline{MS}}^{\gamma\gamma}$ is defined as $F^{\gamma\gamma}$ with simply subtracting the divergent piece Δ defined in Eq. (A.26). Similarly for the quantity $A_{\overline{MS}}^{\gamma Z}$. Also, $\overline{s}_{\theta}^{2}$ is $\sin^{2}\theta$, defined below, in the \overline{MS} scheme and $\overline{c}_{\theta}^{2} = 1 - \overline{s}_{\theta}^{2}$. Therefore, one finds

$$\overline{\alpha} = \frac{\alpha}{\left[1 - F_{\overline{MS}}^{\gamma\gamma}(0) - \frac{2\overline{s}_{\theta}}{\overline{c}_{\theta}} \frac{A_{\overline{MS}}^{\gamma Z}(0)}{M_{Z}^{2}}\right]} \equiv \frac{\alpha}{1 - \Delta \overline{\alpha}}.$$
(A.32)

Choosing the renormalization scale to be $\mu=M_Z$, one can evaluate the running coupling $\overline{\alpha}$ at the M_Z scale. Notice that the top quark mass enter the quantity $\Delta \overline{\alpha}$. However, the dependence is only logarithmic. Numerically, one finds, for $m_t=180\pm12$ GeV, [14]

$$(\overline{\alpha})^{-1} = 128.08 \pm 0.02 \pm 0.09$$
, (A.33)

where the first error corresponds to $m_t = 180$ GeV and the second error to the interval ± 12 GeV around the central value of the top quark mass.

The renormalized masses in the $\overline{\rm MS}$ scheme do not correspond to the physical masses. In chapter 1, we found that summing loop corrections leads to the result

$$\frac{1}{q^2 - M_{Z0}^2} \to \frac{1}{q^2 - M_{Z0}^2 + A^{ZZ}(0) + q^2 F^{ZZ}(q^2)}.$$
 (A.34)

Writing the bare mass in terms of the renormalized MS mass

$$M_{Z0}^2 = \overline{M_Z^2} - \delta \overline{M_Z^2} \,, \tag{A.35}$$

one finds

$$\frac{1}{q^2 - M_{Z0}^2} \to \frac{1}{q^2 - \overline{M_Z^2} + A_{\overline{MS}}^{ZZ}(0) + q^2 F_{\overline{MS}}^{ZZ}(q^2)},$$
(A.36)

where the counterterm $\delta \overline{M_Z^2}$ has been chosen to cancel the divergence in $A^{ZZ}(0)+M_Z^2F^{ZZ}(M_Z^2)$. The on-shell condition relate the on-shell mass to the $\overline{\rm MS}$ mass as follow,

$$q^2 - \overline{M_Z^2} + A_{\overline{MS}}^{ZZ}(0) + q^2 F_{\overline{MS}}^{ZZ}(q^2) = 0$$
, at $q^2 = M_Z^2$. (A.37)

Therefore, one has

$$M_Z^2 - \overline{M_Z^2} + A_{\overline{MS}}^{ZZ}(0) + M_Z^2 F_{\overline{MS}}^{ZZ}(M_Z^2) = 0.$$
 (A.38)

Thus, for the W and Z mass we have the relations between the on-shell and the $\overline{\rm MS}$ schemes

$$M_Z^2 = \overline{M_Z^2} - A_{\overline{MS}}^{ZZ}(0) - M_Z^2 F_{\overline{MS}}^{ZZ}(M_Z^2), \qquad (A.39)$$

$$M_W^2 = \overline{M_W^2} - A_{\overline{MS}}^{WW}(0) - M_W^2 F_{\overline{MS}}^{WW}(M_W^2). \tag{A.40}$$

The weak mixing angle can be defined in different ways, I choose the definition

$$\overline{s}_{\theta}^2 = 1 - \frac{\overline{M_W^2}}{\overline{M_Z^2}}. \tag{A.41}$$

One can relate the weak mixing angle in the on-shell scheme to the one defined in the \overline{MS} scheme as follow

$$\overline{s}_{\theta}^{2} = 1 - \frac{M_{W}^{2}}{M_{Z}^{2}} \left[1 + \frac{A_{\overline{MS}}^{WW}(0)}{M_{W}^{2}} + F_{\overline{MS}}^{WW}(M_{W}^{2}) - \frac{A_{\overline{MS}}^{ZZ}(0)}{M_{Z}^{2}} - F_{\overline{MS}}^{ZZ}(M_{Z}^{2}) \right]
= s_{\theta}^{2} + c_{\theta}^{2} X_{\overline{MS}},$$
(A.42)

where I defined

$$X_{\overline{\rm MS}} \equiv \frac{A_{\overline{\rm MS}}^{ZZ}(0)}{M_Z^2} - \frac{A_{\overline{\rm MS}}^{WW}(0)}{M_W^2} + F_{\overline{\rm MS}}^{ZZ}(M_Z^2) - F_{\overline{\rm MS}}^{WW}(M_W^2). \tag{A.43}$$

Also, we have

$$\bar{c}_{\theta}^2 = 1 - \bar{s}_{\theta}^2 = c_{\theta}^2 (1 - X_{\overline{\text{MS}}}) .$$
 (A.44)

The on-shell gauge boson masses can be related using the $\overline{\text{MS}}$ quantity \overline{s}_{θ}^2

$$M_W^2 = c_\theta^2 M_Z^2 = \frac{\overline{c}_\theta^2}{1 - X_{\overline{\text{MS}}}} M_Z^2 \equiv \overline{c}_\theta^2 \overline{\rho} M_Z^2, \qquad (A.45)$$

where I defined

$$\overline{\rho} = \frac{1}{1 - X_{\overline{\text{MS}}}} \,. \tag{A.46}$$

The weak mixing angle \overline{s}_{θ}^2 can also be related to the Z-pole scheme by calculating the μ decay in terms of the $\overline{\rm MS}$ quantities. We found earlier

$$\frac{G_F}{\sqrt{2}} = \frac{\pi \alpha_0}{2s_{\theta 0}^2 M_{W0}^2} \left[1 + \frac{A^{WW}(0)}{M_W^2} + (\text{vertex, box}) \right]. \tag{A.47}$$

Writing the bare quantities in terms of the MS renormalized quantities on finds

$$\frac{G_F}{\sqrt{2}} = \frac{\pi \overline{\alpha}}{2\overline{s}_A^2 \overline{M_W}^2} \left[1 + \frac{A_{\overline{\text{MS}}}^{WW}(0)}{M_W^2} + \delta(V, B)_{\overline{\text{MS}}} \right], \tag{A.48}$$

where $\delta(V, B)_{\overline{\rm MS}}$ is all the one-loop corrections to the μ decay except the W self-energy calculated in the $\overline{\rm MS}$ scheme. Using Eq. (A.45), one finds

$$\frac{G_F}{\sqrt{2}} = \frac{\pi \overline{\alpha}}{2\overline{s}_{\theta}^2 \, \overline{c}_{\theta}^2 \, M_Z^2} \left[1 - X_{\overline{\text{MS}}} - F_{\overline{\text{MS}}}^{WW}(M_W^2) + \delta(V, B)_{\overline{\text{MS}}} \right] \,. \tag{A.49}$$

Summing higher order corrections yields [14]

$$\frac{G_F}{\sqrt{2}} = \frac{\pi \overline{\alpha}}{2\overline{s}_{\theta}^2 \, \overline{c}_{\theta}^2 \, \overline{\rho} M_Z^2} \frac{1}{1 - \Delta \overline{r}},\tag{A.50}$$

where

$$\overline{\rho} = \frac{1}{1 - X_{\overline{\text{MS}}}},\tag{A.51}$$

$$\Delta \bar{r} = -F_{\overline{\text{MS}}}^{WW}(M_W^2) + \delta(V, B)_{\overline{\text{MS}}}. \tag{A.52}$$

For more details on the $\overline{\text{MS}}$ scheme, the reader can refer to the discussion in Refs. [14, 29].

Appendix B

The S, T, U parameters

In this appendix, I present briefly a well-known parameterization for the low energy data different from the epsilon parameterization. For more details the reader can refer to Refs. [24, 25]. The parameterization I will discuss in this appendix is similar in spirit to the epsilon parameterization.

First, the assumption made are [25]

- The electroweak gauge group of the effective low energy theory at the weak scale is the standard $SU(2)_L \times U(1)_Y$. Therefore, the only relevant electroweak gauge bosons are the photon, W^{\pm} , and Z.
- The only relevant new physics to consider are the oblique corrections, *i.e.*, the corrections to the gauge boson vacuum polarization functions, with the exception of the non-oblique correction to Z-b- \bar{b} vertex.
- The earliest use of this parameterization [24], was based on a third assumption, namely, the new physics scale is large compared to the W and Z masses. Therefore, one can expand new physics contributions to the gauge boson vacuum polarization functions around $q^2 = 0$. Recent efforts have been toward retaining more higher order terms in the expansion of the vacuum polarization

functions [25].

I start the discussion concentrating on the oblique corrections. The parameters S, T, and U are chosen to parameterize the oblique new physics corrections. The convention used is to subtract the new physics effects from the SM contributions and then define the S, T, and U parameters in term of the remnant new physics effect. To do this, one must know the top quark and the Higgs boson masses. However, since our knowledge of theses masses is not precisely established, one simply picks reference masses for the top and the Higgs boson masses. Then one calculates the SM prediction using these reference masses and define the new physics contributions to low energy observables as the difference between the experimental data and the SM predictions (using reference m_t and m_H).

The third assumption mentioned above allows one to expand the vacuum polarization functions around $q^2 = 0$ in powers of q^2/Λ^2 , where Λ is the scale of new physics. Using my notation for the vacuum polarization functions in Eq. (1.49) and the Z-pole renormalization scheme, the S, T, and U parameters are defined as follow

$$\alpha S = 4\sin\theta\cos\theta F^{30}(0), \tag{B.1}$$

$$\alpha T = \frac{A^{ZZ}(0)}{M_Z^2} - \frac{A^{WW}(0)}{M_W^2} \,, \tag{B.2}$$

$$\alpha U = 4\sin^2\theta \left[F^{33}(0) - F^{WW}(0) \right] , \tag{B.3}$$

where

$$F^{30}(0) = -\sin\theta\cos\theta F^{ZZ}(0) + (\cos^2\theta - \sin^2\theta)F^{\gamma Z}(0) + F^{\gamma\gamma}(0), \qquad (B.4)$$

and

$$F^{33}(0) = \cos^2 \theta \, F^{ZZ}(0) + 2\sin \theta \cos \theta F^{\gamma Z}(0) + \sin^2 \theta \, F^{\gamma \gamma}(0) \,. \tag{B.5}$$

Using the latest data [12], a fit for the S, T, and U parameters yields [25]

$$S = -0.33 \pm 0.19$$
,
 $T = -0.17 \pm 0.21$,
 $U = -0.34 \pm 0.51$. (B.6)

The above fit is extracted for $m_t = 180$ GeV, $m_H = 300$ GeV, $\alpha^{-1}(M_Z^2) = 128.9$, and $\alpha_s = 0.123$ [25].

Recent efforts have been implemented to relax the third assumption by allowing the new physics scale to be comparable with the Z-mass scale [25, 70]. In this case, one retains more higher order terms in the expansion of the vacuum polarization functions. It was shown in Ref. [70] that it is sufficient to introduce three more parameters and increase the total number to six. The definition of S and U, but not T, is slightly modified as follows [70]

$$\alpha S = 4\sin\theta\cos\theta F^{30}(0) + 4\sin^2\theta\cos^2\theta \left[F^{ZZ}(M_Z^2) - F^{ZZ}(0) \right],$$
 (B.7)

$$\alpha T = \frac{A^{ZZ}(0)}{M_Z^2} - \frac{A^{WW}(0)}{M_W^2} \,, \tag{B.8}$$

$$\alpha U = 4\sin^2\theta \left[F^{33}(0) - F^{WW}(0) \right] + 4\sin^2\theta \left[F^{WW}(M_W^2) - F^{WW}(0) \right] + 4\sin^2\theta \left[F^{ZZ}(M_Z^2) - F^{ZZ}(0) \right], \tag{B.9}$$

The S, T, and U parameters are in one to one correspondence with the oblique corrections e_3 , e_1 , and e_2 defined in chapter 1 [see Eqs. (1.117)-(1.119)]. The quantities e_3 , e_1 , and e_2 constitute the leading contributions to the parameters ϵ_3 , ϵ_1 , and ϵ_2 . Therefore, concentrating on the possible large new physics contributions one can

relate the two set of parameters as follows

$$S = \frac{4\sin^2\theta}{\alpha}\delta\epsilon_3 ,$$

$$T = \frac{1}{\alpha}\delta\epsilon_1 ,$$

$$U = -\frac{4\sin^2\theta}{\alpha}\delta\epsilon_2 ,$$
(B.10)

where, $\delta \epsilon_1$ is the new physics (beyond the SM) contribution to ϵ_1 . Similarly, for $\delta \epsilon_2$ and $\delta \epsilon_3$.

Parameterizing the non-oblique correction to the Z-b- \bar{b} vertex has been implemented recently [25, 119]. In Ref. [119] the non-oblique corrections from new physics to the Z-b- \bar{b} vertex are expressed in terms of the effective left- and right-handed couplings of the b quark to the Z boson as

$$g_L^b = (g_L^b)_{SM} + \frac{1}{3}\delta \sin^2 \theta + \delta g_L^b,$$
 (B.11)

$$g_R^b = (g_R^b)_{SM} + \frac{1}{3}\delta \sin^2 \theta + \delta g_R^b,$$
 (B.12)

where $\delta \sin^2 \theta$ expresses the shift of the effective weak mixing angle due to oblique corrections, and δg_L^b and δg_R^b express non-oblique vertex corrections due to new physics. The quantities $(g_L^b)_{\rm SM}$ and $(g_R^b)_{\rm SM}$ are the left- and right-handed couplings of the b quark to the Z boson in the SM, where

$$(g_L^b)_{SM} = -\frac{1}{2} + \frac{1}{3}\sin^2\theta$$
,
 $(g_R^b)_{SM} = \frac{1}{3}\sin^2\theta$. (B.13)

The decay width Γ_b depends on one combination of δg_L^b and δg_R^b . While the observable A_{FB}^b depends on another combination. This parameterization is similar to the one I used in chapter 1 (see Eq. (1.123)). The relation between the cases is simply as follow

$$\delta g_L^b = -\frac{1}{2} \left(e_b + \frac{\delta g_{Vd} + \delta g_{Ad}}{2} \right) ,$$

$$\delta g_R^b = -\frac{1}{2} \left(+ \frac{\delta g_{Vd} - \delta g_{Ad}}{2} \right) , \qquad (B.14)$$

where one should remember that, in the above equation, e_b , δg_{Vd} , and δg_{Ad} contain only the new physics effect defined as the difference between new physics and the SM case using reference m_t and m_H . Using the recent data [12], excluding R_c , one obtains the fit [25]

$$\delta g_L^b = 0.0004 \pm 0.0037,$$

$$\delta g_R^b = 0.036 \pm 0.017,$$
(B.15)

where $m_t = 180$ GeV, $m_H = 300$ GeV, $\alpha^{-1}(M_Z^2) = 128.9$, and $\alpha_s = 0.123$ [25].

The conclusion is that, one can express new physics effects in terms of the S, T, U, and the two non-oblique parameters δg_L^b and δg_R^b . Notice that δg_R^b does not involve large m_t effects since the large m_t effects are coming at one-loop through the left-handed W-t-b coupling.

From this brief discussion one notes some differences between the epsilon parameters and the parameterization discussed in this chapter.

- In the epsilon parameterization, the parameters ϵ_1 , ϵ_2 , ϵ_3 , and ϵ_b are written directly in terms of physical observables, rather than in terms of two-point functions which is the case for S, T, and U.
- The parameters ϵ_1 , ϵ_2 , ϵ_3 , and ϵ_b incorporate the SM contribution in addition to possible new physics. On the contrary, the other parameterization only contains the new physics effect.

Appendix C

Heavy Mass Expansion

In this appendix I discuss how to use the heavy mass expansion and tabulate some relevant integrals if there is a heavy mass in the loop calculation [120]. Loop integrals will be performed using dimensional regularization. A general two-point function has the typical integral

$$\int \frac{d^n k}{(2\pi)^n} \frac{k_\mu k_\nu \dots}{(k^2 - m^2)((k+p)^2 - M^2)} , \qquad (C.1)$$

where m, M are mass scales and p is an external momentum. The heavy mass M is satisfying the conditions $M \gg m$ and $M \gg p^2$. The heavy propagator is expanded as follow

$$\frac{1}{((k+p)^2 - M^2)} = \frac{1}{(k^2 - M^2)} \left(1 - \frac{2k \cdot p + p^2}{(k^2 - M^2)} + \dots \right). \tag{C.2}$$

For a three-point function a similar treatment can be done. In this case one encounters the typical integral

$$\int \frac{d^n k}{(2\pi)^n} \frac{k_\mu k_\nu \dots}{(k^2 - m_1^2)((k+p)^2 - m_2^2)((k+p+q)^2 - M^2)},$$
 (C.3)

where m_1 and m_2 are two light mass scales and $M \gg m_1, m_2$. The external momentums p and q satisfy the condition $M^2 \gg p^2, q^2$. The heavy propagator is expanded

as follow

$$\frac{1}{(k+p+q)^2 - M^2} = \frac{1}{k^2 - M^2} \left(1 - \frac{2k \cdot p + 2k \cdot q + (p+q)^2}{k^2 - M^2} + \dots \right). \tag{C.4}$$

Determining the order of the expansion depends on the desired heavy mass M dependence to be retained. For example, to keep contributions up to $\ln M^2$ needs more expanded terms than keeping terms up to M^2 only. To determine this consider the general integral

$$\int \frac{d^4k}{(2\pi)^4} \frac{M^d k_\mu k_\nu \dots}{(k^2 - m_1^2)((k+p)^2 - m_2^2)((k+p+q)^2 - M^2) \dots} , \qquad (C.5)$$

where d is an integer and where the dependence on the heavy mass M in the numerator can come from propagators as in the fermions' propagators or it can come from couplings as in the Yukawa couplings to a heavy fermion (top quark). To determine the number of propagators to retain I will use the following quantities. Denote the number of propagators to be retained by the integer N_p . The number of explicit momentums in the numerator by N_m . The desired power of the heavy mass M to be retained by N_M . Then the number of retained propagators is fixed by counting the dimension of the integral. The total dimension of the integral is $4 + d + N_n - 2N_p$ where the term 4 is coming from the integral measure d^4k , therefore the following inequality must be satisfied

$$4 + d + N_m - 2N_p \ge N_M \,, \tag{C.6}$$

After doing the expansion, one can use the identity

$$\frac{1}{(k^2 - m^2)(k^2 - M^2)} = \frac{1}{M^2 - m^2} \left(\frac{1}{(k^2 - M^2)} - \frac{1}{(k^2 - m^2)} \right). \tag{C.7}$$

Then using the integrals below becomes straight forward.

Here I tabulate some useful integrals in the heavy mass expansion and using dimensional regularization. First I define

$$\Delta = -\frac{2}{n-4} - \gamma - \ln 4\pi \,, \tag{C.8}$$

where n is the space-time dimension and $\gamma = 0.577...$ is the Euler's constant. Also I define the quantity $g_{\mu\nu\lambda\sigma}$

$$g_{\mu\nu\lambda\sigma} = g_{\mu\nu}g_{\lambda\sigma} + g_{\mu\lambda}g_{\nu\sigma} + g_{\mu\sigma}g_{\nu\lambda} \tag{C.9}$$

$$\int \frac{d^n k}{(2\pi)^n} \frac{1}{k^2 - M^2} = -\frac{i}{16\pi^2} \left(-\Delta - 1 + \ln M^2 \right) , \qquad (C.10)$$

$$\int \frac{d^n k}{(2\pi)^n} \frac{1}{(k^2 - M^2)^2} = -\frac{i}{16\pi^2} \left(-\Delta + \ln M^2 \right) , \qquad (C.11)$$

$$\int \frac{d^n k}{(2\pi)^n} \frac{1}{(k^2 - M^2)^3} = -\frac{i}{16\pi^2} \frac{1}{2M^2},$$
(C.12)

$$\int \frac{d^n k}{(2\pi)^n} \frac{1}{(k^2 - M^2)^4} = \frac{i}{16\pi^2} \frac{1}{6M^4}$$
 (C.13)

$$\int \frac{d^n k}{(2\pi)^n} \frac{k_\mu}{k^2 - M^2} = \int \frac{d^n k}{(2\pi)^n} \frac{k_\mu k_\nu k_\lambda}{k^2 - M^2} = \dots = 0,$$
(C.14)

$$\int \frac{d^n k}{(2\pi)^n} \frac{k_\mu k_\nu}{k^2 - M^2} = -\frac{i}{16\pi^2} \frac{g_{\mu\nu} M^4}{4} \left(-\Delta - \frac{3}{2} + \ln M^2 \right) , \qquad (C.15)$$

$$\int \frac{d^n k}{(2\pi)^n} \frac{k_\mu k_\nu}{(k^2 - M^2)^2} = -\frac{i}{16\pi^2} \frac{g_{\mu\nu} M^2}{2} \left(-\Delta - 1 + \ln M^2 \right) , \qquad (C.16)$$

$$\int \frac{d^n k}{(2\pi)^n} \frac{k_\mu k_\nu}{(k^2 - M^2)^3} = -\frac{i}{16\pi^2} \frac{g_{\mu\nu}}{4} \left(-\Delta + \ln M^2 \right) , \qquad (C.17)$$

$$\int \frac{d^n k}{(2\pi)^n} \frac{k_\mu k_\nu}{(k^2 - M^2)^4} = -\frac{i}{16\pi^2} \frac{g_{\mu\nu}}{12M^2},$$
(C.18)

$$\int \frac{d^n k}{(2\pi)^n} \frac{k_\mu k_\nu k_\lambda k_\sigma}{k^2 - M^2} = -\frac{i}{16\pi^2} \frac{g_{\mu\nu\lambda\sigma}M^6}{24} \left(-\Delta - \frac{11}{6} + \ln M^2 \right) , \qquad (C.19)$$

$$\int \frac{d^n k}{(2\pi)^n} \frac{k_\mu k_\nu k_\lambda k_\sigma}{(k^2 - M^2)^2} = -\frac{i}{16\pi^2} \frac{g_{\mu\nu\lambda\sigma} M^4}{8} \left(-\Delta - \frac{3}{2} + \ln M^2 \right) . \tag{C.20}$$

$$\int \frac{d^n k}{(2\pi)^n} \frac{k_\mu k_\nu k_\lambda k_\sigma}{(k^2 - M^2)^3} = -\frac{i}{16\pi^2} \frac{g_{\mu\nu\lambda\sigma} M^2}{8} \left(-\Delta - 1 + \ln M^2 \right) . \tag{C.21}$$

$$\int \frac{d^n k}{(2\pi)^n} \frac{k_\mu k_\nu k_\lambda k_\sigma}{(k^2 - M^2)^4} = -\frac{i}{16\pi^2} \frac{g_{\mu\nu\lambda\sigma}}{24} \left(-\Delta + \ln M^2 \right) . \tag{C.22}$$

Appendix D

Non-Linear Realization

In this appendix, we are interested in realizing the symmetry described by the Lie group G. The symmetry of the theory is assumed to be spontaneously broken, *i.e.*, we consider the breakdown of G into a subgroup H. Given the symmetry group G (global or local) and the matter fields (leptons and quarks), the problem of constructing the invariant Lagrangian (under G) reduces to the problem of realizing the symmetry, *i.e.*, choosing representations of the Lie group G. The realization of the symmetry can be achieved in two different ways; the familiar linear realization and the less familiar non-linear realization.

D.1 Linear Realization

In this realization, the problem is choosing the natural representations of the fields. By natural representation I mean representations which form a self-consistent theory, i.e., free from of all possible anomalies. Usually the matter fields (fermions) are assigned in the fundamental representation of the group G. On the other hand, the gauge bosons (the force mediators) are assigned in the adjoint representation. To illustrate, consider the Lie group $SU(2)_L \times U(1)_Y$ (the SM group). Left-handed fermions Ψ_L are assigned in doublets (the fundamental representation) under $SU(2)_L$

with the transformation under G as

$$\Psi_L \to \Psi_L' = g_L g_Y \, \Psi_L \,, \tag{D.1}$$

where

$$g_L = \exp(i\frac{\alpha^a \tau^a}{2}) \in SU(2)_L, \qquad (D.2)$$

$$g_Y = \exp(i\frac{\beta Y}{2}) \in U(1)_Y, \tag{D.3}$$

and α^a , a=1,2,3 and y are real parameters of the group G. The right-handed fermions are singlets under $SU(2)_L$. The $SU(2)_L$ gauge bosons are assigned in the adjoint representation with the transformation

$$gW_{\mu}^{a}\tau^{a} \to gW_{\mu}^{a'}\tau^{a} = g_{L}\left(W_{\mu}^{a}\tau^{a} - \partial_{\mu}\right)g_{L}^{\dagger}. \tag{D.4}$$

The $U(1)_Y$ gauge boson B transforms as

$$g'YB_{\mu} \to g'YB'_{\mu} = g_Y \left(YB_{\mu} - \partial_{\mu} \right) g_Y^{\dagger} \,, \tag{D.5}$$

where g and g' are the gauge couplings of $SU(2)_L$ and $U(1)_Y$, respectively.

D.2 Non-linear Realization

A different realization of the symmetry from the linear realization can be implemented, namely, the non-linear realization. The starting point is the spontaneous breakdown of G into H.

The mathematical situation is as follows; consider a real analytic manifold M, together with a Lie group G. Under the action of G, an element x in M transforms as

$$x \to gx \quad x \in M, \quad g \in G.$$
 (D.6)

We assume that there is a special point of M called the origin, described by the null vector 0. The origin 0 is invariant under the action of a subgroup H of G:

$$h0 = 0, \quad h \in \mathcal{H} \,. \tag{D.7}$$

The physical situation is that of a manifold of scalar fields with the origin describing the vacuum configuration. The group G is the global or local invariance group of the theory and the subgroup H is the invariance group of the vacuum. Thus, one is dealing with the spontaneous breaking of G into H [72].

An important point is that for any non-linear realization of the fields, we can redefine the fields in such away that their transformation under H is linear [66], we call this form, in which the fields transform non-linearly under G and linearly under H, the standard form. Furthermore, the standard form as discussed in Ref. [81] still leads to the same S matrix as the original realization.

The group G has n generators Z^a , $a=1,2,\ldots,n$ and the subgroup H has p generators V^b , $b=1,2,\ldots,p$. The symmetry described by G breaks down into the symmetry described by H. Therefore, there are n-p broken generators A^c , $c=1,2,\ldots,n-p$. From the spontaneous breakdown of the theory as described by the breakdown of G into H, there are n-p Goldstone bosons [80]. The Goldstone bosons ϕ^c , $c=1,2,\ldots,n-p$ form the coordinates of the manifold M. Each Goldstone boson ϕ^a is associated with a broken generators A^a . Any element $g \in G$ can be uniquely written as [66]

$$g = e^{i\alpha^a A^a} e^{i\beta^b V^b}, \quad a = 1, 2, \dots, n - p, \quad b = 1, 2, \dots, p,$$
 (D.8)

where α^a and β^b are real numbers. We associate with every broken generator A^a a coordinate ϕ^a with the transformation

$$ge^{i\phi^a A^a} = e^{i\alpha^a A^a} e^{i\beta^b V^b} e^{i\phi^a A^a} = e^{i\phi^{a'} A^a} e^{iu^b V^b}. \tag{D.9}$$

Notice that the object $e^{i\phi^a A^a} \in G$, therefore, the transformed object $ge^{i\phi^a A^a} \in G$, this is why we wrote the result of the transformation in the above form. The transformation of ϕ written as

$$\phi^a(x) \to {\phi'}^a(\phi(x))$$
, (D.10)

constitutes a non-linear representation of G. The above equation is taken as the definition of the transformed fields ϕ' in terms of the original fields ϕ and the group element g.

Matter fields ψ (quarks and leptons) are required to possess definite transformation properties only with respect to element $h \in H$, *i.e.*,

$$\Psi \to \Psi' = D(h)\Psi, \tag{D.11}$$

where D(h) denotes a certain linear representation of H. Therefore, the non-linear realization of the whole group G is established as

$$\phi^a \to \phi^{a\prime}(\phi)$$
, $\Psi \to D(h)\Psi$. (D.12)

In general, even in the case of a global transformation one is forced to introduce covariant derivatives for the matter fields, because of the x dependence in ϕ (see Eq. (D.10). In the case of local transformations with gauge bosons W^a , a = 1, 2, ..., n and with their transformation under G as

$$\Omega'_{\mu} = g\Omega_{\mu}g^{\dagger} - g\partial_{\mu}g^{\dagger}, \qquad (D.13)$$

where

$$\Omega_{\mu} = g_a W_{\mu}^a Z^a \,, \tag{D.14}$$

one defines the operator [66]

$$L_{\mu} = e^{-i\alpha^{\bullet}A^{\bullet}} (\partial_{\mu} - \Omega_{\mu}) e^{i\alpha^{\bullet}A^{\bullet}} = \pi_{\mu}^{a} A^{a} + \omega_{\mu}^{b} V^{b}, \qquad (D.15)$$

where ω_{μ}^{b} transforms as a gauge boson under the subgroup H. On the other hand π_{μ}^{a} transforms as a matter field (not as a gauge boson). The covariant derivative of the fermion field Ψ is defined as

$$D_{\mu}\Psi = (\partial_{\mu} + \omega_{\mu}^{b}V^{b})\Psi, \qquad (D.16)$$

with the transformation

$$D_{\mu}\Psi \to D(h)D_{\mu}\Psi \,. \tag{D.17}$$

To proceed I will consider a specific example, namely the electroweak group $G=SU(2)_L \times U(1)_Y$ and $H=U(1)_{em}$. There are 3 broken generators associated with 3 Goldstone bosons ϕ^a , a=1,2,3. The generators of G are the Pauli matrices $\tau^a/2$, a=1,2,3 and the hypercharge generator Y/2. The $U(1)_{em}$ generator can be taken as

$$V = Q = \frac{\tau^3}{2} + \frac{Y}{2} \ . \tag{D.18}$$

The broken generators can be taken as

$$A^a = \frac{\tau^a}{2} \ . \tag{D.19}$$

Rather than working directly with the complicated transformation of the scalar fields ϕ^a , we define the object

$$\Sigma = e^{i\frac{\phi^a r^a}{v^a}},\tag{D.20}$$

where the parameters v^a are introduced for dimensional purposes. Under a general transformation $(g \in G)$, we have (see Eq. (D.9))

$$\Sigma \to g\Sigma = e^{i\frac{\phi^{a'}r^a}{v^a}}e^{iu\frac{r^3+Y}{2}},\tag{D.21}$$

where

$$g = e^{i\alpha^{\alpha} \frac{\tau^{\alpha}}{2}} e^{i\beta \frac{Y}{2}}. \tag{D.22}$$

We can write the above transformation as

$$e^{i\alpha^{\bullet}\frac{\tau^{\bullet}}{2}}\Sigma = \Sigma' e^{iu\frac{\tau^{3}}{2}}e^{i(u-\beta)\frac{Y}{2}}.$$
 (D.23)

Since the left-hand side of the above equation is an element in $SU(2)_L$, it follows that the right-hand side of the equation must be independent of the hypercharge generator Y. Thus, we conclude that $u = \beta$ and the transformation of Σ reduces to

$$e^{i\alpha^{\alpha}\frac{r^{\alpha}}{2}}\Sigma = \Sigma' e^{i\beta\frac{r^{3}}{2}}.$$
 (D.24)

One can write the above transformation as

$$\Sigma' = e^{i\alpha^{a}\frac{\tau^{a}}{2}} \Sigma e^{-i\beta\frac{\tau^{3}}{2}} = g_{L}\Sigma g_{R}^{\dagger}, \tag{D.25}$$

where

$$g_L = e^{i\alpha^4 \frac{r^4}{2}}, \quad g_R = e^{i\beta \frac{r^3}{2}}.$$
 (D.26)

It is clear that under $G=SU(2)_L\times U(1)_Y$, the field ϕ^a has a complicated transformation, while, under the subgroup H, the field ϕ^a transforms linearly. For $h\in H$ and $h=e^{i\beta(r^3+Y)/2}$

$$he^{i\phi^{\mathbf{a}}A^{\mathbf{a}}} = e^{i\phi^{\mathbf{a}'}A^{\mathbf{a}}}h. \tag{D.27}$$

Thus,

$$e^{i\phi^{\bullet\prime}A^{\bullet}} = h e^{i\phi^{\bullet}A^{\bullet}} h^{\dagger} = e^{ih\phi^{\bullet}A^{\bullet}h^{\dagger}}. \tag{D.28}$$

From which it is clear that, for $G=SU(2)_L\times U(1)_Y$, the transformation

$$\phi^a \tau^a \to \phi^{a\prime} \tau^a = h \phi^a \tau^a h^{\dagger} = g_R \phi^a \tau^a g_R^{\dagger} \tag{D.29}$$

constitutes a linear transformation.

We also find that

$$\pi_{\mu}^{a} = \Sigma^{\dagger} D_{\mu} \Sigma \tag{D.30}$$

transforms as a matter field under G, namely

$$\pi^a_\mu \to g_R \pi^a_\mu g_R^\dagger \,, \tag{D.31}$$

where the covariant derivative $D_{\mu}\Sigma$ is

$$D_{\mu}\Sigma = \partial_{\mu}\Sigma - igW_{\mu}^{a}\frac{\tau^{a}}{2}\Sigma + ig'\Sigma B_{\mu}\frac{\tau^{3}}{2}.$$
 (D.32)

Under G, the covariant derivative transforms as

$$D_{\mu}\Sigma \to (D_{\mu}\Sigma)' = \exp\left(i\frac{\alpha^a \tau^a}{2}\right) D_{\mu}\Sigma \exp(-iy\frac{\tau^3}{2}).$$
 (D.33)

A gauge invariant (under G) can be easily seen in the following term

$$\frac{1}{4} v^2 \operatorname{Tr} \left(D_{\mu} \Sigma^{\dagger} D^{\mu} \Sigma \right) . \tag{D.34}$$

This terms can be shown to give the gauge bosons their masses. In the unitary gauge, this term reduces to

$$\frac{1}{4} v^2 \operatorname{Tr} \left(D_{\mu} \Sigma^{\dagger} D^{\mu} \Sigma \right) \to \frac{1}{4} v^2 \operatorname{Tr} \left(\left[-g W_{\mu}^a \frac{\tau^a}{2} + g' B_{\mu} \frac{\tau^3}{2} \right]^2 \right)$$

$$= \frac{1}{8} v^2 \left(g^2 W_{\mu}^a W^{\mu a} - 2g g' W_{\mu}^3 B^{\mu} + g'^2 B_{\mu} B^{\mu} \right) . \tag{D.35}$$

Using the field definitions in Eqs. (1.11) and (1.12) one recovers the gauge boson masses given in Eq. (1.17)

$$\frac{g^2v^2}{4}W^+_{\mu}W^{\mu-} + \frac{g^2v^2}{8\cos^2\theta}Z_{\mu}Z^{\mu}. \tag{D.36}$$

Thus, the W and Z masses are

$$M_W^2 = \frac{g^2 v^2}{4} , \quad M_Z^2 = \frac{g^2 v^2}{4 \cos^2 \theta} .$$
 (D.37)

The difference between the non-linear and the linear realizations is that in a general gauge, the non-linear realization produces other complicated terms in powers of the Goldstone bosons. In general, one finds

$$\mathcal{L}_{m} = M_{W}^{2} W_{\mu}^{+} W^{\mu -} + \frac{M_{Z}^{2}}{2} Z_{\mu} Z^{\mu} + \partial_{\mu} \phi^{+} \partial^{\mu} \phi^{-} + \frac{1}{2} \partial_{\mu} \phi^{3} \partial^{\mu} \phi^{3} + \dots,$$
 (D.38)

where the fields ϕ^{\pm} are defined as

$$\phi^{\pm} = \frac{\phi^1 \mp i\phi^2}{\sqrt{2}} \,. \tag{D.39}$$

Fermions can be included in the context of the chiral Lagrangian by assuming that they transform under $G = SU(2)_L \times U(1)_Y$ as [74]

$$f \to f' = e^{iyQ} f \,, \tag{D.40}$$

where Q is the electromagnetic charge generator. One finds that the fermionic covariant derivative is

$$D_{\mu}f = (\partial_{\mu} + \omega_{\mu}Q)f, \qquad (D.41)$$

where

$$\omega_{\mu} = B_{\mu} \,. \tag{D.42}$$

Thus surprisingly, the gauge field is the B field and not the photon field A as one would expect.

Out of the fermion fields f_1 , f_2 , with the condition $Q_{f_1} - Q_{f_2} = 1$, and the Goldstone bosons matrix field Σ the usual linearly realized fields Ψ can be constructed. For example, the left-handed fermions $[SU(2)_L$ doublet] are constructed as

$$\Psi_L = \Sigma F_L = \Sigma \begin{pmatrix} f_1 \\ f_2 \end{pmatrix}_L. \tag{D.43}$$

One can easily show that Ψ_L transforms under G linearly as follows

$$\Psi_L \to \Psi_L' = \exp\left(i\frac{\alpha^a \tau^a}{2}\right) \Sigma \exp\left(-iy\frac{\tau^3}{2}\right) \exp\left(iy\left[\frac{\tau^3}{2} + \frac{Y}{2}\right]\right) F_L$$

$$= \exp\left(i\frac{\alpha^a \tau^a}{2}\right) \exp(iy\frac{Y}{2}) \Psi_L. \tag{D.44}$$

Therefore, under the group $G=SU(2)_L \times U(1)_Y$,

$$\Psi_L \to \Psi_L' = g \, \Psi_L \,. \tag{D.45}$$

In constructing the invariant Lagrangian, one can define the composite fields as

$$\Sigma_{\mu}^{a} = -\frac{i}{2} \text{Tr}(\tau^{a} \Sigma^{\dagger} D_{\mu} \Sigma) . \tag{D.46}$$

Under the gauge transformation element $g \in G$ and using Eqs. (D.25) and (D.33), one finds that the composite fields transform as:

$$\Sigma_{\mu}^{a} \to \Sigma_{\mu}^{\prime a} = -\frac{i}{2} \text{Tr} \left(\exp(-iy\frac{\tau^{3}}{2}) \tau^{a} \exp(iy\frac{\tau^{3}}{2}) \Sigma^{\dagger} D_{\mu} \Sigma \right) . \tag{D.47}$$

From which one concludes that under a general gauge transformation

$$\Sigma_{\mu}^{3} \to \Sigma_{\mu}^{\prime 3} = \Sigma_{\mu}^{3} \tag{D.48}$$

and

$$\Sigma_{\mu}^{\pm} \to \Sigma_{\mu}^{\prime \pm} = e^{\pm iy} \Sigma_{\mu}^{\pm} \,, \tag{D.49}$$

where

$$\Sigma_{\mu}^{\pm} = \frac{1}{\sqrt{2}} (\Sigma_{\mu}^{1} \mp i \Sigma_{\mu}^{2}).$$
 (D.50)

The field Σ^3_{μ} behaves as a neutral matter field while the two fields Σ^{\pm}_{μ} behave as charged matter fields with $Q=\pm 1$. By a matter field I mean a field which does not transform as a gauge boson field under the symmetry group H.

In a general gauge, Σ^3_μ can be expanded as

$$\Sigma_{\mu}^{3} = \frac{1}{v^{2}} \partial_{\mu} \phi^{3} - \frac{1}{2} \frac{g}{\cos \theta} Z_{\mu} - \frac{ig}{v} \left(W_{\mu}^{+} \phi^{-} - W_{\mu}^{-} \phi^{+} \right) - \frac{i}{v} \left(\phi^{+} \partial_{\mu} \phi^{-} - \phi^{-} \partial_{\mu} \phi^{+} \right) + \dots$$
(D.51)

The composite field Σ_{μ}^{+} can be expanded as

$$\Sigma_{\mu}^{+} = \frac{1}{v^{2}} \partial_{\mu} \phi^{+} - \frac{1}{2} g W_{\mu}^{+} - \frac{ig}{v} \left(\phi^{+} \left[\cos \theta Z_{\mu} + \sin \theta A_{\mu} \right] - \phi^{3} W_{\mu}^{+} \right) + \frac{i}{v} \left(\phi^{+} \partial_{\mu} \phi^{3} - \phi^{3} \partial_{\mu} \phi^{+} \right) + \dots$$
(D.52)

The component Σ_{μ}^{-} is just the Hermitian conjugate of Σ_{μ}^{+} . In the unitary gauge $\Sigma = 1$ one finds that the composite fields reduce to the physical gauge bosons, *i.e.*,

$$\Sigma_{\mu}^{3} = -\frac{1}{2} \frac{g}{\cos \theta} Z_{\mu} \,, \tag{D.53}$$

and

$$\Sigma_{\mu}^{\pm} = -\frac{1}{2}gW_{\mu}^{\pm} \,. \tag{D.54}$$

BIBLIOGRAPHY

- [1] F. Halzen and A.D. Martin, Quarks and Leptons: An Introductory Course in Modern Particle Physics, John Wiley & Sons, Inc., 1984.
- T.-P. Cheng and L.-F. Li, Gauge theory of Elementary Particle Physics, Oxford University Press, Oxford, England, 1984;
 F. Mandl and G. Shaw, Quantum Field Theory, John Wiley & Sons, Inc., 1984.
- [3] G. Kane, Modern Elementary Particle Physics, Addison-Wiley, Inc., 1987.
- [4] P. Renton, Electroweak Interactions: An Introduction to the Physics of Quarks and Leptons, Cambridge University Press, 1990.
- [5] J.F. Donoghue, E. Golowich and B.R. Holstein, *Dynamics of the Standard Model*, Cambridge University Press, 1992.
- [6] A. Olchevski, presented at the International Europhysics Conference on High Energy Physics, Brussel, July 1995; LEP internal notes LEPEWWG/51-01, LEPHF/95-02.
- [7] M. Veltman, Ann. Phys. B8, 475 (1977);
 D. Picus and V. Mather, Phys. Rev. D7, 3111 (1978).
- [8] B.W. Lee, C. Quigg, and H. Thacker, Phys. Rev. D16, 1519 (1977);
 D. Dicus and V. Mathur, Phys. Rev. D7, 3111 (1973);
 M. Chanowitz and M. Gaillard, Nucl. Phys. B261, 379 (1985)379.
- [9] L. Montanet et al., Phys. Rev. **D50**, 1173 (1994) and 1995 off-year partial update for the 1996 edition (URL:http://pdg.lbl.gov/).
- [10] CDF Collaboration (F. Abe et al.), Phys. Rev. Lett. 74, 2626 (1995).
- [11] M. Narain (for the DØ collaboration), presented at Les Rencontres de Physique de La Vallee D'Aoste, La Thuile, Italy (Mar. 1996).
- [12] The LEP Collaborations and the LEP Electroweak Working Group, CERN-PPE/95-172.

- [13] UA2 Collaboration, J. Alitti et al., Phys. Lett. B276, 354 (1992);
 CDF Collaboration, F. Abe et al., FERMILAB-PUB-95/033-E, Phys. Rev. D52, 4784 (1995);
 DØ Collaboration, C.K. Jung et al., FERMILAB-CONF-94-334-E, Presented at 27th International Conference on High Energy Physics (ICHEP), Glasgow, Scotland, 20-27 Jul 1994. Published in ICHEP 1994:429-432 (QCD161:H51:1994).
- [14] W. Hollik, KA-TP-4-1996. Talk given at 5th Hellenic School and Workshops on Elementary Particle Physics, e-Print Archive: hep-ph/9602380.
- [15] B. Mele, in XIV Encontro Nacional de Fisica de Campos e Particulas, Caxambu, Brazil, 29 Sept.-3 Oct., 1993;
 J. Lefrancois, LAL-93-64, in Proceedings of the Int. Europhysics Conference on High Energy Physics, Marseille, France, 1993.
- [16] R. Barbieri, IFUP-TH-23/93, July 1993, in Lectures given at the Symposium on Particle Physics at the Fermi scale, Beijing, May 27 -June 4, 1993. Published in CCAST Symposium 1993:163-212 (QCD161:S12:1993).
- [17] W. Beenakker, F.A. Berends, S.C. van der Marck, Z. Phys. C46, 687 (1990); and the references therein.
- [18] For a discussion on the status of $\alpha(M_Z^2)$ see T. Takeuchi, CERN-TH/96-79, hep-ph/9603415; and the references therein.
- [19] For a review, see D. Soper and L. Surguladze, OITS-577, hep-ph/9506244.
- [20] V.A. Novikov, L.B. Okun, A.N. Razanov, and M.I. Vysotskii, Mod. Phys. Lett. A9, 2641 (1994).
- [21] F. Jegerlehner (PSI, Villigen), PSI-PR-91-08. Lectures given at the Theoretical Advanced Study Institute in Elementary Particle Physics, (TASI), Boulder, Colo., Jun 3-29, 1990. Published in Boulder TASI 90:476-590 (QCD161:T45:1990).
- [22] G. Altarelli, R. Barbieri, and F. Caravaglios, Nucl. Phys. B405, 3 (1993).
- [23] G. Altarelli and R. Barbieri, Phys. Lett. B253, 161 (1990);
 G. Altarelli, R. Barbieri and S. Jadach, Nucl. Phys. B369, 3 (1992).
- [24] M.E. peskin and T. Takeuchi, Phys. Rev. Lett. 65, 964 (1990);
 D.C. Kennedy and P. Langacker, Phys. Rev. Lett. 65, 2967 (1990);
 B. Holdem, Phys. Lett. B259, 329 (1991);
 A. Ali and G. Degrassi, DESY-91-035 (1991). In Islamabad 1990, Proceedings, High energy physics and cosmology, 70-86;
 M.E. peskin and T. Takeuchi, Phys. Rev. D46, 381 (1992).
- [25] J.L. Hewett, T. Takeuchi, S. Thomas, SLAC-PUB-7088, CERN-TH/96-56. To appear as a chapter in Electroweak Symmetry Breaking and Beyond the Standard Model, ed. by T. Barklow, et al., World Scientific.
- [26] G. Altarelli, R. Barbieri, and F. Caravaglios, Phys. Lett. B349, 145 (1995).
- [27] M. Veltman, Acta. Phys. Pol. B8, 475 (1977); Phys. Lett. 70B, 253 (1977);
 M. Einhorn and J. wudka, Phys. Rev. D39, 2758 (1989); ibid D47, 5029 (1993).

- [28] A. Denner, W. Hollik, and B. Lampe, Z. Phys. C60, 193 (1993);
 - J. Fleischer, F. Jegerlehner, and O.V. Tarasov, Phys. Lett. B319, 249 (1993);
 - J. Fleischer, F. Jegerlehner, P. Raczka, and O.V. Tarasov, Phys. Lett. **B293**, 437 (1992);
 - G. Buchalla and A.J. Buras, Nucl. Phys. **B398**, 285 (1993);
 - G. Degassi, Nucl. Phys. **B407**, 271 (1993);
 - S. Fanchiotti, B. Kniehl, and A. Sirlin, Phys. Rev. bf D48, 307 (1993);
 - k. Chetyrkin, J. Kuhn, Phys. Lett. B 248, 359 (1990);
 - k. Chetyrkin, J. Kuhn, and A. Kwiathowski, Phys. Lett. B 282, 221 (1992);
 - B. Kniehl, Nucl. Phys. B347, 86 (1990).
- [29] P. Gambino, NYU-TH-05-01-95, hep-ph/9505366. Ph.D. Thesis.
- [30] K. Hagiwara, KEK-TH-461. Talk given at LP'95: International Symposium on Lepton Photon Interactions (IHEP), Beijing, P.R. China, 10-15 Aug 1995.
- [31] The SLD Collaboration, K. Abe et al., Phys, Rev. Lett. 73, 25 (1994).
- [32] A. Bhatti, for the CDF and DØ Collaborations, FNAL-CONF-95/192-E. Presented at 10th Tropical Workshop on Proton-Antiproton Collider Physics, Batavia, IL, 9-13 May 1995. Published in Batavia Collider Workshop 1995:518-527 (QCD161:W64:1995).
- [33] M. Shifman, TPI-MINN-95-32-T. Talk given at Int. Symp. on Particle theory and Phenomenology, Kazimierz, Poland, 1995 and at International Symposium on Particle Theory and Phenomenology, Ames, Iowa, 22-24 May 1995, hep-ph/9511469.
- [34] M. Shifman, Mod. Phys. Lett. A10, 605 (1995).
- [35] The LEP Collaborations ALEPH, DELPHI, L3, OPAL and The LEP Electroweak Working Group, CERN/PPE/93-157 (1993);
 W. Hollik, in Proceedings of the XVI International Symposium on Lepton-Photon Interactions, Cornell University, Ithaca, N.Y., Aug. 10-15, 1993;
 M. Swartz, in Proceedings of the XVI International Symposium on Lepton-Photon Interactions, Cornell University, Ithaca, N.Y., Aug. 10-15, 1993.
- [36] G. Altarelli, CERN-TH/96-05. Lectures presented at the Hellenic School on Elementary Particle Physics, Corfu, Greece, Sep 3-11, 1995 and Rencontres du Vietnam, Ho Chi Minh City, Vietnam, Oct 21-24, 1995.
- [37] S. Dittmaier, D. Schildknecht, and G. Weiglein, BI-TP-96/06, hep-ph/9602436.
- [38] G. Altarelli, CERN-TH-95/196; and the references therein.
- [39] D.O. Carlson, E. Malkawi and C.-P. Yuan. Phys. Lett. B337, 145 (1994).
- [40] E. Malkawi and C.-P. Yuan. Phys. Rev. **D50**, 4462 (1994).
- [41] E. Malkawi and C.-P. Yuan. Phys. Rev. **D52**, (1995) 472.
- [42] D.J. Muller and S. Nandi, hep-ph/9602390, 1996.
- [43] R.S. Chivukula, E.H. Simmons, and J. Terning, Phys.Rev. D53, 5258 (1996).

- [44] G.L. Kane, R.G. Stuart, J.D. Wells, Phys. Lett. B354, 350 (1995).
- [45] H.E. Haber, CERN-TH/96-08, hep-ph/9601331. Talk given at International Europhysics Conference on High Energy Physics (HEP 95), Brussels, Belgium, 27 Jul 2 Aug 1995.
- [46] P.Q. Hung, hep-ph/9604271.
- [47] R.S. Chivukula, E.H. Simmons, and J. Terning, Phys. Lett. B331, 383 (1994).
- [48] E. Malkawi, T. Tait, and C.-P. Yuan. MSUHEP-60315, hep-ph/9603349.
- [49] B. Holdom, UTPT-95-13, hep-ph/9506428;
 - B. Holdom, Phys. Lett. **B351**, 279 (1995);
 - B. Holdom, Phys. Lett. **B339**, 114 (1994).
- [50] G. Altarelli et al., CERN-TH/96-20, hep-ph/9601324;
 - P. Chiappetta, et al., PM/96-05, hep-ph/9601306;
 - J. Layssac, et al., PM/96-09, hep-ph/9602327.
- [51] F. Caravaglios, G.G. ross, Phys. Lett. **B346**, 159 (1995).
- [52] M, Wiest, D.R. Stump, D.O. Carlson, and C.-P. Yuan, Phys. Rev. **D52**, 2724 (1995); and the references therein.
- [53] C. Arzt, M.B. Einhorn, and J. Wudka, Phys. Rev. **D49**, 1370 (1994); and the references therein;
 - X.-G. He and B. McKellar, Phys. Lett. **B320**, 165 (1994);
 - K. Hagiwara et al., Phys. Rev. **D48**, 2182 (1993);
 - U. Baur and E.L. Berger, Phys. Rev. **D41**, 1476 (1990);
 - K. Hagiwara et al., ibid. 2113;
 - T. Helbig and H. Spiesberger, Nucl. Phys. B373, 73 (1992);
 - C.S. Kim et al., YUMS 93-15, SNUTP 93-44, hep-ph/9309212.
- [54] F. Boudjema et al., to appear in Physics at LEP2, edited by G. Altarelli, T. Sjostrand, F.Zwirner, CERN, 1996. Presented at the 3rd General Meeting on Physics at LEP2, CERN, Geneva, Switzerland, Nov 2 3, 1995, hep-ph/9601224
- [55] H.E. Haber, CERN-TH/96-07, hep-ph/9601330. Talk given at International Europhysics Conference on High Energy Physics (HEP 95), Brussels, Belgium, 27 Jul 2 Aug 1995.
- [56] J.L. Lopez, D.V. Nanopoulos, G.T. Park, X. Wang and A. Zichichi, Phys. Rev. D50, 2164 (1994);
 - G. Belanger and G. Feldman, JHU-HET 8406, Aug 1984;
 - G. Bhattacharyya, Phys. Lett. **B331**, 143 (1994).
- [57] G. Kane, C. Kolda, L. Roskowski, and J.D. Wells, Phys. Rev. D49, 6173 (1994);
 R. Arnowitt and P. Nath, CTP-TAMU-52/93, NUB-TH-3037-93. Published in Brazil Summer School 1993:3-63 (QC174.45:J58:1993); and the references therein.

- [58] K. Lane, BUHEP-94-2. Lectures given at Theoretical Advanced Study Institute (TASI 93) in Elementary Particle Physics: The Building Blocks of Creation From Microfermius to Megaparsecs, Boulder, CO, 6 Jun 2 Jul 1993. In Boulder 1993, Proceedings, The building blocks of creation 381-408; and the references therein.
- [59] R.S. Chivukula, E. Gates, E.H. Simmons and J. Terning, Phys. Lett. **B311**, 157 (1993).
- [60] P. Langacker, hep-ph/9412361, to be published in Precision Tests of the Standard Electroweak Model, ed. by P. Langacker (World Scientific, 1994).
- [61] H. Georgi, Nucl. Phys. B361, 339 (1991).
- [62] M. Golden and L. Randall, Nucl. Phys. B362, 3 (1991);
 R.D. Peccei and S. Peris, Phys. Rev. D44, 809 (1991);
 A. Dobado et al., Phys. Lett. B255, 405 (1991);
 M. Dugan and L. Randall, Phys. Lett. B264, 154 (1991).
- [63] W. Buchmüller and D. Wyler, Nucl. Phys. **B268**, 621 (1986).
- [64] F. Gursey, Nuovo Cim. 230, 230 (1960).
- [65] S. Weinberg, Phys. Rev. 166, 1568 (1968).
- [66] S. Coleman, J. Wess and Bruno Zumino, Phys. Rev. D177, 2239 (1969);
 C.G. Callan, S. Coleman, J. Wess and Bruno Zumino, Phys. Rev. D177, 2247 (1969).
- [67] T. Appelquist and J. Carazzone, Phys. Rev. **D11**, 2856 (1975);K. Symanzik, Comm. Math. Phys. **34**, 7 (1973).
- [68] J. Wudka, Int. J. Mod. Phys. A9, 2301 (1994); and the references therein.
- [69] H. Georgi, Weak Interactions and Modern Particle Theory (The Benjamin/Cummings Publishing Company, 1984).
- [70] C.P. Burgess, D. London, and I. Maksymyk, Phys. Rev. D50, 529 (1994);
 C.P. Burgess et al., Phys.Rev. D49, 6115 (1994);
 C.P. Burgess, NEIP-94-012, invited talk at 3rd Workshop on High Energy Physics (WHEPP III), Madras, India, 10-22 Jan 1994, hep-ph/9411257.
- [71] S. Weinberg, Physica 96A, 327 (1979).
- [72] F. Feruglio, Int.J. Mod. Phys. A8, 4937 (1993); and the references therein.
- [73] A. Longhitano, Nucl. Phys. B188, 118 (1981);
 T. Appelquist and C. Bernard, Phys. Rev. D23, 425 (1981).
- [74] R.D. Peccei and X. Zhang, Nucl. Phys. B337, 269 (1990).
- [75] B. Holdom and J. Terning, Phys. Lett. 247B, 88 (1990).
- [76] H. Georgi, Nucl. Phys. B363, 301 (1991).

- [77] F. Feruglio, A. Masiero, and L. Maiani, Nucl. Phys B387, 523 (1992).
- [78] T. Appelquist and Guo-Hong Wu, Phys. Rev. D48, 3241 (1993).
- [79] For a review see G. Ecker, CERN-TH-6660/92. Published in Cargese Summer School 1992:101-148 (QCD161:S77:1992); and the references therin.
- [80] Y. Nambu, Phys. Rev. Lett. 4, 380 (1960);
 - Y. Nambu and G. Jona-Lasinio, Phys. Rev. 122, 345; (1961);
 - Y. Nambu and G. Jona-Lasinio, Phys. Rev. 124, 246; (1961);
 - J. Goldston, Nuovo Cimento 19, 154 (1961);
 - J. Goldston, A. Salam, and S. Weinberg, Phys. Rev. 127, 965 (1962).
- [81] S. Coleman, in Hadron and their interactions, ed. A. Zichichi (Academic Press Inc., New York, 1968).
- [82] K. Wilson, Phys. Rev. B4, 3184 (1971);
 - K. Wilson and J. Kogut, Phys. Rep. 12C, 75 (1974);
 - D. Callaway, Phys. Rep. 167, 2241 (1988).
- [83] M. J. Herrero, FTUAM-96-1, hep-ph/9601286. Talk given at 23rd International Meeting on Fundamental Physics: The Top Quark, Heavy Flavor Physics and Symmetry Breaking, Comillas, Spain, 22-26 May 1995.
- [84] S. Dawson and H.E. Haber, BNL-HEP/TH-96/5, hep-ph/9604354. To be published in 'Electroweak Symmetry Breaking and New Physics at the TeV Scale,' ed. by Barklow, T. L., Dawson, S., Haber, H. E., and Siegrist, J. L.
- [85] G. Altarelli, and G. Isidori, Phys. Lett. **B337**, 141 (1994).
- [86] P. Hasenfratz and J. Nager, Z. Phys. C37, 477 (1988);
 - P. Hasenfratz and T. Neuhaus, Nucl. Phys. B297, 205 (1988);
 - J. Kuti, L. Lin, and Y. Shen, Phys.Rev.Lett. 61, 678 (1988);
 - M. Luscher and P. Weisz, Phys.Lett. 212B, 472 (1988).
- [87] N. Cabibbo et al., Nucl. Phys. **B158**, 295 (1979);
 - M. Sher, Phys. Rep. 179, 273 (1989); and references therein;
 - M. Linder, Z. Phys. 31, 295 (1986);
 - M. Linder, M. Sher, and H.W. Zaglauer, Phys. Lett. **B228**, 139 (1989);
 - C. Ford et al., Nucl. Phys. **B395**, 17 (1993);
 - M. Sher, Phys. Lett. **B317**, 159 (1993).
- [88] J.A. Casas, J.R. Espinosa, and M. Quiros, Phys. Lett. B342, 171 (1995);
 J.R. Espinosa and M. Quiros, Phys. Lett. B353, 257 (1995).
- [89] For a review see, H.E. Haber, SCIPP-91-06. Invited lectures given at Theoretical Advanced Study Inst. (TASI-90), Boulder, CO, Jun 3-29, 1990. Published in Boulder TASI 90:340-475 (QCD161:T45:1990)
- [90] Y. Nambu. In Proc. of the 1988 International Workshop on New Trends in Strong Coupling gauge Theories, Nagoya, Japan, eds. by M. Bando, T. Muta and K. Yamawaki (World Scientific, Singapore, 1989);

- W.A. Bardeen, C.T. Hill and M. Lindner, Phys. Rev. **D41**, 1647 (1990);
- R. Bönisch and A. Leike, DESY-93-111, hep-ph/9308346;
- B. A. Kniehl and A. Sirlin, Phys. Rev. D51, 3803 (1995).
- [91] M. Chanowitz and M.K. Gillard, Phys. Lett. B142, 85 (1984);
 J. Bagger et al., Phys. Rev. D49, 1246 (1994).
- [92] G.L. Kane, UM-TH-91-32, Dec 4,1991, Invited Lectures at the Workshop on High Energy Phenomenology, Mexico City, July 1-10, 1991. Published in Mexico City HE Phenom.1991:241-289 (QCD161:W568:1991).
- [93] S. Abachi et al., Phys. Rev. Lett. 72, 2138 (1994).
- [94] F. Abe et al., The CDF Collaboration, Phys. Rev. **D50**, 2966 (1994).
- [95] R.D. Peccei, S. Peris and X. Zhang, Nucl. Phys. B349, 305 (1990).
- [96] For a review, see C.-P. Yuan, published in Perspectives on Higgs Physics, edited by G. Kane, World Scientific, 1992, pp 415-428.
- [97] See, e.g., P. Chen, Phys. Rev. **D46**, (1992) 1186; and the references therein.
- [98] K. Fujikawa and A. Yamada, Phys. Rev. **D49**, 5890 (1994).
- [99] C.P. Burgess and David London, Phys. Rev. D48, 4337 (1993).
- [100] M.B. Einhorn, UM-TH-93-12. In Coral Gables 1993, Proceedings, Unified symmetry in the small and in the large, 407-420.
- [101] X. Zhang, Mod. Phys. Lett. A9, 1955 (1994).
- [102] M. Veltman, Nucl. Phys. **B123**, 89 (1977).
- [103] A.C. Longhitano, Phys. Rev. **D22**, 1166 (1980).
- [104] C.-P. Yuan, et al., Report of the subgroup on the Top Quark, Proceedings of Workshop on Physics at Current Accelerators and Supercolliders, edited by J. Hewett, A. White and D. Zeppenfeld, 1993, pp 495-505; and the references therein.
- [105] G. Kane, G.A. Ladinsky and C.-P. Yuan, Phys. Rev. **D45**, 124 (1992).
- [106] D.O. Carlson, MSUHEP-050727, Ph.D. thesis.
- [107] G.A. Ladinsky and C.-P. Yuan, Phys. Rev. D49, 4415 (1994).
- [108] R. Barbieri et al., Nucl. Phys. B409, 105 (1993);
 R. Barbieri et al., Nucl. Phys. B288, 95 (1992).
- [109] S. Naculich and C.-P. Yuan, Phys. Rev. D48, 1097 (1993).
- [110] C. T. Hill, Phys. Lett. **B345**, 483 (1995).
- [111] X. Li and E. Ma, Phys. Rev. Lett. 47, 1788 (1988); ibid. 60, 495 (1988); Phys. Rev. D46, 1905 (1992); J. Phys. G19, 1265 (1993).

- [112] H. Georgi, E.E. Jenkins, and E.H. Simmmons, Phys. Rev. Lett 62, 2789 (1989); *ibid.*, Nucl. Phys. B331, 541 (1990);
 R.S. Chivukula, E.H. Simmons and J. Terning, Phys.Lett. B346, 284 (1995).
- [113] The ALEPH Collaboration, CERN-PPE/95-127.
- [114] The OPAL Collaboration, Z. Phys. C67, 555 (1995).
- [115] S. Abachi et al., Phys. Rev. Lett. 75, 1456 (1995);F. Abe et al., Phys. Rev. Lett. 73, 220 (1994); and references therein.
- [116] CDF Collaboration, F. Abe et al., Phys. Rev. Lett. 75, 2900 (1995).
- [117] CDF Collaboration, F. Abe et al., Phys. Rev. **D51**, 949 (1995).
- [118] e⁺e⁻ Collisions at 500 GeV: The Physics Potential, Hamburg, Germany,1993, Ed. P.M. Zerwas; and Physics and Experiments with Linear e⁺e⁻ Colliders, Waikoloa, USA, 1993, Ed. F.A. Harris, et al.; and references therein.
- [119] T. Takeuchi, A.K. Grant, and J.L. Rosner, FERMILAB-CONF-94-279-T, presented at DPF 94, Albuquerque, NM, Aug 2-6, 1994. Published in DPF Conf. 1994:1231-1235 (QCD161:A6:1994), hep-ph/9409211
- [120] M. Veltman, Acta Phys. Pol., vol B8, 475 (1977).